Optimising process quality and cost for closed, automated and commercial scale manufacture of allogeneic stem cell therapy products

Optimising Process Quality and Cost for Closed, Automated and Commercial Scale Manufacture of Allogeneic Stem Cell Therapy Products

by

William David Mitchell

Centre for Biological Engineering

Wolfson School of Mechanical, Electrical and Manufacturing Engineering

Loughborough University

A Doctoral Thesis submitted in partial fulfilment of the requirements

for the award of

Doctor of Philosophy of Loughborough University

September 2020

Abstract

Embryonic stem cell (ESC) derived therapies offer huge potential for clinical and economic benefit; however, their development is currently restricted by the suitability of available equipment and limited scalability of common processing techniques. Although several current cell manufacturing technologies are hypothetically suitable, systems developed for more mature cell therapies such as mesenchymal stem cells are not scalable down to processing scales suitable for allogeneic ESC derived therapies, while small scale systems developed for autologous therapies such as chimeric antigen receptor T cells lack the processing capabilities required for adherent cells. This thesis explores the complexities faced in transferring allogeneic ESC derived cell therapy products (CTP) from manual processing, where such processes are typically developed, to closed, automated and commercial scale production systems.

This work first documents the intricacies of technology transfer in CTP production. The case example is a protocol to produce 5 x 10^8 mesencephalic dopaminergic (mesDA) progenitor cells on the CliniMACS Prodigy cell processing platform system from Miltenyi Biotec to Loughborough University. Numerous complex device and process robustness interactions are identified, with TrypLE and DTI contamination of above 3.31% for H9 cells and 1.95% for RC17 cells during cell seeding as a result of insufficient purification established as a key point of failure. This work highlights how a cell with a high level of environmental sensitivity compounds typical issues in multi-site protocol transfer and verification processes. Downstream processing techniques compatible with closed and automated processing are then explored, including the effects of physical manipulation on cell harvesting, the efficiency of closed and automated purification techniques, as well as the effects on cryopreservation of increased batch sizes and closed cryopreservation containers, with improved techniques determined in each case.

Based upon the knowledge obtained as a result of the technology transfer and downstream processing investigation, a process economics model is presented establishing baseline costs of £12,960 for manual processing and £20,106 for closed and automated processing against which process improvements may be compared. The TrypLE and DTI contamination issue highlighted during the technology transfer is explored in depth, with the cost and quality impacts of potential process improvements calculated and an optimal improvement plan proposed, providing potential savings of up to £444 for a H9 based process and £330 for an RC17 based process. This investigation highlights the possibility of successfully performing the protocol on the Prodigy and highlights a lack of data driven process change performed by protocol developers as part of their troubleshooting process. Finally, the complexity of CTP manufacturing processes is discussed and the importance of process robustness and fit for purpose process verification is underlined.

Acknowledgements

I would first like to thank my supervisor Dr Mark McCall for his insight and guidance throughout my PhD, and for always providing me with the confidence and motivation to explore this exciting field. I would also like to thank my secondary supervisors, Dr Samantha Wilson and Professor Robert Thomas, as well as my colleagues within the Centre for Biological Engineering, most notably Dr Preeti Holland for her hard work and patience when jointly performing laboratory work.

I would also like to acknowledge the support of the Engineering and Physical Sciences Research Council (EPSRC) for funding my PhD, and to those within the Centre for Doctoral Training in Regenerative Medicine without whom I would never have considered it possible for me to work in the fields of bioengineering and cell therapy product manufacturing.

I would like to thank my parents and grandparents for always encouraging and enabling me to do my best, and my sister for always being there and allowing me to unwind over the phone. Finally, I would like to thank my wife Sophie for her enormous and unwavering support and understanding throughout the PhD and writing up process.

Table of Contents

List of Figures

List of Tables

List of Abbreviations

AA - Ascorbic acid

ATMP - Advanced therapy medicinal product

BDNF - Brain-derived neurotrophic factor

BMP - Bone morphogenetic proteins

BSC - Biological safety cabinet

CAR-T - Chimeric antigen receptor T cells

CBE - Centre for Biological Engineering (Loughborough University)

CCU - Centri-cult chamber

COGS - Cost of goods

CQA - Critical quality attribute

CRF - Controlled rate freezer

CTP - Cell therapy product

DAT - Dopamine transporter

DMEM - Dulbecco's modified eagle medium

DMSO - Dimethyl sulfoxide

DTI - Defined trypsin inhibitor

EDTA - Ethylenediaminetetraacetic acid

ESC - Embryonic stem cell

EU - European Union

FDA - Food and Drug Administration

FITC - Fluorescein isothiocyanate

FMEA - Failure mode and effects analysis

FOX - Forkhead box protein

FSC - Forward scatter

GBX2 - Gastrulation brain homeobox 2

GLP - Good laboratory practice

GMBH - Gesellschaft mit beschränkter Haftung (company with limited liability)

GMP – Good manufacturing practice

GSK3 - Glycogen synthase kinase 3

HEC - Heat exchange cartridge

hESC – Human embryonic stem cell

HSA - Human serum albumin

IAP - Integrin-associated protein

ICH - International Council for Harmonisation of Technical Requirements for Pharmaceuticals for Human Use

ISPE - International Society for Pharmaceutical Engineering

IQOQ - Installation qualification, operational qualification

ISCBI - International Stem Cell Banking Initiative

L-DOPA - Levodopa / l-3,4-dihydroxyphenylalanine

LMX1A - LIM Homeobox Transcription Factor 1 Alpha

MACS - Magnetic-activated cell sorting

MCB - Master cell bank

ME - Mixed ester

mPES - Modified polyethersulfone

NACK - Negative acknowledge

NB - Neuro-brew

NC - NucleoCounter

NDM - Neural differentiation medium

NIM - Neural induction medium

NPM - Neural proliferation medium

NSCR - Neuro stem cell repair

OTX2 - Orthodenticle Homeobox 2

PBS - Phosphate-buffered saline

PCD - Passive cooling device

PD – Parkinson's disease

PEB - Protein extraction buffer

PES - Polyethersulfone

PITX3 - Pituitary homeobox 3

PS - Polysulfone

PSC - Pluripotent stem cell

QA - Quality assurance

QC - Quality control

RCF - Relative centrifuge force

REA - Recombinant antibodies

ROCK - Rho-associated protein kinase

RPM - Revolutions per minute

SD - Standard deviation

SHH - Sonic hedgehog

SOP - Standard operating procedure

SSC - Side scatter

SSEA - Stage-specific embryonic antigen

TACSI - Terumo automated centrifuge and separator integration

TCP - Tissue culture plastic

TFF - Tangential flow filtration

TS - Tubing Set

UKSCB – UK Stem Cell Bank

US – United States of America

VM - Ventral midbrain

VMAT2 - Vesicular monoamine transporter 2

WHO – World Health Organisation

1 Introduction

1.1 Aims and Objectives

The aim of this PhD is to explore closed, automated and commercial processes for the manufacturing of adherent human pluripotent stem cells as well as human mesencephalic dopaminergic (mesDA) progenitor cells, with the aim of optimising process quality and cost through scalable and good manufacturing practice (GMP) compliant processes. The work will demonstrate development of process understanding and manufacturing strategies that will enhance the clinical utility of a process designed in collaboration with the University of Lund and Cambridge University, integrating automation technology from Miltenyi Biotech GMBH and others. The project builds upon differentiation protocols developed at Lund University to produce mesDA cells from pluripotent stem cell lines, as well as work by Miltenyi to adapt adherent cell protocols for use with the CliniMACS Prodigy closed and automated cell processing system. This PhD aims to demonstrate a closed and automated process for the expansion and differentiation of the GMP human embryonic RC-17 cell line into mesDA progenitors on the CliniMACS Prodigy and will inform manufacturing process changes for a cell replacement therapy for the treatment of Parkinson's disease.

The work first focuses on a technology transfer of a process to expand and differentiate H9 human embryonic stem cells (hESCs) into mesDA cells on the CliniMACS Prodigy, with the objective of demonstrating comparability between the process as run by Miltenyi in Germany with the process performed at the Centre of Biological Engineering at Loughborough University. The process will then be adapted for use with the GMP compatible hESC RC-17 cell line, the intended input material to the final Parkinson's disease cell therapy product. A second workstream will focus on downstream process development, exploring currently available purification and cryopreservation techniques to identify an optimal process for the mesDA product and determine the comparability of open and closed purification and cryopreservation processes. Process and equipment changes required for closed downstream processing will also be explored. Finally, cost and quality implications of key compatibility issues will be explored, with the aim of identifying where new technology and techniques are most required to enable future allogeneic stem cell-based therapies.

1.2 Areas of Investigation

The central question of this research was originally: what key process changes are required to transition from open, manual, small-scale production of cellular therapies to closed and automated commercial scale manufacture? Over the course of this PhD, the research focus shifted from specific process improvements to improvements of process development methodology. The new research question therefore became: what are the key challenges to process transfers and development at present, and what approaches may be used to overcome these challenges and achieve robust and optimised cell manufacturing processes?

This work focusses on allogeneic embryonic stem cell-based therapies and utilises a process for the expansion and differentiation of hESCs into mesDA neural progenitors as a demonstrator. This work is therefore performed with an expected dose size on the order of 2×10^6 cells.

1.3 Context

Cell therapies are a disruptive technology with the potential to treat and cure many currently untreatable diseases and to replace or eliminate the need for many established pharmaceuticals. The biologically active material delivered in these therapies present challenges to manufacturing not seen in other industries which, together with the stringent regulatory landscape, present significant barriers to commercialisation. The unique challenge of manufacturing living biological cells with no option of terminal sterilisation means that sterile conditions must be maintained throughout all product processing steps. Cells are also dynamic and responsive to their environment, resulting in a sensitive product with a high degree of potential variability.

Manufacturing of cell therapy products is highly dependent upon technology, especially when processing at commercial scales where a degree of automation is required. Due to the lack of demand from an established allogeneic product base, much of the technology employed in the manufacture of stem cell derived products is repurposed from related products and not ideally suited for the process for which it is used. Much currently available technology relevant to allogeneic stem cell manufacturing was developed to meet the needs of mesenchymal stem cell manufacture, and the expectation that large volumes of this adherent and allogeneic source material would be required for many therapies. As a result of this, much currently available technology is of too large a scale to ideally fit comparatively low dose embryonic stem cell (ESC) therapies. More recent technology development has focussed on

hematopoietic and immunotherapeutic applications, with the market approval of chimeric antigen receptor T cells (CAR-T) therapies such as Kymriah (Novartis, Switzerland) and Yescarta (Kite Pharma, US) attracting attention and funding for similar therapies. While these therapies require processing are at a comparable scale to low dose ESC products, there are significant differences in manufacturing requirements between processing of the autologous and suspension-based CAR T therapies compared to allogeneic and adherent ESC based therapies.

The therapies of the future are dependent upon technologies optimised for the therapies of the present, as the small number of approved cell therapy products and large potential for profitability mean that new technology development is heavily dictated by industry trends. Due to the dependence of cell therapy manufacture on technology such as plasticware and processing systems, industry trends form a positive feedback loop of innovation in an area of focus, enabling rapid product development through new enabling technologies. Conversely, cell therapies outside of areas of focus are subject to a lack of innovation, with development of new enabling technologies limited by a lack of demand from an established product base. Such therapies therefore face an uphill battle and must either wait for success of a product with similar manufacturing requirements to refocus industry attention and provide enabling technologies or pioneer a viable manufacturing process through improvisation of available technology.

Utilising the appropriate tools from established manufacturing industries will be essential in increasing process reliability, reducing manufacturing costs and enabling commercially viable cell therapies. Key to enabling quality cell therapy manufacture is the replacement and simplification of manual handling steps through automation. Cell therapies are typically produced by highly skilled operators performing hand tool manipulations in a cleanroom environment, resulting in high labour costs and numerous opportunities for operator induced variability. Automation has been widely used across manufacturing industries to achieve standardisation and control of complex processes, however its adoption into biomanufacturing is currently limited. A second enabling technology for quality manufacturing is the use of closed or contained manufacturing systems which provide a constant physical barrier between the cell therapy product (CTP) and outside environment. This technology is already utilised in several automated cell processing systems to reduce contamination risk and provide tighter environmental control and is recommended in current regulatory guidance.

1.4 Thesis Structure

This thesis is comprised of seven chapters. This first introductory chapter is followed by chapter two, a literature review, and chapter three, materials and methods, which detail the technology and techniques which underpin the work performed in further chapters. Chapter four presents the process knowledge and lessons learned during the transfer of a process to expand and differentiate cells on the Prodigy system. Chapter five examines the suitability of currently available purification and cryopreservation technology and techniques for small scale cell therapy manufacture. Chapter six explores the quality implications of transferring to closed and automated processing and presents a process economics model for the mesDA manufacturing process which is used to determine the cost implications of process changes. Finally, chapter seven summarises the knowledge gained for each stage of a closed and automated manufacturing process and discusses the implications for future therapies and the cell manufacturing industry. This chapter then ends with a discussion of limitations and suggestions for future work.

2 Literature Review

2.1 Cell Therapies

Cell therapies are treatments in which living cells are implanted into a patient to deliver a clinical benefit (European Medicines Agency, 2019). Stem cell therapies are a category of cell therapy which utilise stem cells to replace damaged cells and restore biological function, exploiting their unique capability to differentiate into other cell types or divide to produce more stem cells (Mason and Dunnill, 2008). Stem cell therapies offer opportunities to treat diseases in ways not currently possible with pharmaceuticals, with the potential benefits approaching the level of a cure for many diseases (Heathman *et al.*, 2015). Many stem cell therapies are regenerative medicines, defined as medicine which "replaces or regenerates human cells, tissue or organs, to restore or establish normal function" (Mason and Dunnill, 2008). While many stem cell therapies harness the regenerative properties of stem cells, other applications include reduction of inflammation and improved bacterial clearance (Mei *et al.*, 2010) and protective effects for several tissue types (Magnasco *et al.*, 2008; Yang *et al.*, 2015) .

2.1.1 Types of Cell Therapy

Regulatory bodies distinguish between minimally manipulated therapies such as transplants and transfusions, and more manipulated cell products including somatic cell therapy, gene therapy and tissue engineered products. More-than-minimally manipulated products are regulated as biologics or medicinal products and are required to meet high standards of manufacturing quality and consistency (Hourd *et al.*, 2008).

Cell therapies derived from human cells may be either autologous, meaning from the same individual, or allogeneic, meaning from the same species (Mason and Dunnill, 2008). Autologous therapies are patient specific and avoid issues of immune rejection associated with allogeneic therapies, however they require an individual product batch for each patient. Allogeneic therapies utilise a common cell source to produce a standardised product for many patients. This approach allows for significantly increased batch sizes and the use of standardised and well characterised input cells, and is therefore highly preferable from a manufacturing and quality perspective (Mason and Dunnill, 2009).

Many vertebrate cell types including pluripotent stem cells are anchorage dependent, meaning that they require adherence to a surface to proliferate. Suspension cells such as hematopoietic cell lineages grow suspended in liquid. The anchorage dependency of cells has important implications for ease and cost of bioprocessing, with additional manipulations required to transfer adherent cells into suspension for further processing. This review will focus on adherent manufacturing of allogeneic stem cell derived cell therapy products (CTP).

The most mature allogeneic CTPs are mesenchymal stem cells (MSCs) and fibroblast derived therapies (Pigeau, Csaszar and Dulgar-Tulloch, 2018), while recent developments have focussed on autologous chimeric antigen receptor T cells (CAR-T) therapies utilising gene editing of patient specific cells for the treatment of cancers. Of the over 1000 regenerative medicine clinical trials underway as of Q3 2019, approximately 62% relate to oncology, 5% to musculoskeletal disorders and 5% to disorders of the central nervous system (Alliance for Regenerative Medicine, 2019). Approximately 21% of current trials are for cell therapies (Alliance for Regenerative Medicine, 2019).

2.2 Parkinson's Disease as a Target Therapy

Parkinson's Disease (PD) is a progressive neurological disorder caused by the degeneration of dopamine producing neurons in the substantia nigra (Parent and Parent, 2010). PD is characterised by the motor symptoms: resting tremor, muscle rigidity, slowness of movement and postural instability (Jankovic, 2008), as well as non-motor symptoms including depression, dementia, sleep disorders, bladder and bowel problems and fatigue thought to originate from non-dopamine cell degeneration in nearby structures (Chaudhuri, Healy and Schapira, 2006). There is no currently available therapy capable of slowing or reversing the degeneration of neural tissue or altering disease progression. The total annual direct health care cost of PD is estimated to be £5022 per patient (Weir *et al.*, 2018), with household costs including higher social care costs, loss of earnings and out of pocket expenditure averaging £16,582 per patient per year (Parkinsons UK, 2017). It is expected that the global prevalence of PD will increase significantly with increased life expectancy and aging populations worldwide (Pringsheim *et al.*, 2014).

Parkinson's disease is a prime candidate for cell therapy treatment as it is caused by the localised loss of a relatively small number of dopamine producing cells (Kirkeby, Parmar and Barker, 2017). Cell therapies have been proposed for the treatment of Parkinson's disease and several other neurodegenerative diseases as they offer the opportunity to replace dead or damaged cells, restoring

local psychologically stimulated dopamine release, restoring normal biological function and providing effective symptom relief.

2.2.1 Mesencephalic Dopaminergic (mesDA) Neuron Manufacturing Process

Foetal midbrain transplants are an allogeneic cell therapy which produce symptom relief for PD when paired with sufficiently long term immunosuppression (Freed *et al.*, 2001; Piccini *et al.*, 2005), findings which have been mirrored in animal models for embryonic stem cell (ESC) based PD cell therapies (Kim *et al.*, 2002).

Development of cell therapies for the treatment of PD began in the late 1970s when groups including Anders Björklund's at Lund University began exploring the survival and regenerative properties of neurons implanted in to rats (Björklund and Stenevi, 1979; Perlow *et al.*, 1979; Björklund *et al.*, 1980). A technique for transplanting cells in suspension was developed resulting in more widespread innervation, and was demonstrated to restore nigrostriatal pathway function and result in behavioural recovery (Dunnett *et al.*, 1983), form synapses with host neurons (Freund *et al.*, 1985), and to correctly regulate dopamine production (Strecker *et al.*, 1987). Transplants of foetal tissue in human PD patients began in 1987 and were shown to achieve similar levels of survival and recovery of motor function found in animal models (Lindvall *et al.*, 1990), with efficacy shown to be dependent upon the number of cells surviving following implantation as well as level of integration between graft and host (Piccini *et al.*, 2000). Long-term follow up studies have demonstrated prolonged symptom relief in humans 10 years after implantation (Piccini *et al.*, 1999).

While foetal trials have provided a proof of concept for cell therapies for PD, a high degree of variability was found in patient outcomes, ranging from near complete symptom relief to severe graft-induced dyskinesia (Freed *et al.*, 2001; Olanow *et al.*, 2003; Lindvall and Björklund, 2004). Outcomes are thought to be affected by patient age (Freed *et al.*, 2001) and spread of pathology (Piccini *et al.*, 2005), graft placement (Piccini *et al.*, 2005) , immunological response (Piccini *et al.*, 2005) and follow up period (Freed *et al.*, 2001). Of note for future cell therapies is that the age, composition and preparation of the foetal cells plays a significant role in patient outcome (Lindvall and Björklund, 2004), and may be improved through the use of a standardised cell source as in the case of an allogeneic stem cell therapy.

Following varied success of foetal tissue trials, the TRANSEURO organisation was formed to reassess trial methodologies with the aim of performing a new trial building upon the developments in trial design, patient selection and tissue and transplantation protocols. This new foetal VM based trial

(NCT01898390) is currently underway in Europe and expected to complete is 2021 (Barker *et al.*, 2019). The TRANSEURO trial forms part of a larger set of EU funded programmes aiming to being ESC derived therapies to a phase I clinical trial in Europe, as shown in Figure 1. An initiative called G-Force PD has also been created to align trial efforts and standards with centres in the US and Japan (Barker *et al.*, 2015). The first trial under this initiative began recruiting in August 2018 and is currently ongoing, having transplanted an induced pluripotent stem cells (iPSC) derived therapy to at least one patient to date (Takahashi, 2019).

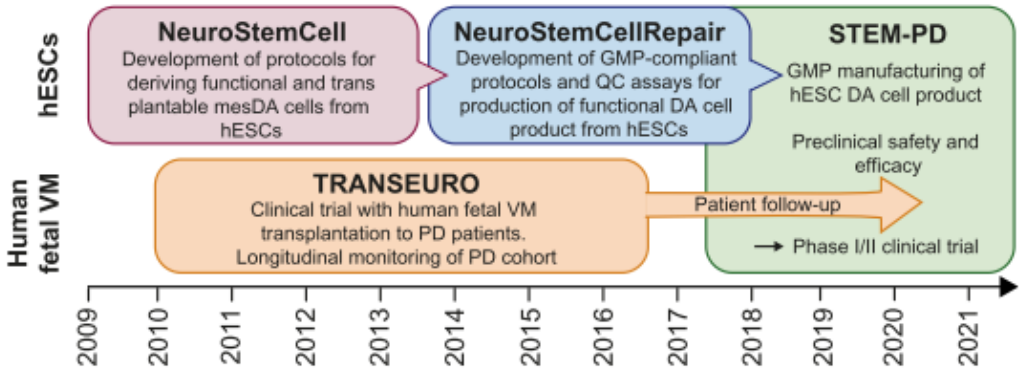

Figure 1 – Overview of EU programs leading to trials of an ESC derived PD therapy (Kirkeby, Parmar and Barker, 2017).

2.2.2 Sourcing

Allogeneic stem cell therapies utilise a common cell source for all product batches, allowing for a high degree of characterisation and standardisation of source material (Mason and Dunnill, 2009). Due to the high potential for self-renewal, a single stem cell source may provide source material to many stem cell therapies for the life of the CTP.

Although shown to be effective in PD symptom relief (Lindvall *et al.*, 1990), minimally manipulated foetal tissue is unsuitable for a large-scale commercial product due to the ethical and practical limits on availability, as well as issues with graft variability and freshness (Lindvall and Björklund, 2004; Fricker-Gates and Gates, 2010). The expansion of foetal neural stem cells does not offer a suitable solution due to low cell survival and regeneration potential of therapies derived from these cells compared to direct transplants, with cells also shown to lose the potential to differentiate into neural lineages following long term culture (Brundin and Björklund, 1998).

Other cell sources including adult neural stem cells, mesenchymal stem cells and parthenogenetic stem cells have also been explored, however protocols for differentiation into functional dopamine neurons have yet to be demonstrated (Fricker-Gates and Gates, 2010; Barker, Drouin-Ouellet and Parmar, 2015; Barker *et al.*, 2016).

ESCs are obtained from the inner cell mass of a blastocyst prior to implantation and are commonly sourced from unused embryos produced by fertility treatments. They were first derived in 1981 by (Evans and Kaufman, 1981), and first isolated and grown in vitro in 1998 (Thomson *et al.*, 1998) where they were shown to maintain self-renewal and pluripotency through extended culture periods, allowing for large numbers of cells to be generated from a single source embryo and providing an effectively unlimited source of standardised and controllable graft material.

In 2001, human ESCs were differentiated into neural progenitors in vitro and transplanted into neonatal mice, where they integrated with host tissue and differentiated into neurons with no detected teratoma formation (Zhang *et al.*, 2001). Two seminal publications in 2002 demonstrated the ability of ESCs to survive and restore motor function in rat models of PD. The first demonstrated the ability of undifferentiated mouse ESCs to differentiate into dopaminergic neurons and restore motor functionality when implanted into the striatum of a rat PD model (Bjorklund *et al.*, 2002), while the second showed that mouse ESCs differentiated into neurons in vitro were also able to restore functionality in rat PD models (Kim *et al.*, 2002). More recently, human ESC (hESC) derived transplants have been shown to integrate into the basal ganglia of rat PD models with varying levels of striatum denervation (Adler *et al.*, 2019).

Protocols to produce large numbers of dopamine neurons from ESCs in vitro have continued to improve, allowing for extended culture periods capable of producing higher numbers of neurons and greater degrees of phenotypic control (Kirkeby *et al.*, 2012; Kirkeby, Nelander and Parmar, 2012). As a result, ESC differentiation protocols are currently able to produce dopamine neuron progenitor cells with higher purity and control than achievable from foetal sources (Kirkeby *et al.*, 2017; Nolbrant *et al.*, 2017). A comparison of dopamine neurons derived from hESCs and foetal tissue transplant showed that neurons from both sources can survive, mature and restore dopamine pathways in rat PD models for at least 6 months following grafting, with near identical morphology, marker expression and potency (Grealish *et al.*, 2014). ESC derived neurons were also shown to achieve similar axon projection distances to foetal derived neurons in adult rat brains and showed a similar dosage response to foetal neurons in in drug-induced rotation tests. Of high clinical relevance is that ESC derived neurons achieved up to 10 mm of outgrowth from the graft, enough to provide recovery of dopamine pathways in human PD patients.

iPSCs are stem cells which are derived from adult tissues and reprogrammed to gain properties similar to ESCs. The generation of iPSCs was first shown in 2006 (Takahashi and Yamanaka, 2006). The production of dopamine neurons from iPSCs obtained from PD patients has also been demonstrated (Soldner *et al.*, 2009), and iPSCs derived from skin biopsies have been shown to improve motor functionality in non-human primate models (Hallett *et al.*, 2015). Despite the benefits of reduced immunological rejection risk and circumvention of ethical issues associated with foetal and embryonic sources, iPSCs have numerous drawbacks including reduced genome integrity, epigenetic memory, increased aggression of teratomas and reduced differentiation speed (Puri and Nagy, 2012). Artificial induction techniques have also been shown to produce cells with dopamine neuron markers which do not perform neurogenesis, raising the difficulty of creating potency assays (Sonntag *et al.*, 2004). While iPSCs offer an autologous approach, cells obtained from PD patients may also feature a genetic predisposition for PD pathology (Stoker et al., 2017).

2.2.2.1 Cell Lines

A cell line is a culture of characterised cells with a high potential for self-renewal, of which sub-populations may be banked and distributed. Cell lines may be used for research purposes such as drug discovery and pre-clinical development, for manufacturing purposes such as protein production, or for clinical use as source material for CTPs (Thomson *et al.*, 1998). Although ESCs are considered to perform similarly between lines, differences in growth rate and long term stability have been observed (Allegrucci and Young, 2006). The first approval for a hESC derived therapy used a cell line initially derived under research conditions, then later qualified for clinical use through comprehensive testing (Alper, 2009). As regulators employ a risk-based approach, cell lines created under entirely good manufacturing practice (GMP) conditions may become a requirement for future therapies (De Sousa, Downie, *et al.*, 2016). Standards for cell line derivation have developed in efforts to produce lines suitable for clinical use, with trends away from the use of animal products and towards greater degrees of control and monitoring. Whether a cell line is of acceptable quality ultimately depends upon whether a product based upon it gains regulatory approval. The high level of quality required for cell banking mean cell lines are expensive to establish, with estimated costs in 2017 of £60,000 for research grade lines and £1,000,000 for clinical grade lines (Stacey, 2017). The cost of establishing clinical grade lines means that few are established. Of the 1200 ESC lines reported in 2015, around 50 were derived under GMP conditions and are therefore potentially suitable as source material for cell therapies (Canham *et al.*, 2015).

2.2.3 Differentiation Process

Differentiation is the process of progressing a cell from a state of pluripotency to a more specialised state (Evans and Kaufman, 1981). In stem cell derived cell therapy products, it is the process of moving from highly proliferative pluripotent cells into tissue specific progenitor cells, and possibly terminal differentiation to a non-proliferative cell type.

Generation of neural cell lineages from pluripotent cells is achieved by replication of the bio-chemical environment present in the natural development of an embryonic central nervous system (Kirkeby and Parmar, 2012). In vivo, cells first differentiate to form the three germ layers from which a population of ectodermal cells form the neural plate. The edges of the neural plate then fold dorsally until a groove is formed, folding then continues to form the neural tube. The tube then closes at both ends and the tube develops into three vesicles, the proenkephalin (forebrain), mesencephalon (midbrain) and rhombencephalon (hindbrain) (Kandel *et al.*, 2000). Dopaminergic progenitors of interest for PD therapy are formed in the mesencephalic floor plate (Kirkeby and Parmar, 2012).

Early protocols to generate dopaminergic neuron lineages from pluripotent stem cells focussed on PAX6 positive lineages and achieved differentiation through the use of embryoid bodies (Zhang *et al.*, 2001), induction by stromal cells (Kawasaki H, Mizuseki K, Nishikawa S, Kaneko S, Kuwana Y, Nakanishi S, Nishikawa SI, 2000) and inhibition of SMAD proteins (Chambers *et al.*, 2009). Although these protocols produce large numbers of cells capable of producing tyrosine hydroxylase, the enzyme responsible for the production of the dopamine precursor L-DOPA, they were found to perform poorly when grafted into PD rat models

Midbrain dopamine neurons were later found to originate from the ventral midbrain (VM) rather than the neuroepithelium (Kirkeby *et al.*, 2012). Recent protocols have therefore focussed on generating cells positive for transcription factors found in the midbrain floor plate such as FOXA2, LMX1A, OTX2, EN1 and CORIN, and negative for pluripotency or non-neuronal floorplate markers including PAX6, FOXG1 and GBX2 (Kirkeby and Parmar, 2012). Midbrain dopamine neurons derived from human ESCs and differentiated using these methods have been shown to survive, mature and restore dopamine pathways in rat PD models (Grealish *et al.*, 2014), with grafted neurons expressing TH, DAT, VMAT2, PITX3, GIRK2 (Kirkeby and Parmar, 2012).

Protocol development has continued at Lund, with neural induction and patterning towards ventral midbrain progenitors currently achieved through several differentiation and patterning factors (Nolbrant *et al.*, 2017):

- Differentiation from hESCs to neural lineages is achieved through dual SMAD inhibition using SB and Noggin differentiation factors (Chambers *et al.*, 2009).
- The GSK3 inhibitor CHIR99021 (CHIR) is used to activate canonical WNT signalling (Frame, Cohen and Biondi, 2001), a gradient of which influences early anterior-posterior neural plate patterning (Bally-Cuif, Cholley and Wassef, 1995). Dose dependant activation of canonical WNT signalling via controlled CHIR exposure allows for direction of cells toward midbrain fates (Kirkeby and Parmar, 2012).
- Sonic Hedgehog C24II (SHH) and bone morphogenetic proteins (BMP) influence cell fate along the dorsal-ventral axis of the neural tube, with SHH being present in floor plate and BMP in the roof plate. SHH is therefore used to direct cells towards floor plate lineages (Ye *et al.*, 1998).
- Purmorphamine is an optional small molecule agonist of the SHH signalling pathway and may be used to increase the ventralization capability of SHH (Nolbrant *et al.*, 2017).
- N2 serum-free supplement is used to support cell growth and viability.

Following maturation and ventral midbrain patterning, maturation into mesDA progenitors is then achieved (Nolbrant *et al.*, 2017):

- Brain-derived neurotrophic factor (BDNF) is a neurotrophic factor that supports the growth, survival, and differentiation of mesDA neurons, increasing their survival in culture (Hyman *et al.*, 1991).
- Ascorbic Acid is an antioxidant and increases dopamine neuron yield in vitro, possibly by reducing damage by oxidative stress (Bagga, Dunnett and Fricker-Gates, 2008).
- Fibroblast growth factor 8b (FGF8b) influences cell fate along the anterior–posterior axes axis of the neural tube. It is present at the boundary between the mid and hindbrain and is essential for late patterning of mature neuron types including dopaminergic neurons (Ye *et al.*, 1998).
- B-27 serum-free supplement is used to support high density cell growth and viability.

2.3 Manufacturing Requirements

CTPs are developed to deliver a clinical benefit to a patient, as well as an economic benefit to the project sponsors. To achieve these goals, cell therapy products must meet standards of product quality at an

acceptable cost (Stanton, 2019). Quality enables a cell therapy to deliver its clinical benefit, and comprises factors such as identity, potency and purity, which together also dictate product efficacy and safety (Lipsitz, Timmins and Zandstra, 2016). Costs are key to the wider adoption of cell therapies, and include aspects such as materials, labour, facilities and equipment, as well as covering the substantial cost of new product research and development (Bubela *et al.*, 2015). Cost and quality are heavily interlinked, as quality improvements may incur additional costs while cost savings may cause quality losses. The driving factor in development of a commercial product is therefore the optimisation or maintenance of an acceptable standard of quality for the minimum possible cost.

It is understood within the field of quality management that the level of resource allocated to quality should be proportional to the cost of failure, and that the cost of implementing effective quality management is often less than the costs associated with handling product quality failures, summarised in the statement "quality is free" (Crosby, 1979). For CTPs, the cost of product failure is extreme and challenging to quantify, as quality losses impacting product safety have the potential to cause loss of life as well as economic loss. These failures may also impact the regulatory status of the therapy, jeopardizing the potential for future profitability regardless of quality improvement efforts. For autologous therapies, the human costs may be significant even for quality failures detected prior to release, as a patient may deteriorate in the time taken to re-harvest the autologous source material and remanufacture the therapy (Bersenev and Kili, 2018). For allogeneic therapies, detection of a quality failure prior to product release is less likely to inflict a human cost as patients may be treated from an alternative product batch. The impact of process failure and out of specification product is high for cell therapy products, as batch failure rates are currently high at approximately 5 to 10% (Julien and Whitford, 2008; Langer, 2008, 2016).

Medicines are highly regulated both in terms of product quality, safety and efficacy as well as the processes of their manufacture, storage and distribution (World Health Organization, 2019). Regulatory bodies distinguish between minimally manipulated therapies for homologous use such as transplants and transfusions, and more manipulated products for non-homologous use. These products are classified as advanced therapy medicinal products (ATMPs) in Europe and include including somatic cell therapies, gene therapies, tissue engineered products and combination products (European Medicines Agency, 2019). The FDA employ a similar definition for cellular and gene therapy products as set out in (FDA, 2018a). Regulations for minimally manipulated products focus on limiting loss of quality and disease spread from donor to patient. Stem cell therapies are more manipulated and are therefore regulated as medicines, requiring highly controlled and well-documented manufacturing processes capable of delivering consistent quality assured products (Williams *et al.*, 2012).

The ATMP industry largely considers the regulatory landscape to be challenging due to its high requirement for product data and the regularity of changes (Plagnol *et al.*, 2009), with this situation exacerbated by the UK's uncertain position within the EU's regulatory architecture.

2.3.1 Quality

Quality during cell product manufacture is typically discussed in terms of critical quality attributes (CQAs), each of which is a "physical, chemical, biological, or microbiological property or characteristic that should be within an appropriate limit, range, or distribution to ensure the desired product quality" (ICH, 2009). CQAs contribute towards meeting a quality target product profile, which is "a prospective summary of the quality characteristics of a drug product that ideally will be achieved to ensure the desired quality, taking into account safety and efficacy of the drug product" (ICH, 2009). These definitions are part of the quality by design (QbD) framework, defined as "a systematic approach to development that begins with predefined objectives and emphasizes product and process understanding and process control, based on sound science and quality risk management" (ICH, 2009).

Language for defining cell therapy quality has developed out of definitions for drug quality, which typically includes specification of identity, strength and purity, as well as suitability for intended use (ICH, 1999). For drug products, identity relates to the molecular composition, however, notionally identical cells vary between themselves and change over time, complicating the concept of cell identity. For product release purposes, cell identity is typically demonstrated through surface marker expression with acceptable ranges defined (Lipsitz, Timmins and Zandstra, 2016). Strength of a drug product describes the dosage, or amount of active ingredient per dose and may be defined by weight. For cell therapy applications, potency is a more useful measure and describes the level of activity of an active ingredient, measured through functional assays (Lipsitz, Timmins and Zandstra, 2016). Purity of cell therapy products includes the absence of unwanted cell types, dead cells, adventitious agents, liquids and particles. The inability to terminally sterilise cell products and resulting requirement for sterility throughout the manufacturing process is a key difference between pharmaceutical and cell therapy manufacture and a significant source of additional cost during manufacture. Typical requirements for a cell therapy product include a definition of cell identity through surface marker expression, a threshold of acceptable viability, a range of acceptable cell concentration, specification of a single cell suspension, and a threshold of acceptable impurities (Pattasseril *et al.*, 2013).

2.3.1.1 Good Manufacturing Practice (GMP)

Quality for a cell therapy product means managing variability to meet requirements of identity, potency and purity, which due to *the product is the process* paradigm means that process knowledge and control are of utmost importance to product quality (Williams *et al.*, 2012). Guidelines for GMP, or the US variant, current good manufacturing practice (cGMP), form the basis of quality manufacturing and specify standards of control and record keeping which enable reproducible and auditable processes. These standards are described in EudraLex in Volume 4, Good Manufacturing Practice guidelines for the EU (EudraLex, 2017) as well as by the FDA under Code of Federal Regulations Title 21 for the US (FDA, 2008). As EU and US guidance is based on broadly similar principles and harmonisation is increasing (ICH, 2000), references to GMP will refer to both standards unless stated otherwise.

A high degree of input material control is required for GMP processing. All reagents in the process must be replaced with GMP compliant alternatives which are xero-free and feature higher grades of production and accountability throughout the manufacturing process. The transfer to GMP compatible processes may mean sacrificing some level of efficiency from a sensitive research grade process and a requirement for re-optimisation. Variation will typically be reduced through the use of more standardised and controlled reagents, resulting in increased reproducibility and granting the standardisation and control required for clinical trial approval (Kirkeby *et al.*, 2017).

Difficulty in meeting GMP standards and management of variability are key limiting factors for ATMP development, with approximately 90% of current regenerative medicine clinical trials yet to progress to phase III (Alliance for Regenerative Medicine, 2019). Control of process variability is a prerequisite for progression through clinical trials, as efforts to quantify biological effects require a stable product produced by a validated process. GMP manufacture has presented challenges even to large established organisations, with Pfizer Kansas having receiving 8 repeat observations for inadequate procedures and repeated violation of GMP and sterility standards (FDA, 2018b). Full GMP compliance is not a requirement for phase 1 trials under FDA legislation (the requirement for a fully validated manufacturing process is waived and packaging and storage conditions are relaxed), however partial adherence and appropriate quality control procedures for product safety are required (FDA, 2008). EU regulations do not define specific exemptions, but do permit flexibility in GMP requirements dependent upon the stage of development of the product (EudraLex, 2014). Although there is a requirement for market released products to be comparable to clinical trial products upon which their safety and efficacy claims are based, GMP requirements rise at each stage of approval according to the perceived product risk. It is intended that full GMP compliance is built up to with the understanding gained

throughout early development, typically informed by early contact with regulators. GMP has evolved from guidance for the manufacture of biopharmaceuticals and therefore translates most clearly for large scale manufacture of autologous therapies. GMP and can therefore be at odds with practices for autologous therapies, where release of "out of specification" product may be beneficial to a patient (Bersenev and Kili, 2018).

One of the most significant challenges in GMP manufacture is creating and maintaining a culture of protocol compliance within the manufacturing environment, minimising deviations (operators not complying with instructions) and preserving best practice. Deviations such as failure to comply with hygiene and sterility instructions have been highlighted as a leading risk in quality manufacturing (Lopez *et al.*, 2010). The issue of operators implementing off-protocol process changes and performing tasks based on personal judgement rather than as prescribed has been highlighted in conference discussion panels and in informal settings, but rarely examined in literature. Protocols must also be designed to be understandable by non-experts. As an industry based on scientific and technological innovation, most ATMP manufacturing is performed by highly qualified operators with a high degree of contact with process development scientists and engineers. As ATMP manufacturing transitions to a more mature manufacturing model, processes must be performed by less costly operators with less training and who may not fully appreciate the consequences of protocol non-adherence. While this challenge is faced in many industries, ATMPs are highly complex products with a high degree of sensitivity to variation in the manufacturing process and environment.

2.3.1.2 Quality Control and Assurance

Quality control (QC) is the process of determining whether a product fulfils quality requirements (ISO, 2015). QC techniques may be broadly split into offline measurements, performed on product removed from the manufacturing process and typically destructive, and online measurements, performed on product within the manufacturing process and typically passive (Zeng and Bi, 2006). CTP measurement techniques are highly product and quality attribute specific and are discussed further in Section 3.5. As autologous products produce very low dose numbers for a single patient, every dose may undergo QC to ensure safety and suitability for purpose. In traditional manufacturing and production of allogeneic therapies, QC is performed on only a small quantity of an overall batch and must therefore be paired with quality assurance (QA) to provide confidence that untested product meets quality requirements (ISO, 2015).

Effective QA ensures that untested product meets quality requirements and requires understanding and control of sources of variability within a process to produce a reliable process output. Robustness is the "ability of a process to tolerate variability of materials and changes of the process and equipment without negative impact on quality" (ICH, 2009). Process robustness is key for production of a repeatable CTP and is achieved through the design of processes which avoid situations of positive feedback for variability. Adequate process knowledge provides a means to identify and manage sources of variability within a process, and therefore predict variability and its impact on CQAs. There are two sources of variability for CTPs, process input material and manufacturing process conditions (Williams *et al.*, 2012). As this work focusses on allogeneic CTPs, the cell input material is common and offers a far greater degree of standardisation than cell input material for autologous therapies, which by definition are unique for each patient and feature a high degree of variability. For allogeneic therapies, variation is contributed and controlled largely by the process, however cryopreservation is a key contributor to process variation, leaving open the possibility of variability within banks for allogeneic therapies (Mitchell *et al.*, 2014).

2.3.2 Commercialisation

Commercialisation refers the process of bringing a product to market, with a marketable product being fit for purpose, of adequate quality to achieve regulatory approval, and of sufficiently low cost to provide profitability. The primary obstacle for commercialisation of cell therapies is the cost of their development and manufacture, and therefore the challenge of reimbursing such high cost therapies (Bubela *et al.*, 2015). There is currently a gap in funding between basic science research, which is typically funding by the public sector in academia, and commercialisation, initially funded by venture capital investors and later by product sales. This is due to the prohibitively high cost of clinical trials for academic funding as well as the significant risk of trial failure dissuading private sector investment. It is essential to reduce the manufacturing costs and provide realistic reimbursement strategies for continued cell therapy funding.

As previously stated, approximately 90% of current regenerative medicine clinical trials are at phase I or II (Alliance for Regenerative Medicine, 2019) meaning that a high number of potential regenerative medicine products are transitioning from a state of basic research into a period of product development and scale up. This period in the lifecycle of a CTP is the period over the product is at most risk of failure due to lack of funding, as illustrated in Figure 2.

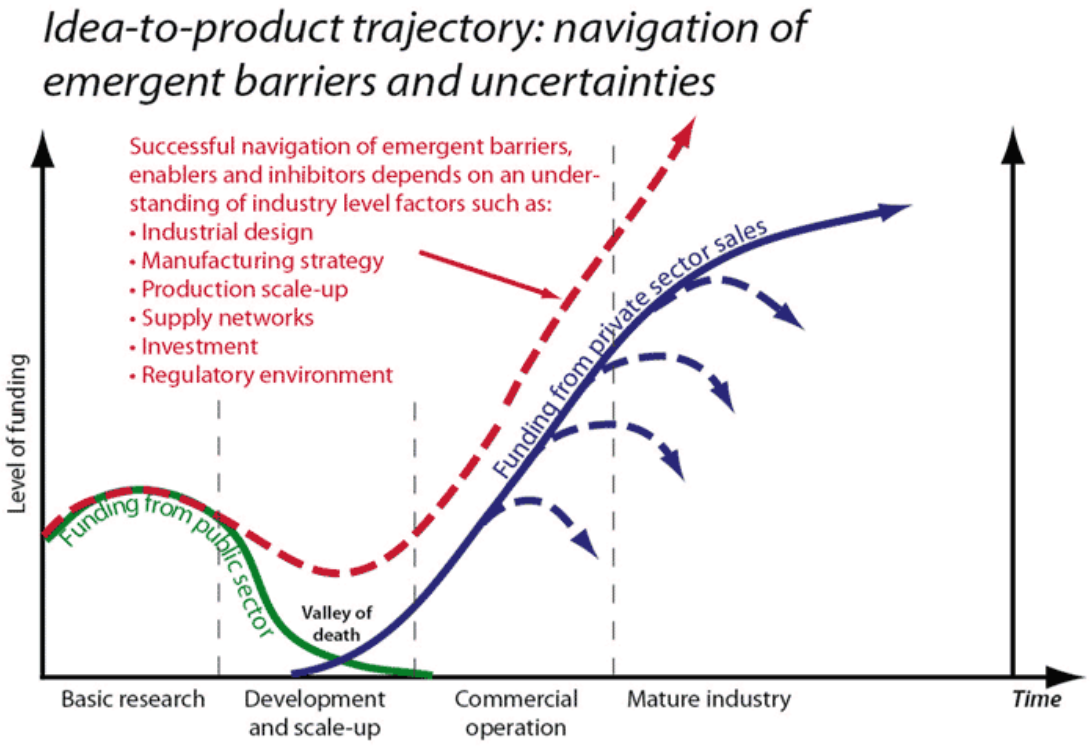

Figure 2 – The "valley of death" between public and private sector funding during manufacturing development stages of project development (Cambridge University Institute for Manufacturing, 2016)

Geron Corporation's GRNOPC1 product was the first ESC derived therapy to receive FDA approval for phase I trials (Lineage Cell Therapeutics, 2010), and is an excellent example of a promising therapy which failed to cross from development to commercial availability. GRNOPC1 was an ESC derived oligodendrocyte therapy, providing remyelination and nerve growth to address spinal cord injury (Lineage Cell Therapeutics, 2010).

The approval for phase I human trials by the FDA in 2009 created much optimism in the field of regenerative medicine, with hopes that other ESC derived therapies would begin to receive approval in the near future (Alper, 2009). Alongside this early optimism, there were also concerns over product safety around possible teratoma formation, product efficacy due the complexity of addressing spinal cord injuries, and difficulty separating a given therapy from controls, with fears that failure of GRNOPC1 may negatively impact the regulation of future stem cell therapies (Alper, 2009).

Safety concerns for GRNOPC1 caused the FDA to halt phase I trials prior to first patient receiving treatment for nearly two years due to the presence of cysts in regenerated tissue sites in animal trials (DeFrancesco, 2009). As the first trial for ESC derived products, difficulties in safe trial design were highlighted as key issues, with stem cells being effectively an irreversible intervention unlike any drug, and the lack of convention treatments for spinal cord injuries providing no benchmark against which to

benchmark the efficacy of the therapy (Strauss, 2010). Other issues including patient selection, animal model relevance and trial aims were critiqued and rebutted in literature, adding to regulatory uncertainty (Bretzner *et al.*, 2011; Wirth, Lebkowski and Lebacqz, 2011). A lack of regulatory precedence also hindered progress, with challenges in characterisation of cell quality and a lack of a proven regulatory pathways hindering progress (Strauss, 2010). Human trials did eventually commence in October 2010, with 4 patients receiving the therapy (Scott and Magnus, 2014)

In November 2011 Geron halted the phase I trial for GRNOPC1 due to financial difficulties, choosing to focus on its lower risk cancer therapies. Despite overcoming significant scientific, manufacturing and political challenges, expected costs of $25 million per year with the potential for another 10 years with no guarantee of eventual approval ultimately proved too costly to support, forcing Geron to exit the ESC field. Despite the failure of this highly visible therapy and lack of efficacy data despite huge investment, the lack of a negative safety outcome was highlighted as a hopeful sign for future ESC derived therapies (Frantz, 2012).

In the time since the failure of GRNOPC1, regulatory pathways have been established and are developing as other biologics such as CAR-T therapies pave the way. Despite recent progress, ESC therapies face similar problems today, with huge development costs and mixed efficacy evidence not providing a clear improvement over established pharmaceutical therapies. Translational development is particularly expensive and not easily publishable, while the high risks associated with early stage trials dissuade venture capitalists (Frantz, 2012).

A direct result of development and manufacturing costs is affordability, with CAR-T therapies such as Kymriah (Novartis, Switzerland) and Yescarta (Kite Pharma, US) priced at $475,000 and $373,000 respectively and the Luxturna (Spark Therapeutics, US) gene therapy priced at $425,000 per eye. A significant reason for these high prices is the high cost of goods (COGS) due to the costs associated with GMP compliant clean rooms, highly trained operators and expensive input material (Stanton, 2019).

2.3.2.1 Closed Processing

Closed processing offers the possibility of reducing COG through reduced cleanroom requirements, while increasing process reliability through the removal of opportunities for contamination (Woods and Thirumala, 2011; Moutsatsou *et al.*, 2019). This thesis will distinguish between closed processes (those for which a continuous physical barrier is maintained between the product and environment),

functionally closed processes (those for which a physical barrier is at times compromised to allow open manipulations), and open processes (those for which airflow barriers are used to maintain sterility).

The potential cost benefits for closed systems are substantial as they may be performed in substantially lower grade clean room environments, however the use of such processes is currently limited by a lack of equipment standardisation and options for fluid manipulation. Closed systems offer complete isolation from the outside environment and theoretically do not require a clean room to operate; however, functionally closed preparation and transport manipulations necessitate the use of cleanrooms, negating much of the cost benefit.

The primary way in which closed processing is achieved at the small and medium scale is through the use of single use plasticware. Single use systems have the potential to reduce COGs through the avoidance of costs associated with validation of cleaning processes, as well as reduced instances of contamination due to closed processing. Closed single use systems are not compatible with traditional operator manipulations and are therefore commonly combined with automation.

2.3.2.2 Automation

Automation has been widely used across manufacturing industries to reduce operator costs and operator induced variability in complex processes. Cell therapies are typically produced by highly skilled operators performing labour intensive manual work in a cleanroom environment, resulting in high labour costs and multiple opportunities for operator variation. Automated systems are capable of operating with no downtime for extended periods, enabling continuous process monitoring and increasing overall throughput and facility utilisation. The removal of manual processing steps reduces operator variability, while automated monitoring and control reduce variability. By removing opportunities for operator variability, variations and costs associated with a process reduce and the risk of process failure is substantially reduced. Automation also eases scale out, simplifying process moves to new sites and reducing the dependence on operator training (Harris, Meacle and Powers, 2016).

Automated systems generally sacrifice a degree of flexibility and require a large initial investment, making them less suited for process changes than manual processing. There is therefore a higher requirement of product and process understanding for automated systems, however, such knowledge also offers opportunities to streamline and remove overcomplicated and inadequately beneficial process steps (Harris, Meacle and Powers, 2016). Automated manipulations are unlikely to offer the same degree of fine control as manual work, meaning that actions such as automated volume reduction

are typically inferior to their manual alternative, aspiration following centrifugation for example. A second issue is dose control of reagents during manufacturing, as current automated systems are unable to match the precision of manual pipette work.

A key limitation of current automation is a lack of standardisation and therefore ability to integrate both hardware and software from different manufacturers (Ball *et al.*, 2018). At present much software is bespoke and hardware is proprietary. De facto standards and flexible software tools may emerge as technologies become more widely adopted, however this will be in tension with manufacturer pressure to preserve revenue through proprietary consumables and promote their own equipment through software limitations.

The challenges faced by automation of ATMP manufacturing mirror those seen in diagnostic immunology, clinical chemistry and haematology, which first emulated human manipulations before moving onto more efficient methods (Tomar, 1999). Key problems identified during this transition were the lack of accepted standards between manufacturers and long payback period for equipment, as well as changes in staff requirements from chemists and biologists to engineers and computer scientists (Tomar, 1999).

Although there has been movement towards automation by the ATMP industry and regulators for some time (FDA, 2004), current equipment has a high dependency on operator interaction and is far removed from automation as implemented in mature manufacturing industries. Much current automation serves simply as an enabling technology for closed systems, providing the mechanisms necessary to manipulate closed systems while making minimal reductions in operator dependency. Current automation efforts also typically involve the replacement of manual processing steps with automation equipment. While this model offers a simple method of transitioning into automated processing, it is unlikely to reap benefits to the same degree as processes that are designed with automation in mind (Ball *et al.*, 2018; Moutsatsou *et al.*, 2019). The current lack of scalable solutions means that automated process development may be too costly to pursue at early stages of development.

Continuous processing, where material may flow continuously into and out of process which may run indefinitely (Doran, 2013), may be required to realise the full benefits of automation due to the otherwise incomplete utilisation of equipment and facilities. A lack of industry familiarity and regulatory clarity regarding continuous techniques means that a significant investment into unestablished and unfamiliar technology would be required for the transition to continuous processing (Munk, 2017). These reasons coupled with the high level of monitoring and control required for continuous processing mean that batch-based manufacturing is likely to remain the dominant technology for cell therapy manufacture at least until automation technology has matured.

2.3.2.3 Scalability

Scalability refers to the capability of a process to be performed with varying levels of output. Manufacturing for PSC derived therapies in development and early stages of clinical evaluation is typically performed using manual processes at small scales (Pigeau, Csaszar and Dulgar-Tulloch, 2018), however, manufacturing output must be increased to meet the increased demands of later clinical trials and eventual commercial release. Increasing production output may be achieved in two ways, either by scale-up, increasing batch sizes and process throughput to increase output per batch, or by scale-out, where unit operations or an entire manufacturing process is replicated to increase the number of batches (Hourd *et al.*, 2008).

Scale-up implies large scale centralised manufacturing of a product, and offers advantages of reduced batch to batch variation and simplified regulatory oversight, as well as the use of familiar business models which align closely with those used with biopharmaceutical manufacture (Williams *et al.*, 2012).

Scale-out frees production from a single facility, offering simplified logistics and increased robustness of supply due to redundancy in the manufacturing network (Harrison *et al.*, 2017). The drawbacks of non-centralised manufacture include increased challenges in quality and regulatory oversight and additional complexity in demonstrating comparability and transferring process changes between manufacturing sites (Harrison *et al.*, 2017; Shariatzadeh *et al.*, 2020).

Personalised therapies such as autologous cell therapies are not compatible with large batch production, as each batch must be produced for an individual patient. Scale out is therefore required for autologous therapies, whereas allogeneic therapied may be manufactured using either model. It may be beneficial for allogeneic therapies to employ equipment and strategies developed as a result of investment in the scale out of autologous therapies.

Mesenchymal based therapies have seen cost reductions of two orders of magnitude as cell yields per lot have increased by three to four orders or magnitude in transitioning from single-layer planar culture through multi-layer vessels and onto microcarrier based production (Simaria *et al.*, 2014). For autologous and small-scale allogeneic therapies, scale up is of limited utility, and so COG improvements must be made through increased process efficiency.

The mesDA manufacturing process which is the focus of this thesis was developed for single layer cellSTACKs with an area of 636 cm^2 and produce a yield of 1.95 x 10^6 cells per cm^2 (Nolbrant et al., 2017). This equates to a per batch yield of 1.24 x 10^9 cells, equal to 620 doses given a dose size of 2 x

10^6 cells per patient (Kirkeby *et al.*, 2017). Given an incidence of 17 per 100,000 (Hirsch *et al.*, 2016) and an approximate UK population of 66,500,000 (ONS, 2019), 19 batches per year would be sufficient to meet ongoing UK demand. This process may be scaled up using multiple layer cell stacks or scaled out using multiple Prodigy systems, or by maintaining multiple cellSTACKs on a single Prodigy device.

2.3.2.4 Technology Transfers

As cell therapies progress towards commercialisation, it is likely that their production will be migrated from a small academic or product development setting into a larger commercial manufacture setting. This migration commonly includes movement of the process between laboratories, sites, and nations; and possibly to a contract manufacturer (Eaker *et al.*, 2013), therefore, a cell therapy must be transferrable in order to progress to a state of commercial operation.

Technology transfers are defined by the World Health Organisation (WHO) as "a logical procedure that controls the transfer of any process together with its documentation and professional expertise between development and manufacture or between manufacture sites." (World Health Organization, 2011). A key element of this definition is that technology transfers are a logical procedure and are ordered to enable validation at each project stage, as summarised in Figure 3. For example, it is important that no process changes or improvements resulting from engineering runs are implemented before completing process qualification runs. Faithful transfer of an existing process depend upon approval and subsequent execution of a protocol frozen from further changes (Eaker *et al.*, 2013).

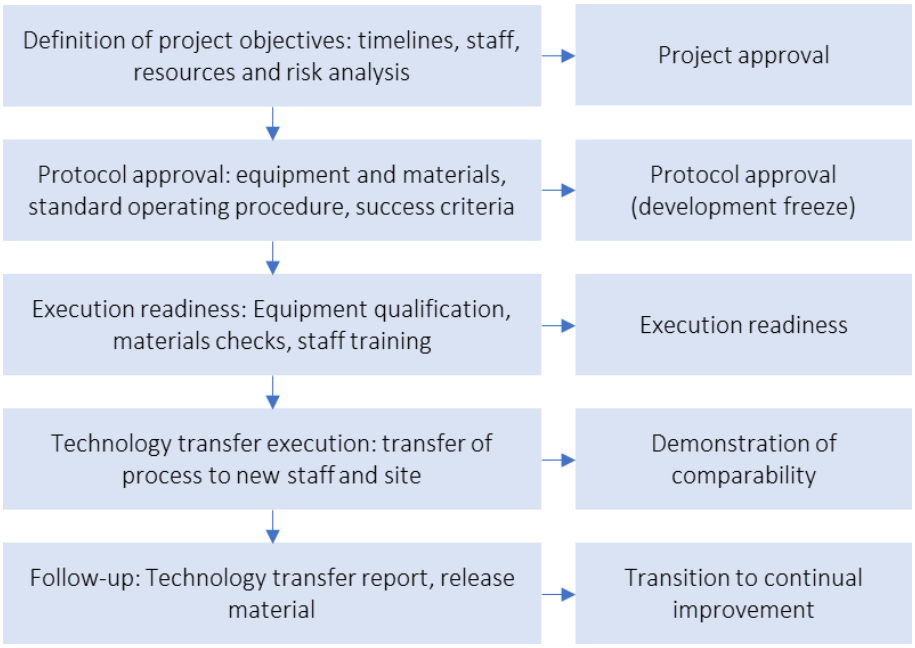

Figure 3 - Flow diagram of an ideal process transfer timeline

The second element of the technology transfer definition is the transfer of documentation, facilitating the transfer of knowledge and providing accountability and traceability for the process. The ICH Q10 guideline builds upon WHO definition, adding that "[transferred] knowledge forms the basis for the manufacturing process, control strategy, process validation approach and ongoing continual improvement" (ICH, 2008). Due to the breadth of knowledge required for successful and robust processing, a significant amount of documentation is required for a technology transfer operation. A list of documents stated as requirements by the Cell and Gene Therapy Catapult (London, UK) is provided in Table 1.

Table 1 – Documents required for transfer of an AMTP manufacturing process (Kerby *et al.*, 2017).

Area	Documents Required
Equipment	Specification and standard operating procedures (SOPs).
Materials	Source, purchasing information, storage, stability and specification.
Process	Development reports including design space knowledge, flow diagrams, detailed process description, SOPs, batch manufacturing records.
Analysis	Development tests (in-process and release), development reports, flow diagrams, process description, SOPs, specification.
Process Risk Assessment	Failure mode and effects analysis (FMEA).
Training records	Manufacturing team training at development laboratories, including test results to assess qualitative judgements.
Health and Safety	Material safety data sheets, risk assessments.
Supply Chain	Starting material, samples, temperature, packaging, monitoring and 3rd party service providers.
Storage and Stability	Labelling, samples and drug product.

The final key element of the technology transfer definition is the transfer of expertise from the development to the manufacturing site. Staff education is essential for the transfer of a process as performed by the originating site, and equips staff to troubleshoot problem aspects of the process and develop further process controls for GMP compliance (Eaker *et al.*, 2013). It is important that technology transfer is a collaborative effort, as a lack of available information will translate to repeated and misdirected effort.

Technology transfers have been highlighted as an area of difficulty at conferences and in trade publications but are rarely discussed in academic literature. The International Society for Pharmaceutical Engineering (ISPE) good practice guide for technology transfers identifies robust planning and exchange of information as the key elements of robust technology transfer efforts (ISPE, 2003). Limited experience of technology transfers and lack of product or process definition have also been identified as key risk factors (Perry, 2010). The difficulty of validation has also driven convergence towards the use of proven technologies such as stirred tank bioreactors. Small scale verification is noted as a key tool for identification of protocol problems before committing to full scale runs, saving time and cost (Perry, 2010). A technology transfer represents a simplified and focussed validation effort more suitable for products in early stages of development, avoiding the considerable time and expenditure required for full formal validation. Formal validation efforts are typically represented in a V-model as shown in Figure 4.

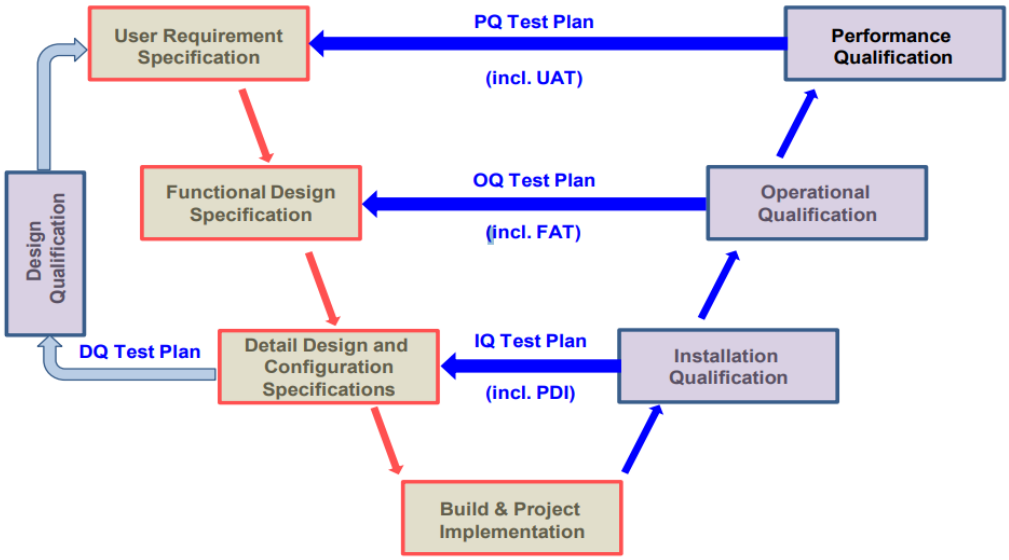

Figure 4 – Formal validation efforts typically follow a V-model, in which the left arm represents design and specification, the centre represents implementation, and the right arm represents validation against the specifications developed in the left arm (WHO, 2016).

2.3.2.5 Cost Modelling

Cost models offer a method to assess the costs associated with a product, and typically include functionality to alter input values and assess varying cost options. The cost of producing a CTP is essential knowledge for assessing commercial viability, however there is often a high degree of uncertainty at early stages of product and manufacturing process development (Girling *et al.*, 2010). Cost modelling provides utility at all stages of product and process development, supporting direction decisions in early development, identifying key areas for product cost effectiveness in the middle stages, and contributing towards reimbursement decisions in later stages (Vallejo-Torres *et al.*, 2008).

Cost models for cell therapy manufacturing may be split into holistic cost of goods (COGs) style models which aim to include a wide array of cost elements to inform process-wide manufacturing and reimbursement decisions (Lipsitz *et al.*, 2017; Lopes, Sinclair and Frohlich, 2018a, 2018b; Pereira Chilima, Moncaubeig and Farid, 2018; Rotondi, Costariol and Rafiq, 2019), and technically focussed models which aim to provide a decision support tool when contrasting a small number of competing technologies or techniques for a particular processing stage (Want *et al.*, 2012; Simaria *et al.*, 2014; Hassan *et al.*, 2015; Specht and Ph, 2020).

Holistic models incorporate a greater breadth of data as required to inform process-wide decisions, and may be capable of capturing sensitivity to aspects not considered impactful (Lipsitz *et al.*, 2017). A lack

of informative data and resulting inclusion of data with higher degrees of uncertainty is however highlighted as a key factor in model inaccuracy (Abou-El-Enein *et al.*, 2013), suggesting that technically focused models more accurately reflect real world costs at the price of their limited scope.

2.4 Process Architecture

Allogeneic cell therapy manufacturing processes may be abstracted into distinct stages as summarised in Figure 5. These include sourcing of input material, establishing a master and working cell bank, expansion to reach appropriate batch size, differentiation of stem cells into the desired product lineage, followed by formulation and cryopreservation of the product. The process steps which contribute most to cost cell therapy manufacturing costs are expansion, downstream processing and cryopreservation (McCall, 2009).

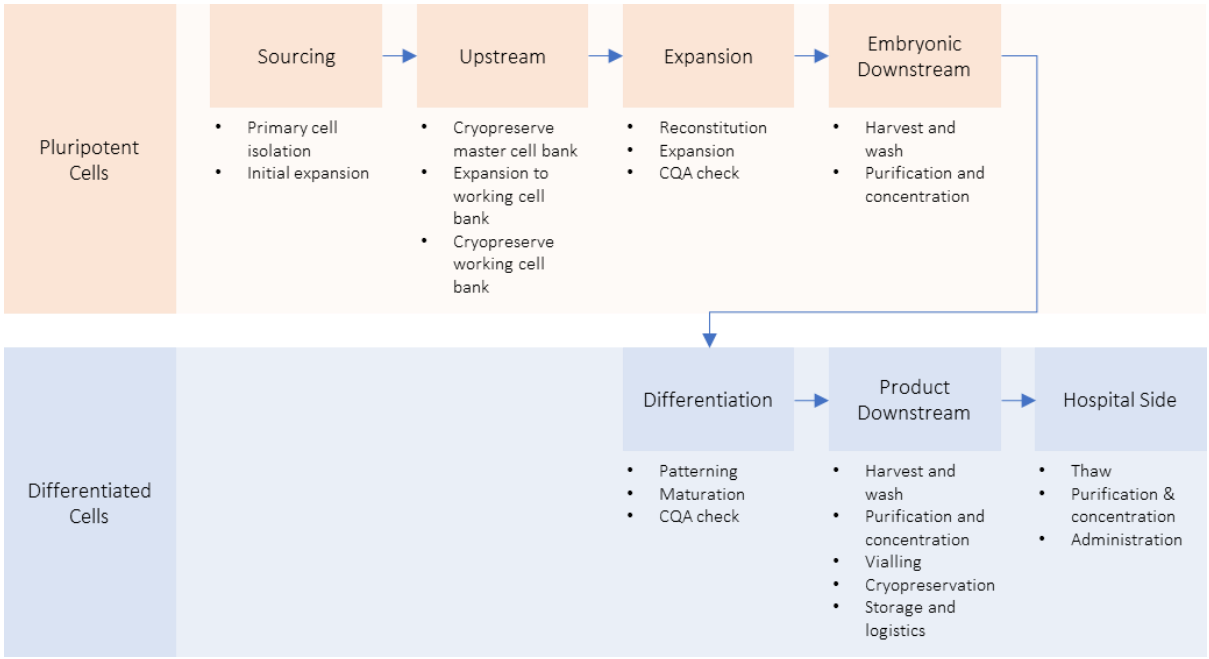

Figure 5 - Manufacturing process map for ESC derived dopaminergic neurons

The term “upstream” is commonly used to refer to any cell processing before product harvest, while “downstream” is used to refer to processing after product harvest. These terms are also used to refer to specific processing steps. For example, centrifugation for volume reduction is typically referred to as a downstream processing step despite its use in upstream processing during cell bank preparation. This

review will distinguish between “embryonic” processing steps for the intermediate product, ESCs, and “product” processing steps for the differentiated dopaminergic neuron product where appropriate. As the preparation of ESCs for differentiation includes mainly downstream processing steps, it will be referred to as “embryonic downstream”.

The key processing technologies which enable CTP manufacture are summarised in Table 2. The areas of expansion and differentiation, purification, and cryopreservation broadly cover all activities required for allogeneic CTP manufacture. Upstream and hospital side processing involves these three categories at a reduced scale, while sourcing is performed only once per allogeneic therapy.

Table 2 – Summary of the processing steps most amenable to improvement via new technology, and the processing technologies currently in frequent use.

Expansion and Differentiation	Purification	Cryopreservation
• Single-layer culture vessels • Multi-layer culture vessels • Packed bed bioreactors • Suspension bioreactors	• Open centrifuge tubes • Closed centrifugation tubes • Closed centrifugation bags • Counterflow centrifugation • Dead end filtration • Tangential flow filtration	• Screw-top vials • Needle-fill vials • Tube weldable vials • Tube weldable bags

2.4.1 Upstream

Upstream processing refers to the process of expanding an initial small cell population into a larger number of cryopreserved cells which will act as the starting material for later process steps. For an allogeneic stem cell therapy, this typically means expanding a small number of cells from a master cell bank into a large number of cells to form a working cell bank, with stringent quality checks throughout the process.

Cryopreservation enables the long-term banking of cells and allows for the creation of standardised and controlled stem cell lines. The quality of banked cells is paramount for both research and clinical grade cell banking. Cell banks are typically organised into a master cell bank (MCB), which is formed from a single pool of cells derived from the source material under defined conditions, and working cell banks (WCB), derived from culture of master cell bank cells and intended for use as the source material for manufacturing runs (ICH, 2001). Standardised and controlled biological input material from cell lines avoids numerous problems of long-term cell culture and gives availability of consistent quality-controlled cells as input material for manufacturing processes.

Quality is essential in cell banking, with potential risks including contamination with adventitious agents or other cells lines, as well as genetic alterations and viability loss. Early banking strategies have highlighted numerous problems with quality control. A 1999 study showed cross contamination affected 18% of human tumour cell lines at source (MacLeod *et al.*, 1999), while 14% of early submissions to the European Bank for induced pluripotent Stem Cells (EBiSC) were later highlighted to be from the incorrect donor (Stacey, 2017). In response to these issues, cell banking centres such as the UK Stem Cell Bank (UKSCB) have been established in many nations to provide quality stem cell lines

for research and clinical applications. A key benefit to the centres is assurance of good practice. The International Stem Cell Banking Initiative (ISCBI) is a network of stem cell banking centres who have developed guidelines on best practice for procurement, testing and distribution of research grade hESC lines (The International Stem Cell Banking Initiative, 2009).

Quality assurance (QA) and quality control (QC) during banking are essential to meet the requirements of research and clinical grade cell lines. QA is process oriented and covers the management, operational, ethical and legal systems of a cell bank. QC is product oriented and ensures that banked cells are as expected. A comprehensive quality management system is required to ensure high quality cell banks, an overview of which is shown in Figure 6. This system must cover all aspects of QA and QC, including cell selection process, ethical process, staff training, equipment monitoring and maintenance, input material, record keeping, release criteria, adherence to relevant regulations and current good practice (Kallur *et al.*, 2017). Good laboratory practice (GLP) is applied to research grade cell lines, while GMP is required for clinical grade cells (EudraLex, 2017). Both regulatory frameworks include general standards for QA and QC which are applicable to cryopreservation and banking of hESCs (Kallur *et al.*, 2017).

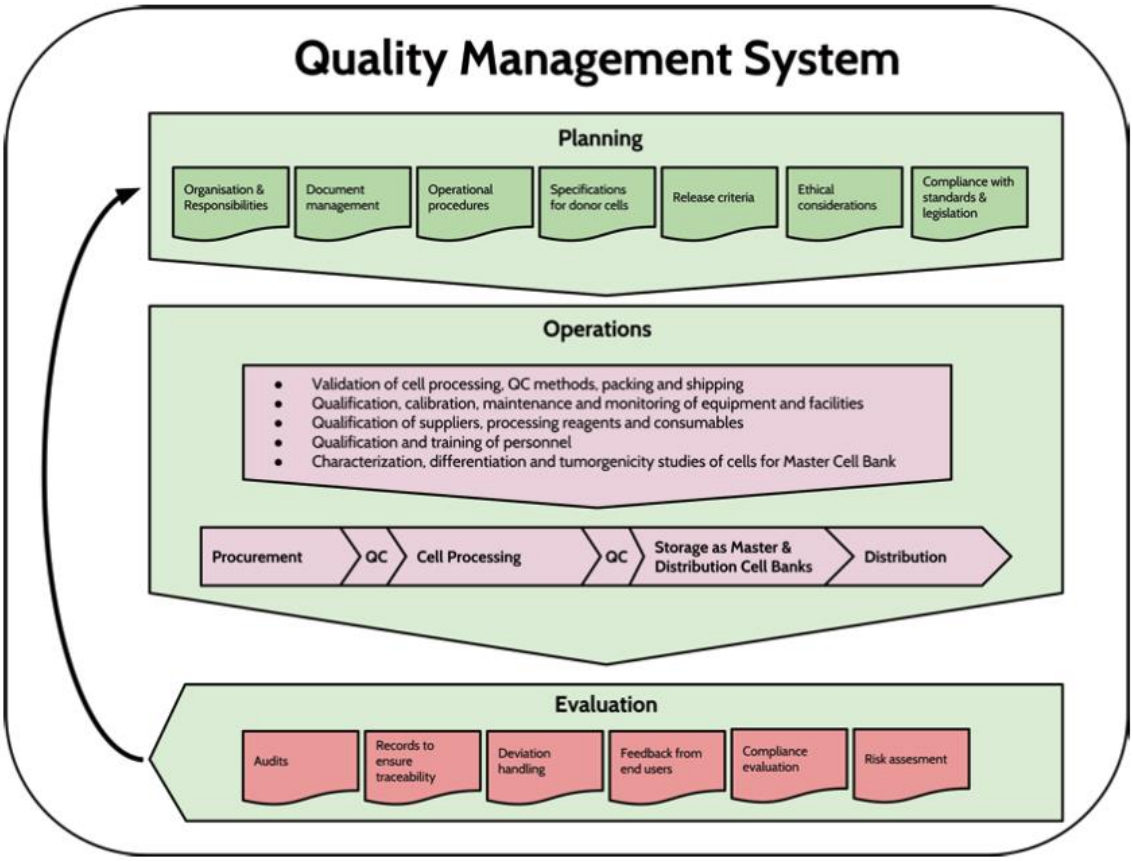

Figure 6 - Example of a comprehensive cell banking quality management system (Kallur *et al.*, 2017)

2.4.2 Expansion

Expansion refers to the process of exponentially increasing cell number in order to reach a desired quantity of cells. Cell expansion is performed in upstream processing to produce adequate cells to form a master and working cell bank, but mainly refers to the primary expansion from working cell bank vial to a cell number appropriate for a product batch.

At research scales, adherent cells are typically grown in multi-well plates or planar flasks. Scaling of this approach may be achieved through the use of multi-layer vessels such as the Corning CellSTACK® and Nunc™ Cell Factory™ systems. The limiting factor for scale out of these systems is the requirement for manual labour or throughput of automated systems, with lot sizes of between 50 and 70 having been demonstrated with 10-layer vessels (Rowley *et al.*, 2012). Multilayer systems are available with up to 40 layers, translating to approximately 25000 cm^2 culture area and 4×10^9 hESCs per vessel. Heterogeneity of the culture environment may be a concern at these scales (Rafiq, Coopman and Hewitt, 2013), while sterile manipulations also grow challenging with increased vessel size, as shown in Figure 7.

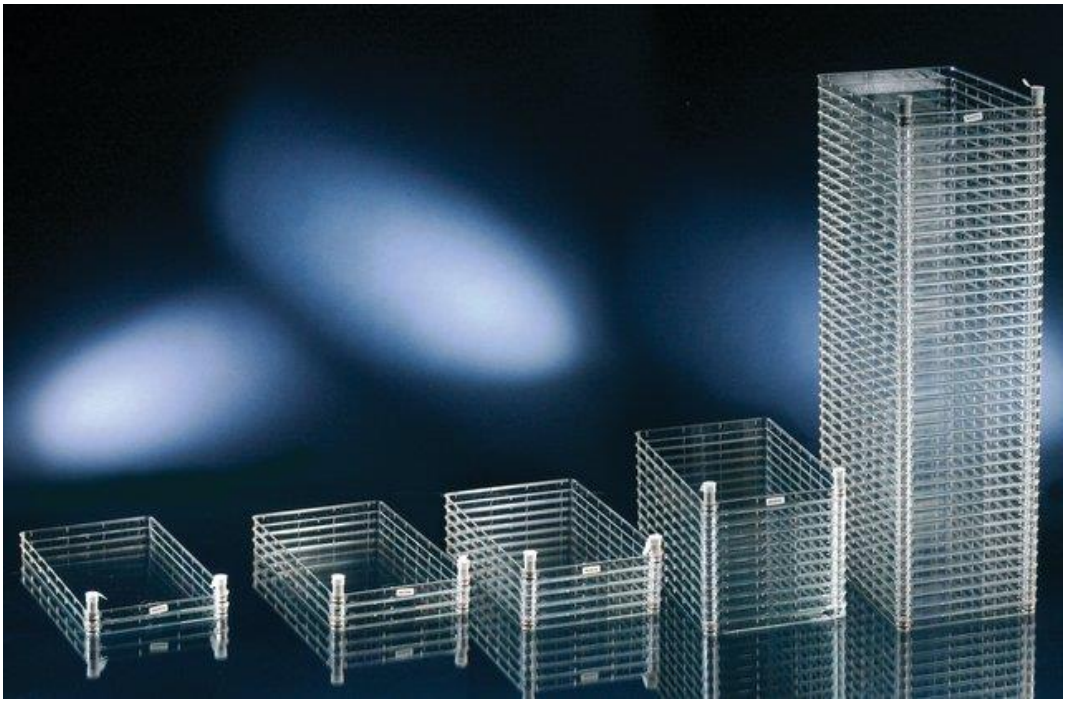

Figure 7 – Nunc Cell Factory systems (ThermoFisher, US), available in 1, 2, 4, 10, and 40-layer configurations, with each layer providing 632 cm^2 growth area. The Corning CellSTACK system is comparable, featuring 1, 2, 5, 10, and 40-layer configurations with each layer providing 632 cm^2 growth area.

The development of gas permeable growth layers in the Corning HYPERStack system has enabled more compact multi-layer systems, with 36-layer systems providing 18,000 cm² of growth area per vessel, translating to yields comparable to a 40-layer CellSTACK in the same volume as a 10-layer CellSTACK. Lot sizes of up to 50 are feasible, equating to 900000 cm^2 culture area and 1.8×10^{11} hESCs per lot, as shown in Figure 8. The suitability of HYPERStacks for rapid scale up of viral vector and gene therapy production resulted in supply shortages and six-month waiting times in mid-2018, highlighting the dependence of the ATMP industry on technology and the lack of diversity in supply (Stanton, 2018c).

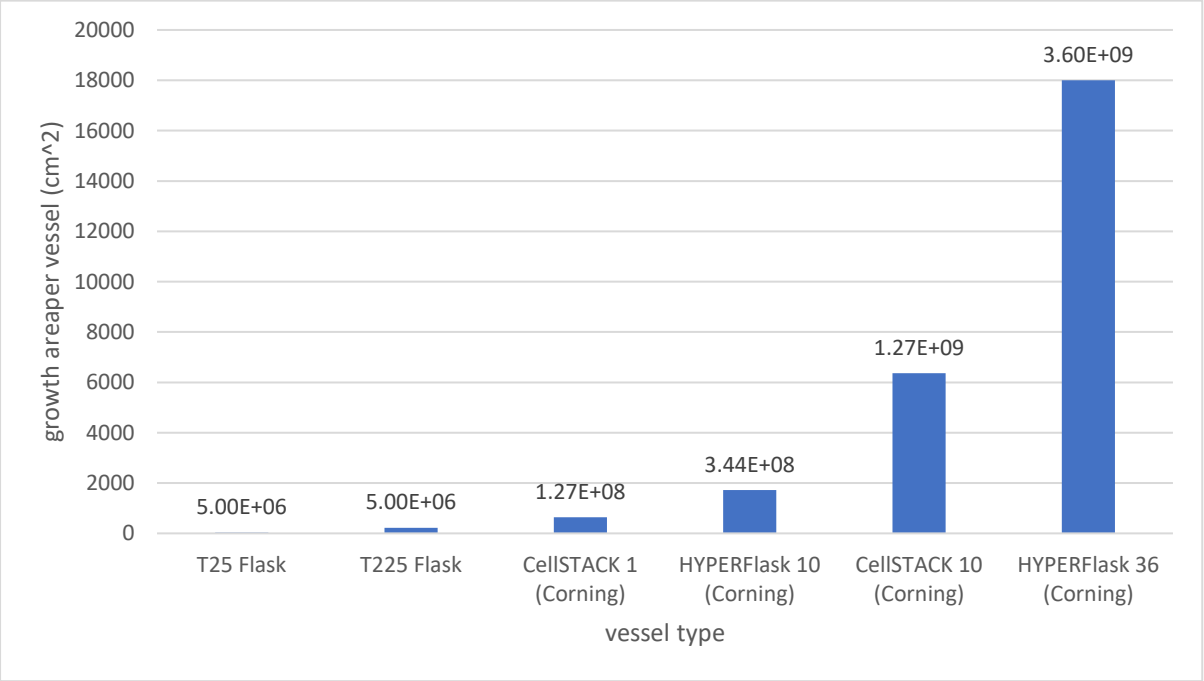

Figure 8 - Growth area and theoretical cell yield for planar culture vessels usable in manual culture without specialist manipulation equipment. 40-layer CellSTACKs have not been included, as their extreme size. Bar labels represent cell yield per vessel assuming a harvest density of 2 x 10^5 cells per cm^2.

For large scale cell production beyond planar culture, as summarised in Figure 9, a degree of automation is required to perform manipulations and maintain ongoing cell culture. Automation of cell expansion takes several forms, with the most analogous to manual processing being the use of a robotic arm to perform manipulations. This strategy is utilised in systems such as the SelecT or CompacT SelecT (TAP Biosystems, UK) and AUTOSTEM Platform (AUTOSTEM Consortium, EU). Other systems based upon gantry style manipulators have more limited manipulation abilities and are limited to proprietary culture vessels, such as the Biomek Cell Workstation (Beckman Coulter), which uses CELLSTAR AutoFlasks (Greiner) and the Cellerity automated cell culturing system (Tecan) which uses RoboFlasks (Corning). Another approach avoids the need for vessel manipulation through bioreactor style

maintenance of a planar surface with flowing medium. Systems employing this approach include the CellCube system (Corning) and Xpansion Multiplate Bioreactor System (Pall).

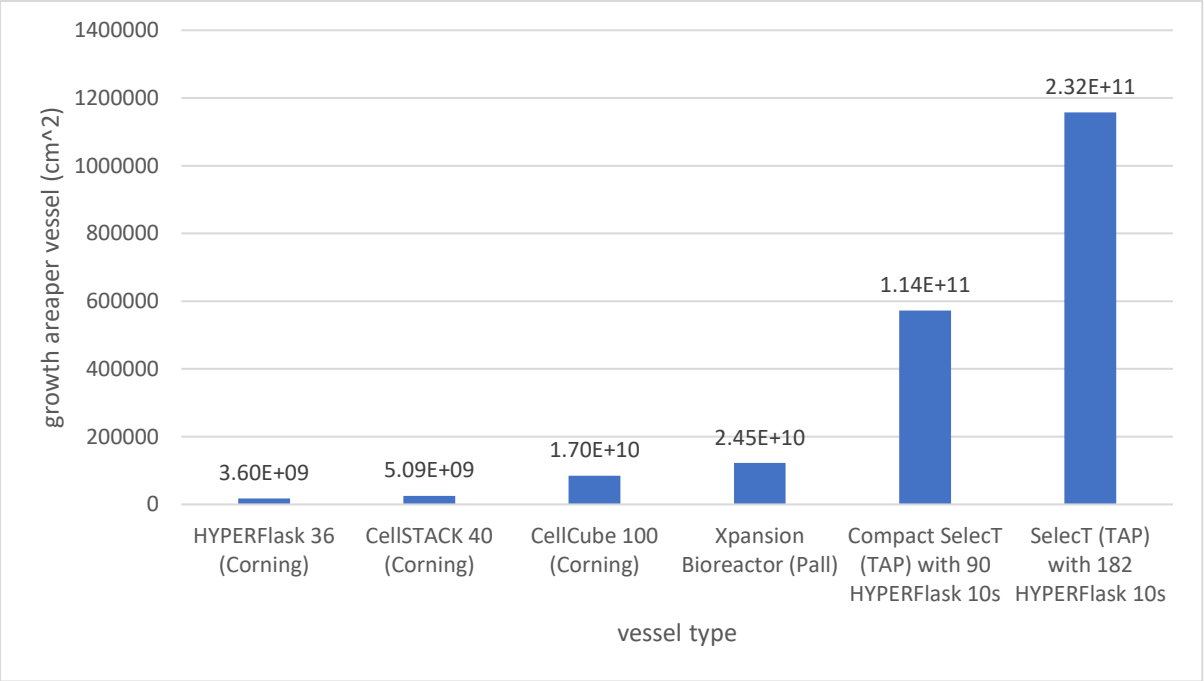

Figure 9 - Growth area and theoretical cell yield for automation compatible planar culture systems. Bar labels represent cell yield per vessel presuming a harvest density of 2 x 10^5 cells per cm2.

Packed bed and suspension bioreactors provide scale up potential beyond that achievable in planar culture and are only cost effective at higher scales than is required for the small dose size of a mesDA therapy (Simaria *et al.*, 2014). Packed bed bioreactors are systems in which cells grow attached to a substrate such as beads or fibres which are placed within a medium reservoir. Examples include the Pall iCELLis Bioreactor and Terumo Quantum Cell Expansion System, and are scalable to around 40L and at 1×10^8 ESCs per mL, or 4×10^{12} ESCs per reactor (Rowley *et al.*, 2012). Beyond this, the most scalable solution to cell expansion is adapting adherent cells to culture in suspension bioreactors (Want *et al.*, 2012). This is achieved by either providing microcarriers for cell adherence, or culturing cells as aggregates. These systems are capable of densities of around 3×10^6 ESCs per mL, equating to yields of 3×10^{12} ESCs for a 1000 L bioreactor, with the possibility of further scale up (Rowley *et al.*, 2012).

Expansion of ESCs is performed with the intention of later differentiation into a product cell. It is therefore essential that both proliferative ability and differentiation potential are maintained during expansion. Proliferative ability is monitored through microscopy during culture and via cell counts between passages, while pluripotency is typically measured via flow cytometry. Key markers for

pluripotency include positive expression of Oct3/4 which regulates renewal and differentiation potential (Nichols *et al.*, 1998), Sox2 which regulates Oct3/4 expression (Masui *et al.*, 2007), and Nanog which restricts differentiation potential (Chambers *et al.*, 2003). Other markers typically used for identification or separation of pluripotent cells include low SSEA-1 expression, as well as positive expression of SSEA-3 positive, SSEA-4, TRA-1-60 and TRA-1-81 (Adewumi *et al.*, 2007).

Long term cell culture has been shown to cause differences in cell properties such as proliferative ability and differentiation potential, however there is disagreement in the literature and conflicting evidence about the degree of change and speed of onset. The mechanism for change is thought to be selectivity in culture for chromosomally abnormal cell sub-populations which come to overtake the original cell population (Draper *et al.*, 2004). Chromosomal changes emerge from complex interactions between and within source cells and culture conditions; therefore, the exact effects of long-term cell culture are impossible to predict while general patterns are guided by natural selection. A common pattern seen in long term cell culture is an increase in proliferative ability. Typical cell culture conditions aim to supply cells with adequate nutrients and space for unrestricted growth, inadvertently favouring cell populations with high growth rates and potentially allowing them to outcompete cells with other desirable characteristics (Amps *et al.*, 2011). This increase in proliferative ability has been demonstrated in ESCs and is often associated with a reduction in differentiation potential (Draper *et al.*, 2004; Park *et al.*, 2008), a key quality attribute for expansion in cell therapy manufacturing. A 2004 study showed only subtle differences in genes and marker expression in ESCs for up to 2 years of continuous culture, however it was noted that even stable cells may quickly generate genetic differences and that long term culture requires monitoring (Rosler *et al.*, 2004). A degree of variation in differentiation propensity has also been shown in ESC lines regardless of culture period (Osafune *et al.*, 2008). Conversely, passage number has been shown to increase differentiation ability in iPSCs, however this is thought to be due to the long passage time needed to complete the iPSC reprogramming process (Koehler *et al.*, 2011) and is unlikely to apply to ESCs. Proliferation ability has also been observed to decrease with passage number in MSCs (Choi *et al.*, 2015), however the extended culture time was relatively short at 15 passages and patterns observed in MSCs may not apply to ESCs.

2.4.3 Downstream

Downstream processes are those which prepare the product for shipment, and include volume reduction, washing, fill and finish and cryopreservation. Downstream processing is often less addressed in terms of technology development and cost reduction than expansion; however, it typically has a

major contribution to the overall product cost (McCall, 2009). All downstream processing steps include some amount of product loss, with the effects of stacking potentially producing significant losses for multi-step processes (Doran, 2013). Downstream processing using closed techniques has been found to contribute 55% of the overall cost of goods per product dose at a scale of 1 x 10^9 cells per lot, approximately the scale of the mesDA manufacturing process (Hassan *et al.*, 2015). This value was found to decrease with higher lot sizes down to 20% at scales of 1 x 10^{11}, and increase drastically for microcarrier based systems to between 80% and 50% at the same scales (Hassan *et al.*, 2015).

The use of closed systems in downstream processing may result in increased cell loss, as the increased surface area of tubes and bags as compared to open equipment offers additional opportunities for surface attachment at low shear stresses (Zoro *et al.*, 2009). The simplification and integration of steps offered by continuous and automated approaches are therefore particularly important for downstream processing with minimal product loss. Only label or tagging free approaches are discussed in this review as label based approaches pose problems for therapeutic use in cell products and are generally not suitable for large scale manufacturing (Masri *et al.*, 2017).

While upstream processing steps may be adapted from the manufacture of products such as antibodies and recombinant proteins, downstream processing for cell therapies is fundamentally different as the cell is the product to be recovered with minimal loss to volume and quality rather than a waste product (Pigeau, Csaszar and Dulgar-Tulloch, 2018). Recent reviews of downstream processing technologies for small scale cell therapies have shown limited options overall and few recent developments, with most systems designed for large scale bioprocessing, or designed specifically for blood processing (Pattasseril *et al.*, 2013; Buckler *et al.*, 2016; Masri *et al.*, 2017). The limited options available for downstream processing at the small scale is a significant hinderance in process development and manufacturing of small-scale therapies.

2.4.3.1 Cell Recovery

For adherent cell culture, cell recovery refers to the process of detaching cells from the culture vessel or microcarrier surface and is typically achieved through the use of dissociation enzymes such as Trypsin or a recombinant alternative. Animal derived trypsin carries the risk of transmitting adventitious agents including vertebrate and invertebrate viruses as well as prions from bovine trypsin (European Medicines Agency, 2014). There is currently no specific guidance for the use of plant or bacteria derived recombinant alternatives pending characterisation.

Trypsin products are commonly combined with the chelation agent ethylenediaminetetraacetic acid (EDTA), which aids detachment through chelation of calcium and magnesium molecules from the cell surface, improving efficiency. The cleaving action of trypsin is typically halted once cells are detached to prevent further protein degradation, and this is achieved either through quenching with protein rich culture medium, or through the use of protease inhibitors which occur naturally in plants such as soybeans, pineapples and papaya as a defence mechanism against trypsin created in the digestive systems of many animals.

Dissociation enzymes are typically aided in cell detachment by the addition of shear forces. For microcarrier based systems, shear forces may be induced through a period of high intensity liquid agitation (Nienow *et al.*, 2016). In manual planar culture, it is common practice for the culture vessel to be gently impacted on the BSC surface or the hand of an operator to create shear forces, however these techniques are poorly defined and standardised (Thomas *et al.*, 2009).

2.4.3.2 Purification

Following harvest, cells must be separated from the reagents used during cell detachment and resuspended to a known concentration in a defined liquid for cryopreservation or patient delivery. These steps must be performed with minimal changes to cell integrity and functionality. Efficient downstream processing is important as cells at this point have passed the costly process of expansion and differentiation. Losses during downstream processing translate to loss of saleable product, and a small percentage loss can be a large absolute loss.

2.4.3.2.1 Centrifugation

Centrifugation separates materials of differing densities by subjecting them to heightened g-force through rapid rotation, with processing speed dictated by relative centrifugal force, particle size, relative densities and liquid viscosity (Doran, 2013). Biological cells have a similar density to the suspending fluid, requiring high centrifugation speeds for effective separation.

Dead-end centrifugation is typically performed in a centrifuge with a swinging bucket rotor, with micro and research scale centrifuges typically supporting tubes from 0.5 to 50 ml. Commercial scale open centrifuge tubes are available up to the 2-litre scale, with rotors supporting 8 such tubes per rotor, or

16 litres per run. Swing bucket centrifugation of discrete vessels is the dominant purification technique at the research scale; however centrifugation at higher scales is restricted by safe operating speeds of large equipment (Masri *et al.*, 2017) and challenges in manipulation of multi-litre vessels (Pattasseril *et al.*, 2013), with automation also proving difficult to achieve (Mason and Hoare, 2006).

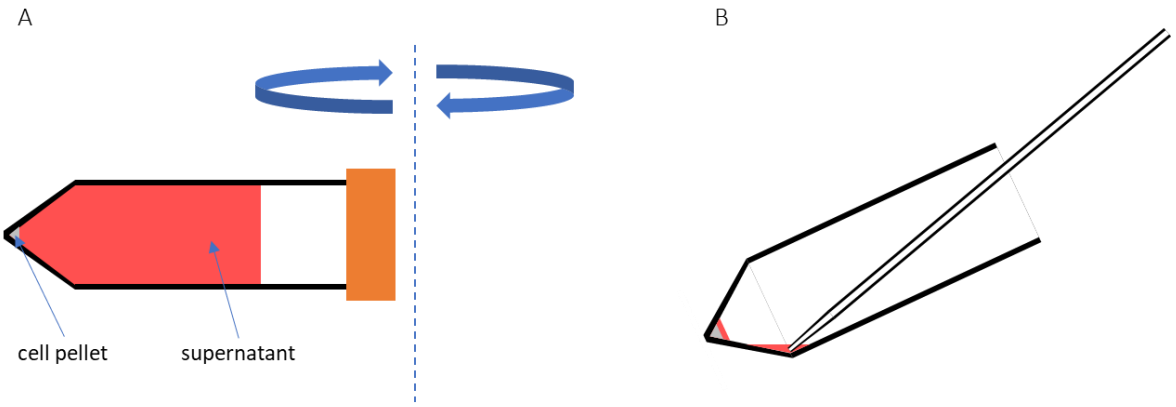

Figure 10 - Dead end centrifugation in a tube. A shows the centrifugation, which is the application of centrifugal force causing the denser than liquid cells to migrate to the bottom of the tube and form a pellet. B shows aspiration of the supernatant with an aspiration pipette, leaving the cell pellet and a small volume of supernatant.

Typical parameters for centrifugation during cell processing are relative centrifuge force (RCF) of several hundred g, with processing times of several minutes. The velocity of liquid during pellet resuspension has been shown to be a key parameter for cell recovery, with near complete recovery achievable even at high RCF values of 10000 and extended periods of 30 minutes (Delahaye *et al.*, 2015).

2.4.3.2.1.1 Closed Vessel Centrifugation

Closure of centrifugation process may be achieved in several ways. Closed centrifugation in conical tubes may be integrated into closed tubing-based systems via tube welding to move batches between equipment. This involving transferring cell solution to a tube, disconnecting the closed tube, performing centrifugation, reconnecting the closed tube, aspirating supernatant and then resuspending and transferring the cell solution. This solution requires operator intervention but preserves a truly closed process while maintaining flexibility and rework opportunity if required. Options for closed centrifuge tubes are limited, with Corning currently producing 50 ml and 500 ml closed system centrifuge tubes. Centrifuges for closed system tubes require rotors with covered chambers to contain the excess tubing

during centrifugation. Rotors are available with capacities of forty 50 ml tubes or four 500 ml tubes, for a maximum capacity of 2 litres per run. Closed centrifugation using 3 input centrifuge tubes has the potential to be a viable option for manual closed processing. Closed bag centrifugation may be performed either with bags taking the place of centrifuge tubes, with multiple bags contained in a rotor, or with a single bag spanning the entire centrifuge, mirroring the method utilised in centrifugation on the Prodigy (Miltenyi Biotec, Germany) system as discussed in Section 2.4.4. Closed bag centrifugation is an established technology for blood processing and provides options for ESC purification with varying levels of automation.

Automated systems with integrated centrifugation vessels offer an approach to automate centrifugation. Integration of purification and cryopreservation processes with closed and automated systems such as the Prodigy have the potential to reducing processing time by eliminating unnecessary product movements and reducing operator dependency, reduce costs by reducing operator requirements and fatigue, as well as reducing risk through process closure and reduction of operator variability. Centrifugation within the CentriCult Unit (CCU) is the purification method built into the Prodigy and is outlined in Figure 11. CCU centrifugation is limited to a start volume of 350 ml. Further liquid may be added without removing the previous batch allowing large quantities of liquid to be centrifuged as part of the same process and with minimal operator input, at the cost of increased process time. Although the Prodigy can add or remove liquid during centrifugation, the peristaltic pump cannot deliver enough pressure to overcome the centrifugal force to aspirate liquid towards the centre of the CCU during full speed centrifugation, preventing continuous purification. For processes featuring cell expansion on the Prodigy, this purification method comes fully integrated into the closed tubing system, however, the cost and complexity of the Prodigy and its consumables means that it is unlikely to be integrated into other closed and automated processes to perform a single process step.

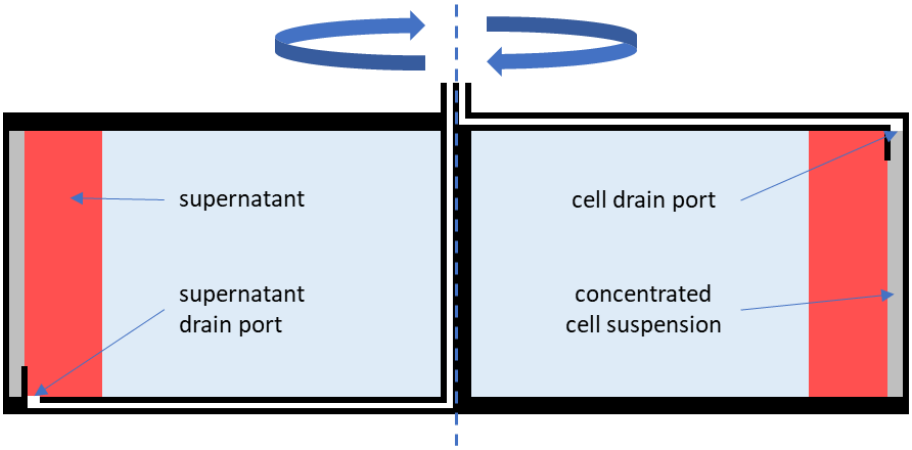

Figure 11 - Overview of centrifugation in the Prodigy CCU. Similar configurations are used for batch centrifugation in proprietary chambers or bags in other closed systems. The cell drain port is located at the chamber edge, while the supernatant drain port is located behind a small barrier several mm away from the chamber edge.

Several systems offer a standalone closed centrifugation including the SynGenX-1000 (Syngen), Sepax C-Pro (GE Healthcare), Sefia Cell Processing System (GE Healthcare) and the COBE 2991 cell processor (Terumo BCT). These systems have all been designed primarily for blood processing and suffer similar drawbacks to CCU centrifugation for cell therapy applications, requiring multiple runs for batch sizes over around 1 litre, resulting in extended processing times and impacts to product quality (Pattasseril *et al.*, 2013). The Centritech Cell II (Carr Seperations) and Unifuge (Carr Seperations) systems use a single-use bag and are able to continuously feed liquid and draw out supernatant and concentrated cell suspension of scales up to 120 litres. These systems have been designed for blood processing and system require additional manipulations for volume exchanges as required by stem cell therapies (Pattasseril *et al.*, 2013).

2.4.3.2.1.2 Counter Flow Centrifugation

Centrifugal counter-flow elutriation offers a scalable and closed approach and is used on the Sartorius kSep (Sartorius) and Elutra (Terumo) cell separation systems (Masri *et al.*, 2017). This technique utilises a conical centrifuge chamber with centrifugal force acting in in one direction and fluid flow force acting in the other, causing particles to settle in the region of the chamber where the forces acting upon them are in balance as shown in Figure 12. Cells are extracted by either increasing the flow rate or decreasing the rotor speed, meaning that this approach is cycle based rather than truly continuous.

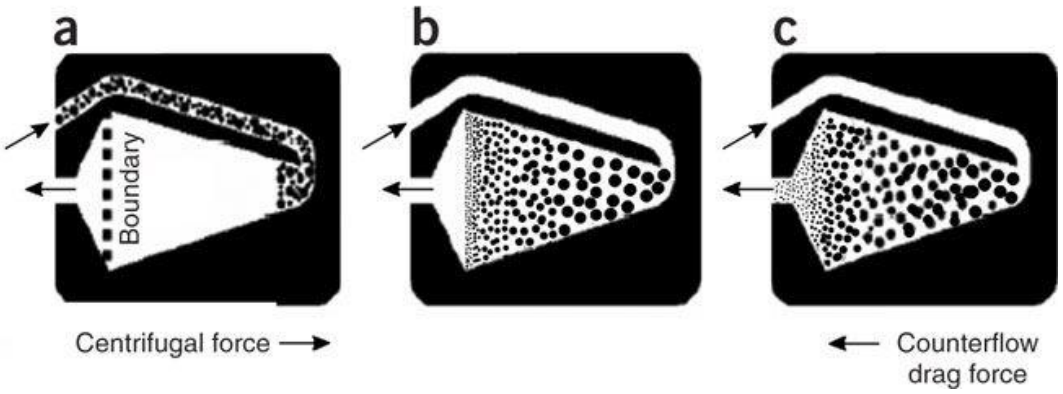

Figure 12 - Counterflow centrifugation (Banfalvi, 2008).

Flexible diaphragms have been employed by systems such as the Terumo Automated Centrifuge and Separator Integration System (TACSI) and Terumo COBE 2991 Cell Processor to allow for continuous material removal during centrifugation. These systems are cost effective at large scales but require a minimum cell yield of approximately 1 x 10^9 to function efficiently (Roberts, 2013). This is due to cell input density requirements as shown in Figure 13, as well as a minimum processing volume of 500 ml dictated by the fixed machine chamber size, making counter flow centrifugation unsuitable for small scale manufacturing and cost prohibitive for many research and process development efforts (Hassan *et al.*, 2015).

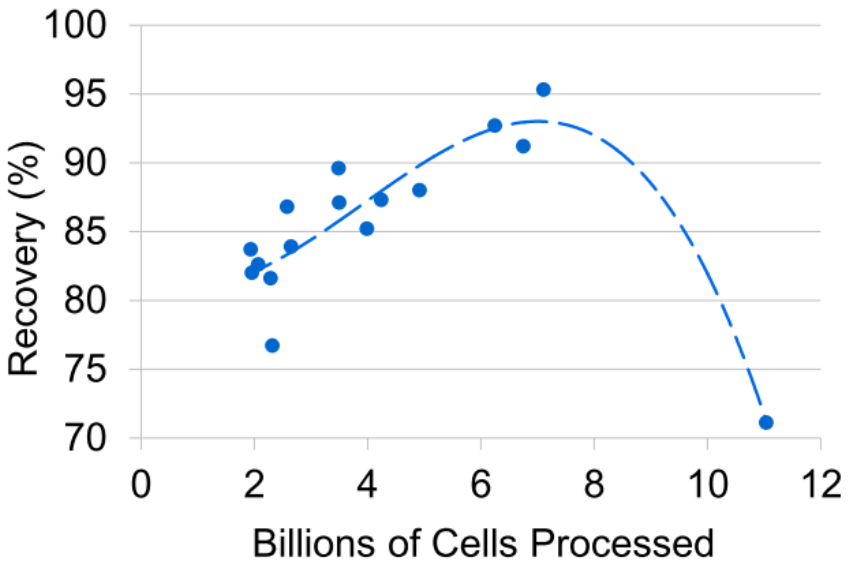

Figure 13 – Cell recovery percentage following counter flow centrifugation on the kSep 400 system in relation to absolute cell count (Roberts, 2013). *These results suggest an optimal cell count of approximately 7 x 10^9 per operation, with reduced cell recovery at lower and higher scales.*

2.4.3.2.2 Filtration

Filtration is the separation of solid particles from a liquid using a filter material which retains particles above a desired size and allows liquid and smaller particles to pass through (Doran, 2013). Filtration may be used to concentrate the desired particles as in a volume reduction, or in the case of diafiltration, small molecules may be passed through a filter while retaining desired particles at a set concentration to achieve a volume exchange.

In traditional direct flow or dead-end filtration, the particle suspension flows perpendicular to the filter with liquid passing through and particles depositing on the filter material. Direct flow filtration is best suited to negative selection in biological processing and is unsuitable for purification of ESCs due to difficulty in recovering cells from the filter cake while maintaining cell quality (Masri *et al.*, 2017).

2.4.3.2.2.1 Tangential Flow Filtration

An alternative to dead end filtration is tangential flow filtration (TFF) shown in Figure 14, in which a particle suspension moves in parallel with the filter material, with a portion of the liquid passing through (permeate) and the portion containing particles (retentate) returning on the retained side. The tangential flow of liquid across the filter reduces membrane fouling and allows for positive or negative cell selection processes.

Diafiltration allows small molecules to pass through a membrane while retaining larger particles, without changing concentration. Continuous diafiltration feeds the replacement buffer liquid into the feed container at the same rate as liquid permeates through the filter, maintaining the volume of the feed container. Discontinuous diafiltration first dilutes the starting volume with a volume of replacement buffer, and then concentrates this volume back to the original volume. Continuous diafiltration requires less input volume to achieve the same level of fluid exchange. Volume exchange may be achieved using less liquid volume by concentrating the product first, however over-concentrating input product increases viscosity and reduces the flow rate of liquid through a filter membrane (Schwartz, 2003).

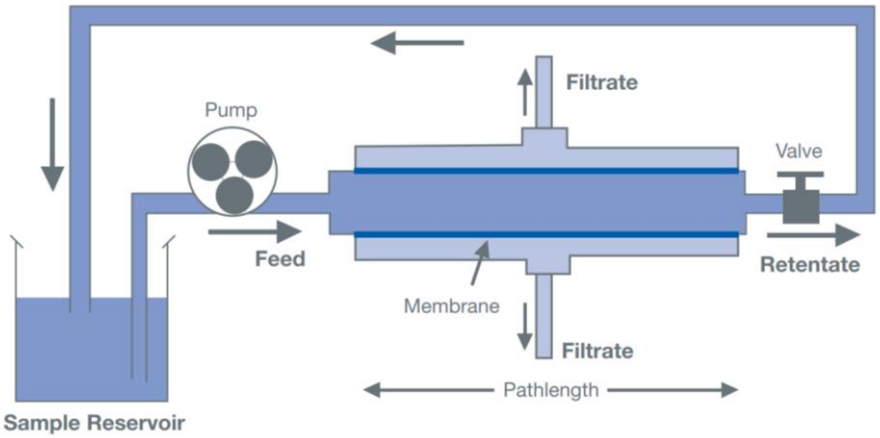

Figure 14 – An example TFF flow path, showing liquid flow from a reservoir, through a peristaltic pump, through a TFF filter and restrictor valve and back to the reservoir. A portion of flow in the filter element passes through the membrane to exit via the filtrate paths, while solids are retained in the retentate path (Pall Life Sciences, 2003).

Balancing recovery rates with throughput is key for filtration processes, as finer filter materials produce higher cell recovery rates with lower liquid flow rates at the cost of higher processing times (Cunha, Peixoto, *et al.*, 2015). Recovery rates of greater than 80% have been demonstrated using continuous TFF with MSCs, with negligible difference in cell quality and a benefit to processing time when used continuously (Cunha, Alves, *et al.*, 2015). If performed discontinuously, TFF approaches may also enable volume reduction and volume exchange steps to be performed by the same filter, reducing equipment requirements at the cost of overall throughput.

The key factors when selecting a TFF filter are flow channel type, membrane pore size, membrane material and membrane surface area. TFF filters may be constructed in either screen channel, suspended screen channel, or open channel configurations. Screen or suspended screen channels cause turbulence in contained fluid which aids with filtration of proteins, while open channels are preferred for cell harvesting to minimise shear forces and cell damage. Membrane pore size controls the size of particles allowed to pass through the filter and dictates the cut off between filtered and retained particles.

Membranes are available with pore sizes ranging from 0.001 µm for biomolecule filtration up to approximately 100 µm to cell filtering applications. High pore sizes of over 0.45 µm have been shown to produce higher cell recovery at higher concentration factors then pore sizes of 0.2 µm and below, and are less prone to fouling (Cunha, Peixoto, *et al.*, 2015; Cunha, Silva, *et al.*, 2017). Typical filter materials include polysulfone (PS), mixed ester (ME), polyethersulfone (PES), and modified polyethersulfone (mPES), with mPES being the most available across different pore size and surface areas. For cell filtering applications, PS has been shown to provide a greater recovery yield than PES

(Cunha, Peixoto, *et al.*, 2015). Membrane surface areas range from approximately 15 cm^2 to approximately 10 m^2. TFF systems are limited by their smallest and largest processing volume, with the smallest filters capable of processing volumes down to around 2 ml, when the limitations of hold up volume limit further volume reduction. The largest manufacturing scale systems are rated as capable of processing batches of up to 5000 litres. Although restrictive in many ways, TFF has the added utility of compatibility with continuous filtration processes (Cunha, Alves, *et al.*, 2015), although continuous processing options for other elements of a stem cell therapy manufacturing are currently limited.

The primary suppliers of TFF filters and systems are Repligen (formerly SpectrumLabs), Pall, GE Healthcare, and MilliporeSigma (formerly Millipore). MilliporeSigma recently announced expansion of filtration manufacturing efforts, citing the success of its TFF range as a primary motivation (Stanton, 2018a). Bioprocessing applications generally treat TFF membranes as single use items, however strategies such as backwashing and alternating flow filtration (Hadpe *et al.*, 2017) are possible to reduce fouling. Several devices such as the Cytomate (Nexell) and Lovo (Fresenius Kabi) systems implement a spinning membrane with counter flow buffer circulation to reduce fouling and maintain a more compact and integrated system as compared to TFF. However, these are limited in scale (Pattasseril *et al.*, 2013).

2.4.3.2.3 Other Purification Techniques

Centrifugation and filtration-based techniques are the dominant purification technologies, with TFF suitable for small and medium scale purification and counterflow centrifugation being more cost effective at large scales (Pattasseril *et al.*, 2013; Hassan *et al.*, 2015; Jossen *et al.*, 2018). Other technologies include field flow fractionation-based techniques which uses waves or fields to cause cells to gather in certain points. This can be achieved in various ways including: acoustophoresis, which uses standing waves to gather cells in nodes and antinodes but is limited in scale, dielectrophoresis, which uses electromagnetic forces to attract or repel cells but is limited by electrode heating and extreme specificity of cell size, and optical sorting of which there are several variants which are also limited in scalability (Masri *et al.*, 2017).

Hydrodynamic techniques rely on flow properties for cell separation and include: deterministic lateral displacement in which rows of micropillars at a slight angle to liquid flow direct large particles to one side, but is affected by clogging, size sensitivity and difficulty of manufacture; hydrodynamic filtration in which a large flow channel with many small exits filter small particles due to their tendency to flow

near side walls, but is challenging to scale and while maintaining laminar flow; and inertial migration in which fluid flows along a channel spiralling outward from the centre allowing cells to moved towards the inner wall due to shear gradient lift and wall effect lift, but has no large scale device availability (Masri *et al.*, 2017).

2.4.3.3 Cryopreservation

Cryopreservation is essential for cell therapy manufacturing as it enables cells to be stored for extended periods, providing standardised and controlled biological input material, simplifying logistics, and avoiding the complications and expenses of long-term cell culture. Cryopreservation is typically considered part of downstream processing but is also essential in upstream processing for preparation of cell banks. Suboptimal cryopreservation has the potential to introduce variation in both cell yield and quality, with the possibility of poor functional recovery, chromosomal damage, and the introduction of selective pressures causing and epigenetic changes (Rajamani *et al.*, 2014). Significant variation in recovery between cell lines has also been observed, with post-thaw recovery values of between 10% and 90% reported across hESC literature (Hunt, 2017). The high degree of variability present in accepted cryopreservation techniques limits their suitability for use in commercial scale products, where regulatory demands for quality and repeatability are high. There is a need to improve the scalability and GMP compatibility of cryopreservation techniques as ESC therapies move towards commercialisation.

The largest potential source of damage to cells during cryopreservation is the formation of ice crystals, with intracellular ice formation having the potential to cause physical rupturing of intracellular membranes, the formation of gas bubbles, protein denaturisation as well as thermal and osmotic shock (Mazur, 1963; Hunt, 2017). Cooling of a cell suspension beyond its equilibrium freezing point will cause ice crystal formation either by homogeneous or heterogeneous freezing. Homogeneous freezing occurs below -35 °C in the absence of an ice nuclei, whereas heterogeneous freezing is ice crystal formation catalysed by surface contact and normally occurs at above -30 °C (Hunt, 2017). Extracellular ice formation also has the potential to cause damage, as cells and solutes grow in concentration in the remaining liquid causing cells to attempt to maintain equilibrium with the extracellular region and so dehydrate, causing damage via increased internal solute concentration (Lovelock, 1953). The “two-factor hypothesis” was first proposed in 1972 (Mazur, Leibo and Chu, 1972) and states that the balance of solution effects and intracellular ice formation cause there to be an optimal cooling rate for conventional cell cooling, with higher rates causing more ice crystal damage and lower rates causing

more solute damage. From a manufacturing perspective, it is also noteworthy that faster cooling rates equate to higher throughput where cooling capacity it limited.

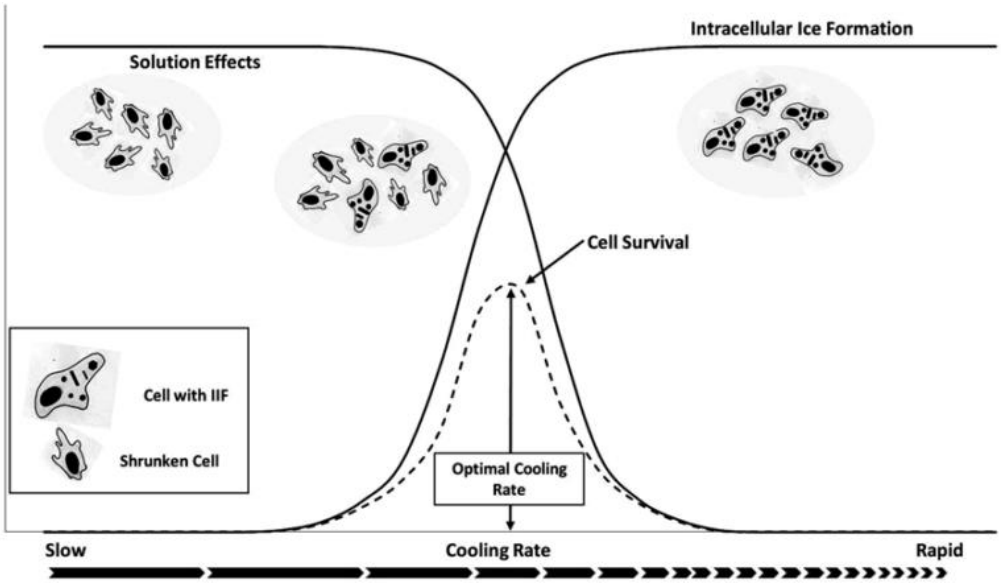

Figure 15 - The influence of cooling rate on cell damage by chemical toxicity and intracellular ice formation forms a peak of cell survival at an optimal cooling rate (Hunt, 2017)

Slow cooling attempts to find the ideal balance between slow and fast cooling, preventing intracellular ice formation while reducing the effects of solute toxicity, allowing cells to gradually dehydrate until no intracellular ice can form. Cryoprotectants are commonly used to reduce the damaging effects of high solute concentrations, enabling cooling rates slow enough to avoid the formation of intracellular ice. Slow cooling is generally achieved either using either a passive cooling device (PCD) or controlled rate freezer (CRF). Passive cooling devices are insulted containers designed to be placed inside a -80 °C freezer and achieve a cooling rates of around 1 °C per minute, depending upon the insulation material. Examples include the Mr Frosty (Nalgene) and the CoolCell (BioCision) and provide a cheap, simple solution with reasonable linearity. Limited changes to cooling rate are possible through altering insulation material and the temperature of the cooling device.

Controlled rate freezing offers a higher degree of control over the freezing process albeit at an increased cost, and allow for custom cooling curves and nucleation control, as well as detailed record keeping. This may be achieved using computer-controlled heating and LN2 delivery as in the CryoMed (Thermo Fisher Scientific) controlled rate freezer or LN2 free using a Stirling engine as in the VIA Freeze system (Asymptote). LN2 based control rate freezers can achieve cooling rates of around 30 °C per

minute, whereas Stirling engine coolers are currently limited to around 2 °C per minute, but have the advantage of being suitable for use in cleanrooms (Massie *et al.*, 2014). Nucleation control offers reduced variability in cryopreservation, as ice crystal formation is forced to occur outside of cells, rather than having the possibility to occur intracellularly (John Morris and Acton, 2013). Controlled rate freezer capacity places a limitation on process throughput, with the largest LN2-free controlled rate freezer, the VIA freeze quad, supporting up to 192 ml of sample material per freezing cycle, each cycle taking approximately 2 hours at a rate of 1 °C per minute (Asymptote Limited, 2017).

An alternative technique used for hESC cryopreservation is vitrification. This approach utilises fast cooling rates and high concentrations of cryoprotectant to prevent ice crystal formation, instead forming a non-crystalline amorphous glass. This solution avoids the issue of intracellular ice, however the high concentrations of cryoprotectant required for vitrification are also damaging to cells (Hunt, 2017). Equilibrium vitrification utilises large concentrations of cryoprotectant to prevent ice crystal formation, typically added in multiple stages to best balance solute concentration damage and osmotic damage. Non-equilibrium vitrification uses less cryoprotectant but requires extremely rapid cooling rates to prevent ice crystal formation. Warming rate is also important for this approach as nucleation must be prevented during the thawing process (Hunt, 2017).

The open pulled straw technique of filling thin straws with small volumes of cell suspension before immersion in LN2 for non-equilibrium vitrification has been used for hESCs cryopreservation due to the high recovery rates attainable (Reubinoff *et al.*, 2001; Richards *et al.*, 2004; Berz *et al.*, 2007). However, the use of open straws prevents this technique from being used in clinical settings due to contamination risk, while the small volumes, technical difficulty and high levels of variation produced by the technique mean it is unlikely to see adoption for commercial cryopreservation (Hunt, 2017).

For both methods, cryopreserved cells are typically stored in vapour phase LN2, as this presents a lower adventitious agent and cross contamination risk than storage in liquid phase LN2.

2.4.3.3.1 Cryoprotectants

The first discovery of a cryoprotectant was of glycerol's protective effect on the cryopreservation of spermatozoa in 1949 (Polge, Smith and Parkes, 1949). This was followed by the finding that dimethyl sulfoxide (DMSO) was capable of similar protective effects but with a drastically increased cell penetration speed, enabling the protection of larger and less permeable cells (Lovelock and Bishop, 1959). DMSO is the most commonly used cryoprotectant and is sometimes combined with others

including ethylene glycol, propylene glycol, hydroxyethylstarch, dimethyformamide, and polyvinyl pyrollidone. DMSO is typically used at 10% concentration with a single addition and removal step, however, lower concentrations such as 5% have been shown to provide comparable levels of protection for hematopoietic progenitor cells (Galmés *et al.*, 1999; Woods *et al.*, 2003) peripheral blood stem cells (Bakken, Bruserud and Abrahamsen, 2003) and porcine MSCs (Ock and Rho, 2011).

Glycerol and DMSO are examples of intracellular agents, non-ionic molecules and strong solvents capable of passing through the cell membrane. These cryoprotectants act by replacing some of the damaging solutes in the cell suspension and therefore reducing overall solute toxicity. Cryoprotectants also have lower freezing points than water, meaning that ice crystals form more slowly. Both effects contribute to having a lower concentration of damaging solvents for any given temperature (Hunt, 2017). Cryoprotectants such as sucrose and trehalose are extracellular agents and are thought to aid the binding together of molecules and cause cell shrinkage, reducing intracellular water and therefore reducing the chance of intracellular ice crystal formation (Hunt, 2017).

Although cryoprotectants provide a net protective effect, they also contribute to damage during cryopreservation. Damage is caused by two effects, volume changes due to osmotic imbalances, and chemical toxicity (Benson, Kearsley and Higgins, 2012). The toxicity of cryoprotectants is dependent on exposure time, temperature and concentration. Individual cells within a suspension may have different permeability values and surface to volume ratios, and so overall recovery may be mixed (Griffiths *et al.*, 1979). Damage may also be caused by the rapid addition or removal of cryoprotectants from a cell suspension. For intracellular cryoprotectants such as DMSO, cells will rapidly dehydrate and reduce in volume due to the initial osmotic imbalance and will then re-hydrate and return to normal volume as the cryoprotectant equilibrates within the cell. Upon removal of DMSO from the extracellular region, for example by centrifugation and resuspension, cells will rapidly rehydrate and swell due to osmotic imbalance in the opposite direction, after which viable cells return to normal volume (Griffiths *et al.*, 1979). Non-viable cells will remain swollen, suggesting that certain subpopulations are less able to recover from volume changes, or that there are volume changes or rates of change beyond which cells cannot recover. For extracellular cryoprotectants, cells will rapidly dehydrate and shrink as the protectant is added, and will remain dehydrated until DMSO has been removed from the extracellular region, at which time rehydration and swelling will occur (Hunt, 2017).

Early cryopreservation of ESCs using slow cooling with 10% DMSO produced significant cell death and loss of Oct-4 pluripotency marker expression (Katkov *et al.*, 2006). These effects were lessened by introduction of ROCK inhibitors which improved the survival rates of general ESC culture with minimal impact on pluripotency or chromosome stability (Watanabe *et al.*, 2007) as well as improved post thaw

survival and cell recovery, effectively enabling the use of slow cooling as a cryopreservation technique (Hunt, 2017). The mechanism of action of ROCK inhibitors on hESCs is not fully understood, however the beneficial effect for cryopreservation of hESCs and hiPSCs has been well demonstrated (Claassen, Desler and Rizzino, 2009; Baharvand *et al.*, 2010). There is however evidence that the ROCK inhibitor Y-27632 reduces expansion and survival in hematopoietic progenitors (Bueno, Montes and Menendez, 2010), as well as reducing post thaw survival and inducing neuronal differentiation in MSCs (Heng, 2009).

DMSO has more recently been used to downregulate Oct-4 expression and aid ESC differentiation (Czysz, Minger and Thomas, 2015). Although active cells were exposed to DMSO for periods far longer than seen during typical cryopreservation and resuscitation, the effect has been observed in DMSO concentrations as low as 0.25% (Adler *et al.*, 2006; Czysz, Minger and Thomas, 2015), a concentration possible assuming sub-optimal purification following thaw. Studies have also shown differences in the cryoprotective effect of DMSO depending on the level of cell lineage commitment. A 1999 study showed that controlled rate freezing with 5% DMSO was optimal for pluripotent progenitors, however 10% was optimal for very primitive pluripotent hemopoietic stem cells. This difference was thought to be due to the P-glycoprotein transport system present in leukemic stem and progenitor cells removing DMSO from cells, and may not be applicable to hESCs (Balint *et al.*, 1999).

DMSO has been shown to induce cell death in neuronal cell lineages at concentrations below 5% (Galvao *et al.*, 2014), and in the developing mouse brain at concentrations of 0.5% (Hanslick *et al.*, 2009), with recommendation that the minimum possible DMSO concentration be used where necessary. Despite the toxicity of DMSO and general loss of cell viability experienced during cryopreservation, foetal mesencephalic tissue cryopreserved in 10% DMSO and subsequently thawed and grafted into rat PD models have been shown to produce functional effects (Sauer *et al.*, 1992), with DMSO concentrations of between 7% and 10% shown to be optimal for preservation of cell viability (Silani *et al.*, 1988). A recent study at Lund University explored the feasibility of cryopreservation for dopaminergic neural progenitors and found no difference in neuron content when comparing in vivo grafts of cryopreserved and fresh cells when transplanted into animal models (Neurostemcellrepair, 2018).

2.4.3.3.2 Fill and Finish

Cryopreservation containers for cell products are largely based on those established in blood banking, with the main approaches being screw top vials and flexible bags (Woods and Thirumala, 2011). As quality control may be limited upon product thaw in a hospital setting, quality and sterility of cells for clinical use is of the utmost importance, driving a trend towards the adoption of closed processing for cryopreservation. Most developments in cell therapy cryopreservation are currently focussed on immunotherapies, which are of similar batch size but one or several doses rather than the several hundred required for allogeneic cell therapy-based therapies. A closed cryopreservation technique capable of freezing volumes of the order of 1mL is desirable for allogeneic cell therapies, where a single production run can produce many doses which require individual packaging.

Automated screw-top vial filling systems such as the Fill-It (TAP Biosystems) have been developed to increase the throughput and standardisation of vialling operations, however screw top cryovials do not provide a perfect seal when closed and must be opened when adding or retrieving cells, resulting in increased contamination risk when the product is at its most valuable (Parisse, 2017).

Luer lock accessed systems such as the CLINIcell (Mabio) gas permeable cassette provide improved process closure but remain open during tube changes (Amps *et al.*, 2010). Needle filled vials such as the AT-Closed Vial (Aseptic Technologies) offer reduced contamination risk compared to screw-top vials, while the needle filled CellSeal (Cook Regentec) system also allows for inlet tube sealing after filling (Woods and Thirumala, 2011), as shown in Figure 16. While needle filling reduces the risk of contamination compared to open screw-tops, it cannot be considered fully closed still results in a period of environment exposure.

Figure 16 – Screw top vials (ThermoFisher, UK), needle accessible AT-Closed vials (Aseptic Technologies, US) and tube welding compatible CellSeal vials (Cook Regentec, US).

Truly closed filling solutions such as the Freeze-Pak (Charter Medical) and CryoMACS Freezing Bags (Miltenyi Biotec) utilise tube heat sealing for entirely closed cell delivery, and allow for sterile cryopreservation outside of a cleanroom facility (Humpe *et al.*, 2007), an example of which is shown in Figure 17. The Finia system (Terumo) automates bag filling at scales of up to 250 ml while agitating bags and maintaining product temperature but is restricted to the filling of 4 bags per lot as it is designed for use with autologous immunotherapies.

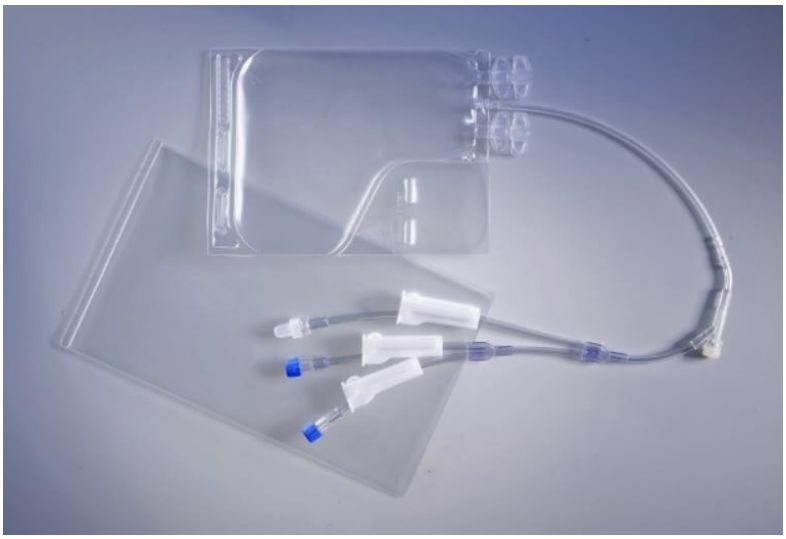

Figure 17 - CryoMACS freezing bag (Miltenyi Biotec, 2020b)

2.4.4 Multifunctional Systems

A key challenge identified for the development of closed and automated manufacturing processes is the lack of standardisation and challenge of device to device integration present in current equipment (Stanton, 2019). A number of multifunctional systems have been developed with the aim of integrating multiple processing steps in a single system. Although most of these systems have been developed for processing of suspension CTPs, this section focusses on the limited number of systems compatible with adherent cell processing.

The Prodigy is a closed and automated GMP compliant cell processing system capable of performing adherent cell culture and centrifugation in a temperature and gas mix-controlled rotating chamber, as well as cell selection through a MACS magnetic separation unit, and liquid manipulations through a closed tubing set with pinch valves and peristaltic pump (Apel *et al.*, 2013). The Prodigy was initially developed for bone marrow stem cell bulking but has seen wider success in the rapidly growing field of

CAR-T therapies due to their similar processing requirements (Kaiser *et al.*, 2015). Processes have recently been developed for the expansion of adherent cell types including MSCs (Godthardt *et al.*, 2019) and ESCs (Miltenyi Biotec, 2018b).

Further examples of closed and automated manufacturing systems are currently limited. The Cocoon manufacturing system (Octane Biotech, Canada) is a patient scale cassette based culture system capable of cell purification, expansion and harvest (Stanton, 2018b). This system appears to replicate the core functionality of the Prodigy in a cassette, as shown in Figure 18, and may be amenable to adherent cell culture, however the system is not yet commercially available.

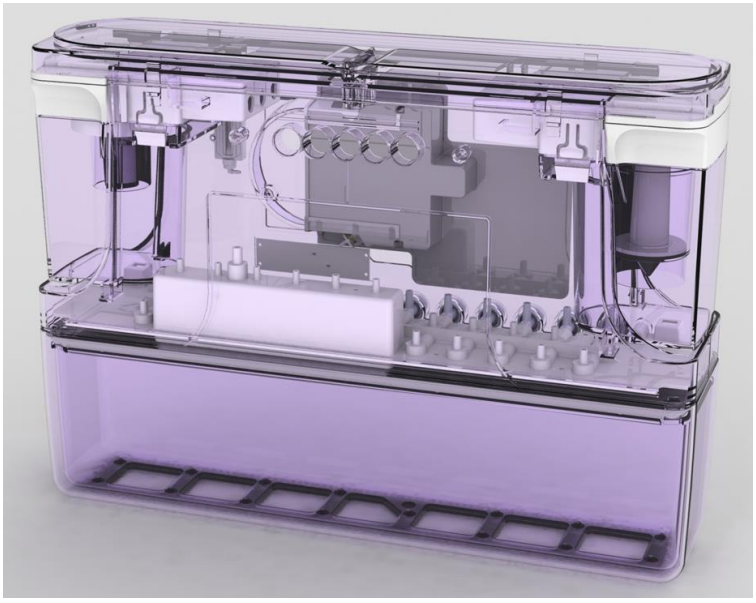

Figure 18 – A cassette of the Cocoon manufacturing system, incorporating cell purification, culture and harvest functionality. The system is not yet available but is supposedly capable of suspension and adherent culture (Stanton, 2018b).

The Compact Select is an automated open cell culture platform based around a robotic manipulator capable of mimicking operator interactions with standard culture vessels. The system has been demonstrated with a range of cell types including MSCs, ESCs, iPSCs and (Thomas *et al.*, 2007, 2009; Soares *et al.*, 2014). It is an established and commercially available device, capable of handling well plates, flasks and HYPERflask flasks with up to 10 layers. The system is limited to open processing and features no integrated purification capability. The AUTOSTEM system represents an advancement of this approach with a focus on bioreactor based culture, integrating culture, sampling, fill and finish and cryopreservation into a single system (Rafiq *et al.*, 2016). This platform is compatible with tube based dead end centrifugation but does not currently support planar culture.

2.5 Gap Analysis

No currently available system fully addresses the need of allogeneic ESC derived CTP manufacture, as summarised in Table 3. While systems based around stirred tank bioreactors are well proven and provide automated and closed cell culture, these systems are only practical for use at large scales and are incompatible with therapies not suited to suspension or microcarrier based culture (Simaria *et al.*, 2014). While robotic arm-based systems achieve increased standardisation and control and represent an important iterative improvement compared to manual processing (Thomas *et al.*, 2008), the strategy of one to one replacement does not realise the advantages of integrated and reduced processing of which automation is capable. Closed tubing-based systems are notionally the closest to fulfilling the requirements of small-scale ESC derived CTP therapies. The most prominent system of this type is currently the CliniMACS Prodigy, which is capable of fully closed and automated cell manipulation (Apel *et al.*, 2013). While the Prodigy is capable of adherent cell culture, dissociation and purification, the required manipulations represent a significant departure from those used in manual processing. There is currently little data available with which to assess the performance of integrated closed tubing-based systems with adherent cell processing, these systems must therefore be considered as potentially suitable but as yet unproven.

Table 3 – Gap analysis of system requirements for manufacture of small-scale allogeneic CTPs, including a summary of the current and desired capabilities.

Requirement	Current State	Desired State
Integrated process	Proprietary hardware, bespoke software and lack of standards. Equipment largely single function.	System compatibility due to hardware and software standards.
Fully closed processing	Dominance of open and functionally closed systems. Fully closed systems require opening to input / retrieve material.	Move from functionally closed to fully closed systems. Increased compatibility to eliminate intermediate vessel changes.
Automation	Automation as an enabler of closed processing and as single unit steps. Little reduction in operator dependency.	Drastic reduction in operator dependency due to entirely automated unit steps and, where required, movement of material between devices.
Adherent cell culture	Most closed and automated systems favour suspension cells processing, some systems adaptable to both cell types.	Industry focus on development of closed and automated adherent cell culture systems.
Cell dissociation	Most systems are not designed with cell dissociation as a requirement.	Systems capable of replicating and enhancing manual dissociation techniques, e.g. shear forces via flask tapping and liquid flow.
Cell purification (e.g. centrifugation or TFF)	Closed and automated solutions for single unit steps. Many techniques at inappropriate scale for allogeneic ESC processing.	Small scale closed purification techniques compatible with closed culture and dissociation systems.

3 Materials and Methods

This chapter details the materials and methods used throughout the thesis that will be referred to in the relevant chapters. These include the protocols utilised for the culture and cryopreservation of pluripotent stem cells, as well as the differentiation of pluripotent stem cells into a mesencephalic dopaminergic (mesDA) progenitor cell product using variations of a process designed at Lund University (hereinafter referred to as Lund). The chapter also provides details of the manipulations required to perform these protocols on the CliniMACS Prodigy (hereinafter referred to as the Prodigy), an automated cell processing system produced by Miltenyi Biotec GmbH (hereinafter referred to as Miltenyi). All consumables and reagents were purchased from Fisher Scientific UK (Loughborough, UK) unless otherwise stated. Work was performed within the Centre for Biological Engineering laboratories at Loughborough University (hereinafter referred to as the CBE and Loughborough).

3.1 Cell lines

The cell lines utilised in this thesis are the human embryonic stem cell lines H9 and RC17 (referred to as pluripotent stem cells), and the human embryonal carcinoma cell line 2102EP. 2102EP cells were used for exploratory pluripotent work as they are a resilient cell line (Josephson *et al.*, 2007) and may be cultured using less costly reagents in comparison to H9 or RC17 cells, whose use are also more ethically restricted. 2102EP cells used in this thesis were from a pre-existing bank at passage 51 which was derived from vials originally purchased from GlobalStem (US) as part of previous project work.

Following the initial exploratory work, the H9 and RC17 cell lines were used for all work relating to the Prodigy system, downstream processing and closed cryopreservation systems. All H9 cells used in this thesis were from a pre-existing bank that had been cultured to passage 8 (Smith, 2014). This bank was derived from vials originally purchased from WiCell (WAe009-A, WiCell, US). H9s have previously been used by Lund and Miltenyi in the development of an automated mesDA production process (Nolbrant *et al.*, 2017) and were therefore used at Loughborough during early Prodigy and downstream processing work. This line was not produced under good manufacturing practice (GMP) or xeno-free conditions (Thomson *et al.*, 1998), and is therefore potentially unsuitable as a source material for cell based therapies.

The RC17 human embryonic cell line (RCe021-A, Roslin Cells, UK) was originally derived in 2011 in compliance with UK and EU quality assurance regulations, and in adherence to international GMP standards for tissue procurement, processing and storage, making it a suitable candidate for source material for cell therapies (De Sousa, Tye, *et al.*, 2016). RC17 cells used in this thesis were from an experimental bank which had previously been cultured to passage 39 and was derived from the expansion of a vial purchased from Roslin Cells (RCe021-A, Roslin Cells, UK).

3.2 Pluripotent Stem Cell Culture and Maintenance

The culture of pluripotent stem cells was used to generate cells as input material for experimental work, including as input material for automated processing on the Prodigy and the subsequent troubleshooting work that was undertaken, as well as at for use in the testing of purification and cryopreservation techniques. Table 4 lists all the reagents and consumables used for pluripotent cell culture and cryopreservation protocols. This section describes the general culture practices common to all experiments unless stated otherwise. Unless otherwise stated, incubation refers to storage inside an incubator at 37°C in an atmosphere of >95% humidity and 5% CO_2, while room temperature refers to approximately 21°C.

Commonly used cell culture reagents and details of the volumes applied for the different culture vessels are provided in Table 5. “Seeding medium” refers to the culture medium used during cell seeding and is prepared by adding Thiazovivin at a concentration of 2 µM to iPS-Brew with the included supplement. “Feed medium” refers to iPS-Brew and is the medium used during pluripotent cell feeding. “Dissociation” volume refers to the volume of TrypLE Select used to dissociate the cells and “Quench” refers to a volume of feed medium used to neutralise the dissociation enzyme. All medium and reagents were warmed to 37°C *via* a water bath prior to use unless stated otherwise. ROCK inhibitor or “ROCKi” refers to Thiazovivin unless stated otherwise.

Table 4 – Pluripotent stem cell culture equipment and reagents

Product	Supplier	Catalogue Number
Corning Cell Culture Treated Flasks T25 (25 cm^2)	Fisher Scientific	10288990
Corning Cell Culture Treated Flasks T75 (75 cm^2)	Fisher Scientific	15350591
Corning CELLSTACK 1-layer (636 cm^2)	Fisher Scientific	10549772
Corning Costar 12-well plate (3.8 cm^2 per well)	Fisher Scientific	10253041
Corning Costar 6-well plate (9.5 cm^2 per well)	Fisher Scientific	10578911
Dulbecco's Phosphate-Buffered Saline (PBS +/+)	Corning	21-030-CVR
Laminin 521	BioLamina	LN521
Mr. Frosty™ Freezing Container	Fisher Scientific	5100-0001
Nunc 15 ml centrifuge tube	Fisher Scientific	339651
Nunc 50 ml centrifuge tube	Fisher Scientific	339653
Nunc™ Cryogenic Tubes (screw top vials)	Fisher Scientific	368632
PBS -/-	Fisher Scientific	14200075
StemMACS Cryo-Brew	Miltenyi Biotec	130-109-558
StemMACS iPS-Brew XF and 50x supplement	Miltenyi Biotec	130-104-368
Thiazovivin	Miltenyi Biotec	130-106-542
TrypLE™ Select Enzyme	Fisher Scientific	12563011

Table 5 – Feed, seed, dissociation and quench volumes used for various growth vessels and growth areas.

Vessel Type	Surface Area	Seed and Feed Medium Volume	Dissociation Volume	Quench Volume
12-well plate	3.8 cm^2	1 ml	0.25 ml	0.25 ml
6-well plate	9.5 cm^2	2 ml	0.5 ml	0.5 ml
T25 flask	25 cm^2	5 ml	2 ml	3 ml
T75 flask	75 cm^2	15 ml	6 ml	9 ml
1-layer CellSTACK	636 cm^2	150 ml	100 ml	100 ml

3.2.1 Coating for Pluripotent Cell Culture

H9 and RC17 cells require coated culture plastic on which to adhere and grow. Laminin-521 was used as the coating for all pluripotent cell growth due to its effectiveness at supporting pluripotent cell growth and previous use by project partners Miltenyi and Lund (BioLamina, 2018). For the expansion of H9 and RC17 cells, tissue culture plastic (TCP) was coated with Laminin-521 at 0.5 µg per cm^2 prior to cell seeding. Laminin-521 was added to TCP with PBS at a volume of 0.2 ml per cm^2 to ensure

adequate coverage of the culture surface. The coated culture plastic was either incubated for at least 2 hours; or alternatively, coated vessels were stored at room temperature for 24 hours and then moved to an incubator for at least 2 hours before use. The coating mixture was then aspirated prior to cell seeding.

3.2.2 Resuscitation

Cryopreservation of cells allows for long term storage and simplified logistics. Screw top vials are the dominant cryopreservation vessel for stem cells in a research setting and were used for long term storage of all banked cells in this thesis. To transfer cells from a state of cryopreservation to one of active culture, cells must be resuscitated.

Cryopreserved cells were resuscitated by thawing individual banked cryovials in an incubator for 5 minutes, or until entirely thawed. Following thawing, the vial was transferred into a biological safety cabinet (BSC) and its contents moved dropwise into a 50 ml tube containing 5 ml of feed medium.

3.2.3 Purification

Cells require the removal of supernatant following resuscitation or dissociation to remove potentially damaging reagents such as cryoprotectants and dissociation reagents prior to seeding. Purification was achieved by centrifugation of the cell suspension at 300 G for 5 minutes in a SIGMA 3-15 centrifuge, before being transferred back into the BSC where supernatant was aspirated. Aspiration was achieved by positioning the tip of a 2ml aspiration pipette at the top of the liquid and tilting the centrifuge tube to an angle at which the shoulder of the conical portion of the tube became the lowest point. The aspiration tube was then slowly moved from the top of the tube towards this shoulder, collecting all liquid as it collected at this point due to gravity, while the pellet remained suspended at the tip of the conical portion of the tube. Following centrifugation, the cell pellet was resuspended first in 1 ml of liquid using a 1 ml pipette tip in order to break up the pellet, with further liquid added to an appropriate dilution (Table 5) using a serological pipette. The liquid used for resuspension was varied depending on the purpose of the purification, with seeding medium used for cells to be passaged and Cryo-brew used for cells to be cryopreserved.

3.2.4 Cell Seeding

Following purification, cells must be transferred from suspension onto a coated culture surface to be seeded for further growth. Following centrifugation and resuspension, a 190 µL sample of the cell solution was collected and a viable cell count obtained using a NucleoCounter NC-3000 (Chemometec, Denmark) (hereinafter referred to as the NucleoCounter). An appropriate volume containing the desired viable cell count was then transferred to freshly coated culture plastic for continued culture. 2 x 10^4 cells per cm^2 was used as the default cell seeding densityfor pluripotent culture for all work unless stated otherwise due to robust growth at this density observed in preliminary work, and convenience of timing of harvest days in experiment scheduling. Each culture vessel was then topped up with an appropriate volume of 37°C seeding medium as shown in Table 5, and the flask gently tilted from side to side to ensure full coverage of the culture surface with cell solution. Following cell seeding, culture plastic was transferred to an incubator.

3.2.5 Culture Maintenance

Following seeding, a medium exchange was performed, and cell growth status checked every 24 hours until reaching a state of confluence. Medium exchanges were performed every 24 hours throughout the culture period using feed medium of volumes listed in Table 5. Cultures were inspected and confluency evaluated visually using light microscopy at each feed, as detailed in Section 3.5.1, and passaged upon reaching approximately 80% confluency as judged visually by an operator. The typical time taken for cells to achieve confluency for various seeding densities is shown in Table 6.

Table 6 – Days to confluence for various seeding densities. Following cell resuscitation, cultures took on average one additional day to reach 80% confluency as compared to cells reseeded under standard passage conditions.

Seeding density per cm^2	Days to confluence for a typical passage	Days to confluence following resuscitation
1 x 10^4	4	5
2 x 10^4	3	4
4 x 10^4	2	3

3.2.6 Dissociation

Upon reaching 80% confluency, further cell growth may be impaired by lack of available space, it is therefore best practice to dissociate cells before they become over confluent and transfer them to new vessels at a reduced density or prepare them for other uses such as cryopreservation or for use in experiments.

To dissociate cells, spent culture medium was first aspirated using a 2 ml aspiration pipette and waste line, and culture surfaces were washed using a volume of PBS -/- equal to the feed volume as shown in Table 5. The PBS wash was then aspirated. Cells were then dissociated through the addition of a dissociation volume of TrypLE as shown in Table 5, and incubated for 7 minutes. Cells were then manually agitated to aid detachment and inspected *via* light microscopy. Following cell detachment, the dissociation enzyme was quenched through the addition of a quench volume of feed medium shown in Table 5, with the resulting cell solution gently pipetted over the surface of the flask to encourage complete detachment. The cell solution was then transferred to a 50 ml centrifuge tube and centrifuged at 300 G for 5 minutes to purify the cells from the dissociation enzyme contaminated supernatant.

3.2.7 Cryopreservation

Cryopreservation of cells enables long term storage and simplifies logistics. In this work, cryopreservation was used to store cells when making intermediate banks, and for the exploration of closed cryopreservation containers. All cell banks used in this thesis use cells cryopreserved in screw top vials and suspended in vapour phase liquid nitrogen.

Cells to be cryopreserved were first harvested using the standard dissociation technique as detailed in Section 3.2.6. Following aspiration of the supernatant, the cell pellet was resuspended in 1 ml Cryo-Brew using a 1 ml pipette tip. Further Cryo-Brew was added to reach a dilution of approximately 2 x 10^6 cells per ml using a serological pipette, then a 190 µL sample collected, and a viable cell count obtained using a NucleoCounter as described in Section 3.5.2. The cell pellet was then further diluted in an appropriate volume of Cryo-Brew to reach the recommended concentration of 1 x 10^6 cells per ml for use with this cryoprotectant. 1ml of cell solution was dispensed per vial into cryogenic storage tubes labelled with cell line name, passage number, date cryopreserved, initials of all operators and cells per vial, until the entire cell solution was dispensed.

Where possible, freezing was performed using a VIA Freeze Research controlled rate freezer (CRF) (Asymptote, Cambridge, UK) for increased robustness and record keeping in comparison to unmonitored methods. For freezing using the CRF, the device was configured for a 4°C hold followed by 1°C per minute cooling profile. The device was initialised prior to cell harvesting and the cooling chamber to reach the 4°C hold temperature. Once cell dissociation and vialling were complete, vials were transferred onto the CRF plate and the program advanced to the 1°C per minute cooling phase. Following controlled cooling to -80°C, vials were transferred for long term storage in vapour phase liquid nitrogen. Vial information and location were then logged within the CBE quality system.

Where a CRF was not available due to equipment or time constraints, slow cooling was achieved using a Mr. Frosty Freezing Container passive cooling device in a -80°C freezer. Prior to cell harvesting, the Mr. Frosty was first checked for adequate filling with isopropyl alcohol and allowed to reach room temperature. Once vialling was complete, vials were quickly transferred into the device prior to being transferred to a -80°C freezer. The device was then left to cool for between 4 and 48 hours before transferring the vials to vapour phase liquid nitrogen. Vial information and location were then logged within the CBE quality system.

3.3 Differentiation of human embryonic stem cells (hESCs) to mesDA Progenitors

The cell therapy product selected as a demonstrator in this thesis is a mesDA progenitor cell therapy for the treatment of Parkinson's disease. A protocol for differentiation of pluripotent stem cells into mesDA progenitors was originally developed at Lund (Nolbrant *et al.*, 2017) (hereinafter referred to as the Lund protocol) and later developed by Miltenyi into an automated process (Miltenyi Biotec, 2018a) (hereinafter referred to as the Miltenyi protocol). These processes share the same 16 day overall run time and passage step on day 11 but vary in multiple ways and are therefore both detailed in this chapter. The reagents and consumables used for differentiation of pluripotent stem cells into mesDA progenitors are shown in Table 7, while plasticware and consumables common with pluripotent stem cell culture and are provided in Table 4.

Table 7 - Medium and reagents used for the differentiation of pluripotent stem cells to mesDA progenitor cells.

Product	Supplier	Catalogue Number
B-27 supplement minus vitamin A CTS	Fisher Scientific	A3353501
Brain-derived neurotrophic factor (BDNF)	Miltenyi	130-096-286
CHIR99021 (CHIR)	Miltenyi	130-106-539
DMEM/F-12	Fisher Scientific	21331020
FGF8b	Miltenyi	130-095-740
Human serum albumin solution (HAS)	Irvine Scientific	9988
L-Ascorbic acid (AA)	Sigma-Aldrich	A4403-100MG
L-Glutamine	Fisher Scientific	25030081
MACS Neuro Medium	Miltenyi	130-093-570
MACS NeuroBrew-21 w/o Vitamin A	Miltenyi	130-097-263
N-2 supplement CTS	Fisher Scientific	A1370701
Neurobasal CTS	Fisher Scientific	A1371201
Noggin	Miltenyi	130-103-456
Purmorphamine	Miltenyi	130-104-465
SB431542	Miltenyi	130-106-543
SHH-C24II	Miltenyi	130-095-727
Thiazovivin	Miltenyi	130-104-461
Y-27632 dihydrochloride	Miltenyi	130-106-538
Laminin-111	Biolamina	LN111

3.3.1 Coating for Differentiation to mesDA Progenitors

All differentiations of hESCs to mesDA progenitors were performed on Laminin-111 coated tissue culture plastic due to its ability to support cells differentiation to neural lineages. Furthermore, this coating method has historically been used by collaboration partner organisations Miltenyi and Lund (BioLamina, 2018). Laminin-111 was added to the culture surface at a concentration of 1 µg per cm^2 along with PBS +/+ at a volume of 0.2 ml per cm^2 to ensure culture surface coverage Table 5. The coated surfaces were then incubated for at least 2 hours before aspirating the coating mixture and seeding cells. Alternatively, cell seeding may be delayed by holding coated flasks at room temperature for 24 hours, then incubating at for at least 2 hours before use.

3.3.2 Lund 2017 Protocol

The Lund 2017 protocol was designed as a xeno-free manual process for the differentiation of pluripotent stem cells into mesDA progenitor cells (Nolbrant *et al.*, 2017). Several changes were implemented to ensure compatibility with T25 flasks and CellSTACK vessels as the protocol was originally developed at the scale of 6, 12, 24, 48 and 96 well plates and requires the use of medium volumes of up to 600 µl per cm^2. This volume is unsuitable for typical adherent cell culture vessels such as flasks or CellSTACKs, equating to 15 ml of medium in a T25 flask and exceeding the vessel capacity when stored horizontally. Similarly, 600 µl of medium per cm^2 in a single layer CellSTACK equates to 381.6 ml, far in excess of the recommended maximum working volume of 200 ml (Corning, 2011). Medium volumes were therefore limited to a maximum of 7.5 ml per T25 and 250 ml per CellSTACK. Other than alterations to feed volumes the described protocol is a faithful reproduction of the process described in (Nolbrant *et al.*, 2017), and is summarised in Figure 19.

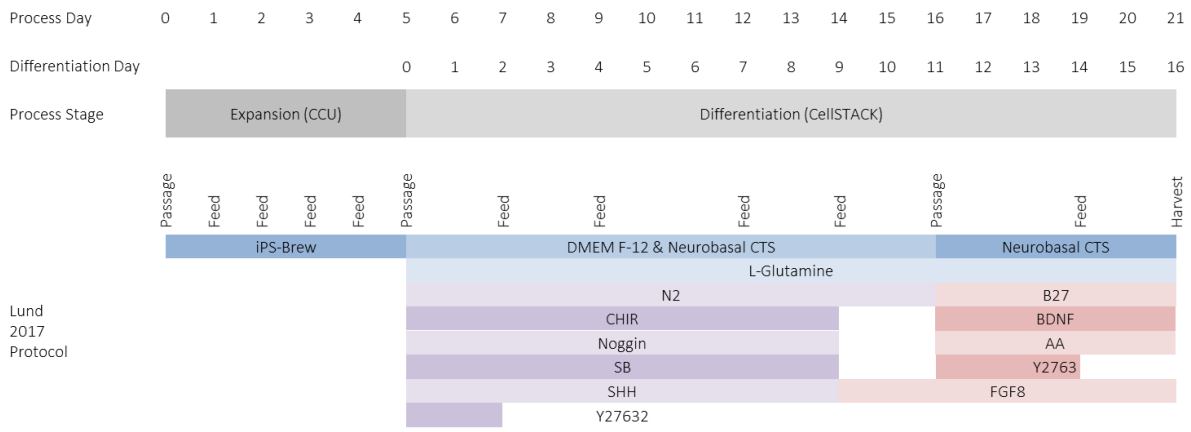

Figure 19 – Summary of the protocol described by (Nolbrant *et al.*, 2017)*, with the addition of 5 days of pluripotent expansion preceeding the differentiation process. On process day 21 (differentiation day 16) the mesDA progenitors are ready for quality control and cryopreservation or direct transplantation, where the terminal differentiation to mesDA neurons will complete in vitro.*

3.3.2.1 Media Preparation

Two base mediums were prepared prior to the start of the differentiation process. The base medium used for culture on days 0 to 11 (hereinafter referred to as N2 medium) contains DMEM F-12 (49% *v/v*), Neurobasal CTS (49% *v/v*), N2 Supplement (1% *v/v*), L-Glutamine (2 mM), while the medium for days

11 to 16 (hereinafter referred to as B27 medium) contains Neurobasal CTS (97% *v/v*), B27 Supplement (2% *v/v*), L-Glutamine (2 mM).

Small molecules additions were prepared freshly on each day as required, mirroring the industry standard practice of caution to minimise small molecule degradation, at the cost of additional manipulations when preparing media. Differentiation days 0, 2, 4 and 7 require N2 Medium with SB431542 (10 µM), Noggin (100 ng / ml), CHIR99021 (0.7 µM), Shh-C24II (300 ng / ml), with Y27632 (10 µM) also included on day 0 only. Differentiation day 9 requires N2 Medium with FGF8b (100 ng/ml) only. Differentiation days 11 and 14 require B27 Medium with BDNF (20 ng/ml), AA (0.2 mM) and FGF8b (100 ng/ml), with Y27632 (10 µM) also added on day 11 only. Cell seeding, maintenance and passage were performed as described in Section 3.2, with feed and passage timings detailed in Figure 19.

3.3.3 Miltenyi 2018 Protocol

The Miltenyi 2018 differentiation protocol shown in Figure 20 was developed from the Lund protocol described in (Kirkeby *et al.*, 2012; Kirkeby, Nelander and Parmar, 2012) by Miltenyi and mirrored many of the changes made to that process as it progressed towards the Lund 2017 method described in (Nolbrant *et al.*, 2017). The Miltenyi protocol has undergone continuous development throughout the technology transfer period with the aim of improving the expression of product purity markers in the final cell therapy product (CTP).

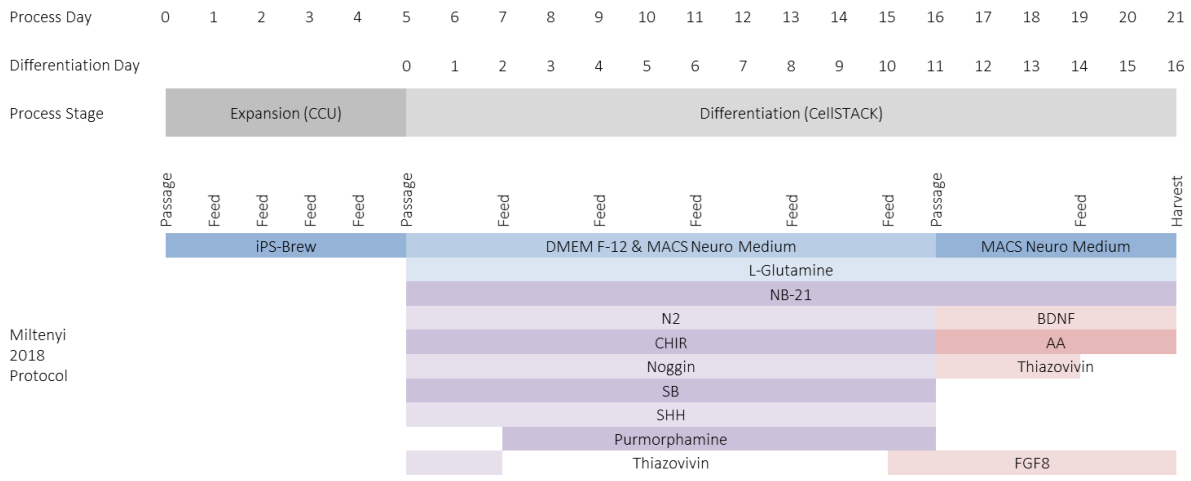

Figure 20 – Summary of the most recent 2018 Miltenyi method. Changes from the previous Miltenyi protocol include the movement of feed day 9 to 10, the addition of purmorphamine from differentiation day 2 to 11, and the addition of FGF8b from differentiation day 10 to 16.

The Miltenyi protocol includes a modified feed schedule to decrease gaps between feeds. Media change days in the Lund 2017 differentiation method were optimised to avoid the requirement for weekend media changes, however this approach may be sub-optimal for the cell product. The Miltenyi 2018 protocol removes the two-day media change gap between days 4 and 7, opting for media changes every two days from day 0 to 10. The Miltenyi protocol also includes several reagent changes, including functionally identical reagent substitutions for Miltenyi products such as MACS Neuro Medium and MACS NeuroBrew-21 (NB-21) in place of Gibco CTS Neurobasal Medium and B-27 supplement, as well as StemMACS Thiazovivin in place of the ROCK inhibitor Y27632.

The neural supplement NB-21 was used throughout the process to support cell growth and reduce cell death (Chen *et al.*, 2008). This addition is listed as a potential solution to excessive cell death on or shortly after differentiation day 4 in the Lund 2017 protocol (Nolbrant *et al.*, 2017), a behaviour described as typical in H9 cells and observed by Miltenyi during process development. Although NB-21 reduces cell death in general, its use early in the process may also contribute towards continued survival of undesirable cell lineages which would otherwise be lost early in the differentiation process (Rajamani *et al.*, 2014).

Purmorphamine was also included between days 2 and 11 to promote ventralization. The use of purmorphamine is recommended in the Lund 2017 protocol as a troubleshooting step if over 90% of cells are expressing OTX2+ but less than 80% are LMX1+/FOXA2, as determined by the flow cytometry analysis detailed in Section 3.5.3. Product cells expressing PAX6 with insufficient FOXG1 may have differentiated towards lateral rather than ventral patterning. Purmorphamine is a small molecule agonist of the SHH signalling pathway and promotes ventralization (Nolbrant *et al.*, 2017). As purmorphamine may also induce cell death (Nolbrant *et al.*, 2017), seeding density at differentiation day 0 was therefore increased from 1 x 10^4 per cm^2 to 2.5 x 10^4 per cm^2.

3.3.3.1 Media Preparation

Media preparation for the Miltenyi process was performed on differentiation day 0, with the exception of the addition of ROCK inhibitor which is prepared freshly on the day of use. Medium for the Miltenyi protocol is split into three types, with reagents and concentrations varied depending upon progress throughout the differentiation.

Neural Induction Medium (NIM) is used on days 0 and 2 and consists of DMEM F12 (50% *v/v*), NeuroMACS (50% *v/v*), L-Glut (2 mM), N2 (1:100), NB-21 (1:50), CHIR (0.7 µM), Noggin (100 ng/ml), SB

(10 µM), SHH (600 ng/ml), with thiazovivin (2 µM) on day 0 only and Purmorphamine (0.1 µM) on day 2 only. Neural Proliferation Medium (NPM) was used from day 4 to 10 and consists of DMEM F12 (50% *v/v*), NeuroMACS (50% *v/v*), L-Glut (2 mM), N2 (1:200), NB-21 (1:100), CHIR (0.7 µM), Noggin (100 ng/ml), SB (10 µM), SHH (600 ng/ml), Purmorphamine (0.1 µ M), with the addition of FGF8b (100 ng/mL) on day 10 only. Neural Differentiation Medium (NDM) is used from day 11 to 16 and consists of MACS-Neuro-Media, L-Glut (2 mM), NB-21 (1:50), BDNF (20 ng/ml), Ascorbic Acid (0.2 mM), FGF8b (100 ng/mL), with thiazovivin (2 µM) added on day 11 only. Cell seeding, maintenance and passage were performed as described in Section 3.2 using feed timings as shown in Figure 20.

3.4 Manipulations for Expansion and Differentiation on CliniMACS Prodigy

Previous sections in this chapter have described manual protocols for the expansion of embryonic stem cells and their differentiation of to mesDA progenitors. A goal of this work was to transfer various manual processing steps onto the Prodigy device for automation within a closed system. The plasticware and consumables specific to automated work are provided in Table 8, while reagents used for expansion and differentiation are common to for both manual and automated methods and are provided in Table 4 and Table 5 respectively.

Table 8 – Closed and automated process specific plasticware and consumables.

Product	Supplier	Catalogue Number
1-chamber CellSTACK	Corning	3268
1-meter tube extension	Miltenyi	130-017-904
500mL Storage bottle w dip-tube	Corning	11665
CellSTACK fill-cap	Corning	3282
CliniMACS-Buffer	Miltenyi	700-25
Corning-bottle 500mL	Corning	430282
Flexboy 500mL bag	Sartorius	FFB102670
Flexboy 50mL bag	Sartorius	FFB102603
TrypLE	Miltenyi	12563-029
Trypsin-Inhibitor	Invitrogen	170750290
TS730	Miltenyi	130-097-187
TSCD wafers	Terumo	W017

3.4.1 Adaption of Manual Aseptic Technique to Automated Processing

Manual aseptic technique utilises rigid containers with screw top lids which are either held or set down onto the sterile surface of a BSC during liquid transfers. Liquid manipulations occur with serological pipettes or pipette tips and either a manual or motorised air displacement controller. Reagent preparation for single use tubing-based systems such as the Prodigy involve liquid transfers to and from flexible bags and dip tube containers (Figure 22) with Luer lock connector (Figure 23). Manipulations with this type of equipment is poorly standardised and rarely described in detail.

Figure 21 – Photograph of the active process during seeding of the CellSTACK during a process run. Shown are the liquid transfer bags (A), Prodigy tubing set (B), Prodigy interface screen (C), Terumo tube welder (D), Prodigy CCU (E), Prodigy waste bag (F), CellSTACK (G) and dip tube bottle (H). A CellSTACK (G) and dip tube media bottle (H) are connected to the tubing set (B) using a tube welder (D).

The key manipulations when working with the Prodigy are addition and removal of liquid from flexible bags, addition of liquid to dip tube bottles, and connection and disconnection of vessels to the Prodigy tubing system.

Liquids were transferred into flexible bags by first removing the plunger from a syringe with a male Luer connection while partly unwrapped. The cap of a female Luer connection on the container was then removed and placed on a sterile surface, and the syringe connected to the tubing. The syringe opening was then treated as the opening on a typical vessel, with liquid added using a serological pipette and care taken to avoid movements above the opening to ensure sterility. After liquid had drained into the container, the syringe was removed and the Luer cap replaced. For removal of liquid from a flexible bag, a male Luer threaded syringe was connected to a female threaded bag or bottle port with its plunger fully depressed. Liquid was then drawn out of the container using the syringe, which was then disconnected, and the liquid dispensed into a separate waste bottle.

For liquid addition or removal from dip tube bottles the lid was unscrewed and the bottle treated as a typical open container. The lid and dip tube attachment were either stored in a second sterile bottle or held by a second operator within the BSC during the manipulation.

Figure 22 - Flexboy bag (Sartorius, 2020) *and dip tube bottle with Luer dip tube connections* (Corning, 2019a).

Connection of closed containers to the Prodigy was achieved using a TSCD-II welder (Terumo BCT) (hereinafter referred to as the tube welder), which forms a connection between two sections of tubing enabling a sterile liquid flow path. Disconnection of containers from the Prodigy tubing set was performed using the tube sealer built into the Prodigy, which compresses and heats the tubing to form a seal. Three seals on the tubing were made for redundancy with the centre seal then cut with scissors.

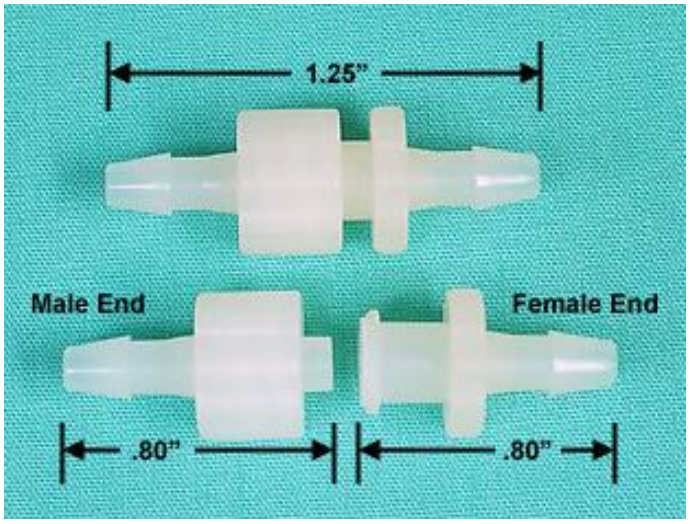

Figure 23 – Connected and disconnected Luer lock connectors (OzoneLab Instruments, 2020)

3.4.2 Automated Expansion and Differentiation Process Steps

Manual cell expansion and differentiation steps were modified for use with the Prodigy by Miltenyi. Key changes required were reductions in feed volumes to within acceptable limits for CCU and CellSTACK containers, and allowances for dead volumes liquid losses due to clearing tubing and are summarised in Table 9. Much of the processing for each process step on the Prodigy is automated. The culture process is initiated by selecting the relevant programme from the Prodigy's touch screen menu. The main operator involvement in these processes is the attachment of the correct liquid in bags prior to running a program, and interventions to take samples and attach / detach vessels according to onscreen instructions during automated processing.

Table 9 – Summary of the Lund 2017 and Miltenyi 2018 differentiation protocols, adapted for use on the Prodigy. Feed volumes are provided for the CCU during the expansion phase and for a single layer CellSTACK during differentiation.

		Lund 2017 Protocol			Miltenyi 2018 Protocol		
Process Day	Differentiation Day	Process Stage	Media	Volume	Process Stage	Media	Volume
-1		Coat CCU with laminin 521			Coat CCU with laminin 521		
0		Start expansion	iPS-Brew + Y27632	40 ml	Start expansion	iPS-Brew + Thiazovivin	40 ml
1		Feed	iPS-Brew	40 ml	Feed	iPS-Brew	40 ml
2		Feed	iPS-Brew	40 ml	Feed	iPS-Brew	40 ml
3		Feed	iPS-Brew	40 ml	Feed	iPS-Brew	40 ml
4		Feed & coat with laminin	iPS-Brew	40 ml	Feed & coat with laminin	iPS-Brew	40 ml
5	0	Seed differentiation	N2 medium + SM, Y27632	150 ml	Seed differentiation	NIM + Thiazovivin	150 ml
6	1						
7	2	Feed	N2 medium + SM	150 ml	Feed	NIM + Purmorphamin	150 ml
8	3						
9	4	Feed	N2 medium + SM	150 ml	Feed	NPM	150 ml
10	5						
11	6				Feed	NPM	250 ml
12	7	Feed	N2 medium + SM	250 ml			
13	8				Feed	NPM	250 ml
14	9	Feed	N2 medium + FGF8b only	250 ml			
15	10	Coat with laminin 111			Feed & coat with lam 111	NPM + FGF8b	250 ml
16	11	Replate	B27 medium + SM, Y27632	250 ml	Replate	NDM + Thiazovivin	250 ml
17	12						
18	13						
19	14	Feed	B27 medium + SM	250 ml	Feed	NDM	250 ml
20	15						
21	16	Harvest			Harvest		

Preparation of medium for automated runs of the Lund 2017 and Miltenyi 2018 processes were performed as described in Section 3.3, with the exception of increased medium volumes and changes to manipulations outlined in this section.

The steps in Figure 24 describe the programmatic process for expansion and differentiation of H9 or RC17 cells as performed on the Prodigy according to the Miltenyi 2018 protocol.

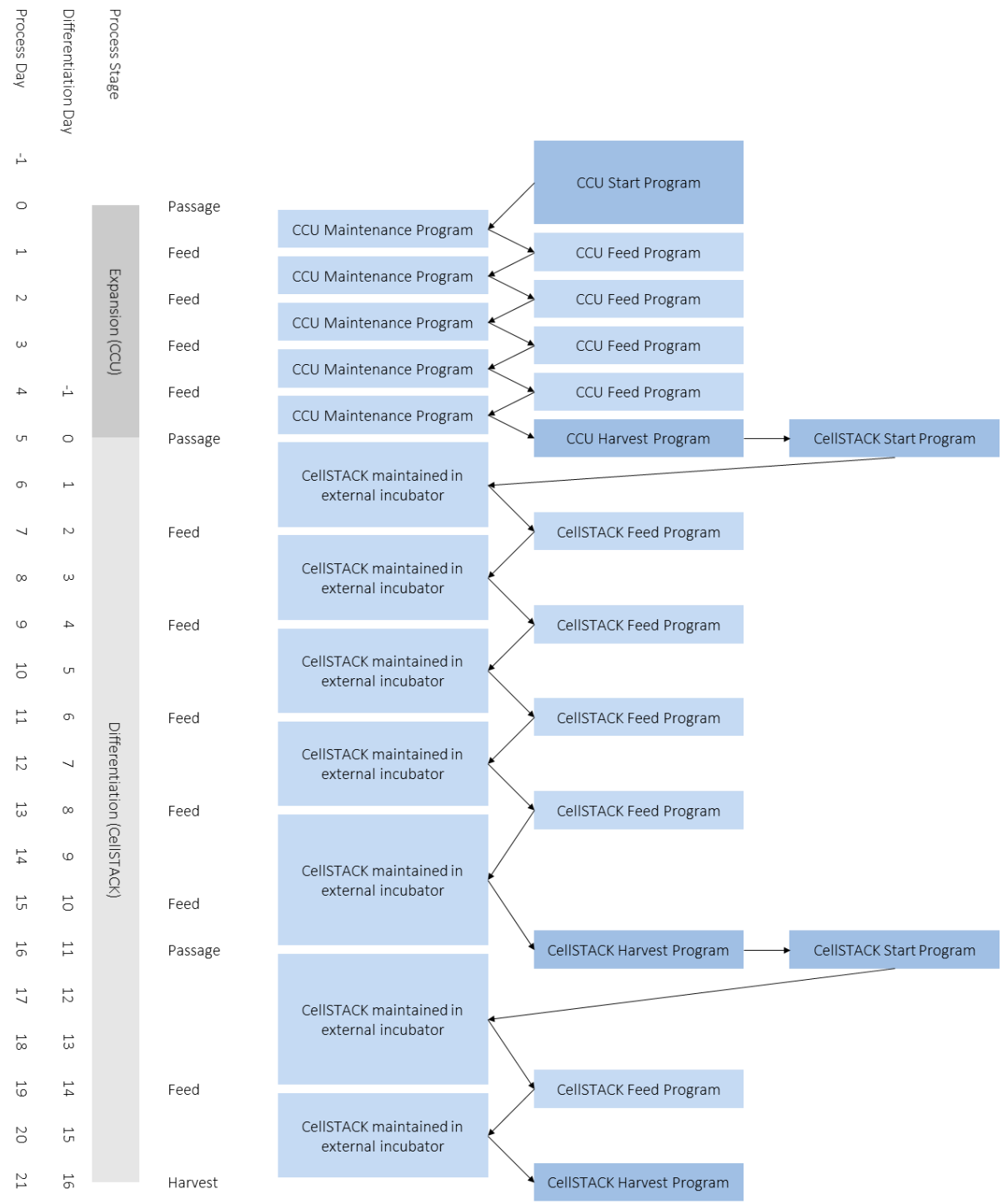

Figure 24 - Summary of the Miltenyi 2018 differentiation protocol showing the programmatic steps required. Dark blue boxes represent steps requiring significant time and user input, with light blue boxes representing minor or passive process stages.

3.5 Analytical Techniques

The following section details analytical techniques used to determine cell health, cell counts and surface marker expression during general cell maintenance and during experiments.

3.5.1 Microscopy

Cells were imaged prior to each feed and passage using light microscopy (Eclipse Ti-S inverted microscope and DS-Fi2 camera, Nikon). Cultures were examined at x4 and x10 magnification for observation of colony trends and x40 magnification to discern cell morphology and to check for bacterial contamination.

The utility of microscopy as a diagnostic tool is high throughout pluripotent expansion and during early differentiation when cells are not fully confluent, allowing growth and morphology to be assessed as shown in Figure 25. For differentiations, microscopy provides qualitative success and failure metrics such as cell attachment, growth and morphology as shown in Figure 26.

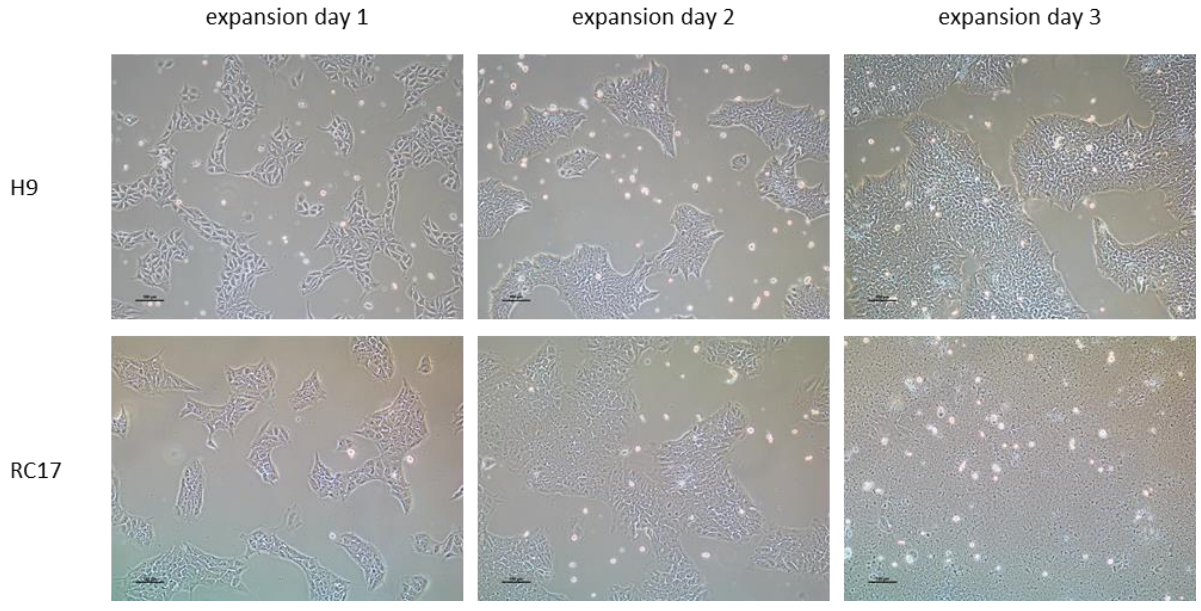

Figure 25 - Example of microscopy for healthy pluripotent cell growth. Cell attachment is visible due to the flattened morphology after 24 and 48 hours. Confluency was increased with each time point. Dead cells have detached and are visible as bright white points, with the number of dead cells low compared to the number of attached cells in all cases. RC17 cells have a higher growth rate in comparison to the H9 cells, reaching confluency by expansion day 3 after seeding at 2 x 10^4 per cm^2. Scale bar equivalent to 100 µm.

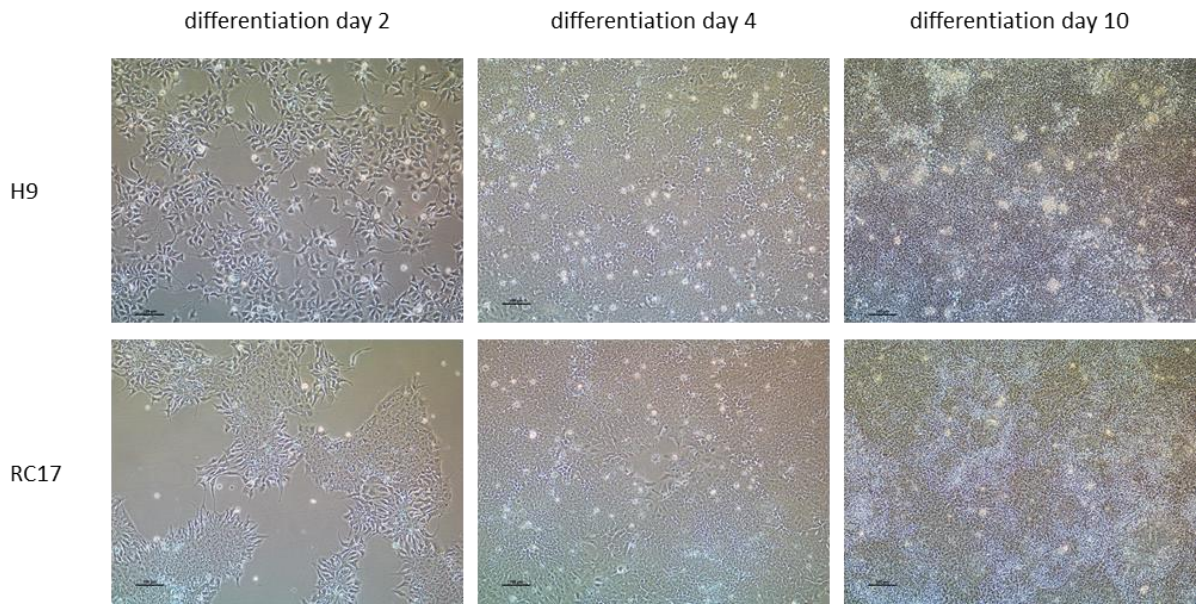

Figure 26 – Example microscopy images of a healthy pluripotent to mesDA progenitor cell differentiation process. It is challenging to see detail by day 4 as no colony edge is visible at full confluence for either cell type. By differentiation day 10, cells are forming multiple layers, and areas of high cell thickness are visible as brighter white regions.

3.5.2 Cell Counting

Cell counts and viability measurements were performed during cell resuscitation, passage and prior to cryopreservation to ensure processes were performed at the desired cell density and as an indicator of process yields and cell health. Cell counts for this work were obtained using a Chemometec NucleoCounter NC-3000 image cytometer using the Viability and Cell Count using NC-Slides - Mammalian Cells assay. This assay comprises acridine orange staining of all cells and DAPI staining of cells with reduced membrane integrity. 10 µL of Solution 13 (Chemometic, 910-3013) was added to a 190 µL sample of cell solution. The sample was then vortexed for 5 seconds to ensure a homogenous cell suspension and 10 µL cell suspension was dispensed per chamber into three chambers of an A8 slide (Sartorius Stedim, 942-0003), or 30 µL per chamber into two chambers of an A2 slide (Sartorius Stedim, 942-0003). Total cell count per ml, viability percentage and viable cell count per ml were recorded for each chamber, with viable cells per ml averaged to obtain an average viable cell count per ml cell suspension.

3.5.2.1 Seeding Volume

During a passage or cell thaw, cells were counted to determine the density of the cell pool. The liquid volume to be seeded into each container was determined as:

$$v = \frac{x_s}{x_p} \quad (1)$$

Where v is the volume to be seeded, x_s is the cell count to be seeded per container and x_p is the cell density of the pool.

3.5.2.2 Specific Growth Rate

Specific growth rate is defined as "the rate of increase of biomass of a cell population per unit of biomass concentration" (Godoy-Hernández and Vázquez-Flota, 2012) and is the gradient of a curve formed where cell number is plotted against time. Specific growth rate is a useful metric of cell performance and may be calculated as:

$$\mu = \frac{ln(x/x_0)}{t} \quad (2)$$

Where μ is the specific growth rate, x is the cell number at the end of the growth period, x_0 is the initial cell number, and t is the duration of the growth period in hours.

3.5.3 Flow Cytometry

Flow cytometry was utilised as a method of measuring cell surface marker expression to determine cell identity. An assay capable of reliably distinguishing correctly patterned mesDA progenitors, as well as cells exhibiting markers of pluripotency and undesired neural lineages, is essential as a quality control (QC) measure for final CTP release. As part of the Neurostemcellrepair (NSCR) Consortium, Miltenyi

developed a flow cytometry assay to assess cell product identity and purity (Neurostemcellrepair, 2018). For this work, patterning of hESCs to mesDA progenitors was assessed *via* flow cytometry using a BD FACSCanto II (BD Biosciences, US). The reagents and consumables required for flow cytometry panels for this work are provided in Table 10.

Table 10 - Flow cytometry consumables for analysis of according to the Neurostemcellrepair quality control assay.

Product	Supplier	Catalogue Number
Anti-FoxA2-APC (clone REA 506)	Miltenyi	130-107-774
Anti-IAP-PE (clone REA 220)	Miltenyi	130-118-962
Anti-Ki67-FITC (clone REA 183)	Miltenyi	130-117-691
Anti-Nkx2.1-Alexa488 (clone EP1584Y) – FITC	Novus Biologicals	NBP234544AF488
Anti-Nkx6.1-Alexa647 (clone R11-560) – APC	BD Biosciences	563338
Anti-Oct3/4-APC (clone REA 622)	Miltenyi	130-109-717
Anti-Otx-2 (pure, monoclonal)	Abcam	ab92326
Anti-Pax6-PE (clone REA 507)	Miltenyi	130-107-775
Anti-Sox1-PE (REA 698)	Miltenyi	130-111-043
EDTA	Gibco	15400054
Fixation/Permeabilization Solution Kit (1 & 2)	BD Biosciences	554714
goat anti rabbit – FITC	Abcam	ab6717
Human Serum Albumin (HSA)	Irvine Scientific	9988
Perm/Wash Buffer (x10 concentrate)	BD Biosciences	554723

3.5.3.1 Sample Preparation

Pluripotent cells from differentiation day 0, as well as unstained cells and three biological repeats of differentiated cells from days 11 and 16 were each analysed via flow cytometry. Each sample had three technical repeats, giving a total of 27 analyses. Antibodies were split into 3 panels as follows:

Panel 1

- Anti-Oct3/4-APC (clone REA 622)
- Anti-Pax6-PE (clone REA 507)
- Anti-Ki67-FITC (clone REA 183)

Panel 2

- Anti-FoxA2-APC (clone REA 506)
- Anti-IAP-PE (clone REA 220)
- Anti-Otx-2 (pure, monoclonal) & secondary antibody (goat anti rabbit – FITC)

Panel 3

- Anti-Nkx2.1-Alexa488 (clone EP1584Y) - FITC
- Anti-Nkx6.1-Alexa647 (clone R11-560) - APC
- Anti-Sox1-PE (REA 698)

Samples were first fixed by resuspending in fixation solution (fix/perm solution 1 (25%), fix/perm solution 2 (7.5%)) for 30 minutes in the dark at 4 °C. Samples were then washed in protein extraction buffer (PEB) (PBS, HSA (0.5%), EDTA (2 mM)) and centrifuged at 300G for 5 minutes, then resuspended in permeabilization buffer (deionised water (90%), fix/perm solution 2 (10%)).

Samples were then centrifuged, and the stained samples resuspended in the staining mix, while unstained samples were resuspended in permeabilization buffer. Samples were then wrapped in foil and transferred to 4 °C for 30 minutes. The cells were then washed by the addition of permeabilization buffer and centrifugation. For the secondary antibody, cells were centrifuged and resuspended in the secondary antibody mix for 10 minutes at 4 °C, followed by resuspension in permeabilization buffer and centrifugation. All samples were then resuspended in PEB buffer and 250 µl transferred to a flat bottom 96 well plate for each analysis. Samples were measured using the following BD FACSCanto II settings:

Table 11 - BD FACSCanto II parameters for samples during flow cytometry.

Flow Parameter	Value
Flow rate	0.5
Sample volume	200 µl
Mixing volume	100 µl
Mixing speed	100 µl
Mixes	5
Wash volume	200 µl
Events Analysed	30,000

3.5.3.2 Gating Strategy

Following flow cytometry analysis, data was gated according to methods defined by Miltenyi (Neurostemcellrepair, 2018). Debris were first excluded by plotting forward scatter area on the X axis (FSC-A) versus side scatter area on the Y axis (SSC-A). Data points with lower FSC-A than the bulk of data points were excluded as debris, and the remaining data points labelled as cells. Doublets and clumps were then excluded as positive and negative cells may have clumped together, allowing negative cells to be counted as positive as the group fluoresces. Forward scatter height (FSC-H) on the X axis was plotted against forward scatter width (FSC-W) on the Y axis with all data points of higher than typical FSC-W excluded as doublets. Finally, gates were applied according to the expected expression levels provided in (Neurostemcellrepair, 2018), as shown in Table 12. Analysis at Loughborough University was performed using the FlowJo software package, while analysis at Miltenyi was performed using FlowLogic software.

Table 12 - Flow cytometry markers with their expected levels. QC thresholds have been defined by the Neurostemcellrepair Consortium for cell therapy product release (Neurostemcellrepair, 2018) *and are highlighted in blue. High +, low -, and intermediate (+) levels are defined by Miltenyi Biotec. Thresholds for IAP and Ki-67 markers have not yet been defined.*

Marker - Stain	Expected mesDA			Description
	D0	D11	D16	
Oct3/4 – APC	+	-	≤ 0.08% detection limit	Pluripotency marker
Pax6 – PE	-	-	< 5%	Non-neuronal floorplate markers (present in dorsal and lateral populations)
Ki67 – FITC	+	+	+	Proliferation marker
FoxA2 – APC	-	+	> 85%	Midbrain floor plate marker (present in the anterior ventral midbrain, posterior ventral midbrain and ventral hindbrain)
IAP – PE	-	+	+	mesDA surface marker
Otx2 – FITC	(+)	+	> 85%	Midbrain and forebrain marker (not expressed in hindbrain, allows discrimination between mid and hindbrain)
Nkx2.1 – FITC	-	(+)	5 - 90%	Anterior ventral midbrain marker
Nkx6.1 – APC	-	-	< 5%	Gli transcription factor, present in lateral midbrain and hindbrain
Sox1 – PE	-	-	< 5%	Present in primitive neuroectoderm, lateral floor plate, marks all non-floorplate neural domains

The key markers for mesDA identification are FoxA2 and Otx2, with expression levels of over 85% deemed acceptable for product release (Neurostemcellrepair, 2018). The threshold for FoxA2 and Otx2 positive cells of >85% set by the NSCR is currently under review by Miltenyi Biotec as expression commonly drops after day 11, resulting in insufficient expression at day 16.

Contamination of the CTP with embryonic cells is identified using the pluripotency marker Oct3/4. Any hESCs present in the CTP are potentially teratoma forming and therefore carry a high risk to the patient. For this reason, the threshold set for acceptable Oct3/4 expression in the CTP is below the detection limit of the flow cytometry system used. Contamination of hindbrain lineages is identified with positive Nkx6.1 and negative Otx2 expression, with Otx2 expression decreasing closer to that anterior than the Nkx6.1 expression increase. Pax6 is also utilised as a negative marker for detection of contamination of non-neuronal floorplate populations, such as those in the dorsal and lateral midbrain. Expression of Ki67 and Nkx2.1 have been found by Miltenyi to be highly variable, while thresholds for IAP and Ki-67 markers have not yet been defined.

3.6 Cost Modelling

A cost model was developed for the mesDA manufacturing process outlined in Section 3.3.3, and is included in Appendix A. This model was used to compare the costs of product produced in open and manual conditions against closed and automated processing using the Prodigy, as well as to provide reference process costs against which potential process changed may be compared.

The excel framework and data summary algorithms of the model were developed by Charlotte Manley as partial fulfilment of the Mechanical and Manufacturing Engineering MSc Major Project module at Loughborough University. Process specific information such as reference costs and algorithms relating to cell growth and material calculations were contributed by the author.

Bill of materials data was collated in July 2019, with price per unit equal to the list prices on supplier websites, not inclusive of any discounts or promotions. Low cost consumables such as pipette tips and centrifuge tubes were not included in the model due to their minimal impact on overall process cost (Lopes, Sinclair and Frohlich, 2018a), however, high cost specialist consumables such as CellSTACK culture vessels and Prodigy tubing sets were included.

Starting material of 1 x 10^6 ESCs from a working cell bank (Miltenyi Biotec, 2018a) and a dose size of 2 x 10^6 mesDA progenitors were assumed (Kirkeby *et al.*, 2017). The model covers processing from retrieval of a vial from a working cell bank, through expansion, differentiation and downstream

processing and on to cold storage of cell product doses. The model includes costs for materials as well operator and cleanroom time required for the manufacturing process, with cleanroom cost represented by the approximate cost per hour for facility hire within CBE laboratories. Costs associated with sourcing, bank creation, and QC and are not included in the model as these are assumed to be common for manual and automated processing.

3.7 Statistical Techniques

T-tests and ANOVA were performed with Origin data analysis software (OriginLab Corporation, USA). Values are given as mean ± standard deviation of biological repeats unless stated otherwise. Statistical significance of results was assessed using Student T test and one-way analysis of variance (ANOVA), with the threshold of significance set at 0.05. The Bonferroni correction was used to adjust the significance threshold in cases where multiple comparisons were performed.

4 Clinical-like Production Scenario

4.1 Introduction

This chapter explores the steps required to close and automate an allogenic stem cell therapy process, an example of which is shown in Figure 27. A process for the expansion and differentiation of human embryonic stem cells (hESCs) into mesencephalic dopaminergic (mesDA) neural progenitor cells for use as a Parkinson's disease therapy, developed at Lund University (Kirkeby, Nelander and Parmar, 2012; Nolbrant *et al.*, 2017), was selected as the demonstrator for this work. This process was selected due to an existing collaboration between Lund University (Lund University, Sweden), Miltenyi Biotec (Miltenyi Biotec GmbH, Germany), Loughborough University (Loughborough University, UK) and the University of Cambridge (Cambridge Biomedical Campus, UK) to advance commercialisation of this therapy.

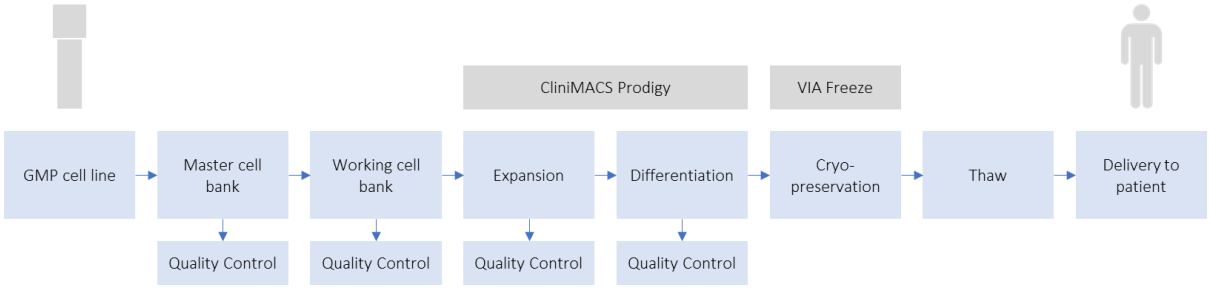

Figure 27 – High level block diagram of the mesDA manufacturing process, from hESC cell line source material to patient delivery in a hospital.

H9 cells (WiCell, USA) were selected as the development cell line due to their frequent use in research and availability for use by Miltenyi Biotec in Germany, where limitations on embryonic stem cell research prevent the use of lines derived after 1st of May 2007 (Schlenke *et al.*, 2008). An initial protocol for a closed and automated mesDA progenitor production from H9 cells was developed by Miltenyi Biotec for the CliniMACS Prodigy system (hereinafter referred to as the Prodigy) and based upon work by Lund University. These protocols will then be adapted for use with the RC17 cell line (Roslin Cells, UK) which are intended as the source material for the proposed Parkinson's disease therapy. This line was selected as it adheres to standards of quality assurance (QA) and GMP required for regulatory approval and achieved positive outcomes during development (Nolbrant *et al.*, 2017).

The Prodigy is a closed and automated cell processing device and was selected for this work due to its ability to automate the culture and centrifugation of adherent cells within a truly closed system at an appropriate scale. The use of closed systems for cell therapy product manufacturing is advised wherever possible in regulatory guidance, as is reduction in the number and complexity of manipulations performed by personnel, with automation and robotics promoted by the FDA as solutions to reduce contamination risk (FDA, 2004). The initial protocol for closed and automated manufacture was further developed in collaboration with Loughborough University during an extended technology transfer process, with the aim of increasing process stability and GMP compliance. This chapter outlines progress towards a clinical-like production scenario as a proof of concept for the transfer of an open manual process to a closed and automated system. This work also highlights challenging areas for process transfers in general, as well as difficulties when working with closed and automated systems and recommendations for solutions to identified problems.

This chapter details manual exploratory work and six automated process attempts, a summary of which is provided in Figure 28. Throughout this chapter, automated process runs will be referred to by their number. Process runs 1, 2 and 3 are discussed in Section 4.3.2 as initial Prodigy expansion runs, while runs 4, 5 and 6 discussed as both demonstrations of the revised expansion process in Section 4.4.4 and as troubleshooting runs for the differentiation process in Section 4.6.1.

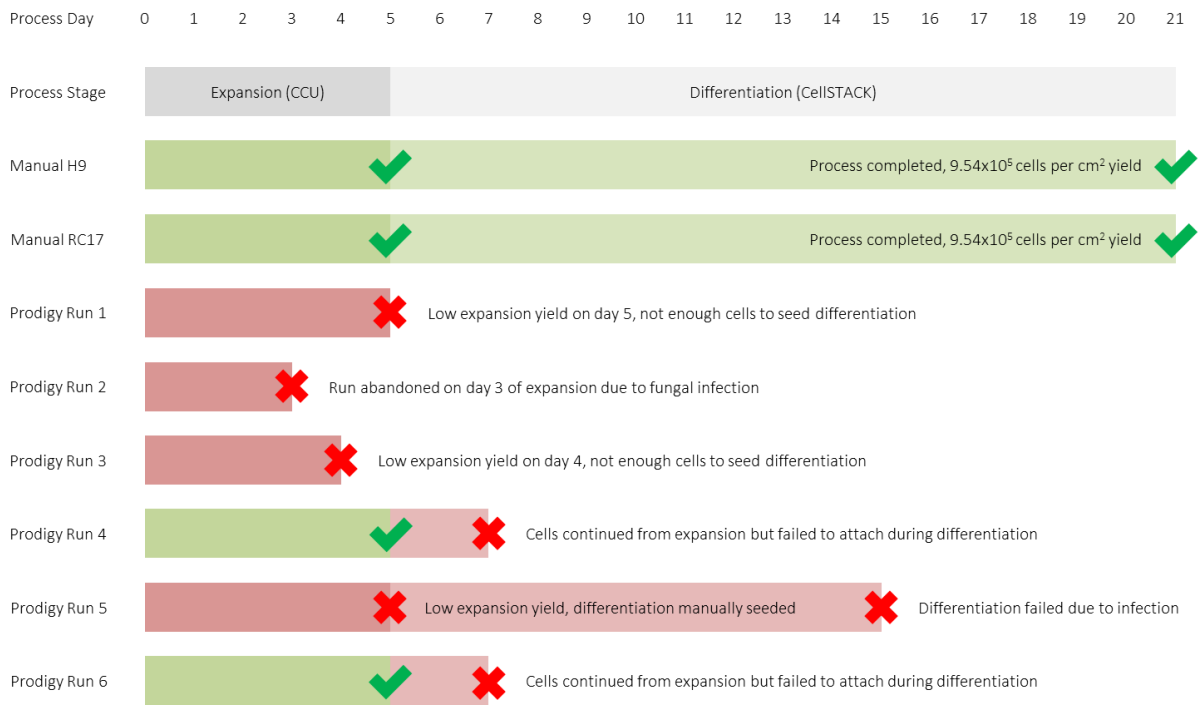

Figure 28 – Summary of manual and automated process runs detailed within Chapter 4. Green bars with ticks indicate successful process steps, while red bars with crosses indicate failed process steps.

4.2 Process Transfer Considerations for the Miltenyi Prodigy

The target device for closure and automation of the expansion and differentiation process is the Prodigy system shown in Figure 29. This system combines a closed single use tubing set, centrifuge, temperature and gassing controlled culture chamber and other components into a single GMP compliant benchtop device (Apel *et al.*, 2013). The Prodigy is optimised for the closed and automated processing of suspension cell types such as blood, and has seen significant use in the field of T cell immunotherapy (Kaiser *et al.*, 2015). A key challenge for this project has been the adaption of a suspension cell processing system for the culture and differentiation of adherent cells such as human embryonic stem cells (hECSs) and neural cell lineages.

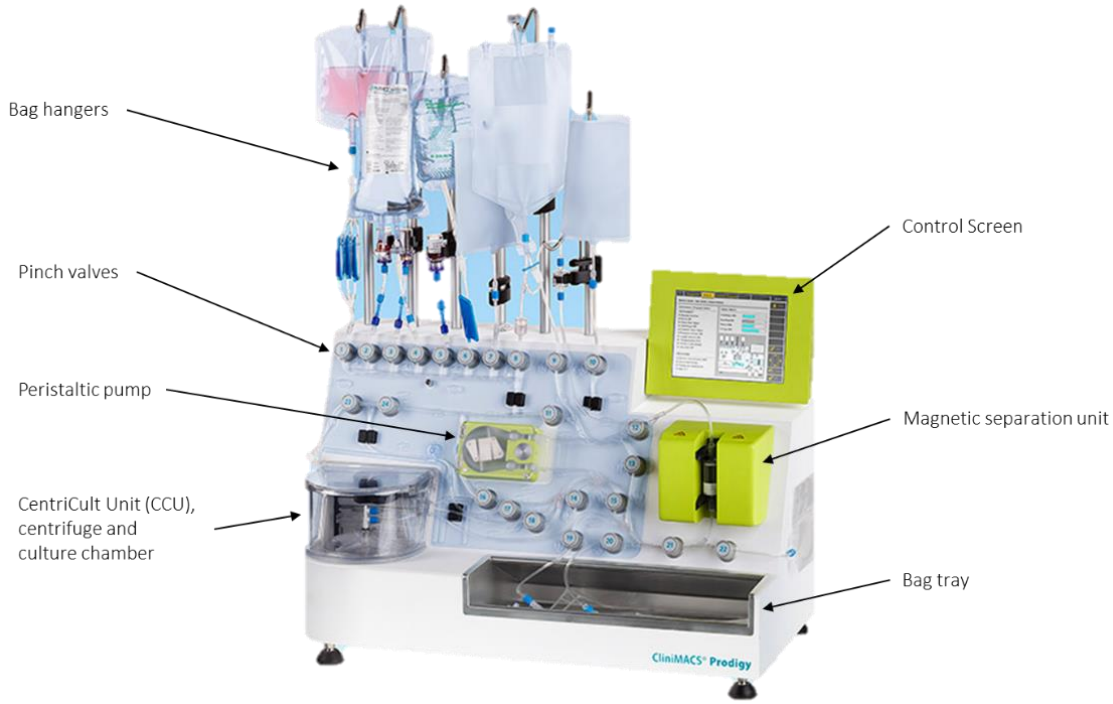

Figure 29 – CliniMACS Prodigy automated cell processing system, produced by Miltenyi. Image adapted from (Miltenyi Biotec, 2020a) *and main components labelled.*

The device features a tubing set through which liquid is transferred using pinch valves and a peristaltic pump. The culture chamber (CentriCult unit, hereinafter referred to as the CCU) shown in Figure 30 is a combined centrifugation chamber and culture vessel whose temperature is controlled via a heated plate at the back of the chamber. Gasses are mixed within the device and transferred to the CCU through an outlet port which connects to the tubing set through a sterile filter. A heat exchange cartridge (HEC) is attached to a heated plate behind the CCU and is used to heat the gas in the chamber as well as liquid as it is pumped from the input ports and into the CCU, avoiding the need to pre-heat liquids. A magnetic separation column also allows for cell sorting through the Miltenyi trademarked magnetic-activated cell sorting (MACS) technology. External culture vessels may also be processed by welding onto the single use tubing set; however, their gassing and temperature must be maintained in external incubators.

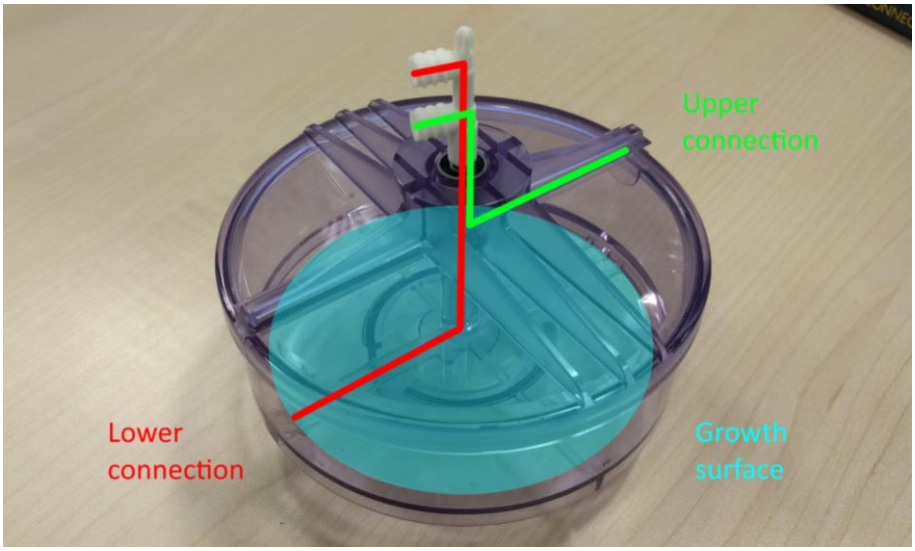

Figure 30 – CCU with highlighted liquid flow paths and cell culture surface.

Single use preassembled tubing sets are used for liquid manipulations on the Prodigy, with specialised and general-purpose tubing sets available. All currently available tubing sets feature a centrifugation chamber, while the heat exchange cartridge (HEC) and magnetic separation columns are included on tubing sets as required. The TS730 tubing set is a general-purpose tubing set and it used for this adherent cell culture process. It includes input and output bag ports, a CCU with HEC gas mix input, and omits a magnetic separation column which is not used in this process.

There is limited opportunity for online analysis during culture on the Prodigy, with processes limited to at-line or offline analysis. Samples cannot be taken from the CCU during culture due to the closed nature of the system and lack of manual sampling ports. There is a microscope camera, but it is incapable of reliably focussing on cells attached to the CCU growth surface and is only available at select points during processing. The CCU chamber has also not been designed with consideration for the requirements of long-term cell culture and features a translucent plastic chamber cover, exposing small molecules to light degradation.

4.2.1 Example Liquid Manipulation Process

Liquid manipulations on the Prodigy are performed through control of the peristaltic pump and pinch valves within a single use tubing set, the layout of which for the mesDA progenitor manufacturing process is shown in Figure 31. Pinch valves compress tubing threaded through them to create an air

and liquid tight seal, with all pinch valves being normally closed to prevent gas and or liquid flow in their resting state.

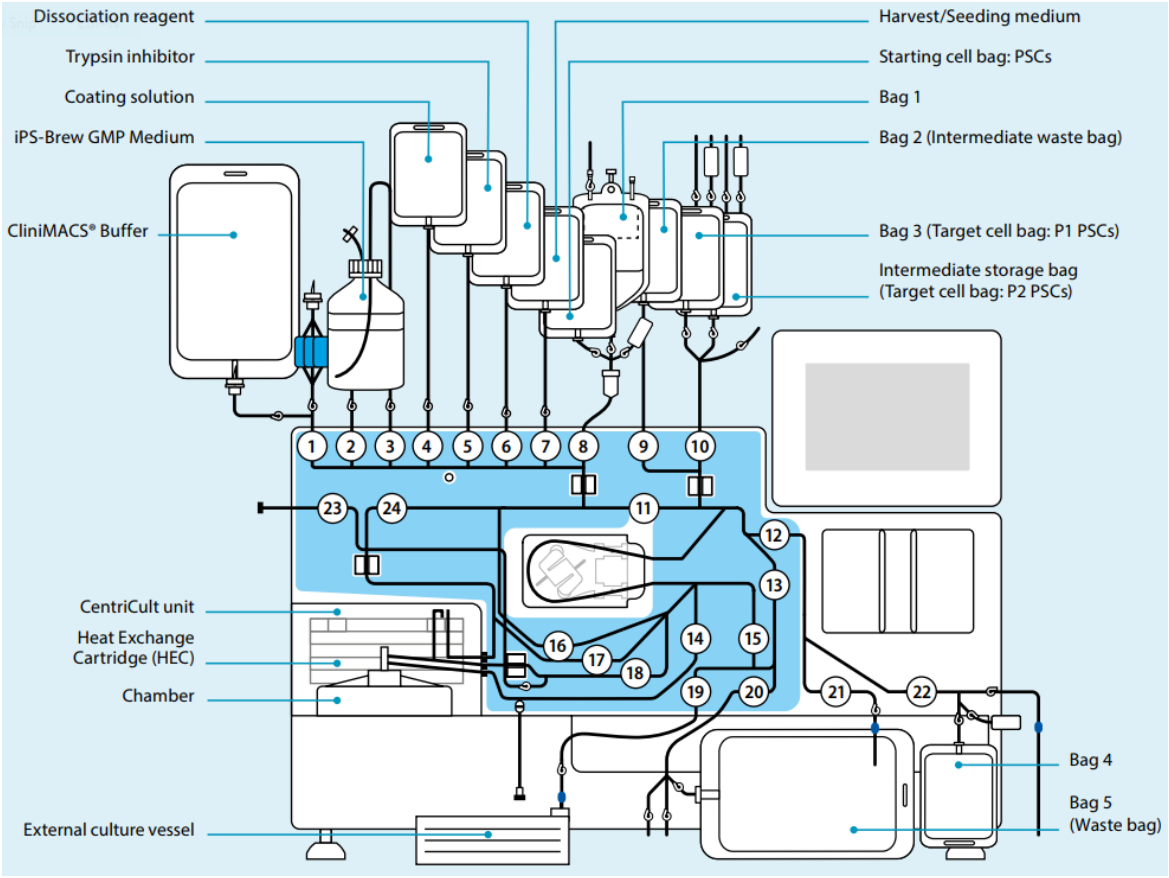

Figure 31 – Layout of the TS-730 tubing set. Numbered circles indicate pinch valve locations while thick black lines indicate tubing. Unlike most tubing sets, the TS-730 is not designed for a specific cell therapy process and is optimised for flexibility. Image from Miltenyi application note (Miltenyi Biotec, 2018b).

To move liquid through the system, all pinch valves on the desired route are opened (from the source, through the peristaltic pump, and on to the destination) while all others remain closed, effectively producing a single open tubing path through which liquid can flow. The peristaltic pump is then rotated to create a pressure differential between the two ends of the open path, causing liquid to flow. The liquid movement technique is illustrated for a medium change in Figure 32. To transfer liquid from the CCU to a waste bag, valves are opened to create a single path from the CCU, through the peristaltic pump and to the waste bag. The pump is then rotated, creating a negative pressure at the source and pumping liquid through to the waste bag destination. New media is added to the CCU by opening pinch valves on the route from input port 1, through the pump and onto the CCU, leaving all other pinch valves closed.

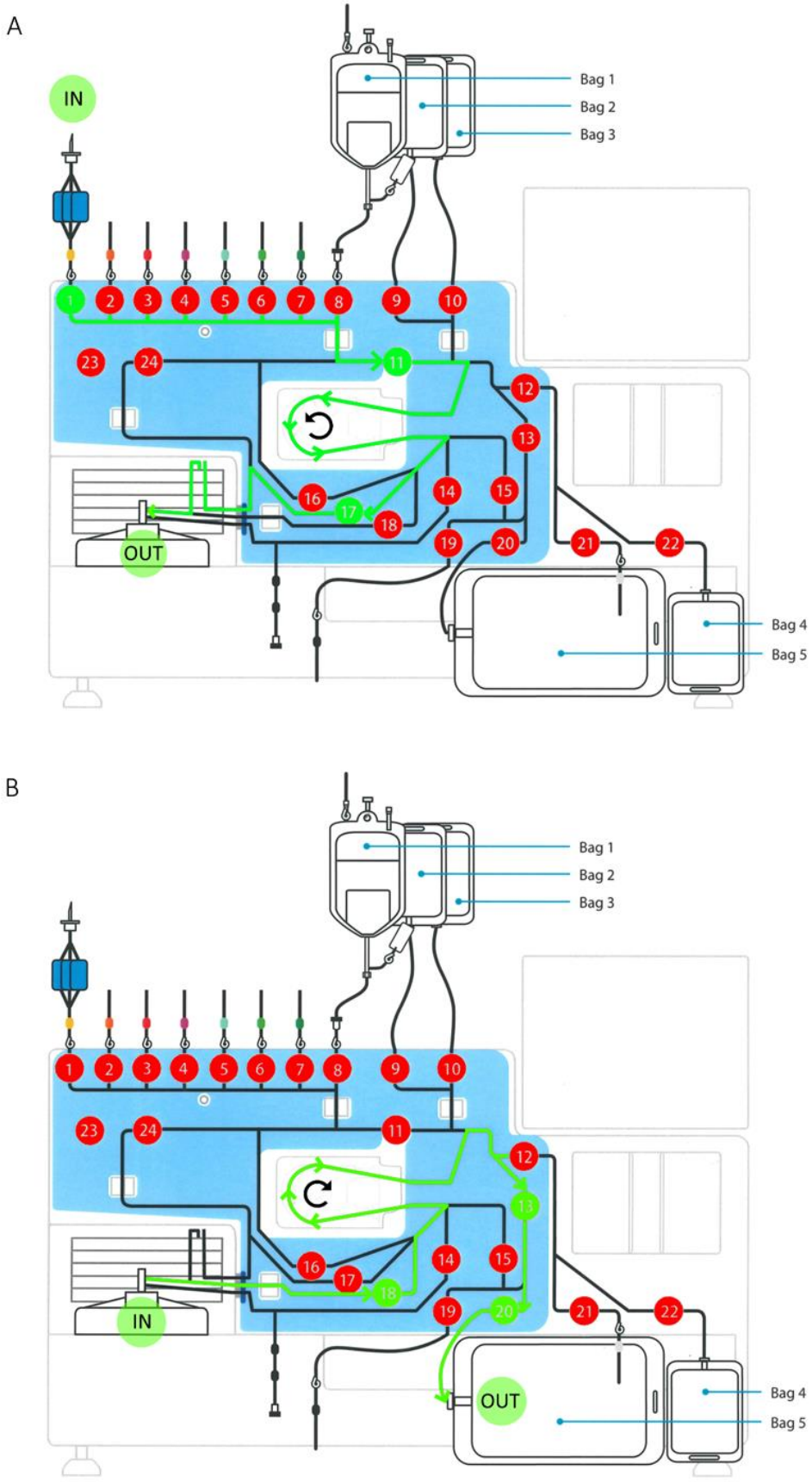

Figure 32 – Liquid manipulations during a routine medium change. Closed valves are shown in red, open valves in green. Step 1 (A): removing spent media from the culture chamber to the waste bag on port 20. Step 2 (B) adding fresh media from input port 1, through the heat exchange cartridge and into to culture chamber. Images adapted from (Miltenyi Biotec, 2018b).

4.3 Technology Transfer Process

The initial aim of this project was to demonstrate comparability between the process for expansion and differentiation of H9s to mesDA progenitors on the Prodigy as performed by Miltenyi compared to the same process performed at Loughborough University. To achieve this goal, a technology transfer was initiated to migrate the process. Two operators from Loughborough University visited Miltenyi at the headquarters in Bergisch Gladbach, Germany from 13/03/2017 to 16/03/2017 and ran through key process steps on the Prodigy, with training lead by a Miltenyi operator. Training included Loughborough operators observing and performing a tubing set installation and removal as well as cell seeding, maintenance and harvest in both the CCU and CellSTACK. Cells prepared by Miltenyi to demonstrate later process stages became infected on day 3, meaning that elements of the training were not possible for Loughborough operators to perform.

The Prodigy was installed at Loughborough University within class 2 laboratories and placed upon a work surface with mounted drawers in the centre of the laboratory room as shown in Figure 33. Following receipt and installation of the Prodigy at Loughborough University, the Miltenyi operator visited Loughborough from 10/10/2017 to 13/10/2017 and performed key parts of the process using PBS and culture medium, with no cells seeded. Training at Loughborough was hindered by the lack of an available tube welder, resulting in manual handling being significantly different to a clinical production scenario. Due to the lack of comparable outputs due to the infection at Miltenyi and the inability to perform sterile processing at Loughborough University, the process transfer effort to migrate the automated mesDA manufacturing process was never formally completed. A full timeline of events performed as part of the technology transfer effort is provided in Appendix B.

Figure 33 - Installation of Prodigy at Loughborough University. The device was placed on a fixed work surface with attached draws and extends into the centre of the room. Although described as suitable by Miltenyi Biotec, the device was later found to be highly sensitive to physical movement due to closing drawers or bumping of the surface, as well as vibrations caused by moving through detents in rotation of the touchscreen display.

4.3.1 Gap Analysis

Following the training at Miltenyi, a gap analysis was produced to assess differences between the process performed in manual culture with the performance of the same process on the Prodigy and is shown in Table 13. The key process risks highlighted by the gap analysis were heightened infection risk due to process complexity and the use of non-standard aseptic technique and equipment, variability in volume delivery due to dead volumes and variability of tube lengths, and insufficient purification due to incomplete aspiration of the CCU during centrifugation. Other important considerations highlighted were the inability to monitor an ongoing CCU process with microscopy and the inability to rework problems due to the locked CCU chamber.

Table 13 – Gap analysis for cell manipulations as performed in manual culture and automated on the Prodigy.

Process Operation	Manual Process	Automated Process	Perceived Risk
Medium preparation	Medium prepared manually in centrifuge tubes or bottles. Large volumes moved with stripettes and small volumes moved via pipette tip. Prior to use, medium warmed to 37°C for 10 min in a water bath.	Medium prepared manually in 500ml Corning bottles. Large volumes moved with stripettes and small volumes moved via pipette tip. Bottles are capped with caps featuring tubing and an air filter. Prior to use, tubing from the bottle cap is welded onto the Prodigy. Media is heated to 37°C by the HEC during transfer to the CCU (but not when transferring directly to CellSTACK).	Medium will not be warmed to 37°C when transferring directly to CellSTACK, i.e. during CellSTACK seeding.
Plasticware preparation	Plasticware unwrapped, disinfected with 1:50 Chemgene and transferred into BSC.	Plasticware unwrapped, disinfected with 1:50 Chemgene and transferred into BSC. Tubing set preparation: close and check clamps, connect CliniMACS-Buffer, parafilm Luer locks. Bags containing cells require rinsing with medium: add medium to bag using syringe, transfer to incubator for 30 mins, drain bag using syringe.	Risk of infection when preparing tubing set due to the number of leur lock manipulations required (reduced for GMP tubing set).
Coat plasticware with laminin	Prepare coating solution in centrifuge tube, transfer to flasks / CellSTACK using stripette.	Prepare coating solution in centrifuge tube, transfer to bag and weld onto Prodigy. Laminin solution is transferred to CCU / CellSTACK during setup program.	Risk of laminin attachment to bags and tubing. Risk of contamination with buffer or medium during coating.
Seed cells into culture vessel	Transfer the cell suspension in an appropriate volume of seeding medium in to a culture flask / CellSTACK using a stripette.	Transfer the cell suspension in an appropriate volume of seeding medium in to a flexible bag. Weld the bag onto the Prodigy and begin the program to pump an appropriate volume of cells into the CCU / CellSTACK.	Risk of cell loss due to dead volumes as well as attachment to bag and tubing. Risk of inaccurate cell seeding due to low precision of peristaltic pump.
Adding liquid to culture vessel	Liquid added to vessels using stripettes.	Liquid is pumped from the input vessel to the CCU or CellSTACK. For the CellSTACK, liquid may be added directly to the stack, or warmed by passing through the HEC and CCU (requiring prior washing).	Low precision of peristaltic pump. Possibiliy of contamination for warmed CellSTACK liquids from incompletely washed CCU contents.
Remove liquid from culture vessel	Liquid removed from flasks using aspiration pipette and pump.	For the CCU, liquid is pumped from the chamber to the waste bag while the chamber is slowly rotated. For the CellSTACK, an operator is required to hold the stack at 90° (tube cap at the bottom, filter cap at the top) while liquid is transferred to the waste bag.	Risk of incomplete liquid removal in both CCU and CellSTACK. Risk of operator error. Instructions to tilt the CellSTACK to 90° risk an operator tilting to stack to a position where liquid may touch and saturate the air filter cap, resulting in potential contamniation.
Cell culture maintenance	Vessels placed in an incubator at 37°C, 5% CO2.	For CCU, running the CCU culture routine holds the CCU chamber at 37°C, 5% CO2. For the CellSTACK, vessels are placed in an incubator at 37°C, 5% CO2.	Risk of incorrect gassing due to sensitivity of Prodigy to gas input pressure fluctuations. Possible halting of maintenance routines due to machine error e.g. magnet alignment error due to bumped work surface.
Verification of cell detachment	Vessels checked via microscope, if cells are not visually rounding up and detaching, a further minute of incubation will be performed.	No ability to check detachment (the device does have a microscope but it performs very poorly for attached cells).	Risk of incomplete detachment.
Centrifuge and remove supernatant	Centrifuge at 300G for 5 minutes. Transfer to BSC and aspirate supernatant using an aspiration pipette at the shoulder of the conical tube buttom.	Prodigy centrifuges at 1500 rpm (350g), then slows to 800 rpm (42g) to remove liquid from bottom port down to 70ml. The speed is then slowed to 275 rpm (5g) and liquid is removed from the bottom port leaving 35ml in CCU.	Risk of insufficient purification. Minimum centrifuge dead volume is 35ml. Maximum centriuge volume is 350ml, which limits dilution.
Resuspension of cell pellet	Resuspend cell pellet in 1ml of medium by gently lifting and dispensing with a 1ml pipette tip, then add additional medium using a stripette.	Liquid added to CCU chamber which is then rotated.	Risk of highly aggregated cells. Note: the process of extracting a sample will reduce aggretation.
Retreive a sample for viability and cell count assay	Mix tube contents with a stripette or laboratory shaker. Using a 300ul pipette tip, transfer a 190ul sample to an Eppendorf tube. Perform a viability and cell count assay on the NC-3000.	Transfer cells to a bag and weld off the Prodigy, transferring to a BSC. Using a syringe, mix the bag contents by gently extracting and dispensing volume several times. Extract a 5ml sample from the bag and transfer to a tube. Using a 300ul pipette tip, transfer a 190ul sample to an Eppendorf tube. Perform a viability and cell count assay on the NC-3000.	Higher than typical wastage in retreiving sample.

4.3.2 Initial Automated Expansion of embryonic stem cells (ESCs), Process Runs 1, 2 and 3

The first three attempts to culture and differentiate H9 cells into dopaminergic neuron progenitors on the Prodigy experienced limited success as shown in Figure 34, with the CCU failing to produce sufficient cells to seed a CellSTACK and proceed to differentiation. These initial process runs were based on a draft protocol provided by Miltenyi, summarised in Section 3.3.3. The first attempt at expansion of H9 cells on the Prodigy was ended prematurely due to negligible growth and a poor harvest of 1.05×10^4 cells per cm^2 from the CCU on day 5, compared to the manual flask yield of 1.72×10^5 viable cells per cm^2 (equivalent to a specific growth rate of 1.97×10^{-2} per hour) harvested the following day due to time constraints. The CCU failed to produce enough cells to seed a differentiation and continue the process, with the failure attributed to a problem during CCU gassing and possible operator errors during setup or coating. The second expansion of H9 cells within the CCU was halted prior to harvesting due to a visible fungal infection within the tubing set and growth chamber. It was not possible to breach the closed system in order to extract a sample for counting due to the infection, however, microscope observations of the CCU revealed a lack of cell growth on day 5. Control flasks for this run produced an average of 4.08×10^5 cells per cm^2 (equivalent to a specific growth rate of 3.08×10^{-2} per hour). The third attempt at the expansion process on the Prodigy produced a low yield of 2.23×10^4 cells per cm^2 (equivalent to a specific growth rate of 8.36×10^{-3} per hour) from the CCU day 4, 7.5% of the average output of three control flasks which produced 2.97×10^5 per cm^2 (equivalent to a specific growth rate of 3.53×10^{-2} per hour). The process was again halted prior to seeding the differentiation as the CCU did not produce the 7×10^6 cells necessary to seed a CellSTACK.

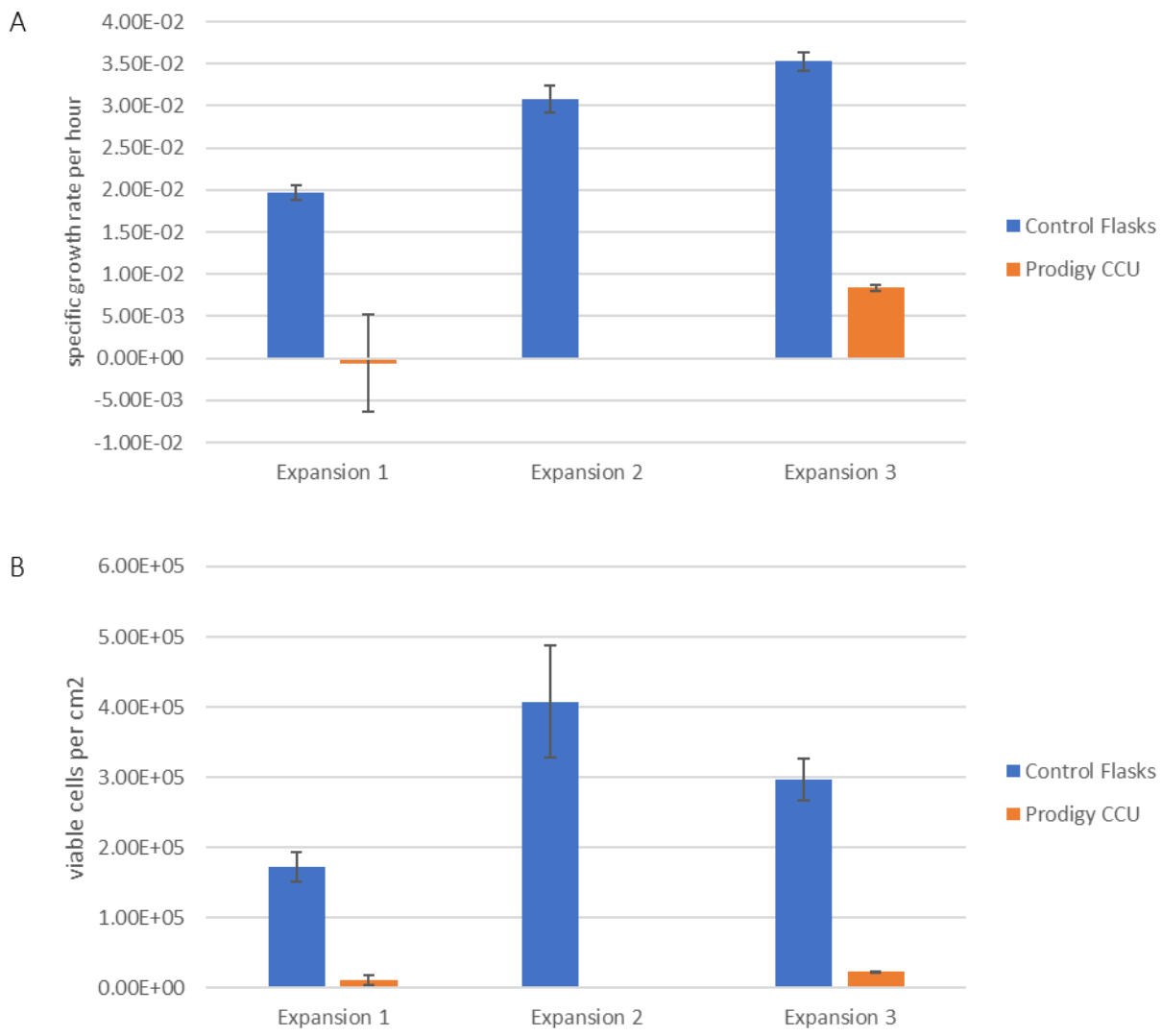

Figure 34 - Specific growth rate per hour (A) and viable cells per cm² (B) for CCU and T-flask grown H9 cells across the initial three expansion attempts. CCU produced very low yield compared to the relatively stable output of control flasks (the specific growth rate of expansion 1 is lower which may be partly attributed to an extra day of growth, having had 6 days of expansion rather than the 5 planned to reach full confluence). Likewise, the high rate of growth seen for expansion 3 may be attributed to 1 day less growth than planned (4 rather than 5), meaning cells were less limited as they grew at lower confluency levels. Error bars shown as mean ± SD for biological and measurement repeats, n=3 for control flasks and n=1 for CCU.

4.3.3 Device Issues

The Prodigy was received as a loan unit from Miltenyi and installed according to provided instructions regarding location and gas inputs. The device and set up was also approved by the Miltenyi development scientist during the initial technology transfer site visit.

4.3.3.1 Prodigy Hardware Issues

During the initial three process attempts the Prodigy was found to be highly sensitive to physical movement, producing a “magnet alignment error” in response to movement of the bench surface (e.g. closing a bench drawer) and rotation of the attached touch control screen. This error triggers a siren requiring operator intervention to clear, and halts the maintenance of CCU temperature and gassing, potentially exposing cells to incorrect temperature and gassing conditions until the error is addressed. This behaviour produces a risk of severe deviations from correct culture conditions if the error is unresolved for some time, which may occur if triggered at night or a weekend. A Miltenyi service engineer confirmed that there was no fault with the system and laboratory users were advised to avoid the surface. Instructions to clear magnet errors and contact Prodigy operators was fixed to the device, and multiple other laboratory users were trained to clear magnet errors if they occur.

The device was also found to be sensitive to gas pressure fluctuations at the lower bound of its acceptable input pressures. The device manual lists 1 to 2.5 bar as the limits for input gas pressure, however, successful gas mixing is unreliable for input pressures of around 1 bar. A Miltenyi service engineer confirmed that a minimum of 1.5 bar input pressure for all gasses is recommended for reliable gassing. This issue was resolved for future process runs by raising the input CO_2 levels to the Prodigy from 1 bar to 1.5 bar.

4.3.3.2 Tubing Set Issues

Luer locks pose a risk to the integrity of the closed system during extended processes. Luer locks rely on friction of a threaded connection to remain mated and preserve sterility, and feature no locking mechanism, making them susceptible to loosening due to vibration and movement. An example Luer lock is shown in Figure 35. A Luer lock loosened and disconnected during manipulation of an adjacent bag during seeding of H9s into the system in the second process attempt and may have contributed to the fungal infection which caused this process to fail. Luer locks are unsuitable for connection alterations performed outside of a BSC. Due to repeated problems in shipping, a sterile tube welder was not available for the first process attempt meaning that bag attachments and detachments were performed via Luer locks, breaching the closed system of the tubing set.

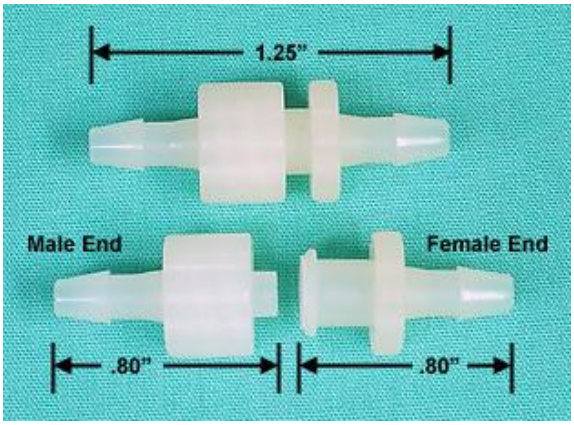

Figure 35 - Luer lock connector, connected (top) and disconnected (bottom) (OzoneLab Instruments, 2020). *Note that Luer locks have no lock or detent mechanism to prevent loosening of the screw thread. They are therefore vulnerable to loosening via vibration and movement.*

Manipulation of tubing and Luer locks on the tubing set and flexible bags is challenging, increasing the likelihood of contamination. The infection on process run 2 may be the result of an error during manual reagent preparation. Securing of Luer locks with parafilm to prevent accidental loosening of connections was added to all future protocol revisions, as well as removal of all liquid pouring steps. Sterile filtering of reagents during transfer to bags was also introduced, although this was later removed as it introduced challenging manual manipulations and was judged to not significantly decrease infection risk.

4.3.3.3 Prodigy Software Issues

Error handling on the Prodigy is problematic as it pauses a running program. Halting a program and requesting operator intervention to continue is an appropriate behaviour during short processes with continuous operator supervision. During the mesDA manufacturing process, the Prodigy is expected to maintain CCU temperature and pressure for periods of several days and may produce an error at any time. With the possibility of no operator intervention for many hours, the maintenance program may halt maintenance of CCU temperature and gas mixing, risking an out of specification event.

A second issue with error handling on the Prodigy is lack of available troubleshooting data following an error detection. A number of errors are delivered as error codes and hardware addresses (e.g. Error #4107 at CANID 1202) which are not listed in available reference material. An example error dialogue is provided in Figure 36. Helpful troubleshooting information would include all relevant information to aid an operator in addressing the error source, e.g. a “NACK” error communicates that a subsystem is

providing a negative acknowledgement and prompts the operator to reset or reinitialise the subsystem but provides limited troubleshooting information, including information such as “nitrogen pressure below acceptable threshold” would prompt an operator to check gas connections before continuing.

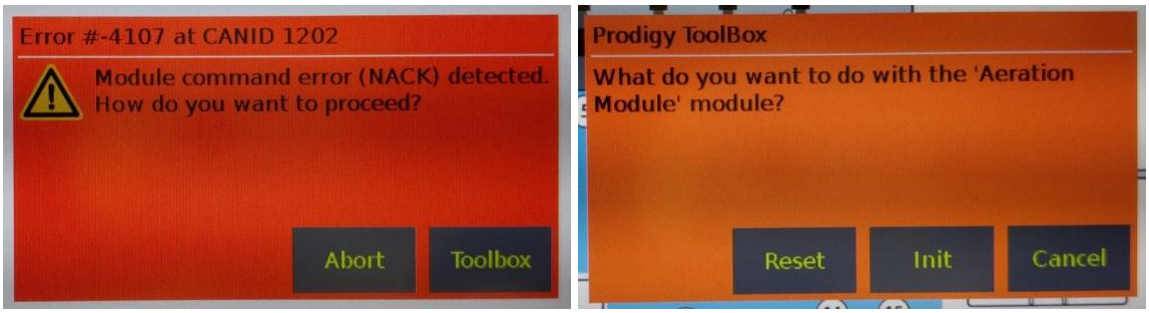

Figure 36 - Example error dialogue boxes during a gassing error caused by low input pressure of CO2.

The lack of troubleshooting data is compounded by the use of ambiguous language in error messages and prompts. Following a gassing error for example, the operator is prompted to reset the Aeration module. Repeated reinitialization of the gas mix unit bypasses the gassing step and advances the running program, resulting in a lack of CCU gassing and therefore lack of gas control during culture. This behaviour is not communicated to an operator at any time, who is likely to assume that gassing has completed successfully on progression of the Prodigy program. This behaviour may also be true for other subsystems such as CCU temperature control.

Another example of ambiguous language is the poor distinction between exiting a programmatic loop to advance to the next step within a program, and aborting the running program, as shown in Figure 37. The CCU setup program was erroneously aborted after 24 hours of laminin-521 coating but before the coating solution was removed from the chamber during run 3. The correct sequence of commands is “OK” followed by “yes”. What was actually entered was “stop” followed by “abort”. This mistake combined with the software bug which prevented draining of the CCU meant that coating solution could not be drained from the CCU prior to cell seeding.

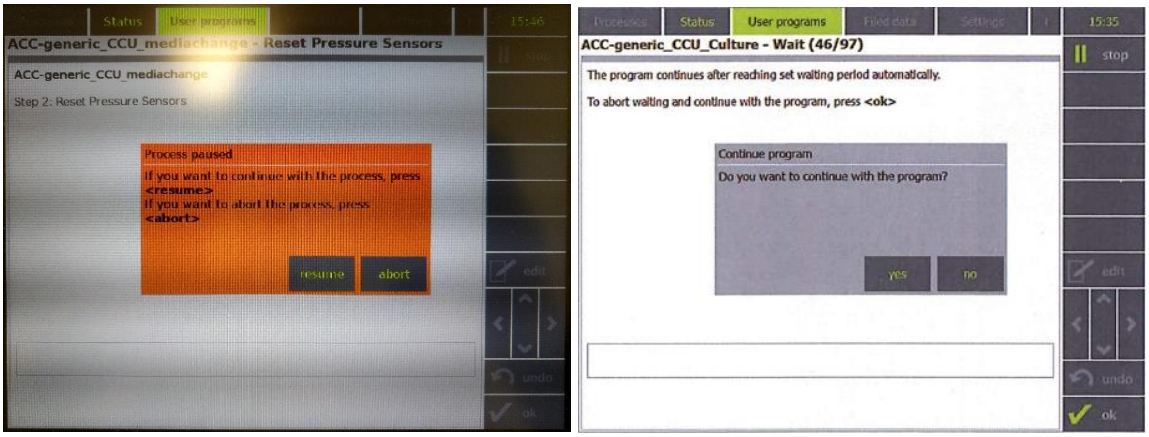

Figure 37 – Dialogue boxes for aborting the current program (left) and exiting a loop to advance to the next step within a program (right). These dialogue boxes use similar language but have drastically different effects on the process. Rewording these options for clarity may prevent operator error and prevent process loss.

Limitations on user actions with regards to both product manipulations and software updates are a further cause of process issues on the Prodigy. Due to the licencing structure of Prodigy software, users may only run programs installed on the Prodigy by a Miltenyi representative and do not have access to single unit operations such as liquid movements. These restrictions are significant barriers to process development, as software bugs identified as causing process issues are not able to be corrected by the user and may contribute to process failure. Secondly, software fixes to bugs cannot be deployed to the Prodigy without a visit from a Miltenyi technician, meaning that during this process transfer effort, several process runs were completed with known software bugs present due to time constraints. The combined effect of these software restrictions is that only users with developer privileges may identify errors, perform online fixes and deploy updated software to the Prodigy, significantly hindering collaborative capability and external process development efforts.

4.3.3.4 Protocol Issues

Miltenyi provided a reagent preparation protocol and software guide, however these documents were not integrated and proved challenging to use when performing the process. The software protocol includes many optional steps and uses ambiguous language which is not consistent with the Prodigy on-screen display. Documents were of a high abstraction level and were not in the format of a step by step protocol. An SOP (step by step instructions in the correct order for each operator interaction with reagents, equipment and system software) was requested from Miltenyi but not made available. A draft protocol was therefore produced at Loughborough University. Much of the required knowledge for this

protocol was known only by development scientists at Miltenyi, and so the incomplete process knowledge and frequent back and forth for detail and clarification lead to slow and error prone SOP development.

4.4 Prodigy Expansion Troubleshooting

The initial three process attempts on the Prodigy highlighted significant issues with the Prodigy system's hardware, software and laboratory setup. Due to the overlapping nature of potential issues and the lack of in process troubleshooting options, a series of experiments were performed to investigate the causes of failure and explore protocol changes to prevent future failures.

4.4.1 Identification of Potential Failure Causes

Following the failure of the initial three process runs performed as part of the technology transfer effort, an analysis of potential causes for the reduced CCU pluripotent cell yield failure mode was performed to prioritise areas for investigation. An Ishikawa diagram (Figure 38) was produced to identify and categorise potential causes of failure for the initial process runs, with the highest priority potential failure modes prioritised for laboratory investigation.

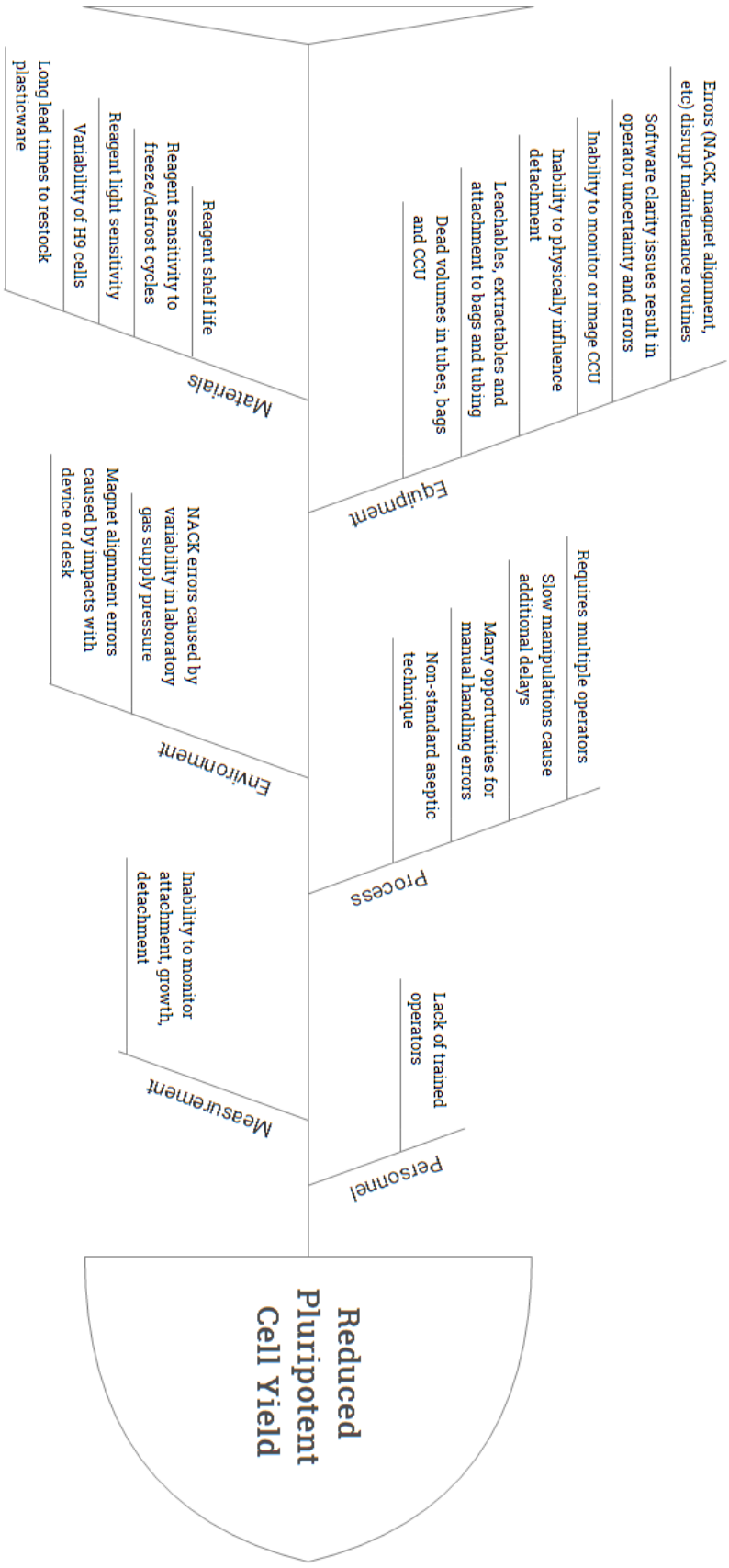

Figure 38 – Cause and effect diagram for the investigation of the low CCU viable cell yield produced by the expansion protocol as run on the CliniMACS Prodigy. Potential causes have informed process changes and areas for further investigation.

The most likely causes for process failure were identified as those relating to the laminin-521 coating process, with many potential causes early in the process contributing to a failure during coating and ultimately to process failure. The expansion process also features numerous opportunities for contamination of the CCU with buffer and feed medium during coating and cell seeding, with this problem compounded by the inability to drain the CCU following an erroneous liquid transfer. Coating had also been mentioned by Miltenyi as a common source of failures during development of the process, leading to process changes such as increased laminin concentration for the CCU, use of chilled PBS+/+ and coating mixture as well as minimising delay between coating mixture preparation and use.

4.4.2 Analysis of Potential Failure Causes

Due to the number of potentially contributing factors, a formal investigation was required to determine possible causes of failure. Experiments were performed to analyse the highest priority potential cause of failures, both to identify the impact of an event on the process, and to increase understanding of errors to aid with development of solutions.

4.4.2.1 Exposure to Feed Medium Prior to and During Coating with Laminin-521

During normal Prodigy tubing set installation, the tubing set is rinsed with a buffer solution (priming) and then again with feed medium (blocking), the CCU is not included in either rinse. A miscommunication during the technology transfer resulted in the CCU being included in the blocking process for the third H9 expansion attempt, exposing the CCU surface to medium containing albumin before exposure to the laminin-521 coating mixture. Albumin is capable of binding to many surfaces and is commonly used to reduce non-specific binding to culture vessels and other surfaces (Pijuan-Galitó *et al.*, 2016). Albumin has also previously been shown to reduce adherent cell attachment and growth by binding to a surface coating (Pijuan-Galitó *et al.*, 2016). The presence of albumin in the culture medium during Prodigy process runs may have reduced the available surface for H9 cell attachment. An experiment was performed to determine if exposure of a surface to medium containing albumin before exposure to a laminin-521 coating solution would lower its potential to support cell H9 cell growth, an overview for which is shown in Figure 39.

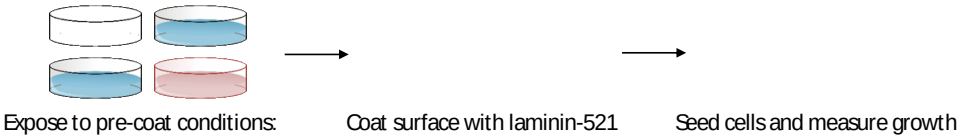

Figure 39 – Overview of the competitive binding experiment. Surfaces were exposed to medium containing serum albumin before coating with laminin-521 and seeding with H9 cells.

An experiment was performed to measure the potential for H9 cell growth on surfaces coated with laminin-521 following exposure to feed medium containing serum albumin. 6-well plates were exposed to one of four conditions each with 3 biological replicates:

1. A control condition in which 2ml of coating solution added to fresh well surface.
2. 1 ml of feed medium was added to a well surface for 2 minutes before being aspirated and followed by a 1ml PBS-/- wash, which was also aspirated prior to coating.
3. 1mL of feed medium was added to a well surface for 2 minutes before being aspirated, followed by coating.
4. 1mL of feed medium was added to a well surface for 2 minutes then followed by 2ml of coating solution, with medium left on throughout the coating period.

All wells were then coated, seeded at 2 x 10^4 cells per cm^2, maintained and harvested after 72 hours according to the methods outlines in Section 3.2.

Any exposure of the culture surface to feed medium prior to coating was found to negatively impact cell growth compared to the control condition. The control group with no medium exposure prior to coating produced the highest number of H9 cells on growth day 3 with a harvest of 1.67 x 10^5 viable cells per cm^2 (equivalent to a specific growth rate of 2.94 x 10^{-2} per hour). Cells in the control conditions showed typical morphology, forming clusters after 24 hours and approaching confluence after 72 hours of growth. Two minutes of medium exposure followed by a PBS wash produced a yield of 9.93 x 10^4 viable cells per cm^2 (equivalent to a specific growth rate of 2.22 x 10^{-2} per hour), a reduction of 40.49% compared to the control condition. Cells in the PBS washed condition branched less after 24 hours and formed smaller more rounded clusters after 48 and 72 hours, with rounded edges visible as a white halo on cluster edges. Two minutes of medium exposure with no wash produced a yield of 4.42 x 10^4 viable cells per cm^2 (equivalent to a specific growth rate of 9.45 x 10^{-3} per hour), a reduction of 73.54% compared to the control condition. Cells in the aspiration condition formed clusters after 24 hours, followed by rounded clusters and cell death after 48 hours, and significant cell death after 72 hours. Leaving feed medium on the surface during the laminin coating produced a yield of 9.60 x 10^2 viable cells per cm^2 (equivalent to a specific growth rate of -4.77 x 10^{-2} per hour), a reduction of 99.42%

compared to the control condition. The variance of each test group is significantly different from all others (P = < 0.00001). Cell attachment after 24 hours is poor compared to controls for surfaces exposed to medium throughout coating. This is followed by near complete cell detachment and death after 48 hours, leaving few cells present after 72 hours. A summary of growth data is provided in cell Figure 40 and growth images are provided in Figure 41.

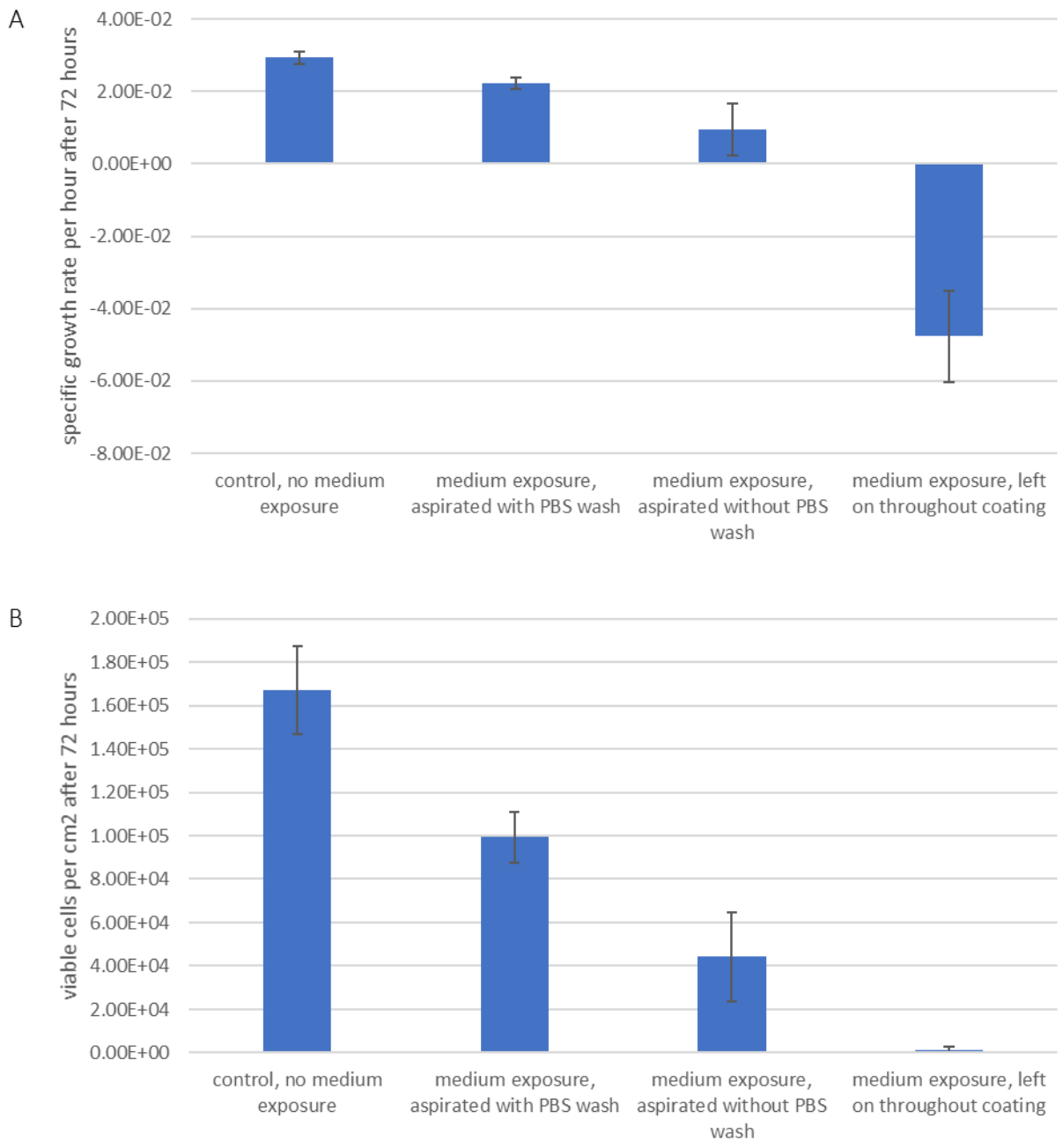

Figure 40 – Specific growth rate per hour (A) and viable cells per cm² (B) of H9 cells after 72 hours of growth on surfaces exposed to culture medium before laminin-521. Average of 3 sample per condition, each with 3 counts of viable cells per cm² following harvest three days after seeding. Data shown as mean ± SD for biological repeats, n=3.

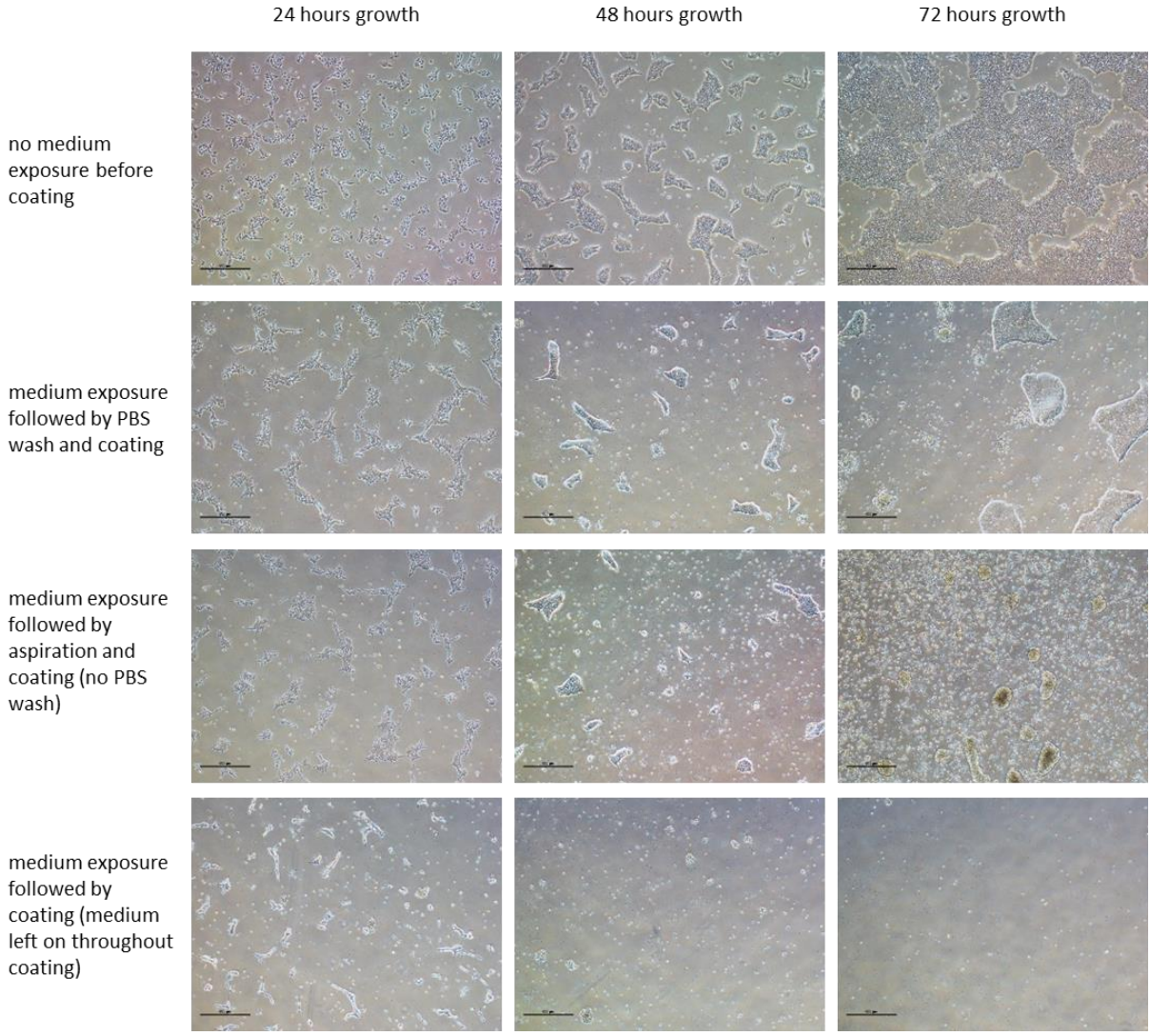

Figure 41 – H9 cell growth over a three-day period for surfaces exposed to feed medium prior to coating with laminin 521. Image scale bars equal to 500 µm.

These results show a significant impact on H9 growth from 2 minutes of feed medium exposure to a surface prior to laminin-521 coating. This result agrees with the literature that a significant portion of the coating capacity of a surface is removed by albumin exposure (Pijuan-Galitó *et al.*, 2016), and suggests that the effect happens within 2 minutes of albumin exposure. The results also show a limited benefit to washing a surface with PBS after exposure, likely due to the small reduction in residual feed medium capable of further coating the surface following medium aspiration. The fault condition in which a Prodigy CCU is exposed to buffer and feed medium prior to laminin coating may significantly reduce the ability of the CCU to support cell attachment and growth and is likely to have been a significant contributor to process failure during the initial expansion attempts.

4.4.2.2 Exposure to Low Concentration EDTA-Buffer

A buffer solution of phosphate buffered saline at pH 7.2 with 1 mM EDTA is used on the Prodigy to prime the tubing set, wash tubing between liquid transfers, and as a volume of neutral liquid when precise control of other liquid volumes is desired. During priming, buffer is pumped throughout the tubing set and CCU, with a dead volume remaining after draining. During washing and volume transfers a residual volume is retained on the tubing walls and is therefore added to any liquid transferred through the tubing set. In these ways, a residual volume of buffer will always be present in the CCU, including during coating with laminin-521.

EDTA is included in the buffer to prevent cell attachment to the tubing set, acting as a metal chelator and bonding to calcium ions required by integrins to attach cells to surfaces. The ability of EDTA to reduce the availability of calcium ions is the mechanism typically used to reduce cell adhesion for dissociation during a harvest (Zeng and Bi, 2006). Although the impact of low concentration EDTA buffer on cell seeding and growth has not been directly explored in the literature, EDTA may contribute towards the effects observed during TrypLE contamination, which has been shown to negatively impact the ability of cells to adhere to the coated CCU surface during cell culture (Thomas *et al.*, 2007). For completeness, experiments were performed to measure the impact of EDTA exposure during laminin-521 coating, between coating and cell seeding, and during cell seeding, with the expectation that cell growth will be lower in cases where EDTA is present during cell seeding or growth process steps.

4.4.2.2.1 Exposure to Buffer Prior to and During Coating with Laminin-521

The effects of buffer exposure before and during coating were measured by adding buffer to 6-well plates under 4 test conditions, each with 3 biological replicates:

1. A control condition in which coating was performed with no prior buffer exposure.
2. Residual buffer with wash, in which 1 ml of buffer was added for 5 minutes before being aspirated and the well washed with 1 ml PBS+/+, then aspirated and coated.
3. Residual buffer without wash, in which 1 ml of buffer was added for 5 minutes before being aspirated, then aspirated and coated.
4. Buffer left on, in which 1 ml of buffer was added for 5 minutes, before coating mixture was added without aspirating the buffer.

All wells were then coated, seeded with RC17 cells at 2 x 10^4 cells per cm^2, maintained and harvested after 72 hours according to the methods outlines in Section 3.2.

Buffer exposure prior to and during laminin coating was found to produce no significant variance in cell growth or cell yields between test cases during the first 72 hours of growth (P = 0.33), as shown in Figure 42. Cell growth and morphology was consistent across the test conditions forming small clusters after 24 hours, large colonies after 48 hours and reaching confluence by 72 hours, as shown in Figure 43. There is no discernible difference in colony size or edge rounding, with cells appearing healthy across all conditions. Given these results and the lack of literature suggesting an interaction between EDTA and laminin-521, it is unlikely that buffer present before or during laminin coating resulted in negative impacts to cell growth during the initial expansion attempts.

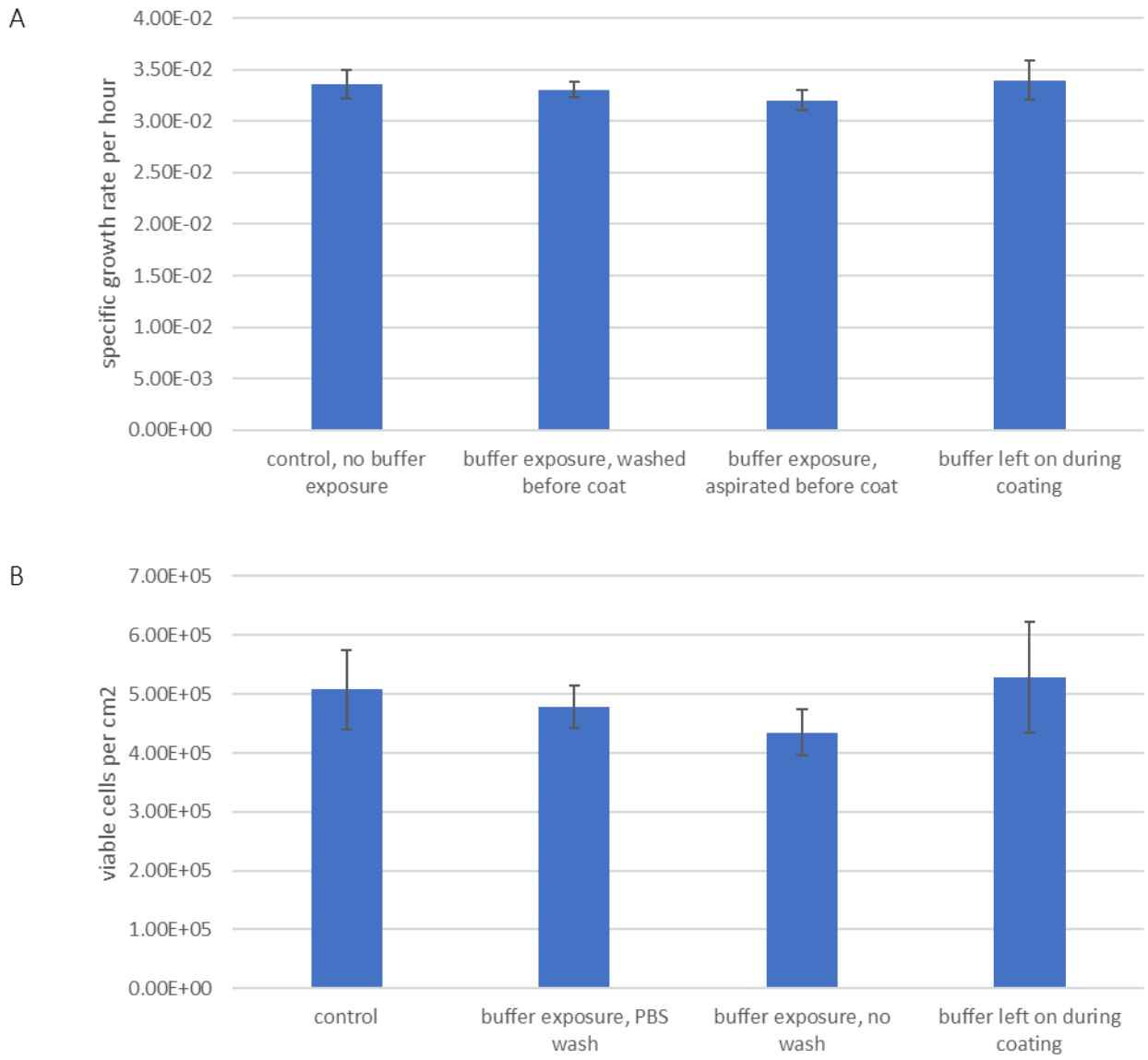

Figure 42 – Specific growth rate per hour (A) and viable cells per cm² (B) following 72 hours of growth of RC17 cells on surfaces exposed to low concentration EDTA buffer prior to coating with Laminin-521. Data shown as mean ± SD for biological repeats, n=3.

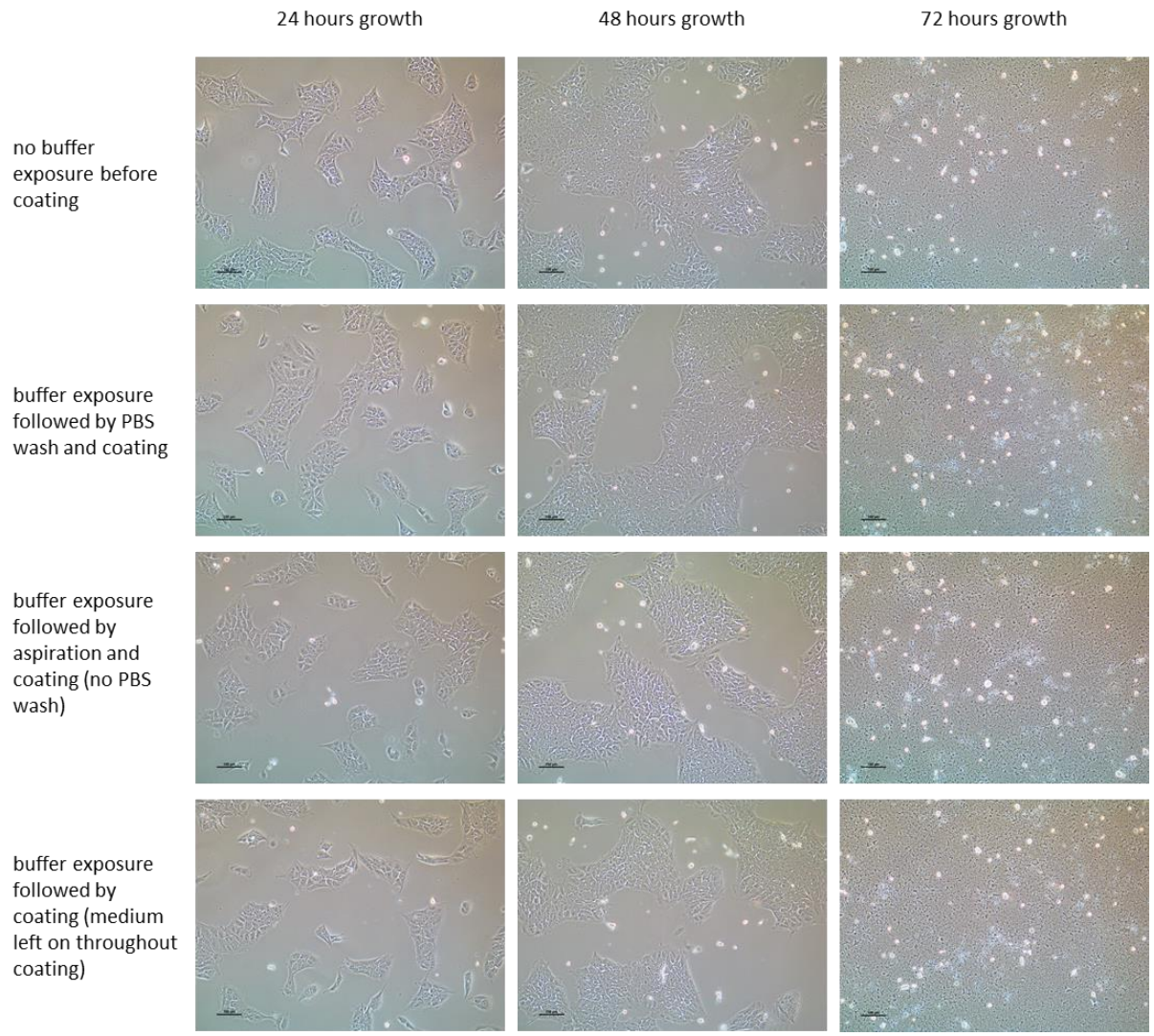

Figure 43 – RC17 cell morphology for 72 hours following various buffer exposure conditions prior to laminin coating. Scale bars are equivalent to 100 µm.

4.4.2.2.2 Exposure to Buffer Following Coating with Laminin-521

An experiment was performed comparing the growth of H9 cells on surfaces exposed to buffer as well as buffer with feed medium after laminin coating but prior to cell seeding, as summarised in Figure 44. 6-well plates were first coated with laminin 521 as detailed in Section 3.2.1. Following coating one set of wells were drained and exposed to low concentration EDTA buffer for 5 minutes before aspirating and seeding. A second set of wells were drained and exposed to low concentration EDTA buffer and

feed medium for 5 minutes before draining and seeding. A third set of wells acted as the control condition and were drained of coating solution and immediately seeded. Two biological repeats per condition were then seeded with H9 cells at a density of 1 x 10^5 per cm^2 and maintained for 96 hours before harvesting. Cell seeding, maintenance and harvesting were performed as detailed in Section 3.2.

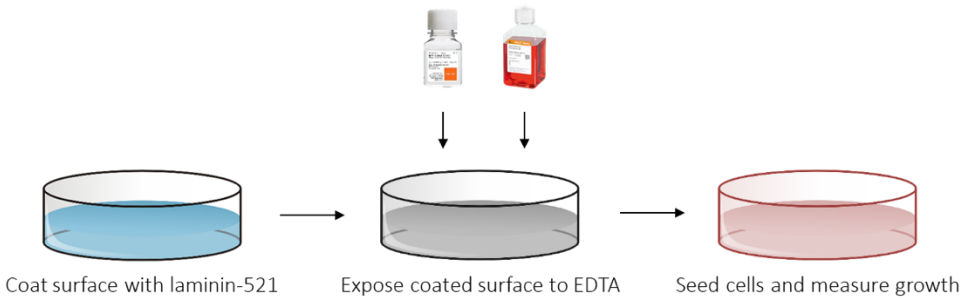

Figure 44 - Overview of the low concentration EDTA buffer laminin exposure experiment. 6-well plate surfaces were coated with laminin-521 before exposing the buffer and feed medium, then seeding with H9 cells.

Neither the addition of buffer or the addition of buffer and feed medium after coating but before cell seeding produced a significant variance in cell growth on the surfaces for 96 hours following seeding (P = 0.68),, as shown in Figure 45. The control surfaces produced an average of 2.89 x 10^5 viable cells per cm^2 (equivalent to a specific growth rate of 1.1 x 10^{-2} per hour), the surfaces exposed to buffer produced an average of 3.05 x 10^5 viable cells per cm^2 on average (equivalent to a specific growth rate of 1.16 x 10^{-2} per hour), while the surfaces exposed buffer and feed medium produced an average of 2.82 x 10^5 viable cells per cm^2 (equivalent to a specific growth rate of 1.08 x 10^{-2} per hour). Cell morphology is also consistent across exposure conditions, with cells forming clusters after 24 hours and approaching confluency after 96 hours, as shown in Figure 46. As in the previous experiment, given these results and the absence EDTA and laminin-521 interactions in the literature, the accidental exposure of the coated CCU surface to low concentration EDTA buffer during the third attempt at H9 expansion on the Prodigy was unlikely to be the cause of the poor cell yields obtained during that process.

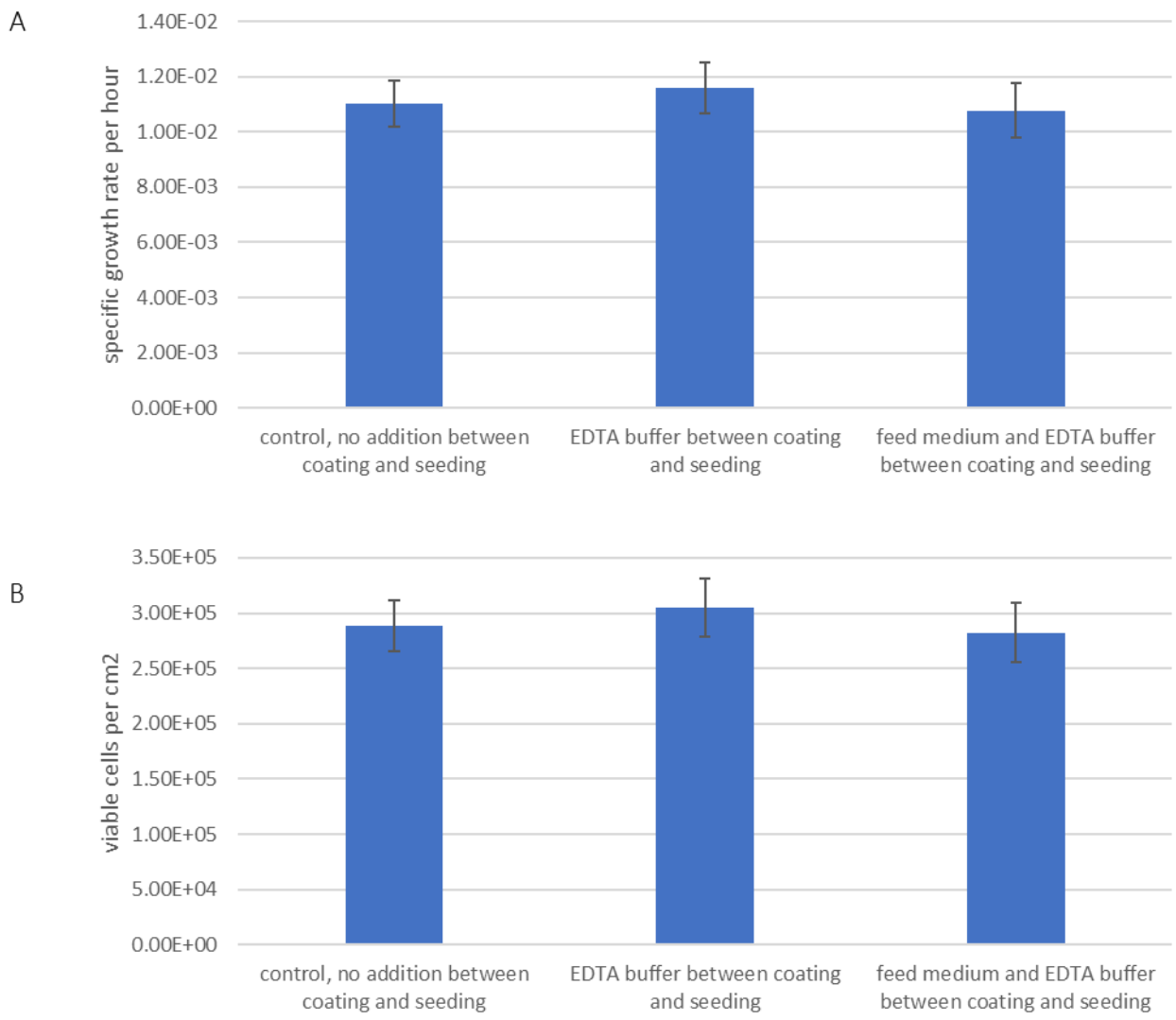

Figure 45 – Specific growth rate per hour (A) and viable cells per cm² (B) of H9 cells following 96 hours of growth with various coating and seeding conditions. All wells produce similar yield, indicating little difference between control and buffer and feed medium exposed conditions. Data shown as mean ± SD for biological repeats, n=2.

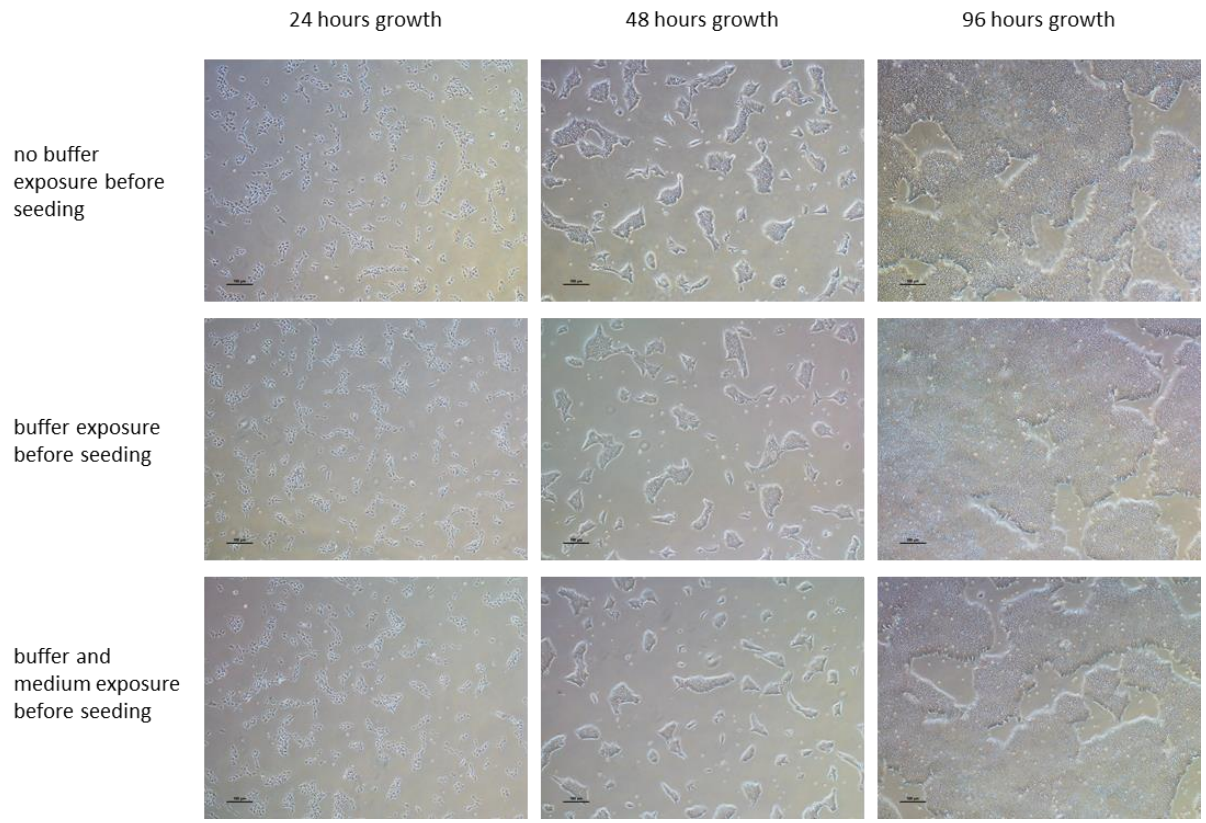

Figure 46 – H9 cell growth across a 96-hour period. Scale bars are equivalent to 100 µm.

4.4.2.2.3 Exposure to Buffer During Cell Seeding

An experiment was performed to determine whether the presence of a low concentration EDTA buffer during cell seeding negatively affects cell attachment and growth. 6-well plates were then coated, seeded and maintained according to the method described in Section 3.2, with the following variations for each condition of three biological repeats:

1. Control condition with no buffer added during cell seeding at 1.5 x 10^4 cells per cm^2.
2. 1% of seeding volume replaced with buffer (1.98ml seeding medium, + 0.02ml buffer), equating to a seeding density of 1.49 x 10^4 cells per cm^2.
3. 10% of seeding volume replaced with buffer (1.8ml cell seeding medium + 0.2ml buffer), equating to a seeding density of 1.35 x 10^4 cells per cm^2.
4. 50% of seeding volume replaced with buffer (1ml seeding medium + 1ml buffer), equating to a seeding density of 7.5 x 10^4 cells per cm^2.

The presence of low concentration EDTA buffer during cell seeding has a statistically significant negative impact on cell growth for concentrations as low as 10% ($p = 0.037$ for 1%, $p = 0.007$ for 10%, $p = < 0$.

0.00001 for 50%, threshold 0.0167 following Bonferroni correction), with negative effects increasing as buffer concentration increases as shown in Figure 47. This outcome suggests that EDTA is a factor in cell losses observed as a result of the presence of TrypLE (containing EDTA) during cell culture in the literature (Thomas *et al.*, 2007). It is plausible that this effect is due to the action of EDTA inhibiting cell attachment and expansion. As shown in Figure 48, cells appear healthy for the control and 1% buffer replacement conditions, transitioning from small clusters after 24 hours to larger colonies after 48 hours, which then join as the cells approach confluence at 96 hours. The 10% buffer replacement condition appears similar but with a lower confluence level and larger proportion of dead cells after 96 hours. The 50% buffer replacement condition has little cell attachment at any point, meaning effective total cell loss. While there is a clear trend of reduced cell growth and resulting yields as buffer concentration increases, buffer during seeding is unlikely to cause process failure for the residual volumes present in a typical process. It may however be a cause of process failure in exceptional circumstances where a large volume of buffer cannot be removed from the CCU prior to seeding.

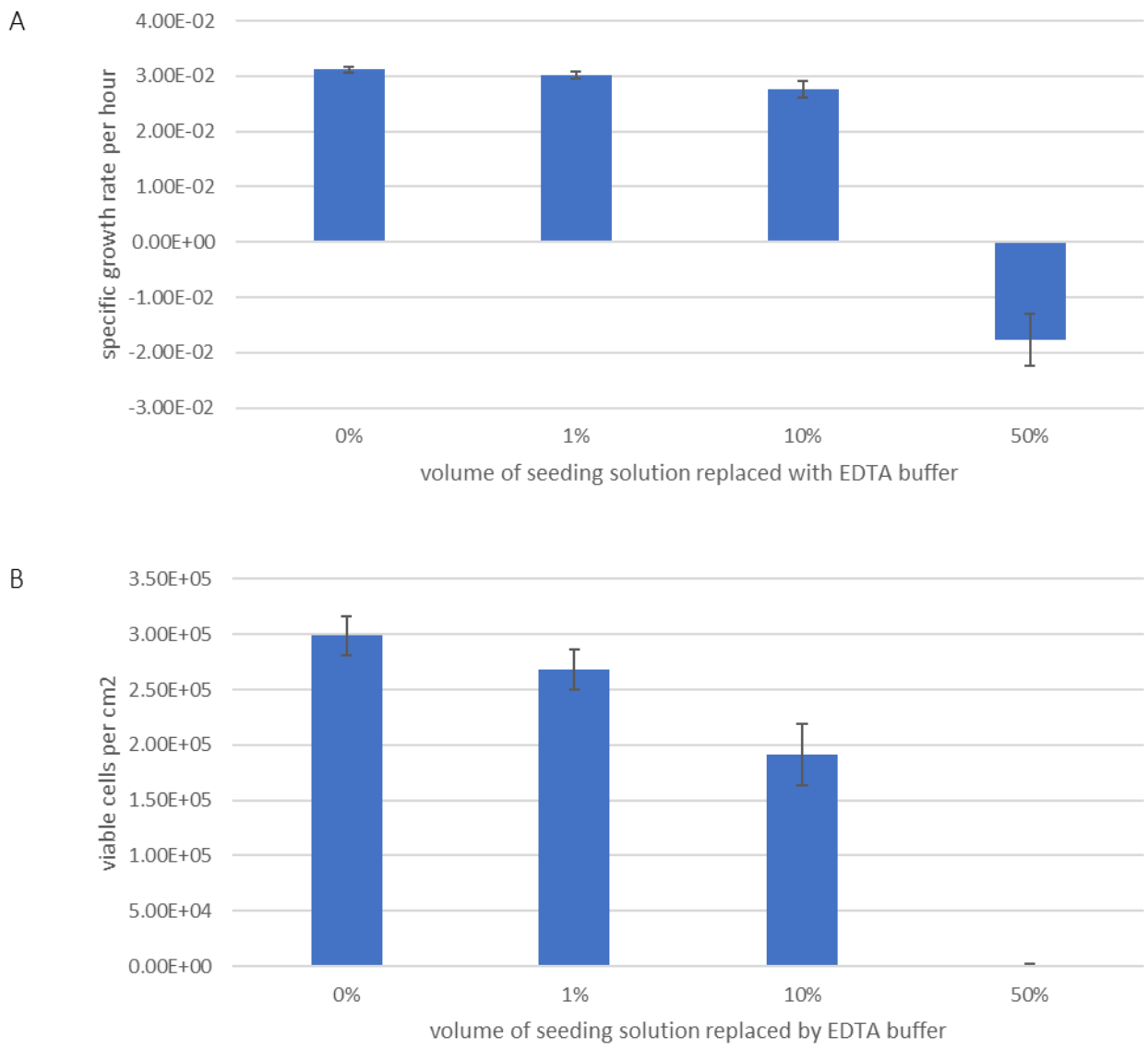

Figure 47 - Specific growth rate per hour (A) and viable cells per cm^2 (B) of H9 cells following 96 hours of growth on surfaces on exposed to low concentration EDTA buffer during seeding onto Laminin-521 coated surfaces. Data shown as mean ± SD for biological repeats, n=3.

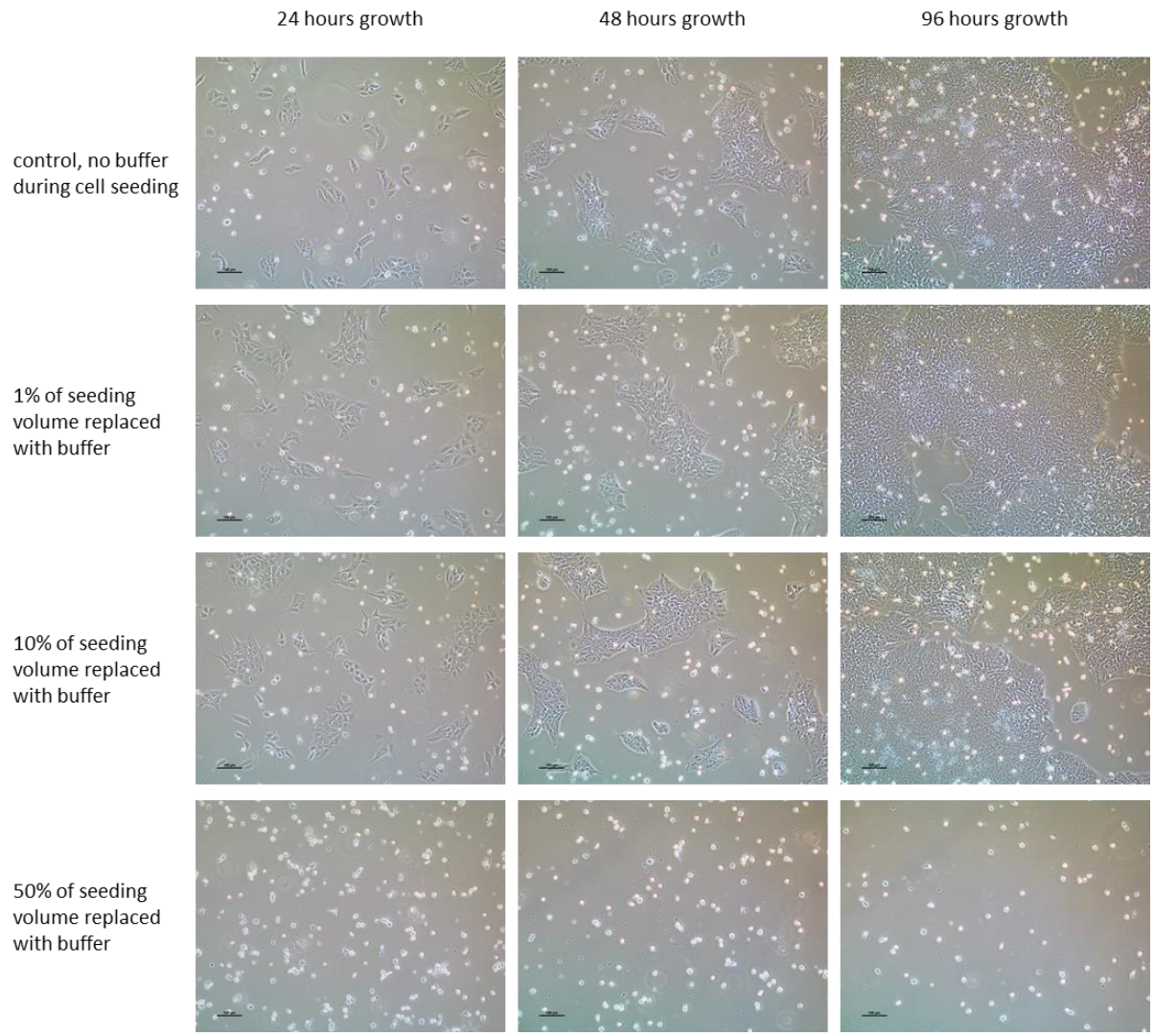

Figure 48 – H9 cell growth over 96 hours for cells with varying degrees of buffer contamination at the point of cell seeding. Scale bars are equivalent to 100 µm.

4.4.2.3 Drying of Laminin-521 Coated Surface due to Evaporation Prior to Cell Seeding

Laminins are proteins which form part of the extracellular matrix and provide structural and biochemical foundations for surrounding cells, influencing cell adhesion, migration and differentiation (Zeng and Bi, 2006). Coating of surfaces with laminin-521 and laminin-111 is detailed in Sections 3.2.1 and 3.3.1 respectively, and involves preparing a coating mixture to the desired laminin concentration in PBS with calcium and magnesium. The coating mixture is then applied to the surface, left in contact for a coating period, then aspirated prior to the addition of culture medium and cells. The time between aspiration of the coating mixture and re-coating the surface with culture medium leaves the layer of laminin proteins with a thin layer of liquid which may evaporate and cause drying of the laminin proteins

(BioLamina, 2018). Manufacturer guidance states that drying of a laminin coating inactivates the coating and causes degradation in its cell attachment properties (BioLamina, 2018), however, there is little information available to quantify the extent or rate of coating degradation available in the literature. Manual aspiration with an aspiration pipette leaves little liquid behind, and manual seeding for a single flask or well typically takes less than 30 seconds. The aspiration technique for the Prodigy CCU is slower, with the coated surface uncovered throughout the aspiration process, during tube clearing and medium pumping steps, and partially after seeding but before the CCU is agitated to spread the liquid over the entire surface. The effect of laminin surface drying on ESC growth has not yet been quantified. Experiments were performed to quantify laminin drying behaviour and to determine an acceptable period of drying time for the mesDA manufacturing process are summarised in Figure 49. The expected outcome of these experiments was that vessels in which laminin had been allowed to dry for periods of over 2 minutes would show significantly reduced cell yields to those with shorter drying periods.

An experiment was performed to measure the performance of laminin-521 and laminin-111 coated surfaces following extended periods of drying. 6-well plates were coated with a coating solution according to the methods given in Sections 3.2.1 and 3.3.1. Deviations from this method include a group of wells coated at the typical 0.5 µg per cm^2 and a second group coated at 0.1 µg per cm^2. Wells were then stored for 24 hours before aspiration of the coating mixture to allow for drying of the laminin coated surface. Wells were aspirated and filled with 2 mL of culture medium at staged intervals to create drying times of 'as fast as possible' (approximately 15 seconds), 2 minutes, 5 minutes, 10 minutes, 30 minutes and 3 hours. Wells were then seeded with H9 cells at 2 x 10^4 per cm^2, maintained for 72 hours and harvested according to the method given in Section 3.2.

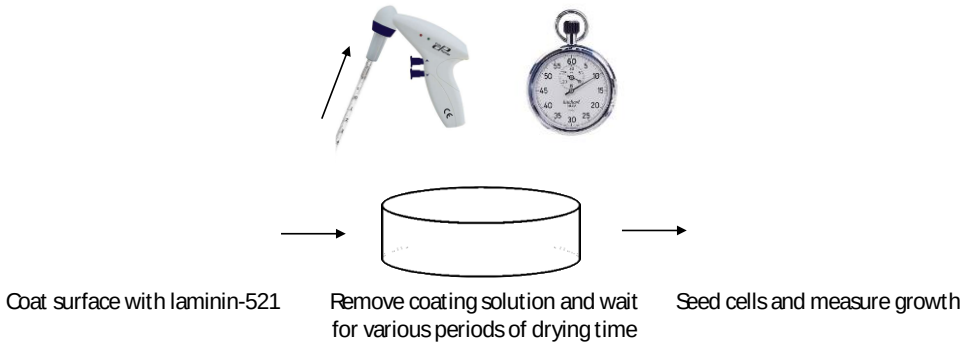

Figure 49 – Overview of the laminin-521 surface drying experiment. Surfaces were first coated with laminin-521, then dried for a range of periods before seeding with H9 cells.

Delays between the aspiration of the laminin-521 coating mixture and addition of seeding medium cause reduced growth potential of the coated surface. The effect is more pronounced for surfaces coated with the lower than recommended coating concentration of 0.1 µg per cm^2 as compared to the recommended 0.5 µg per cm^2. Laminin degradation begins at the moment the coating mixture is removed and continues to degrade approximately logarithmically until at least 3 hours of drying, as shown in Figure 50. The lack of a safe period in which a surface remains wetted demonstrates that a fully dry surface is not necessary to cause laminin degradation and suggests the cause of damage may be related to salt balance or uneven drying of the surface.

A negative impact on cell growth as a result of laminin drying was expected and is in agreement with manufacturer guidance (BioLamina, 2018), however, the relatively small change in growth rate for extreme drying periods when using the recommended laminin coating concentration calls into question the widely used and rarely documented recommendation of a cut-off point at several minutes of drying time. The overall impact of laminin drying on H9 growth was lower than expected for surfaces coated at the recommended concentration, suggesting that laminin drying is insufficient to explain the large decrease in cell yield observed during the third attempt at H9 expansion on the Prodigy. Working as quickly as possible between removal of coating solution and addition of culture medium is recommended practice and is supported by this experiment, however the negative impact of delays is far less pronounced than expected, and unlikely to be a cause of process failure unless combined with other causes.

A

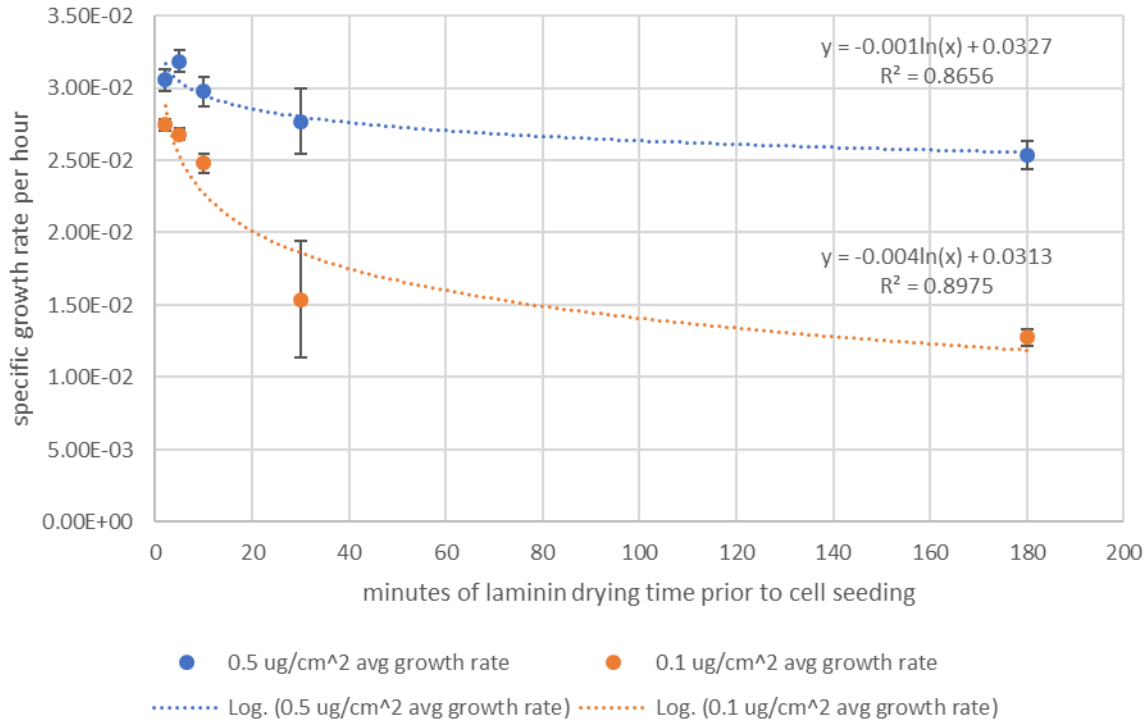

B

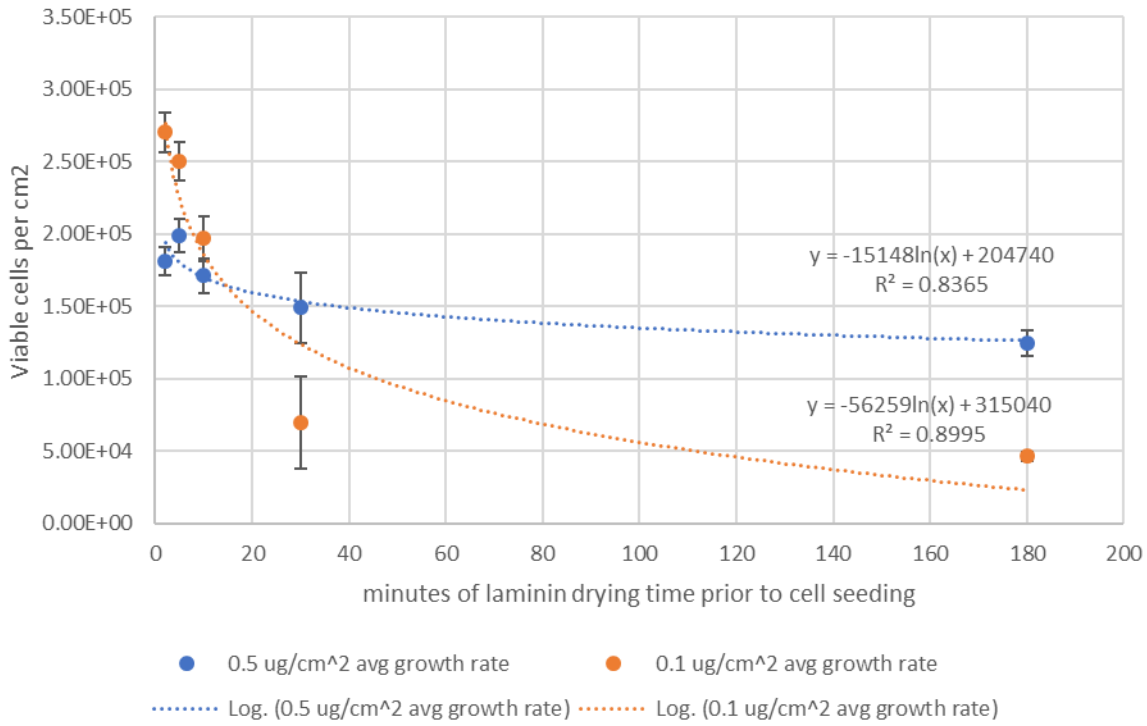

Figure 50 – H9 cells specific growth rate per hour (A) and viable cells per cm² (B) is lower on surfaces which experienced a longer duration between aspiration of the laminin-521 coating mixture and the culture surface being coated with culture medium during seeding. The effect is more pronounced for surfaces coated with a lower concentration of laminin-521. Data shown as mean ± SD for biological repeats, n=2.

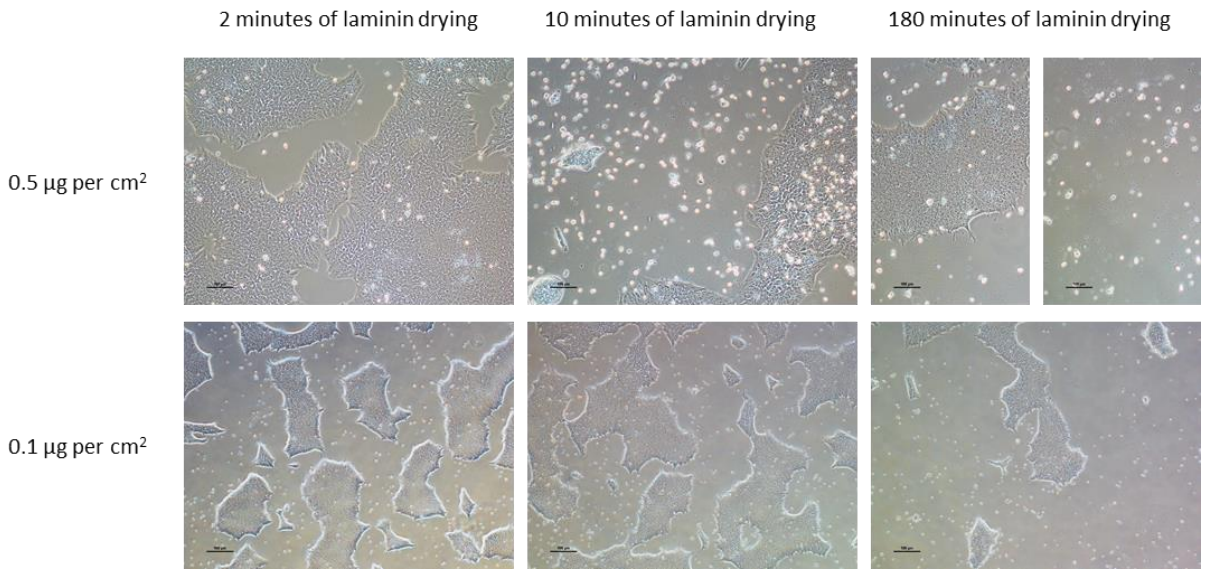

Figure 51 – H9 cell growth 72 hours after seeding cells on surfaces exposed to varying periods of laminin drying. The two images shown for 180 minutes of laminin drying show different areas of the same well, with part showing healthy cell growth and part devoid of cell attachment. Scale bars are equivalent to 100 µm.

4.4.3 Corrective Actions

In response to these potential causes of failure, a new SOP style protocol was developed at Loughborough to be used in place of the fragmented draft Miltenyi protocol, with the aim of producing a single easily followable list of instructions for the entire process.

High priority potential failure modes were explored with laboratory experiments with the aim of preventing further process failure during H9 expansion on the Prodigy. Exposure of the CCU to feed medium prior to and during coating with laminin 521 was found to have a significant impact on cell growth. It is probable that this failure mode was responsible for the failure of the third H9 expansion attempt in which the CCU was erroneously included in the feed medium blocking process and exposed to medium before coating. As a result of this work, the draft protocol document was updated to explicitly state not to include the CCU during blocking with feed medium.

Exposure of the CCU to buffer before, during and after coating were found to have no significant impact on cell growth and no process changes were required to protect against these occurrences. Exposure of the CCU to buffer during cell seeding did produce reduced cell growth at high concentrations possible during error conditions, however the impact was slight for buffer volumes present as residual volumes during normal processing. Drying of laminin surfaces prior to seeding was also found to have a negative impact on cell growth but to a more limited degree than previously thought and would not be sufficient

to cause process failure alone. Due to the nature of processing on the Prodigy, a certain delay period is required for liquid manipulations to occur. Additional checks were implemented to ensure that all possible preparation was completed prior to draining the CCU for cell seeding.

4.4.4 Demonstration of Automated Cell Expansion on the Prodigy

Following troubleshooting work and protocol improvements, three further process runs on the Prodigy were performed using the Loughborough University produced protocol document provided in Appendix C. Of these runs, two cell yields comparable to manual controls during the expansion phase, while one resulted in reduced cell growth. The laboratory setup of the Prodigy and related equipment is shown in Figure 52 and a summary of results is provided in Figure 53.

Figure 52 - CliniMACS Prodigy during expansion process. feed medium is attached via dip tube bottle during feeds.

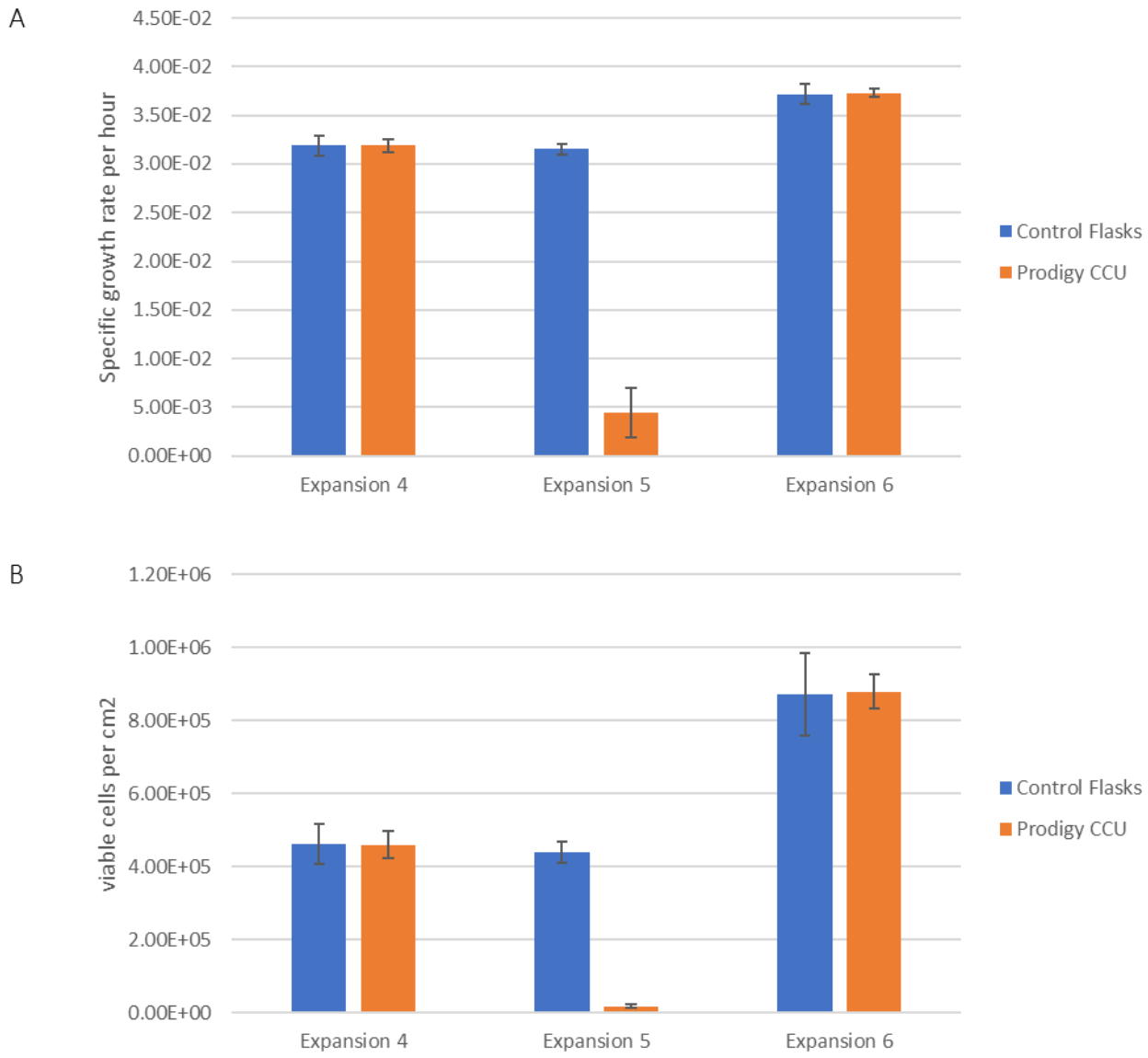

Figure 53 - Summary of specific growth rates per hour (A) and viable cell yields per cm² (B) during Prodigy expansions following troubleshooting. Process attempts 4 and 6 achieved comparable viable cell yields between the Prodigy expanded cells and control flasks as well as with expansions performed at Miltenyi, which achieved yields 5 x 10^5 viable cells per cm², equivalent to a specific growth rate of 3.26 x 10^{-2} per hour (Miltenyi Biotec, 2018a). *The expansion of cells in process run 5 failed in the CCU due to an operator error during tubing set installation which resulted in buffer remaining in the CCU during cell seeding. Expansions 4 and 5 used H9 cells whereas expansion 6 used RC17 cells. Data shown as mean ± SD for biological and measurement repeats, control flasks are n=3 and CCUs are n=1.*

4.4.4.1 Process Run 4, Automated Expansion of ESCs

The fourth process attempt (the first following troubleshooting) was successful, producing comparable cell yields between the CCU and manual control T25 flasks of 4.6 x 10^5 per cm² and 4.61 x 10^5 per cm² respectively. This success of this run partly attributable to close adherence to the SOP style protocol produced by Loughborough, which avoided many of the errors and misunderstandings resulting from

use of the Miltenyi protocol. Two magnet errors were triggered during the expansion phase by laboratory users closing drawers fitted to the desk on which the Prodigy was mounted. Fortunately, an operator was present in both cases and the error cleared without impacting CCU maintenance routines. A visual guide to clearing magnet errors was produced and attached to the front of the machine to mitigate future occurrences.

4.4.4.2 Process Run 5, Automated Expansion of ESCs

The fifth process run produced a significantly reduced cell yield of 1.76 x 10^4 per cm^2 in the CCU compared to an average of 4.4 x 10^5 per cm^2 produced by three manual control flasks, equating to a process failure. Due to updates in Miltenyi products, the fifth process attempt was the first to trial the GMP compliant version of the TS730 tubing set. This new tubing set includes 1 metre tubing extensions on all input and output ports, removing the requirement for an operator to add these during initial setup. The tubing set also includes 3-way branch points on many input and output ports, granting the flexibility of 3 input locations per port. Due to this increase in tubing set flexibility and complexity, the total number of Luer locks and tubing clamps has increased substantially over the non-GMP version of the TS730 tubing set. During initial setup of the fifth process run, a 3-litre bag of CliniMACS buffer was connected to input port 1 on the tubing set without closing the flow restricting tubing clamp. Both the Miltenyi protocol and Loughborough SOP instruct operators to check that clamps are closed during tubing setup, however the complexity of the new tubing set and unknown number of clamps meant that one clamp was overlooked during checks. When the tubing set was lifted onto the Prodigy and the buffer bag attached to the bag hanging hooks, the buffer began to drain through the tubing set into the CCU chamber. Clamps were closed as soon as this error was realised, however, approximately 20ml of buffer was allowed to reach the CCU before the error was corrected. Priming of the tubing set was twice repeated in an attempt to remove the buffer from the CCU, however, an estimated 10ml of buffer remained in the CCU during the coating process, with a portion remaining during seeding. The protocol was updated following this event to list the number of clamps to be checked for future process runs.

During seeding of the CCU for the expansion of the fifth process run, a post attached to the rotating head of the peristaltic pump became caught on the flexible tubing of the TS730 tubing set within the pump chamber as shown in Figure 54, causing the pump to stall and the liquid transfer to fail with no indication of detection or mitigation issued by the Prodigy system. This stall condition was removed by freeing the trapped section of tubing, however the precise effects on liquid transfers at various points

in the process are unknown. It is not known whether this was caused by a problem with the Prodigy pump unit, a tubing set installation error, or an issue with the GMP version of the TS730 tubing set.

Figure 54 - Peristaltic pump tubing lodged between housing and tubing containment posts. This caused the pump to stall and was not detected by the device, allowing the program to continue with an incomplete liquid transfer.

Given the errors known to have occurred during initial tubing installation and the low CCU yield failure mode, it is likely that contamination with buffer during seeding, combined with the CCUs sensitivity to coating issues was the cause of failure for the fifth process run.

4.4.4.3 Process Run 6, Automated Expansion of ESCs

The sixth process attempt achieved comparable yields between the CCU expanded cells and T25 control flasks, averaging 8.80 x 10^5 and 8.72 x 10^5 viable cells per cm^2 respectively. This process run was the first to use the clinically relevant RC17 cell line, which has a marginally higher growth rate than H9 cells resulting in higher cell yields compared to previous process runs. The sixth process run was also performed with the GMP version of the TS730 tubing set, this time with no issues relating to peristaltic pump stalls due to snagging.

4.4.4.4 Summary of Process Runs 4, 5 and 6, Expansion Phase

The automated expansion of H9s during process run 4, and RC17s during process run 6, produced comparable yields to control flasks and to expansions performed by Miltenyi in both cases, demonstrating the possibility of successful cell expansion on the Prodigy for both cell lines. The failure of process run 5 highlights the need for continued protocol revision to avoid operator errors, and the potential for other issues yet to be identified.

4.5 Manual mesDA Differentiation

As detailed in Section 3.3, the protocol for differentiation of ESCs to mesDA neurons on the Prodigy has been designed for the scale of a single layer CellSTACK (Miltenyi Biotec, 2018a), equivalent to 636 cm^2. Due to the high cost of plasticware and reagents required for a differentiation process run at this scale, the Miltenyi differentiation protocol was first performed in T25 flasks to demonstrate successful transfer of the process from Miltenyi to Loughborough University.

4.5.1 Transfer of Manual H9 Differentiation Protocol

Three T25 flasks were coated with laminin-111 at a concentration of 1 µg per cm^2, seeded with H9s at a density of 2.5 x 10^4 cells per cm^2 and fed, maintained and harvested according to the Miltenyi 2018 method outlined in Section 3.3.3, with the exception of all manipulations being performed in manual flasks and liquid volumes scaled down to equal those used in typical pluripotent culture and provided in Section 3.2.

The Lund protocol on which the Miltenyi protocol is based produces an expected yield of 1.15 x 10^6 cells per cm^2 on day 11 and 1.95 x 10^6 cells per cm^2 on day 16 for H9 cells (Nolbrant *et al.*, 2017). Miltenyi lists expected yields of 9.83 x 10^5 for day 11 and 1.19 x 10^6 in the process application note (Miltenyi Biotec, 2018a).

The average observed yield on day 11 was 1.97 x 10^6 cells per cm^2, which was high compared to those achieved at Lund and Miltenyi and provided enough cells to seed the next process stage with a comfortable safety buffer. As shown in Figure 55, harvest of product cells on day 16 yielded an average of 9.54 x 10^5 cell per cm^2, a value comparable to the yield of 1.19 x 10^6 per cm^2 observed by Miltenyi (Miltenyi Biotec, 2018a) but lower than the 1.95 x 10^6 cells per cm^2 achieved by Lund, possibly due to the change in scale from 24-well plates used at Lund to T25 flasks used at Loughborough. During

development an approximate yield of 8.15 x 10^5 per cm^2 was stated as typical for 6 well plates at Miltenyi, with yield described as decreasing at increasing scales.

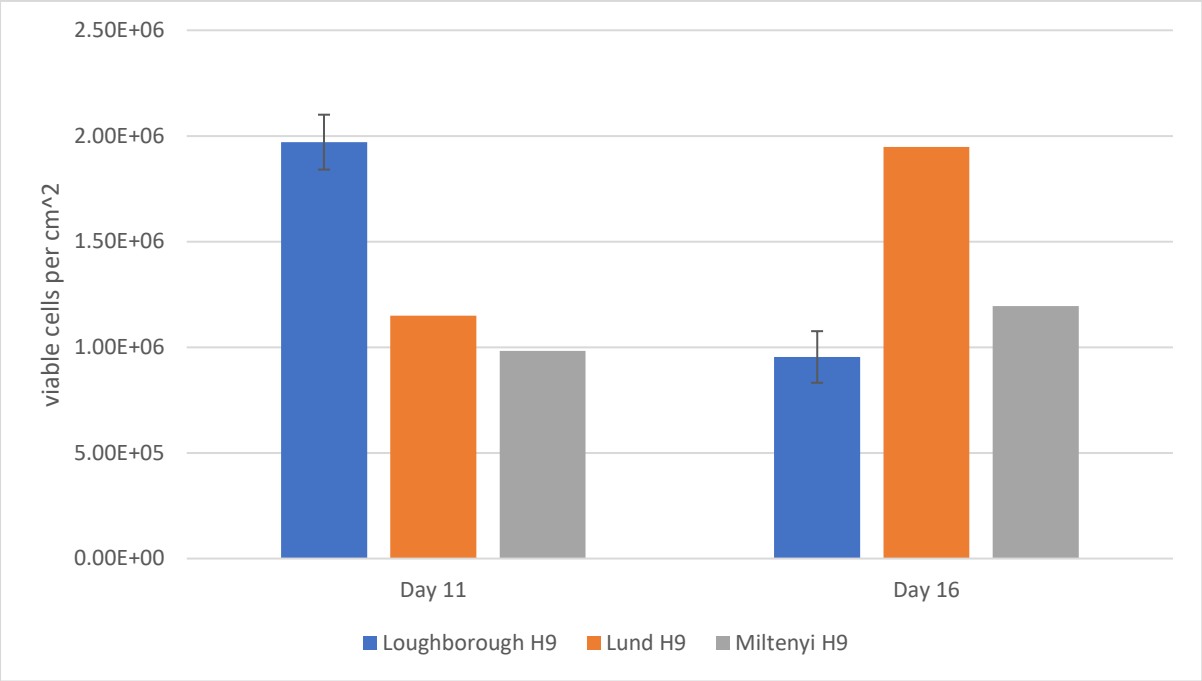

Figure 55 – Viable cell counts on differentiation day 11 and day 16. Loughborough H9 bars shown as mean ± SD for biological repeats, n=3. Data to produce error bars for Lund and Miltenyi values was unavailable.

Cells grew to full confluency by day 4 and continued to proliferate, resulting in clumps of cells detaching or growing in clumps detached from the culture surface due to lack of available binding surface. Clumps are visible in Figure 56 as bright white areas and were visible during microscopy as clumps anchored to the culture surface, but able to sway with liquid movement.

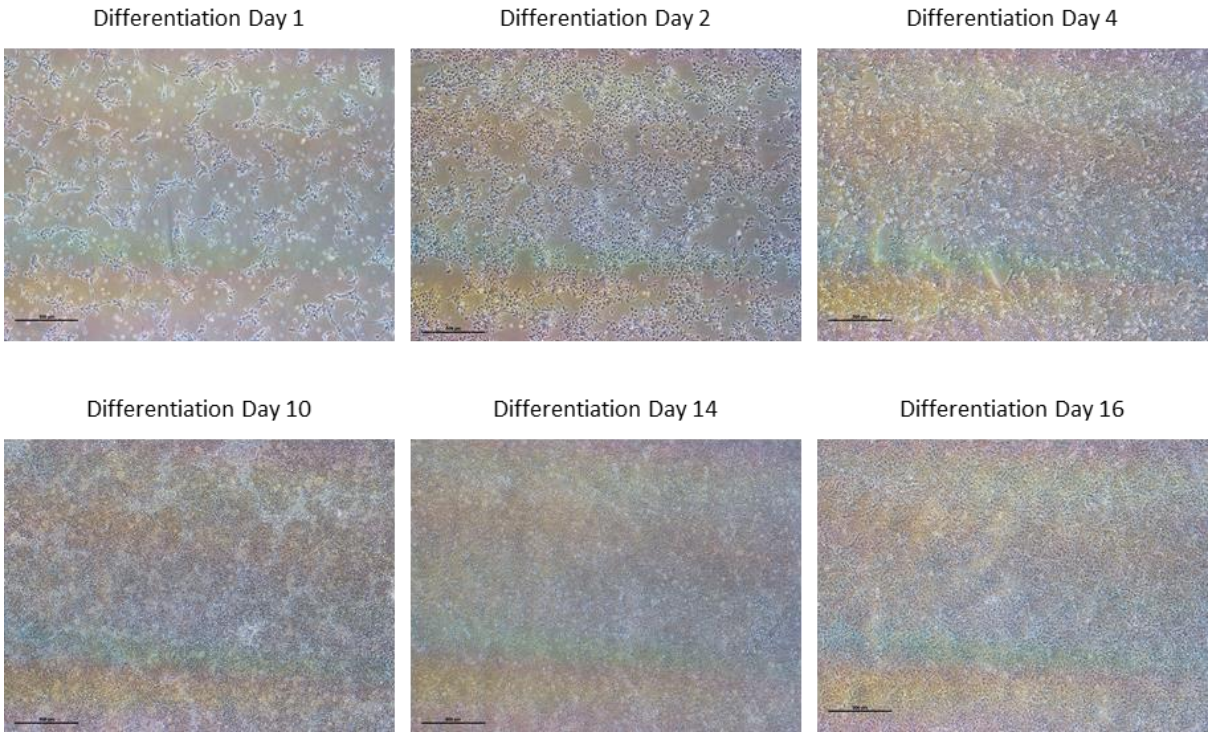

Figure 56 - Cell growth for a manual H9 differentiation process. Cells are seeded on day 0 and reach confluency by day 4, continuing to grow and forming multilayer clumps. Cells were passaged on day and seeded at 11 at 8 x 10^5 cells per cm^2 and so were at full confluency at seeding, with no space to expand into. Scale bars are equivalent to 500 µm.

Flow cytometry was performed on cell samples from days 0, 11 and 16 from each flask according to the methods given in Section 3.5.3. As shown in Figure 57, Oct3/4 showed a clear transition from positive to negative expression between pluripotent cells and those on differentiation days 11 and 16, regardless of differentiation or analysis location. Ki67 was positive for pluripotent cells and produced the expected response of high variation in expression on differentiation days 11 and 16.

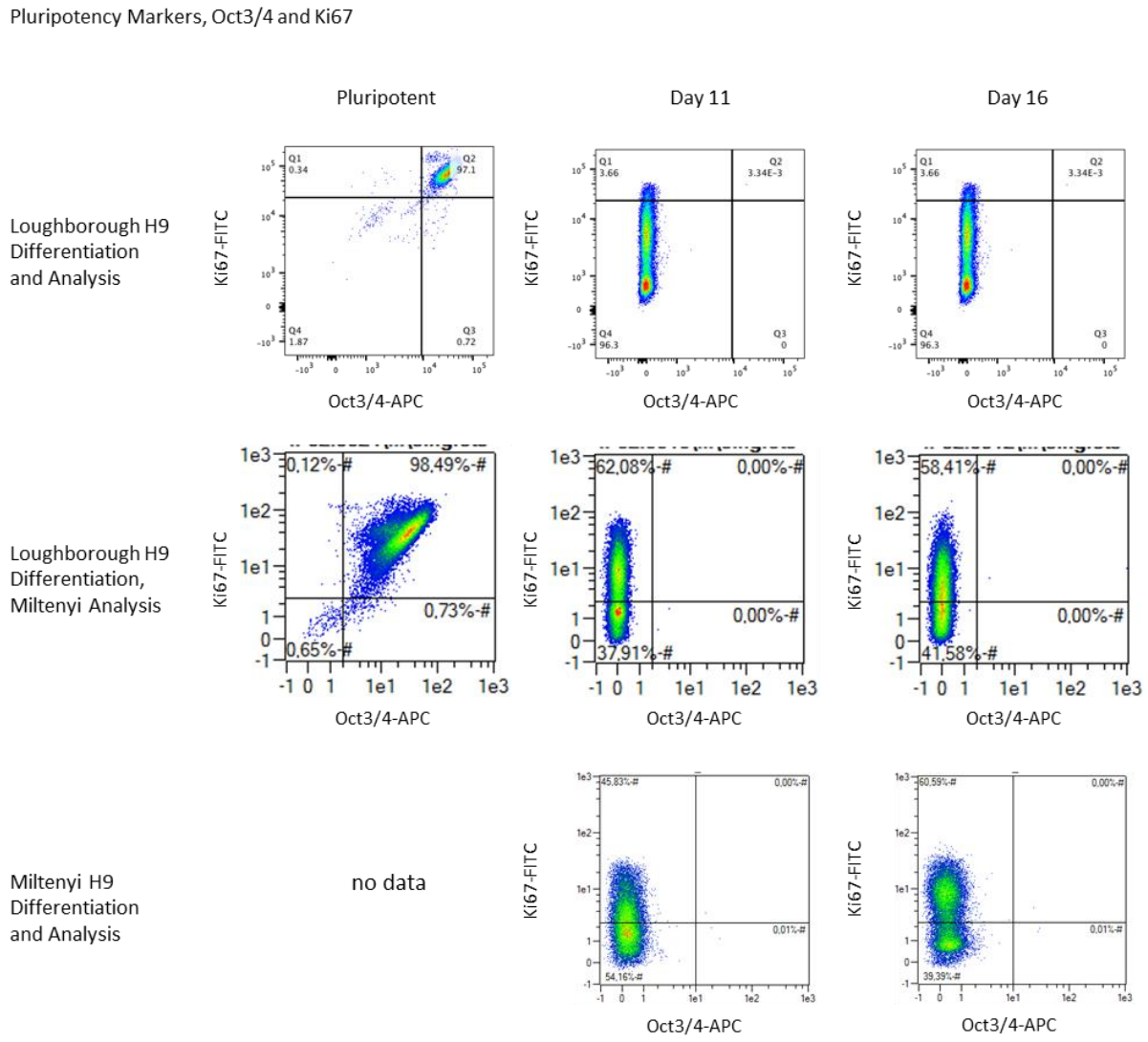

Figure 57 – Summary of key pluripotency markers for H9 cells differentiated at Loughborough and analysed at Loughborough and Miltenyi, as well as H9 cells differentiated and analysed at Miltenyi. Graph scaling is mismatched due to the use of different software across sites, and due to Miltenyi data only communicated as low-resolution images.

As shown in Figure 58, Otx2 expression was positive for pluripotent cells and experienced a small drop in expression by day 11 which persisted until day 16. No Otx2 expression data for pluripotent cells differentiated by Miltenyi was made available. FoxA2 transitioned from low at pluripotent day 0 to high at the intermediate product day 11. The Loughborough analysis showed FoxA2 levels returning to low at day 16, while Miltenyi analysis showed a higher proportion of cells retaining FoxA2 expression on day 16. Miltenyi noted that the threshold of 85% FoxA2 is difficult to meet, and that decreases after day 11 are common.

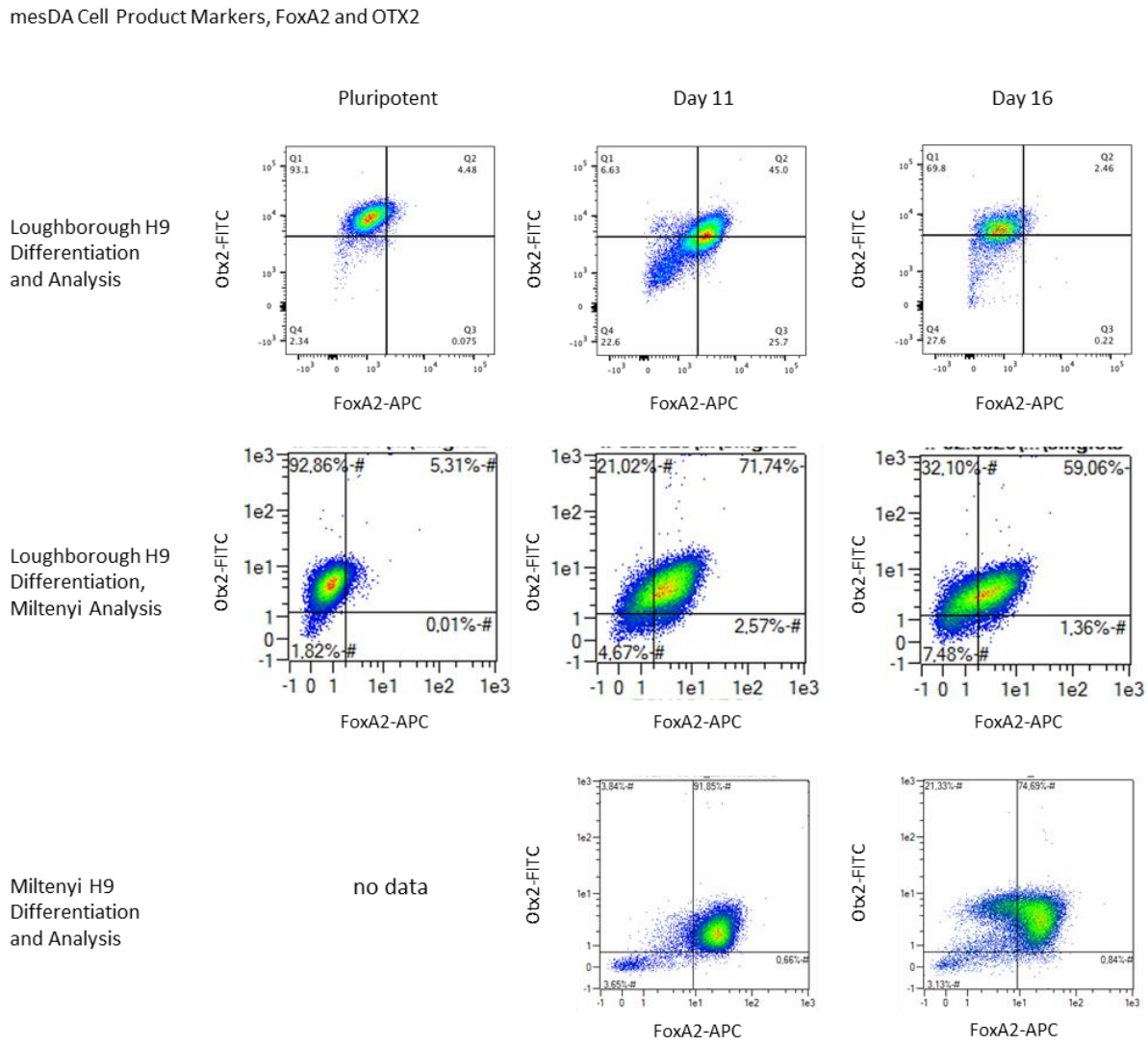

Figure 58 - Summary of key mesDA product markers for H9 cells differentiated at Loughborough and analysed at Loughborough and Miltenyi, as well as H9 cells differentiated and analysed at Miltenyi. Graph scaling is mismatched due to the use of different software across sites, and due to Miltenyi data only communicated as low-resolution images.

4.5.2 Transfer to Clinically Relevant RC17 Cell Line

In order to advance the Parkinson's disease cell therapy towards commercial approval, the use of a GMP compliant cell line as the source material grows increasingly important. A therapy is unlikely to achieve regulatory approval without adhering to modern standards of quality assurance and GMP (De Sousa, Downie, *et al.*, 2016). The H9 cell line was used in development by Miltenyi but was not derived under GMP conditions (Fernandes *et al.*, 2009). Due to legal restrictions in Germany preventing the use of embryonic cell lines derived after the 1st of May 2007, Miltenyi is unable to verify the process using any GMP compliant cell line (Schlenke *et al.*, 2008). The RC17 cell line was selected as the clinical cell

line due to the adherence to GMP guidelines during derivation, and positive outcomes during development (Nolbrant *et al.*, 2017). Details of both cell lines and the establishment of working cell banks is provided in Section 3.1.

An experiment was performed to determine the comparability of the Miltenyi 2018 mesDA manufacturing process given in Section 3.3.3 on H9 and RC17 cells. Three T25 flasks were coated with laminin-111 at a concentration of 1 µg per cm^2 and seeded with RC17s at a density of 2.5 x 10^4 cells per cm^2. Cells were then fed, maintained and harvested as described in the Miltenyi 2018 method outlined in Section 3.3.3, with the exception of all manipulations being performed in manual flasks, and liquid volumes scaled down to equal those used in typical pluripotent culture and provided in Section 3.2.

As shown in Figure 59, yields of day 11 RC17 cells averaged 2.05 x 10^6 viable cells per cm^2, which is comparable to the 1.97 x 10^6 yield obtained for day 11 H9 cells at Loughborough and higher than Lund for both cell types. Yields follow the same pattern across institutions of higher yields for RC17 than H9 cells. Day 16 product cell yields for RC17s averaged 1.78 x 10^6 which is similar to day 16 yields obtained at Lund at 1.7 x 10^6 for H9s and 1.95 x 10^6 for RC17s.

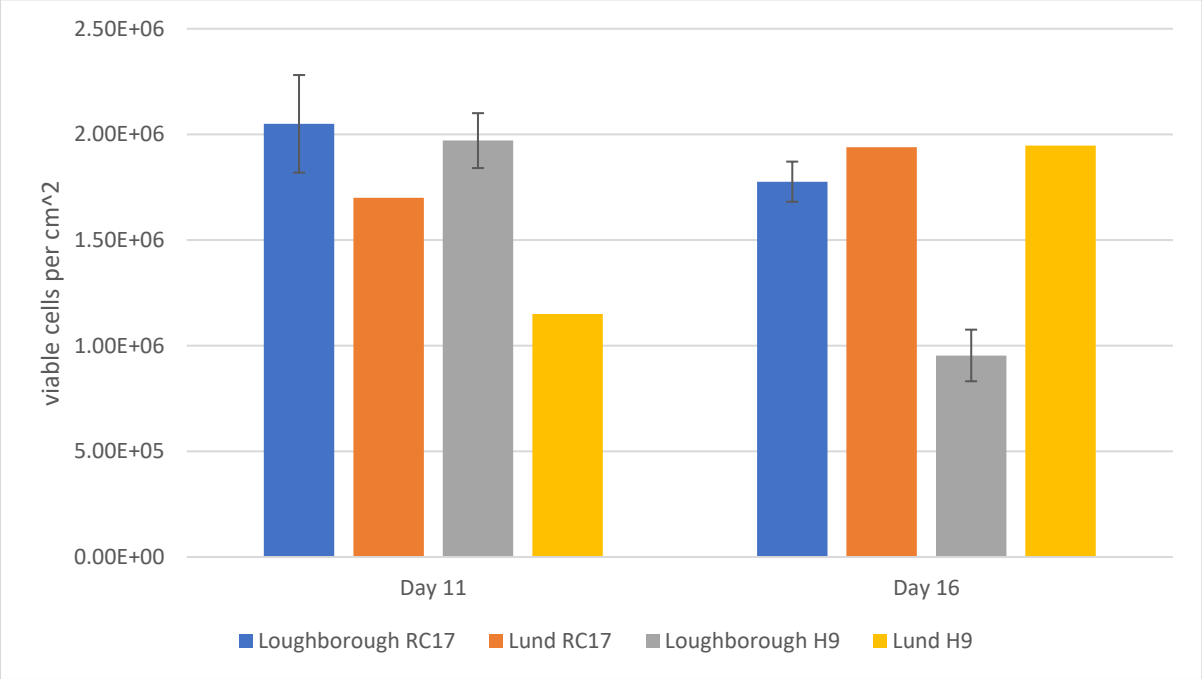

Figure 59 – Comparison of yields at differentiation days 11 and 16 for H9 and RC17 cells at Loughborough and Lund. Loughborough bars shown as mean ± SD for biological repeats, n=3

Cell morphology for H9 and RC17 differentiation processes at Loughborough are shown in Figure 60. RC17s formed culture clusters at day 2 with inner cells beginning to bunch as growth area was restricted, while cells on the edge of culture groups extend into the available space. H9s by comparison appeared more evenly spaced and face no restricted growth area. At day 4, both cell types approached 100% confluency and appeared less spread out as space grew scarce. Areas of high cell density are visible as white patches as light diffracts between rounded up cells, whereas areas of relatively lower cell density appear as larger more transparent cells. This pattern was more pronounced on day 6 for both cell types. By day 10, cells had remained at 100% confluency for several days and were therefore severely restricted by available culture area. High density areas exhibited cell growth on top of laminin attached cells, visible in microscopy as distinct layers of white featuring focussed and unfocussed cells. The pattern of growth area limitation was repeated following reseeding on day 11, with cells at day 14 appearing less severely layered and layering developing more prominently by day 16. Layering for H9 cells on day 16 is less apparent, reflecting the lower yields obtained.

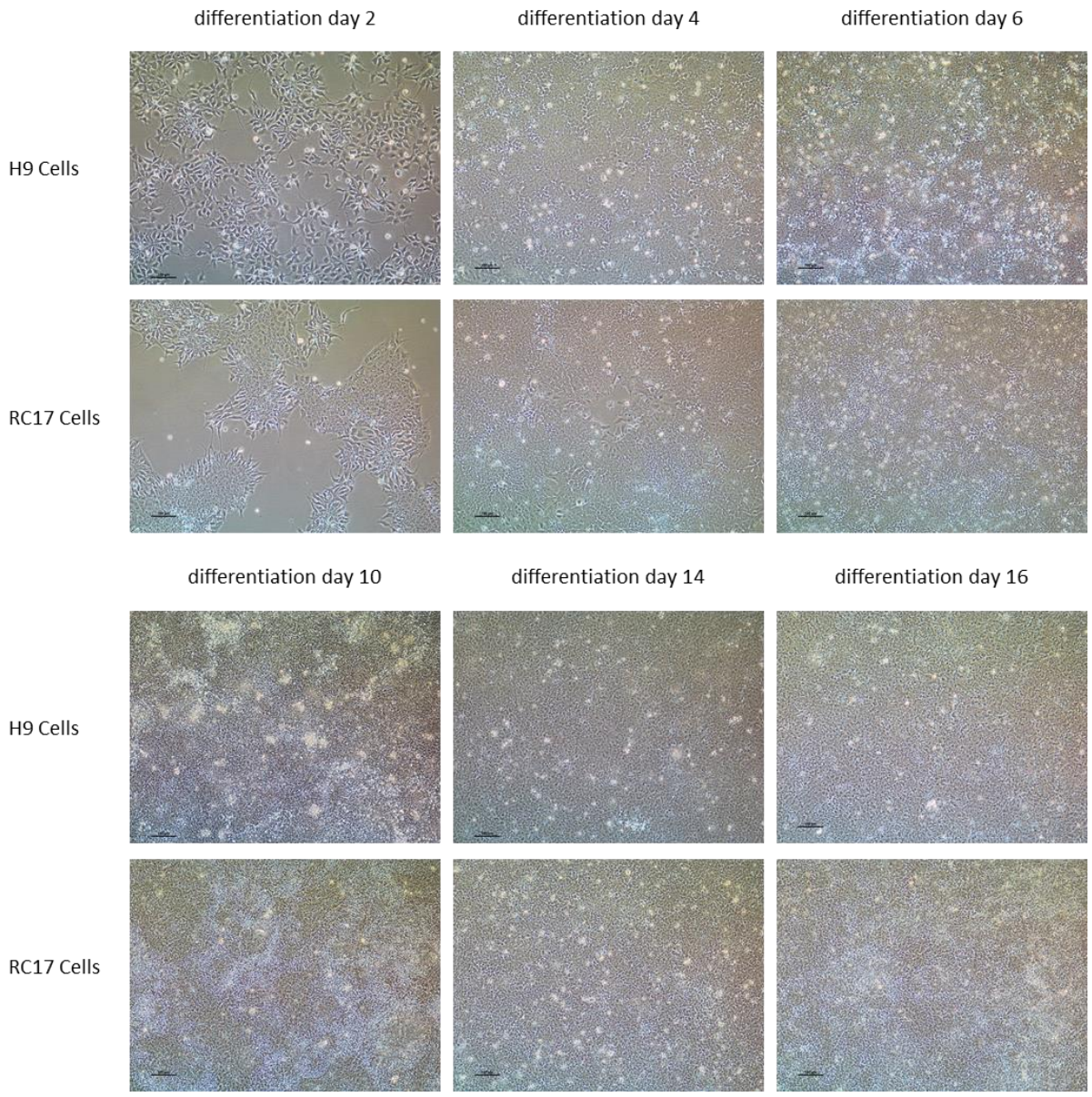

Figure 60 – Cell growth during differentiation of H9 and RC17 using a manual protocol. Both cell types reach full confluence at around day 4 and remain overconfluent for the rest of the differentiation process. Scale bars are equivalent to 100 µm.

As with H9 cells, flow cytometry was performed on cell samples from days 0, 11 and 16 for each flask according to the methods provided in Section 3.5.3, a summary of pluripotency marker results in provided in Figure 61. Oct3/4 transitioned from positive to negative expression between pluripotent cells and those on differentiation days 11 and 16 for both cell types across all analyses. Ki67 was positive for pluripotent cells and highly variable on differentiation days 11 and 16 as expected.

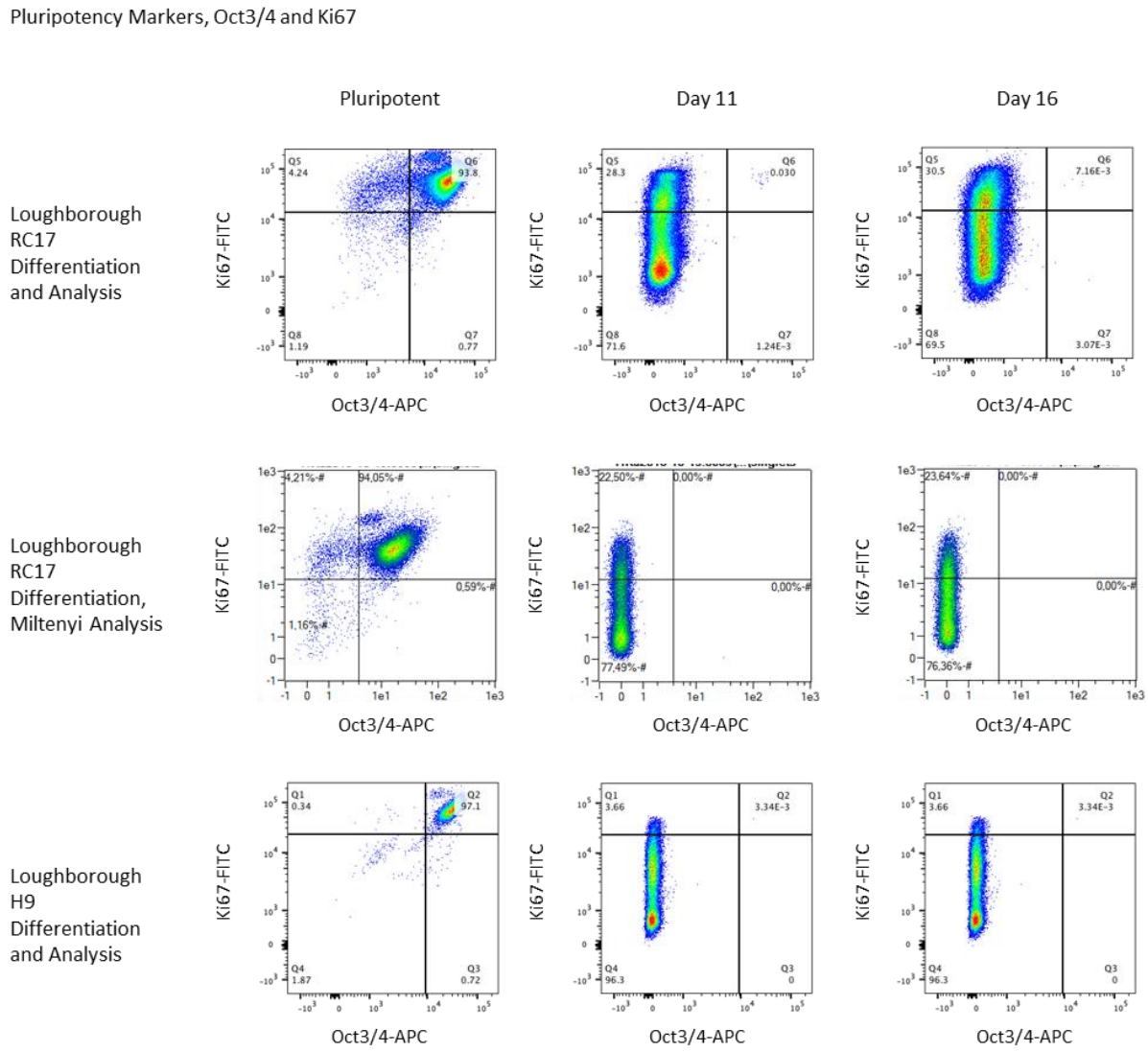

Figure 61 – Summary of key pluripotency markers for RC17 cells differentiated at Loughborough and analysed at Loughborough and Miltenyi, as well as H9 cells differentiated and analysed at Loughborough. Graph scaling is mismatched due to the use of different software across sites, and due to Miltenyi data only communicated as low-resolution images.

A summary of product marker expression is shown in Figure 62. For RC17s, Otx2 expression was positive for pluripotent cells and remained positive throughout the differentiation process. As with H9s, FoxA2 expression transitioned from low at pluripotent day 0 to high at the intermediate product day 11, then highly variable at day 16. Positive FoxA2 expression on day 16 is noted as challenging both in the Lund 2017 protocol (Nolbrant *et al.*, 2017) and in Miltenyi quality control development report (Neurostemcellrepair, 2018).

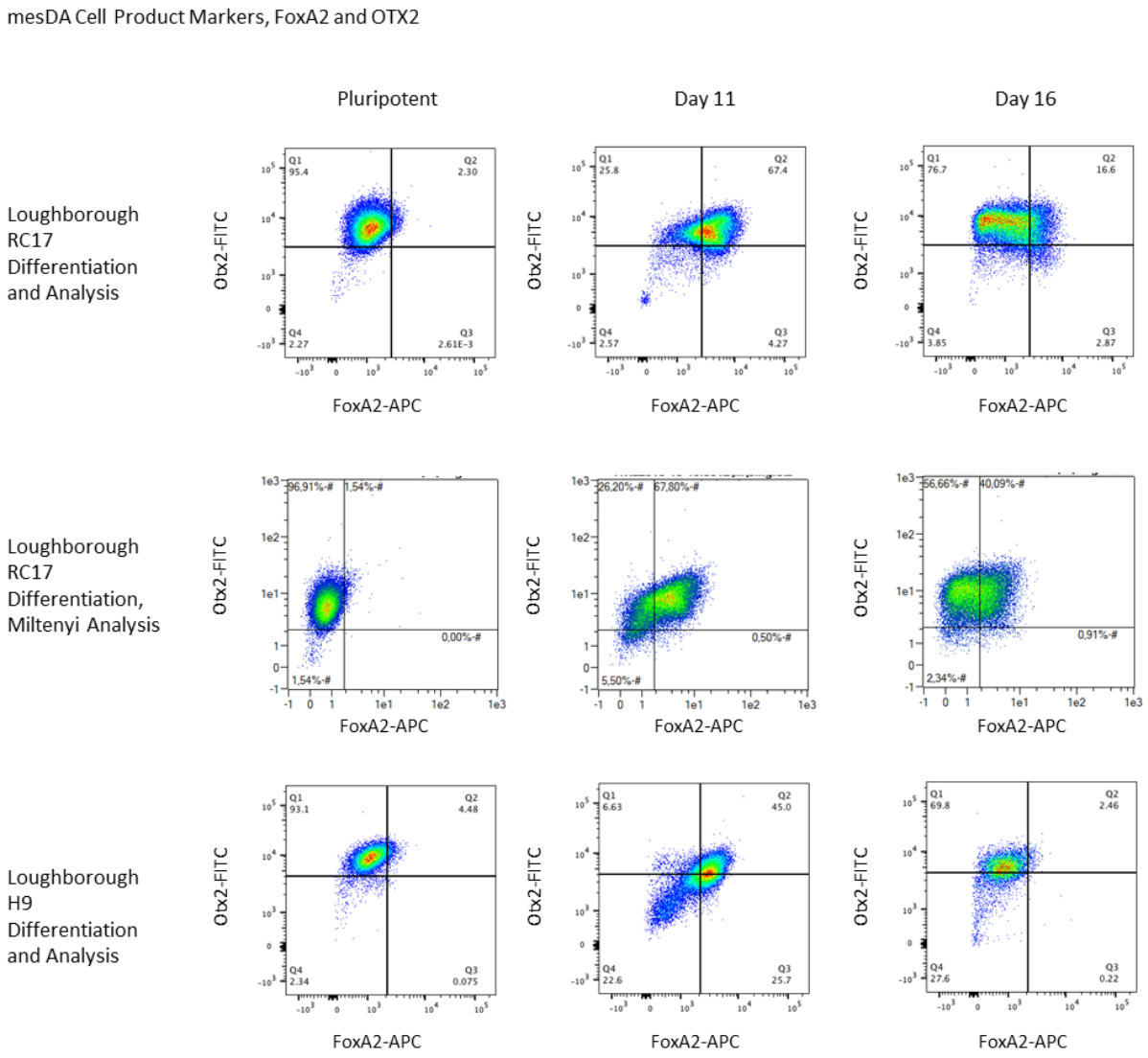

Figure 62 - Summary of key mesDA product markers for RC17 cells differentiated at Loughborough and analysed at Loughborough and Miltenyi, as well as H9 cells differentiated and analysed at Loughborough. Graph scaling is mismatched due to the use of different software across sites, and due to Miltenyi data only communicated as low-resolution images.

4.6 Prodigy Differentiation Troubleshooting

Following the successful expansion of cells within the CCU shown in Section 4.4.4 and the demonstration of comparability between manual differentiation runs shown in Section 4.5.1, three automated differentiation runs were attempted.

4.6.1 Initial Prodigy Differentiation Runs

For automated differentiation runs, CCU grown cells were seeded into a single layer CellSTACK using the Prodigy, with automated liquid manipulations used during seeding, maintenance and cell harvesting as detailed in Section 3.4. For each automated run, three T25 flasks were manually processed in parallel as controls, utilising the same starting cell population and pooled medium and reagent preparation. As discussed in Section 4.1, each automated differentiation described in this chapter followed an automated expansion demonstration, the differentiation runs are therefore referred to as process runs 4, 5 and 6 as they followed the expansion phases of process runs 4, 5 and 6 discussed in Section 4.4.4.

4.6.1.1 Process Run 4, Automated Differentiation to mesDA Progenitors

The successful expansion of H9 cells in the CCU during the fourth Prodigy run described in Section 4.4.4.1 produced 4.6 x 10^7 viable cells which was sufficient to seed a differentiation within a single layer CellSTACK. Due to the ongoing development of the Miltenyi differentiation protocol, this process run was performed using the Lund 2017 differentiation process detailed in Section 3.3.2, with a single layer CellSTACK seeded at a density of 1 x 10^5 viable cells per cm^2 and with liquid manipulations performed via the Prodigy. This process attempt was halted prematurely for both the Prodigy manipulated CellSTACK and manually manipulated controls, with the CellSTACK stopped on day 4 due to lack of cell attachment and the manual controls stopped on day 11 due to detachment and cell death, as summarised in microscopy images shown in Figure 63.

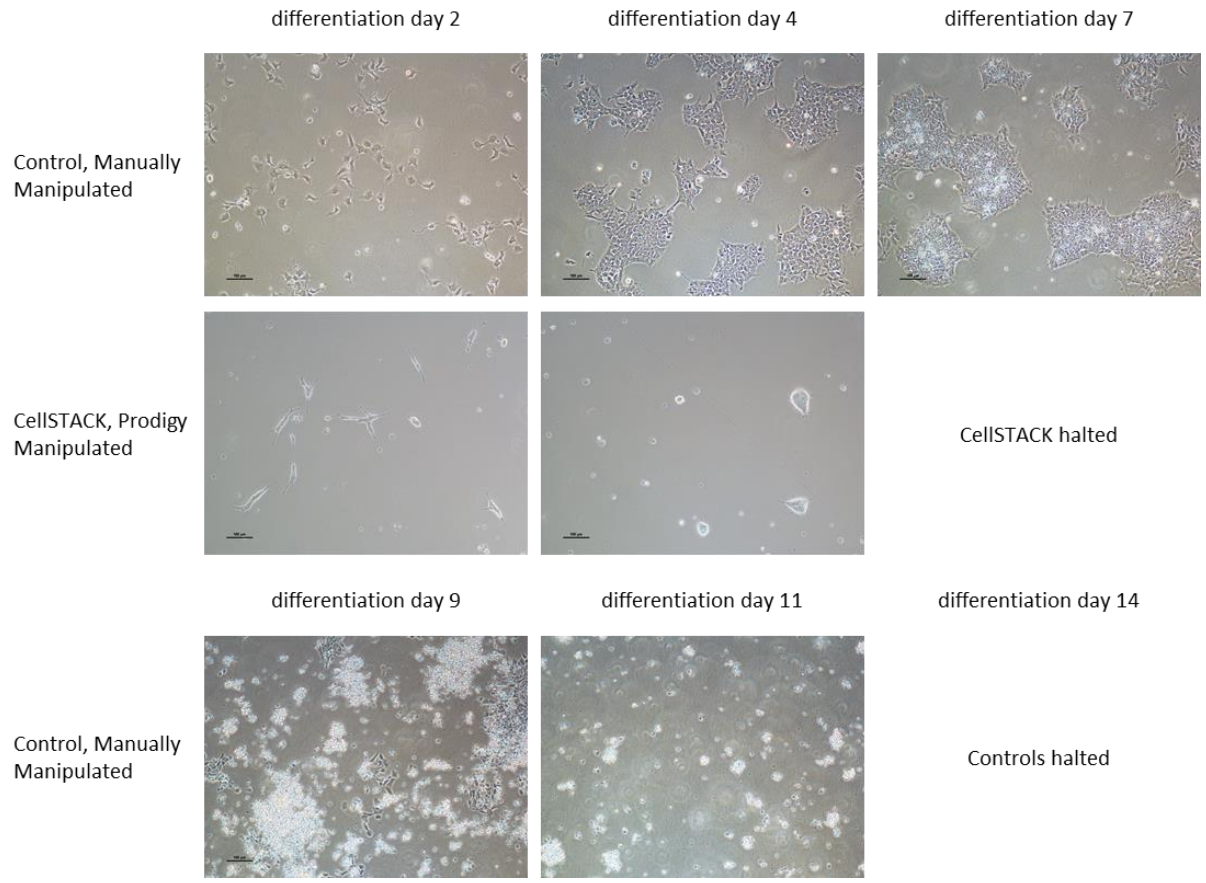

Figure 63 – Cell growth during H9 differentiation in automated process attempt 4. The CellSTACK was stopped on day 4 due to lack of cell attachment, while the control flasks were stopped on day 11 due to cell death. Scale bars are equivalent to 100 µm.

On differentiation day 2 there was visibly more cell attachment in the control flasks than Cell STACK, with only a small amount of variation between controls. By differentiation day 4, cells in the control flasks had begun to form colonies whereas cells in the stack had begun to detach and round up, with little visible growth. It was decided to end the differentiation attempt within the CellSTACK to preserve reagents. A count was performed on the CellSTACK contents giving a density of 1.14×10^4 viable cells per cm^2, equating to a loss of 88.6% cells seeded. Differentiation was continued in the control flasks, which at day 7 had increased in confluency but begun to show signs of cell detachment and rounding. Flasks 1 and 3 exhibited small areas of near total confluency while flask 2 did not. Most of the area for all flasks was at around 50% confluency. At day 9 all control flasks displayed significant cell detachment. Flasks were counted on day 11 and had 5.31×10^4 viable cells per flask, with an average viability of 37.0%.

The differentiation process used during this process run used the reagents and feed schedule of the Lund 2017 protocol provided in Section 3.3.2, with adaptions for compatibility with the CellSTACK and

Prodigy as detailed in Section 3.4. To prioritise correct patterning of the cells, none of the troubleshooting steps advised in the Lund 2017 protocol paper to improve process reliability were utilised (Nolbrant *et al.*, 2017). Increased cell death between differentiation days 4 and 9 are noted in the Lund paper as being typical for H9s, with the recommendation being made to add B27 supplement on differentiation days 0 to 11. Lund also advises that higher CHIR levels are required for correct patterning if B27 is used throughout the differentiation. Following this process attempt, the Miltenyi 2018 protocol was communicated to Loughborough and utilised for future differentiation runs.

4.6.1.2 Process Run 5, Automated Differentiation to mesDA Progenitors

The fifth process attempt was performed according to the Miltenyi 2018 differentiation protocol and includes reagent and feed schedule changes to reduce cell death and improve robustness. As detailed in Section 4.4.4.2, the expansion preceding this differentiation attempt failed due to a buffer contamination within the CCU. Pluripotent cells from the control flasks of the expansion phase were therefore used to manually seed a differentiation in a CellSTACK, with all further liquid manipulations for CellSTACK feeds performed using the Prodigy. Despite comparable cell growth and morphology from days 2 through 6, a bacterial infection was discovered within the CellSTACK on day 10 and the Prodigy process halted. Manual flasks were continued until process completion on day 16.

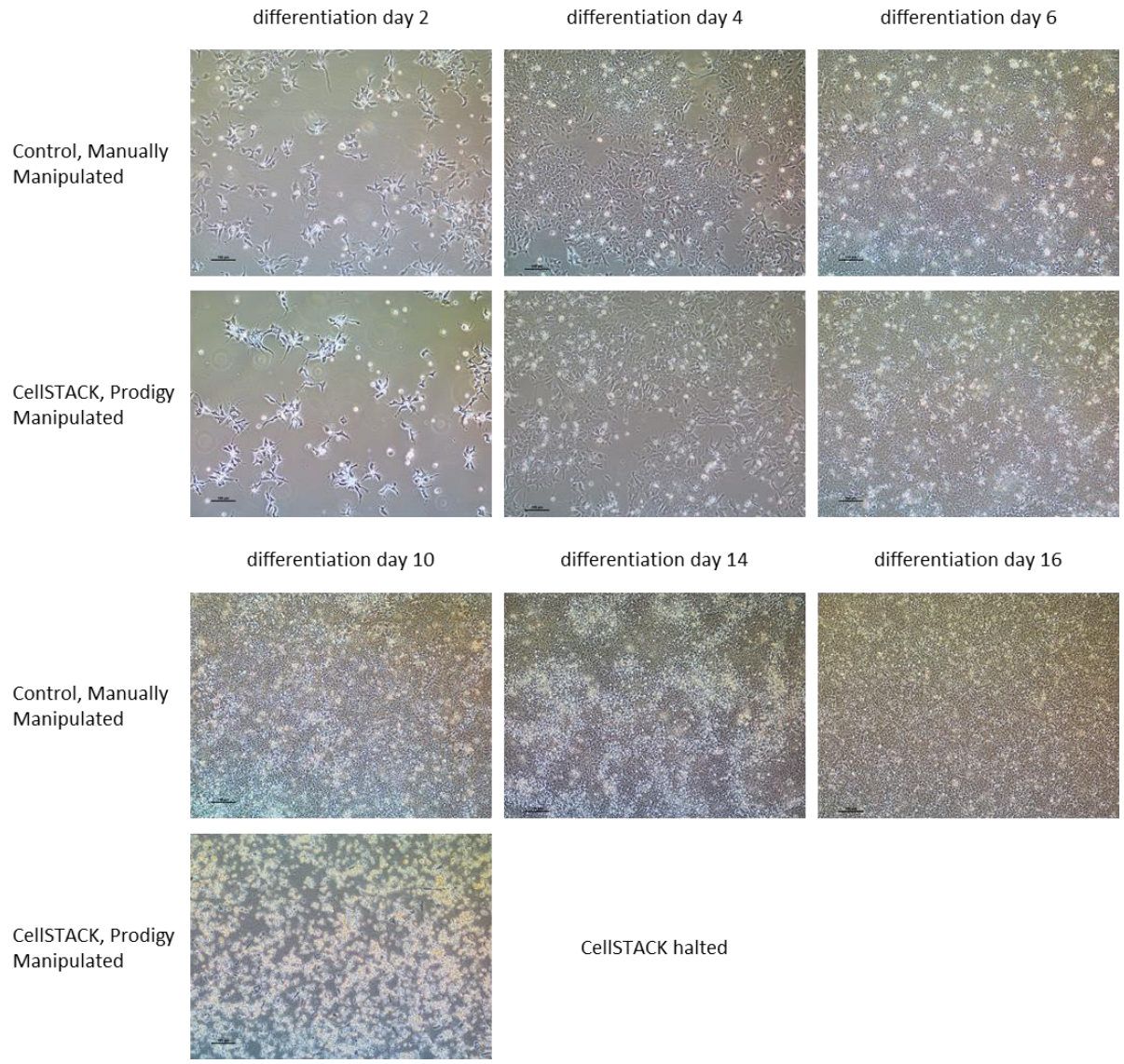

Figure 64 – Cell growth during H9 differentiation of automated process attempt 5. The CellSTACK appeared healthy until day 10 when cells detach from the culture surface due to bacterial contamination, visible as dark debris between cells. Control flasks continued to completion with no signs of infection. Scale bars are equivalent to 100 µm.

The source of infection for the CellSTACK process is unknown as no failed tube welds or loose Luer locks were identified, meaning that the Prodigy and CellSTACK should form a fully closed system. All medium was prepared as a common batch in a dip tube bottle before being split to feed the CellSTACK and control flasks, meaning that compromised reagents were unlikely to be the cause of infection due to success of the control flasks.

4.6.1.3 Process Run 6, Automated Differentiation to mesDA Progenitors

Following a successful expansion of RC17 cells within the Prodigy CCU producing 8.8 x 10^7 viable cells as described in Section 4.4.4.3, the run was continued into a CellSTACK differentiation with manipulations performed by the Prodigy. As detailed in Section 3.4, the Prodigy was used to harvest and purify pluripotent cells from the CCU, which were then counted, and the correct volume of cells transferred to seed a CellSTACK. As shown in Figure 65, cells in the control flasks attached and grew normally, while those seeded into the CellSTACK using the Prodigy under otherwise identical conditions showed little attachment or growth. Control flasks were continued until process completion, reaching confluency by approximately day 6 and producing a day 11 yield of 1.46 x 10^6 per cm^2 and day 16 yield of 2.01 x 10^6 per cm^2.

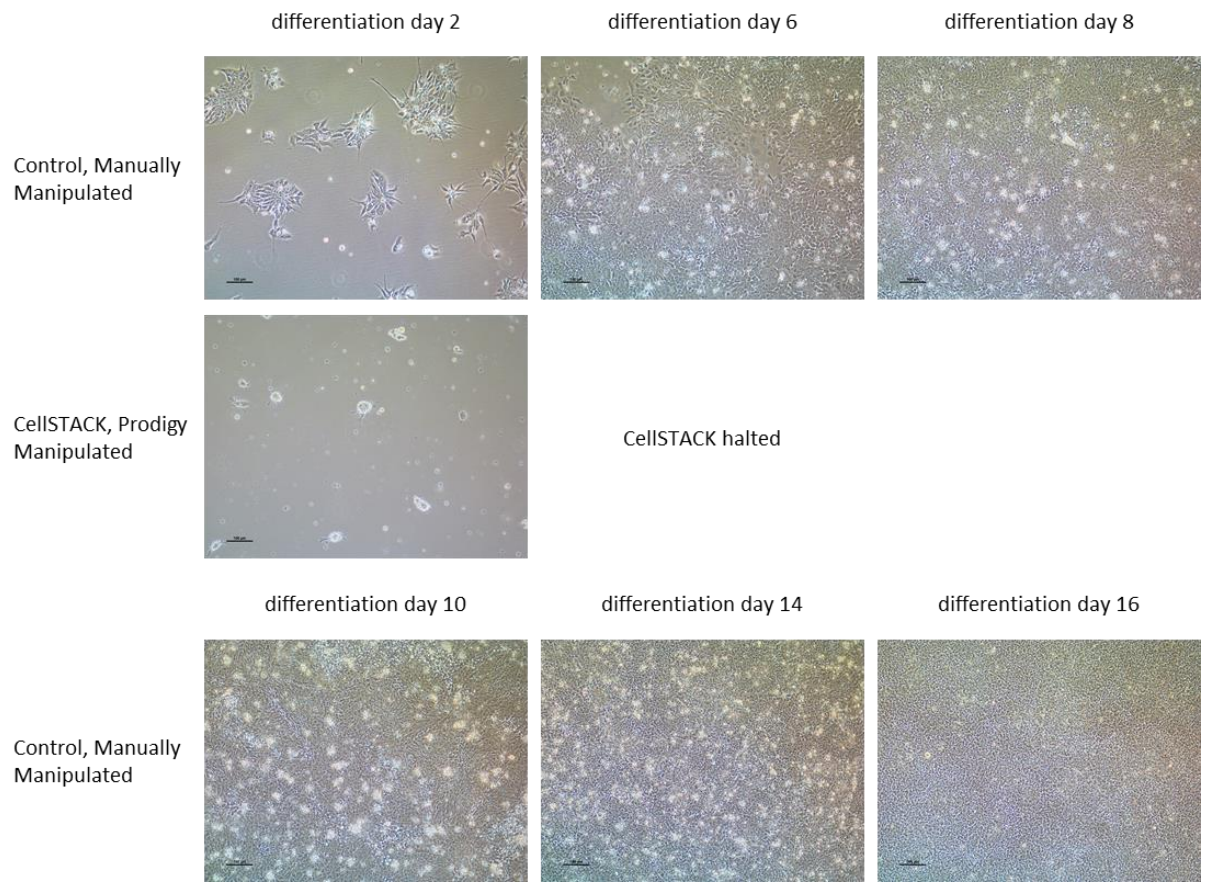

Figure 65 – Cell growth during RC17 differentiation of automated process attempt 6. The CellSTACK was halted on day 2 due to lack of cell attachment, while control flasks continued to process completion. Scale bars are equivalent to 100 µm.

4.6.1.4 *Summary of Process Runs 4, 5 and 6, Differentiation Phase*

Figure 66 shows a summary of differentiation yields for control flasks compared to manual only runs. No day 11 or day 16 yield data is available for any CellSTACK differentiations due to the early failure in every case. Process runs 4 and 6 exhibited similar failure types of a successful expansion followed by cells not attaching to the CellSTACK on day 0, with control cells performing well until process end. Process run 5 failed on day 10 due to an infection with an unknown source. In both cases, the causes of failure had many potential contributing factors and prompted formal failure mode investigation.

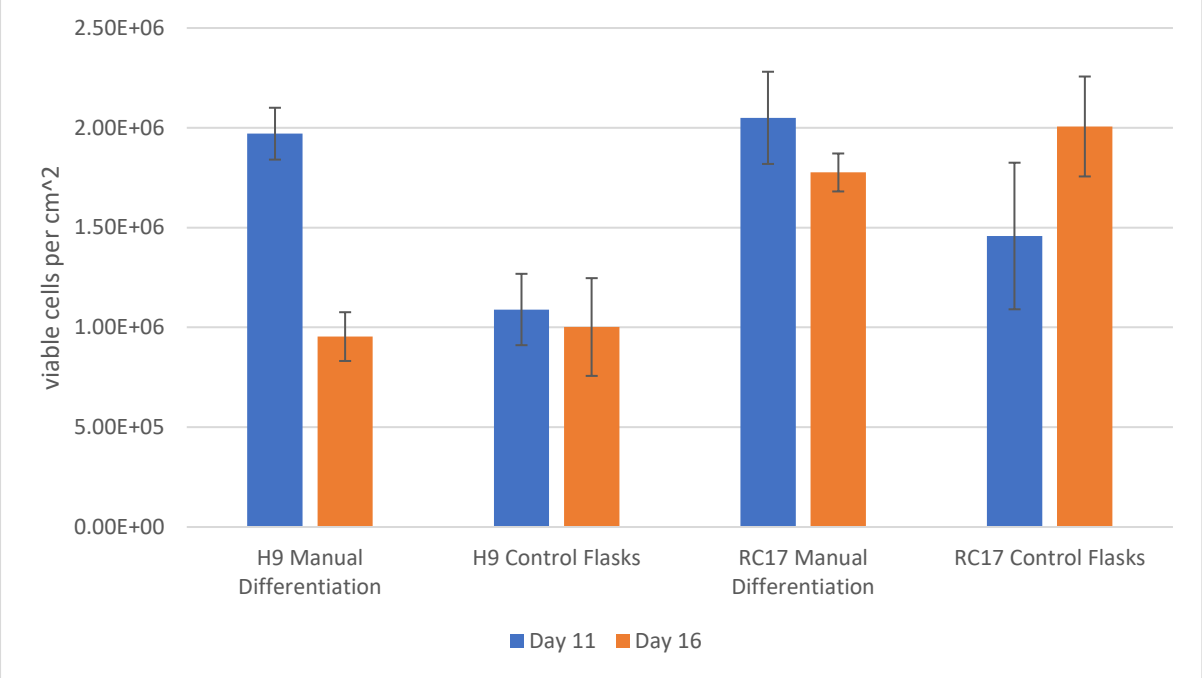

Figure 66 – Differentiation yields for control flasks compared to manual only runs. Day 16 yields demonstrate consistency within cell types with RC17 producing higher yields than H9s. Data shown as mean ± SD for biological repeats, n=3. No data is available for automated differentiation attempts, which all failed prior to the sampling point on differentiation day 11.

4.6.2 Identification of Potential Failure Causes

Based on the differentiations performed in process runs 4, 5 and 6, an Ishikawa diagram (Figure 67) was produced to highlight potential causes of failure for the CellSTACK differentiation process performed on the Prodigy, with potential failure modes then prioritised for further investigation.

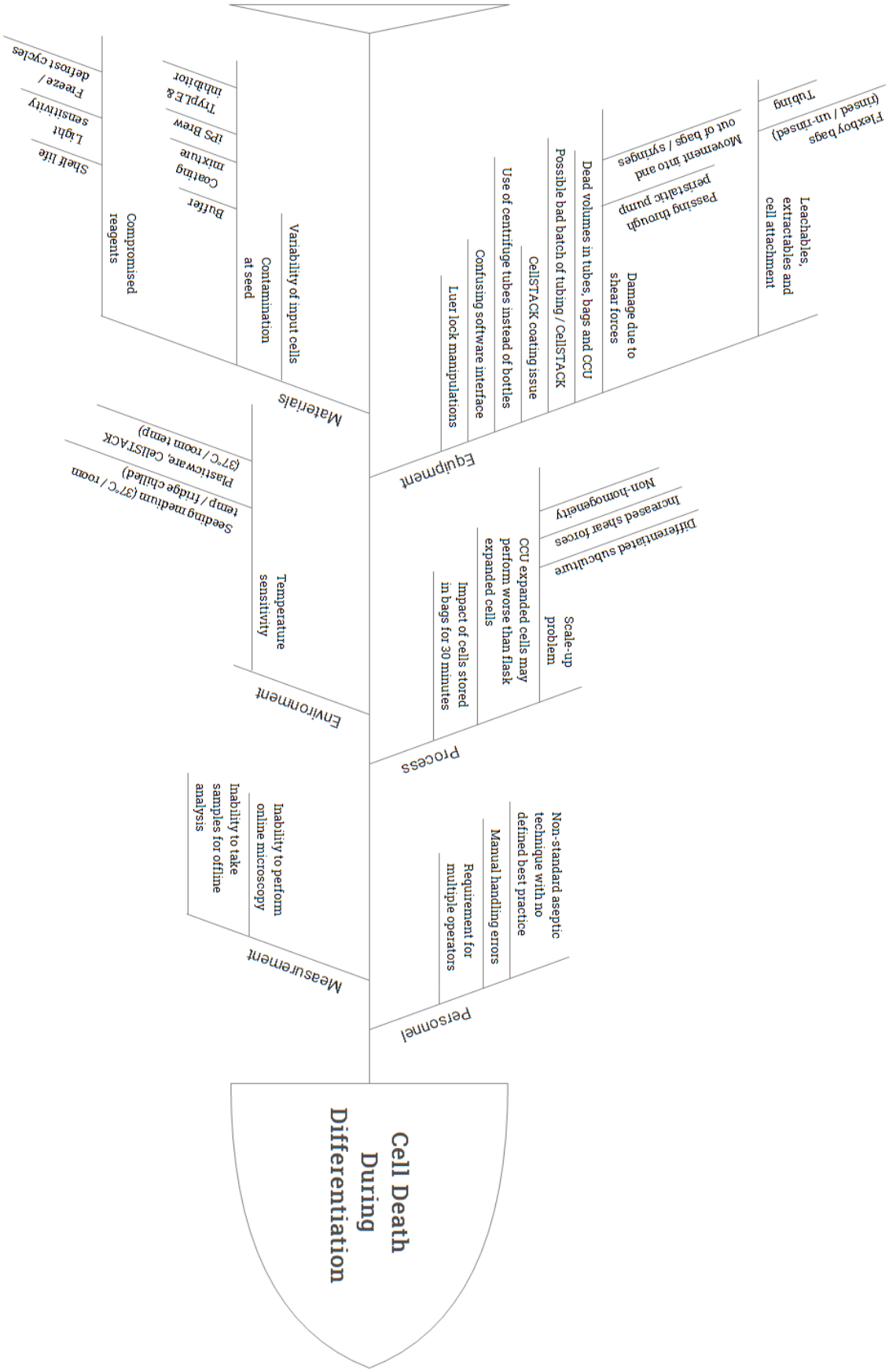

Figure 67 - Ishikawa diagram of potential causes of failure for the CliniMACS Prodigy differentiation process

4.6.3 Analysis of Potential Failure Causes

Two attempts to seed pluripotent cells into a CellSTACK resulted in process failure due to lack of cell attachment after 24 hours, despite successful seeding of manual control cells using the same reagent pool. It was not clear whether the cells attached and detached within this period, or whether the cells never attached at all. Following efforts to identify differences between the process as performed manually and Prodigy run process, key areas were identified as interactions between cells and plasticware (tubing and flexible bags as compared to serological pipettes and centrifuge tubes) and possible contamination due to dead volumes when centrifuging or transferring liquid throughout the Prodigy tubing set.

4.6.3.1 Cell Storage in Flexible Bags

The extraction of a cell sample from the Prodigy after harvesting the CCU was discovered to be a common point for the introduction of process delays, both due to the number and challenging nature of manipulations as well as due to the limited availability of automated cell counting due to other laboratory users. Because of this, harvested cells may remain in a flexible bag for up to 30 minutes. Hold periods during cell processing have been shown to reduce cell membrane integrity (Delahaye *et al.*, 2015). The potential negative impact of this period of bag storage for cells was therefore explored to determine whether hold periods in flexible bags lead to reduced cell yields following seeding, and therefore whether a reduction in hold time should be prioritised for future process revisions.

In a variation of the differentiation method described in Section 3.3.3, a 6-well plate was coated with laminin-111 and a 50 ml bag was rinsed with feed medium and incubated for 30 minutes. Cells were harvested, transferred to a 50 ml centrifuge tube and the average of three viable cell counts obtained, then resuspended in seed medium. Three wells of the 6-well plate were aspirated of coating mixture and seeded with cells at 2.5 x 10^4 viable cells per cm^2 with 2ml seeding medium. The remaining cell suspension was diluted in 50ml seed medium and transferred to a 50ml bag where it remained at room temperature for 30 minutes. Cells were then recovered from the bag and seeded into three wells of a 6-well plate at 2.5 x 10^4 viable cells per cm^2 with 2ml seeding medium. Cells were then cultured for 48 hours before being harvested and counted as described in Section 3.2.

As shown in Figure 68, Cells stored in a bag for 30 minutes prior to seeding averaged 7.53 x 10^4 viable cells per cm^2 on after 48 hours of culture, while the control condition averaged 7.33 x 10^4 viable cells

per cm^2. Bag stored cells show no significantly reduced growth potential compared to a control with no bag storage or delay period (P =0.34). This result was unexpected as hold time has previously been shown to result in reduced membrane integrity (Delahaye *et al.*, 2015), however, any effect of this nature did not translate into reduced cell yields following culture. This outcome suggests that the typical bag hold time that cells experience during processing on the Prodigy is of little impact to later cell yields.

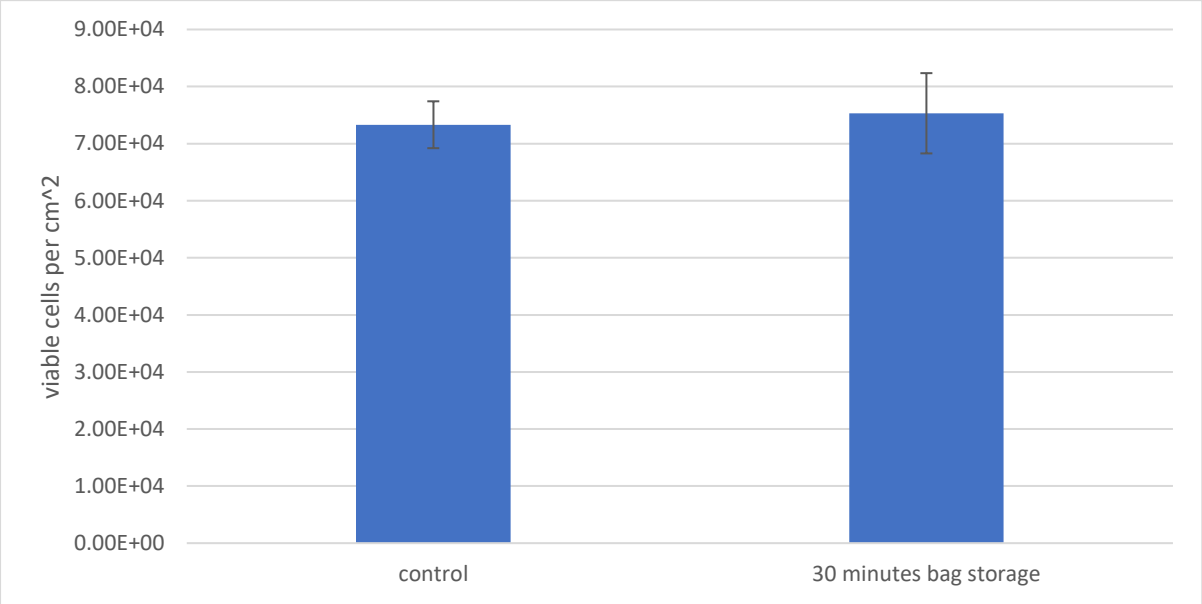

Figure 68 – RC17 cells stored in a flexible bag at room temperature for 30 minutes prior to seeding produced comparable yields to cells seeded immediately after resuspension in seed medium. Data shown as mean ± SD for biological repeats, n=3.

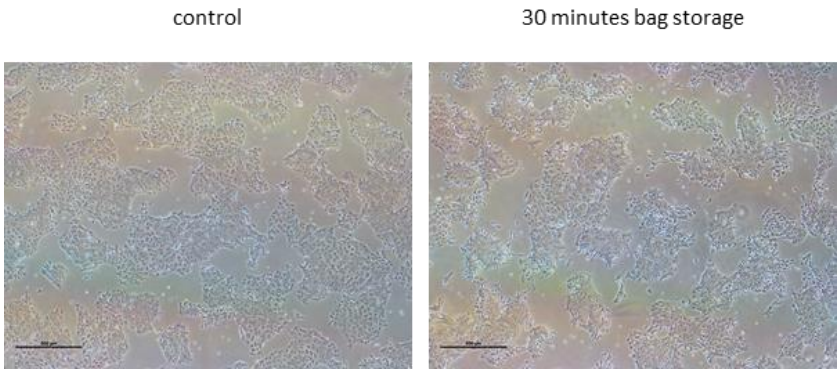

Figure 69 - Comparison of growth of bag stored RC17 cells to non-bag stored controls. Cell growth and number of dead cells appear comparable between conditions. Scale bars are equivalent to 500 µm.

4.6.3.2 Temperature Sensitivity

There are a large number of additional manipulations and delays when passaging cells from the CCU and seeding them into a CellSTACK using the Prodigy, rather than from flask to flask using manual cell culture techniques. Because of this, medium and culture plastic will cool from the incubation warmed temperature of 37°C to room temperature during processing. ESCs are known to be temperature sensitive (Heng *et al.*, 2006), with temperature control and monitoring highlighted as an area of particular consideration in regulatory guidance (ICH, 1995). The reduction in ESC temperature during Prodigy processing may therefore contribute negatively to cell seeding by cooling cells to non-optimal temperatures at the time of seeding.

A first experiment explored the effects of non-warmed culture plastic. Three wells on two 6-well plates were coated with laminin-111 according to the method described in Section 3.3.1. One plate remained in the 37°C incubator until seeding, while the other was removed 30 minutes prior to seeding. RC17 cells were harvested, counted and resuspended in seed medium according to the method described in Section 3.2. The warmed plate was removed from the incubator, coating mixture was aspirated and replaced with 2ml of warmed seeding medium with cells at a density of 2.5 x 10^4 viable cells per cm^2. The non-warmed plate, having cooled to room temperature for 30 minutes, had its coating mixture aspirated and was seeded under the same conditions.

A second experiment looked at the effects of non-warmed seed medium. Nine wells across two 6-well plates were coated with laminin-111 according to the method described in X. Seeding medium was prepared and transferred into three centrifuge tubes, with one stored in a 37°C water bath, the second stored at room temperature and the third in a fridge at 4°C for 30 minutes. Cells were harvested, counted and resuspended in 5ml of warmed seeding medium according to the method described in Section 3.2. Coating mixture was aspirated from all wells and replaced with 2ml of seeding medium, with three wells for each temperature condition (37°C, room temperature and 4°C). Cells were then added to each well to a density of 2.5 x 10^4 viable cells per cm^2.

As shown in Figure 70, cells seeded onto room temperature culture plastic perform with no significantly different variance to cells seeded onto warmed culture plastic following 48 hours of growth (P = 0.27). This suggests that the change in culture plastic temperature possible during processing on the Prodigy is unlikely to have caused the cell death seen on previous differentiation attempts.

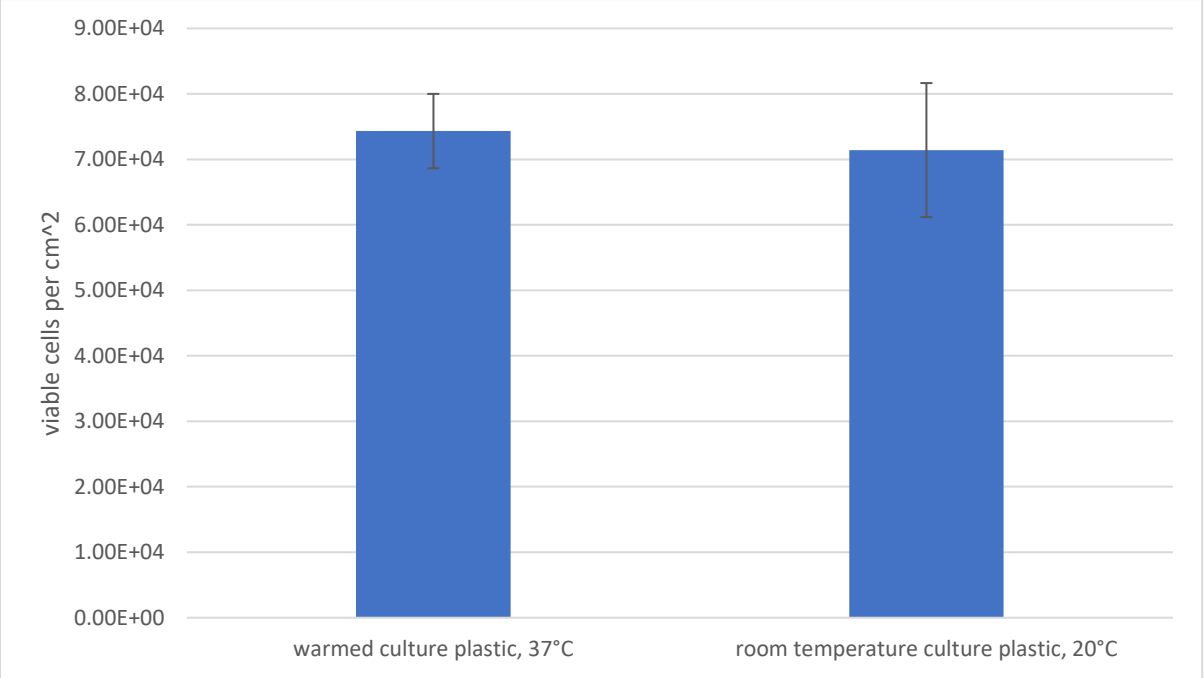

Figure 70 – Comparison of RC17 cell density at differentiation day 2 for cells seeded onto warmed or room temperature culture plastic. Data shown as mean ± SD for biological repeats, n=2.

As shown in Figure 71, cells seeded using room temperature and fridge chilled medium do not produce significantly different variance as compared to cells seeded into medium warmed to 37°C following 48 hours of growth (P = 0.28). It is surprising that the cells did not perform more poorly with fridge chilled medium. This may be because the fridge chilled medium was quickly warmed by the culture plastic soon after seeding. There was a relatively small volume of chilled medium (2ml per well across three wells) compared to a high amount of plastic in a 6-well plate, which would have been warmed to 37°C during the 2-hour coating incubation period. This would likely be worse for larger vessels, as the culture medium to plasticware ratio increases. Given the negligible effect of non-warmed culture plastic and the small effect of fridge chilled medium, temperature changes within the range likely on a Prodigy process are unlikely to have caused lack of attachment present on previous differentiation attempts seeded through the Prodigy. Although temperature is highlighted in the literature as an important factor in cell processing (Heng *et al.*, 2006), the results of this experiment show that medium temperature differences for the time taken to reach equilibrium in an incubator do not cause significant harm to RC17 cells.

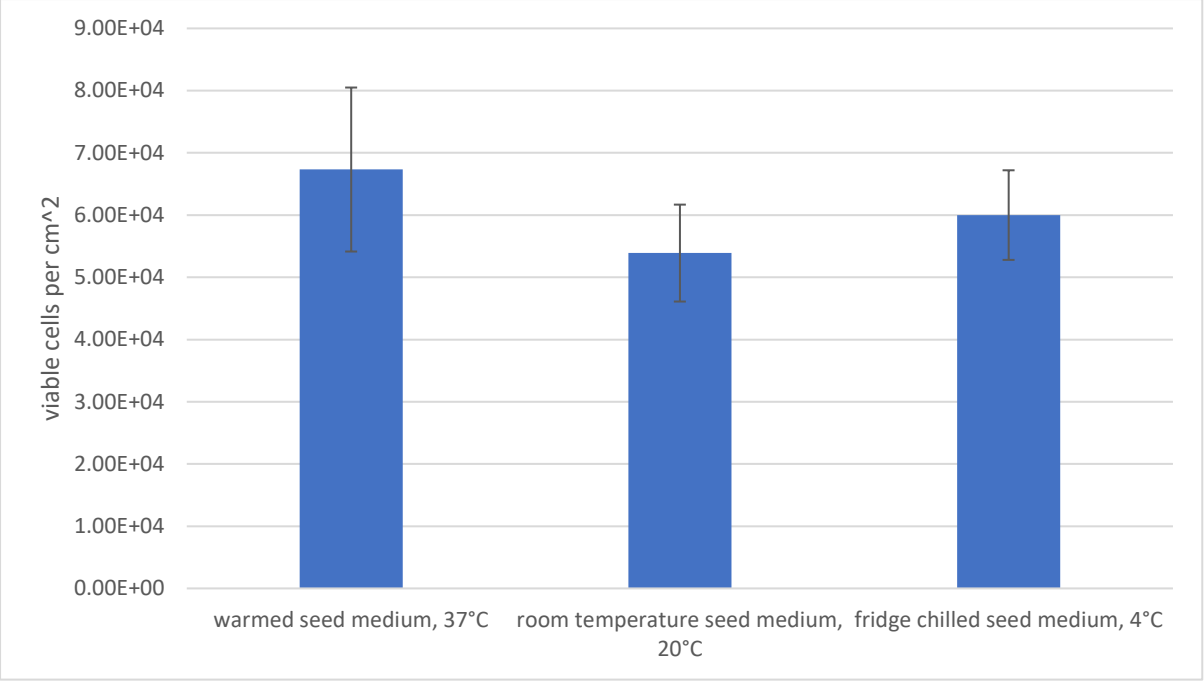

Figure 71 – Comparison of medium temperatures during RC17 cell seeding. The use of room temperature and fridge chilled medium produced. Data shown as mean ± SD for biological repeats, n=3.

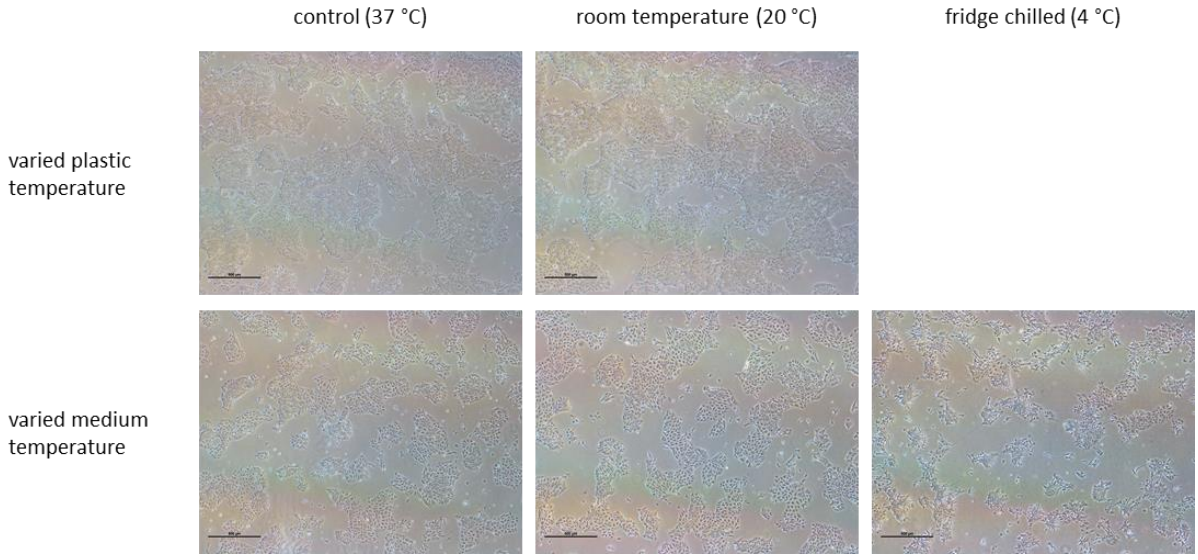

Figure 72 – RC17 attachment and growth for varied culture plastic and medium temperatures during cell seeding. Fridge chilled plastic was not tested as this condition would never occur during normal culture conditions. Scale bars are equivalent to 500 µm.

4.6.3.3 CCU and Manually Expanded Cells

CellSTACK differentiation runs use cells expanded within the CCU whereas manual differentiation runs use cells expanded in manual culture. Little information about the material and surface treatment of the CCU was made available by Miltenyi, however, the CCU was primarily designed for the processing of suspension cell types, meaning that the surface properties of the CCU may differ from standard tissue culture treated plasticware. An experiment was performed to determine whether expansion within the CCU has a negative impact on cells which may contribute towards detachment and lack of growth following seeding of a differentiation.

Due to the prohibitive cost of using the Prodigy for anything other than full process runs, cryopreserved samples from previous Prodigy process attempts were utilised. A vial of CCU expanded pluripotent cells as well as a vial of manually expanded control cells from expansion day 5, differentiation day 0 of the sixth Prodigy process were thawed and transferred to a centrifuge tube with 5ml of feed medium. All processing was performed according to the method described in Section 3.2. Cells were split to allow for four seeding conditions:

- Expansion seeded with manually expanded cells
- Expansion seeded with CCU expanded cells
- Differentiation seeded with manually expanded cells
- Differentiation seeded with CCU expanded cells

Cells for pluripotent expansion were resuspended in expansion seed medium and seeded into laminin-521 coated 6-well plate wells at a density of 2 x 10^5 viable cells per cm^2. Cells for differentiation were resuspended in differentiation seed medium and seeded into laminin-111 coated plates at 2.5 x 10^5 viable cells per cm^2. Each condition comprised of three biological repeats. All conditions were harvested and counted following 48 hours of culture.

As shown in Figure 73, pluripotent expansion using cells sourced from a CCU yielded 28% less viable cells after 48 hours of growth than an expansion using cells sourced from manual controls. CCU sourced cells also performed worse than manual sourced cells during differentiation, producing 2.57 x 10^4 compared to the 4.27 x 10^4 viable cells per cm^2, a 40% reduction in yield. Both the expansion and differentiation results represent a statistically significant difference in 48-hour yield (expansion P = 0.011099, differentiation P = 0.000043). CCU expansion does contribute negatively to cell density for both expansion and differentiation after 48 hours, however this impact does not extend to the near-complete detachment and cell loss experienced during Prodigy process runs.

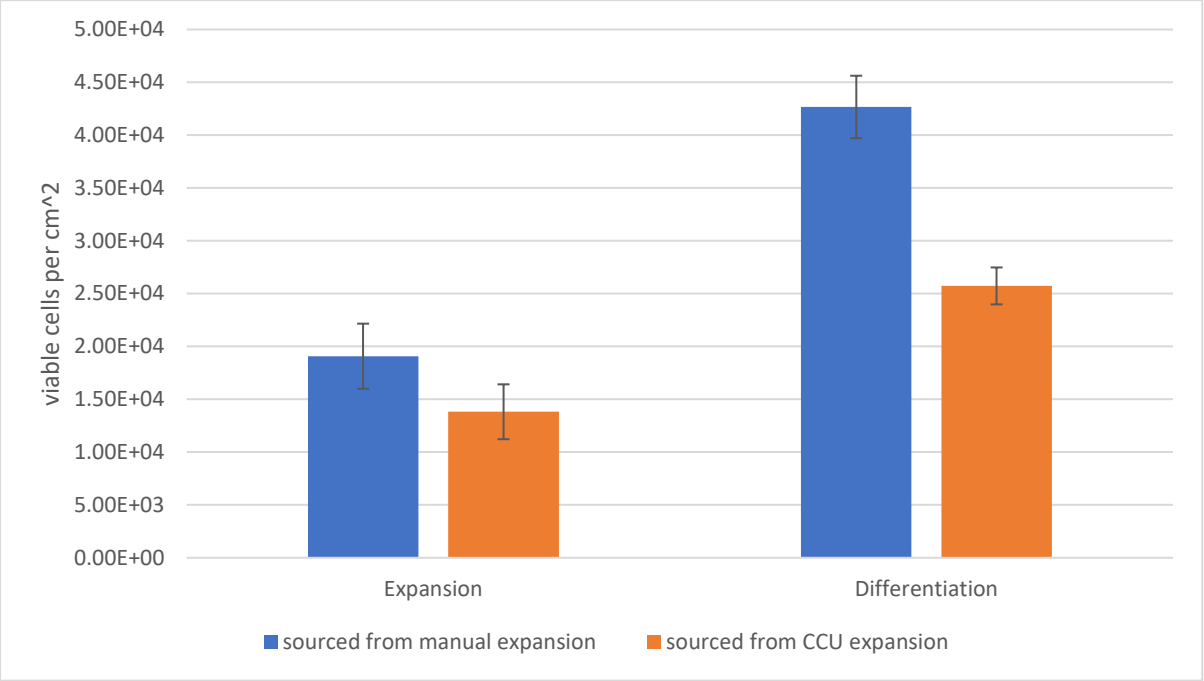

Figure 73 – Yields for 48 hours of RC17 expansion and differentiation with starting material sourced from either manual flask cultured or automated CCU cultured pluripotent cells. Data shown as mean ± SD for biological repeats, n=3.

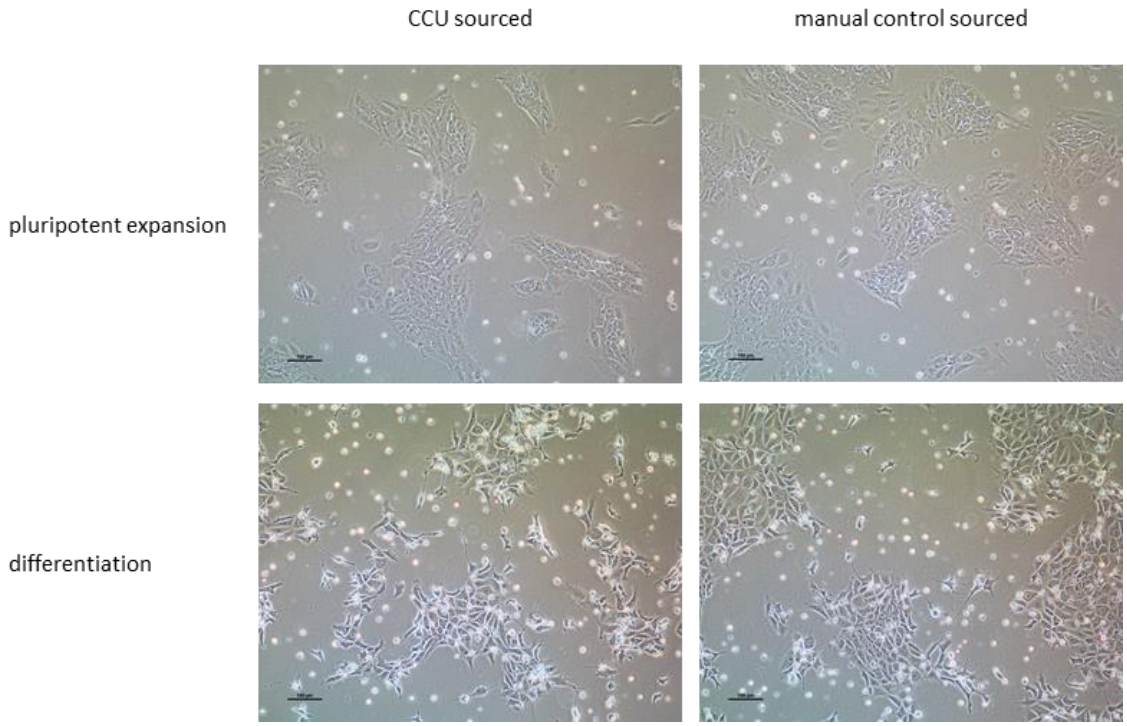

Figure 74 – RC17 attachment and morphology for expansion and differentiation of cells sourced from CCU and manual controls after 48 hours of growth. Cell health appears comparable between conditions. Scale bars are equivalent to 100 µm.

4.6.3.4 Buffer and Coating Solution Contamination During Seeding

Removing liquid from a CellSTACK involves moving the vessel from a horizontal to vertical position along one of its long edges, causing one of the fill caps (with a tubing adaptor attached) to be submerged in liquid to be drained, while leaving the other to provide a filtered air input to balance pressure. Draining the CellSTACK in this way prior to seeding leaves a significant dead volume of laminin-111 coating solution which is lower than the position of the tubing adaptor, possibly impacting cell attachment following seeding.

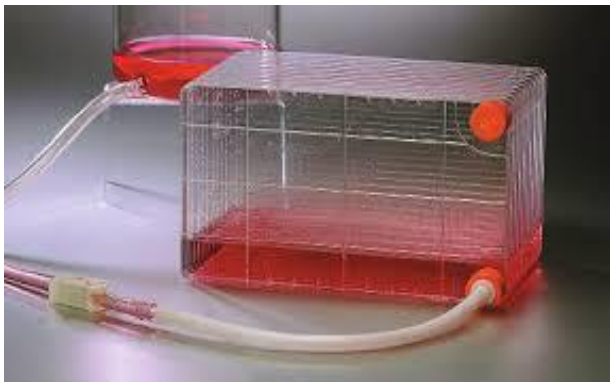

Figure 75 – Multi-layer CellSTACK being drained (Corning, 2011)*. The drainage point is not on the floor of the flask, leaving a dead volume which cannot be extracted at this angle.*

All liquid manipulations within the Prodigy single use tubing set are followed by a rinse with PBS/EDTA Buffer. This buffer is a phosphate buffered saline intended to wash away other residual liquids, and also contains low concentration EDTA buffer to encourage detachment of any cells attached to the single use tubing set. In removing other residual liquids and following draining with gas from the gas mix chamber, a small quantity of the PBS/EDTA buffer remains within the tubing set and is included within the cell seeding volume delivered to the cell stack.

As mentioned in Section 4.4.2.2 the impact of low concentration EDTA buffer has not been explored in the literature, with EDTA commonly referenced as a detachment aid and neutralisation or removal of EDTA commonly included as a required step for cell culture (Chen, 2012). EDTA is commonly included with TrypLE as a detachment aid, and may have contributed to the negative effects on cell yield during TrypLE contamination explored in (Thomas *et al.*, 2007). An experiment was performed to determine whether the inclusion of buffer or coating solution during differentiation seeding caused a lack of cell attachment and reduction in eventual cell yield compared to EDTA free controls.

RC17 cells were seeded into laminin-111 coated 6-well plates at a density of 2.5 x 10^4 cells per cm^2 according to the method described in X. Cells were seeded into either 2 ml seeding medium, seeding medium with 10% PBS/EDTA buffer solution, or seeding medium with 10% coating solution, with 3 wells per condition. Following 48 hours of incubation, wells were harvested and counted.

As shown in Figure 76, both the presence of buffer and coating solution during seeding produce significantly different variance in cell density after 48 hours (buffer contamination P = 0.000325, coating solution contamination P = 0.000336). The inclusion of 10% buffer resulted in 40.3% lower cell density on differentiation day 2, while 10% coating solution resulted in 43.0% lower cell density compared to the control condition with no contaminants. These losses are significant but did not cause complete lack of attachment as seen during automated differentiation. A 40% reduction in cell density after 48 hours is likely to be recoverable during differentiation as the process is normally allowed to reach a state of significant over-confluence by the passage on day 11. The reduced cell yields due to the presence of buffer agree with the literature in that EDTA contributes to reduced yields in cases of cell culture contamination with reagents containing EDTA (Thomas *et al.*, 2007).

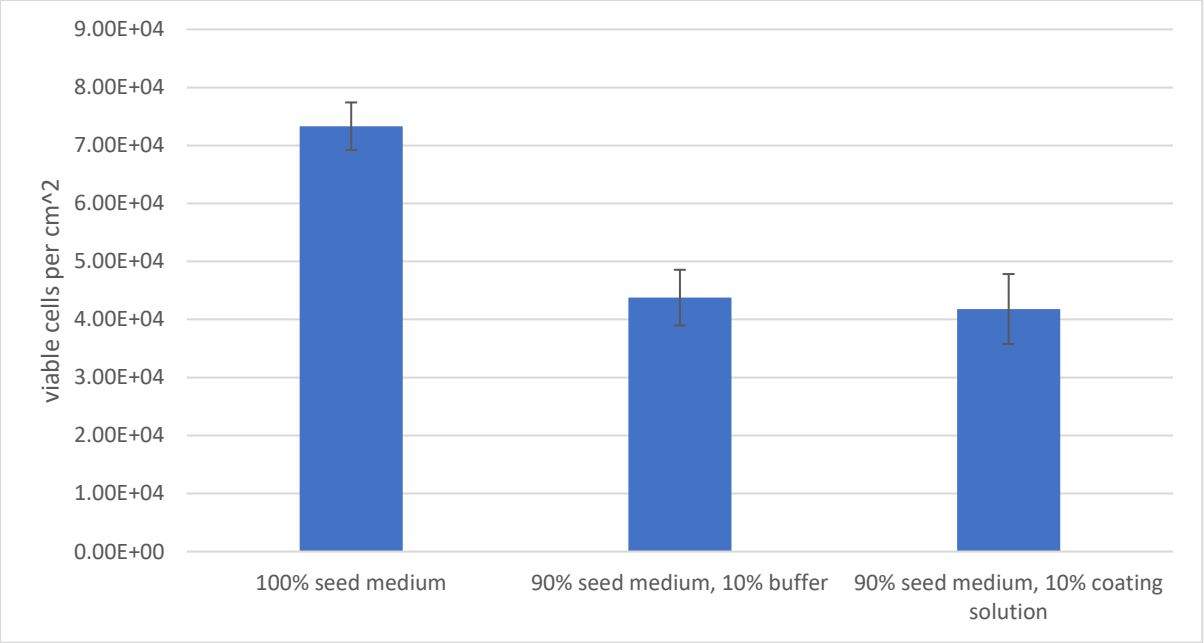

Figure 76 – RC17 yields obtained 48 hours following cell seeding with seed medium, seed medium with 10% buffer contaminant, or seed medium with 10% coating solution contaminant. Data shown as mean ± SD for biological repeats, n=2.

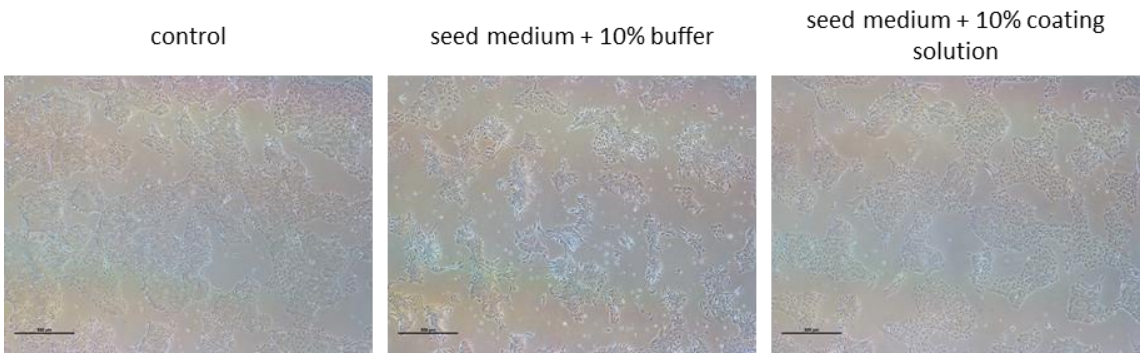

Figure 77 – RC17 growth for 48 hours following differentiation seeding using various conditions of contaminated seed medium. Scale bars are equivalent to 500 µm.

4.6.3.5 TrypLE and Inhibitor Contamination During Seeding

Manual centrifugation and aspiration provide near-complete supernatant removal during a typical passage (Delahaye *et al.*, 2015). During a passage on the CliniMACS Prodigy, CCU centrifugation and aspiration is used to remove TrypLE and Defined Trypsin Inhibitor (DTI) following harvest, before resuspending cells in seeding medium. Purification of cells in the CCU is limited to a start volume of 350ml, limiting initial dilution, and an end volume of 30ml, limiting removal of undesirable reagents. These limitations allow supernatant to persist through the cell resuspension process step and into cell seeding, with this having previously been shown to contribute towards lower cell yields (Thomas *et al.*, 2007). It is expected that the presence of TrypLE and DTI during cell seeing will reduce cell yields, and that cell yields will further reduce with increasing levels of TrypLE and DTI contamination.

During differentiation attempts on process runs 4 and 6, cells seeded into the CellSTACK were purified using the CCU while controls were purified using manual centrifugation. During CCU harvest, 200 ml of TrypLE and inhibitor and 100 ml of medium are reduced to 20ml of TrypLE and inhibitor with 10 ml medium, before diluting in a further 90 ml of medium, placing the TrypLE and inhibitor concentration at approximately 16.67%. During process run 4, 18.25 ml of contaminated seeding solution was transferred to the CellSTACK, while during process run 5, 21.7 ml of cell solution was transferred into the CellSTACK. In both cases, these volumes were topped with seeding medium to 150 ml, placing the TrypLE and inhibitor contamination concentration at 2.03% during process run 4 and 2.08% during process run 6.

An experiment was performed to determine whether the presence of TrypLE and inhibitor in seeding medium could account for the lack of cell attachment and process failure observed during process runs 4 and 6. RC17 cells were harvested from pluripotent culture and counted using the method described

in X. The cell solution was split into 4 conditions prior to seeding, with the first seeded directly to wells, and others receiving 1%, 2% and 5% TrypLE and inhibitor by volume to the cell suspension prior to seeding as a contaminant. Cells were then seeded at 2.5 x 10^5 viable cells per cm^2 into laminin-111 coated 6-well plates and maintained for 48 hours before harvesting and counting according to the methods described in Section 3.2.

As shown in Figure 78, yields after 48 hours of growth are flat for 0% and 1% TrypLE and inhibitor contaminant conditions. A 10.6% reduction in yield is seen for the 2% contaminated condition, while 5% contaminant resulted in a 97.2% reduction in yield, indicating near complete cell loss and irrecoverable crash in the culture.

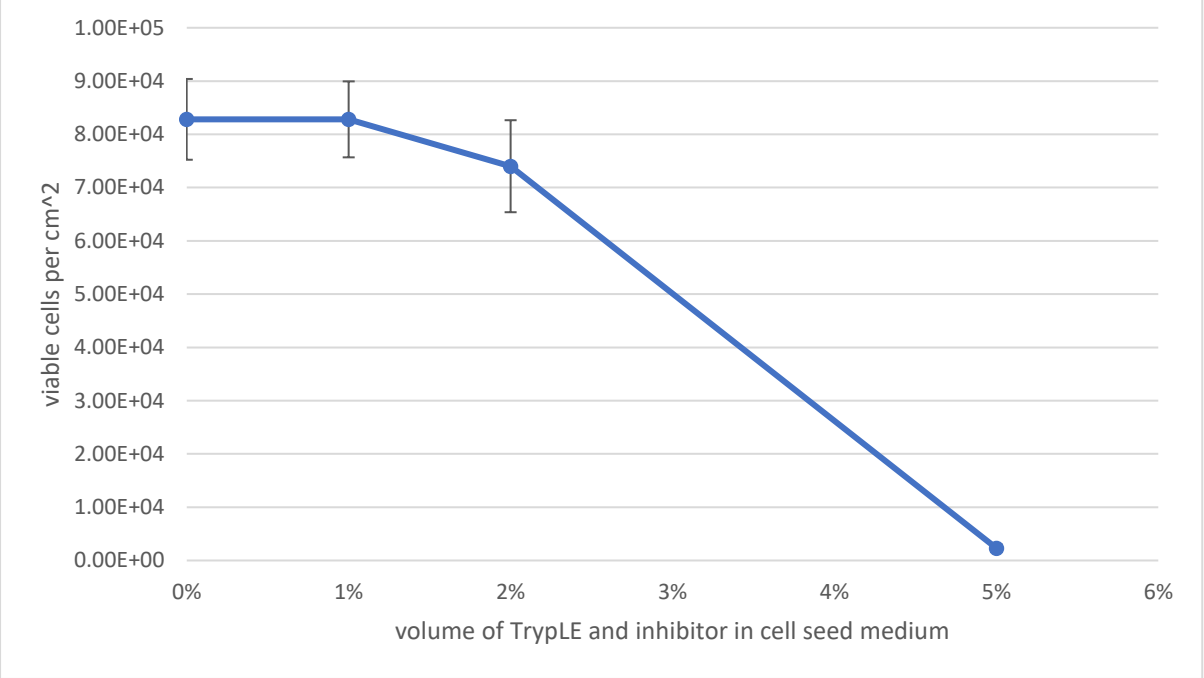

Figure 78 – RC17 yield at differentiation day 2 following seeding with various levels of TrypLE and inhibitor seed medium contamination. Data shown as mean ± SD for biological repeats, n=3.

As shown in Figure 79, the control condition with no TrypLE and inhibitor contamination exhibited typical morphology and reached confluence after 48 hours. 1% TrypLE and inhibitor produced a sparser culture with slightly rounded culture edges while 2% TrypLE and inhibitor contamination produced significantly sparser culture with pronounced risen edges, visible in microscope images as bright white borders. 5% contamination with TrypLE and inhibitor produced loss of culture with no visible cell attachment or growth, only entirely rounded and detached cells.

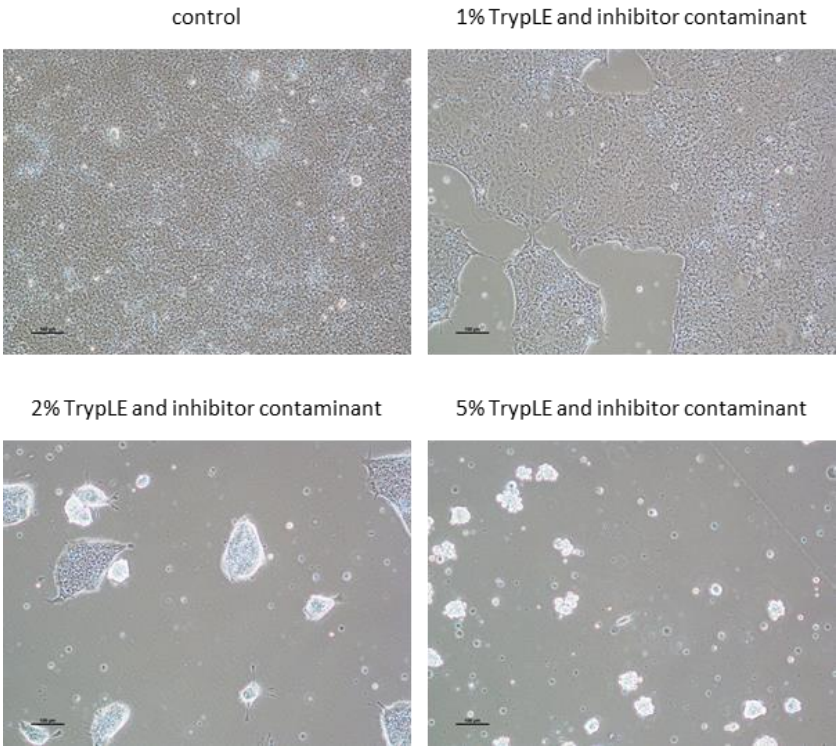

Figure 79 – Images from differentiation day 2 for RC17 cells seeded with various levels of TrypLE and inhibitor contamination. Cell growth is healthy in the control condition, with slightly reduced confluence in the 1% contaminant condition. The 2% contaminated condition features drastically altered culture morphology, while 5% contaminant shows little cell attachment. Scale bars are equivalent to 100 µm.

The lack of attached cells presents in the 5% TrypLE and inhibitor contaminant condition is similar to the failure mode observed in the CellSTACK during automated differentiation runs 4 and 6. The nature and severity of the response at concentrations likely during automated processing on the Prodigy suggests that TrypLE and inhibitor contamination was a likely cause of failure of these automated runs. These results show a similar trend to that seen in the exposure of hMSCs to TrypLE contamination (Thomas *et al.*, 2007), however, ESCs show a higher degree of sensitivity, with higher losses incurred at lower levels of contamination.

4.6.4 Corrective Actions

Exploratory work highlighted low level contamination with TrypLE and inhibitor due to insufficient purification during CCU centrifugation as the most likely cause of failure for automated process runs 4 and 6. The partial success of process run 5 supports this conclusion, as the insufficient yields produced

by the expansion phase of this run meant that the automated differentiation phase was seeded using manually purified cells, effectively removing insufficient purification as a risk factor from this process attempt and allowing cells to be seeded without TrypLE and inhibitor contamination. Trypsin/EDTA has been previously been shown to disrupt mesenchymal cell growth in an automated process using the CompacT SelecT (Thomas *et al.*, 2007). As a result of this work, reduction of TrypLE and DTI contamination during cell seeding was the primary focus of protocol change efforts prior to further runs and is discussed in further detail in Chapter 6.

Buffer and coating contamination of seeded cells were shown to have a moderate impact on later cell yields and may be mitigated by requesting that the Prodigy remove more liquid than was added to the CellSTACK, while holding the CellSTACK with the drain port at the lowest point. For example, to remove 100 ml of liquid, an operator should enter the value of 150 ml, then proceed to hold the CellSTACK at an angle to allow all liquid and bubbles generated during aspiration to drain. The additional liquid removal requested allows liquid to drain the entire length of the tubing attachment to the CellSTACK, allowing for more complete drainage.

Expansions and differentiations seeded using CCU expanded cells produced lower yields than expansions and differentiation seeded using manually expanded cells. The reason for this loss of yield is unknown, and as CCU expansion is a key feature of this process the location of the expansion cannot be easily changed. The reduced growth of CCU expanded cells is unlikely to affect final product yield, as cells are restricted by culture area throughout the later differentiation, allowing adequate time for a slow growing culture to reach confluence.

Storage of cells in flexible bags for periods of up to 30 minutes as well as the temperature of culture plastic and media was shown to have minimal impact on cell yield, and therefore did not require addressing through process changes.

Protocol changes to prevent the future occurrence of potential failure causes identified in this section contributed towards the final protocol, included in Appendix C. A demonstration of comparability between Prodigy manipulated differentiation at Miltenyi and Loughborough was not possible due to time and cost limitations preventing further process runs.

4.7 Discussion

An application note for the expansion and differentiation of pluripotent stem cells into mesDA progenitor cells on the Prodigy was published by Miltenyi as a result of the work described in this chapter (Miltenyi Biotec, 2018a).

4.7.1 Lessons Learned in Technology Transfer for Cell Therapy Applications

An ideal process transfer is shown in Figure 80 and includes observation of a trained operator performing the process at an established site (stage 1), followed by performance of the process by the trainee operator at the established site (stage 2), then followed by performance of the process by the trainee operator at the new site (stage 3). After each process run by the trainee operator, the output is analysed to check for comparability, with further training required should a deviation be present.

Due to the process cost as well as limitations on staff availability and travel costs for a 21-day process, it was not possible to perform the complete automated mesDA manufacturing process at any time during operator training. Training instead focussed on use of the Prodigy system, included coverage of key process steps such as tubing installation and cell seeding and harvesting in the CCUs and on CellSTACKs. Training stage 1 was observed using H9 cells, however the process failed due to infection during the expansion phase of the demonstration. Due to the lack of a full process run, no data was generated with which to judge the success of the process transfer at the decision points following stage 2 (comparability between operators within a site) or stage 3 (comparability between operators at different sites). The lack of data generated during training runs coupled with the limited comparability data provided by Miltenyi as a reference mean that no quantitative success criteria was defined or met. Ultimately, Loughborough operators William Mitchell and Dr Preeti Holland compared results with output data produced by Miltenyi using outdated process versions with variations in feed schedule and differentiation factor concentrations. It is unknown whether Miltenyi ever attempted to perform the mesDA manufacturing process on the Prodigy in its entirety prior to releasing the application note, however the lack of protocol and available data as well as significant issues highlighted during the process transfer suggest that the process has yet to be completed successfully.

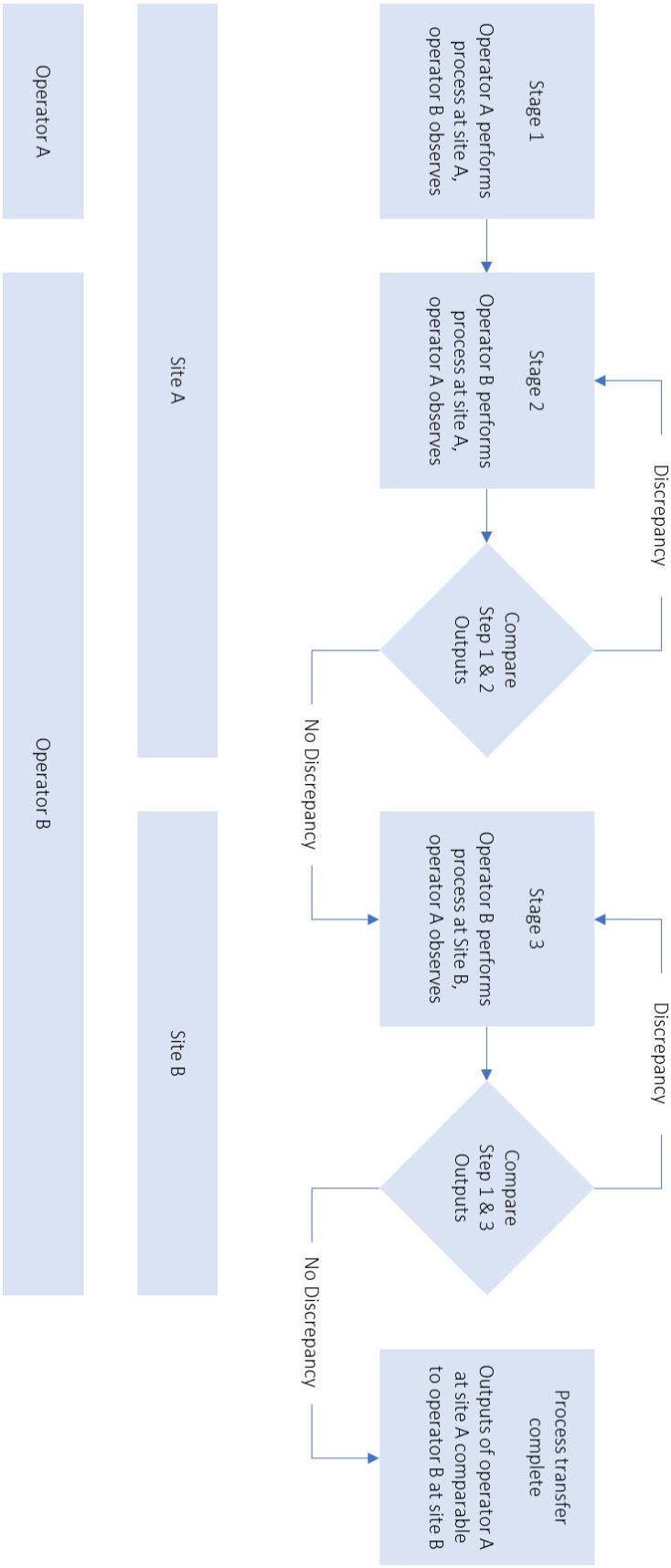

Figure 80 - Flow diagram of an ideal process transfer exercise.

Delays in receiving the Prodigy and a sterile tube welder lead to significant delays between stages of the process transfer, which would ideally be performed punctually to aid with operator training retention. Technology transfer stages 1 and 2 were performed at Miltenyi on the 13th to 16th of March 2017 while stage 3 was performed at Loughborough University on the 10th to 13th of October 2017, a difference of seven months. These delays coupled with the non-permanent nature of academic employment resulted in staff turnover during the technology transfer process. Stages 1 and 2 were performed by William Mitchell and Dr Samantha Wilson. Stage 3 was performed at by William Mitchell and Dr James Crutchley, while the majority of process runs were performed by William Mitchell and Dr Preeti Holland. The process transfer effort would have benefitted from a faster completion and the training of two permanent staff members.

The lack of a development freeze for the process developed by Miltenyi resulted in attempting to transfer a changing process with lacking documentation. The Miltenyi process underwent significant changes throughout the technology transfer, with changes communicated informally. Several changes present in the Miltenyi 2018 method were communicated only during enquiries about previously communicated conflicting or contradictory process steps (e.g. introduction of new molecule on a non-feed day, preparation of less medium than is subsequently transferred for a feed). The lack of a freeze on process development also contributed to the lack of up to date documentation. Attempts to perform the process at Loughborough University, as well as to formalise risk management, faced consistent problems with lacking protocol details such as daily medium volumes and system software clarity. A list of medium volumes required for each day of the automated differentiation process has yet to be provided by Miltenyi.

Data is a key part of a successful technology transfer and was not made available by Miltenyi, limiting the capability to make informed data driven decisions. This may be due to a reluctance to share when unnecessary, as well as due to a high dependence on operator knowledge with lacking documentation. Process output data was frequently not provided when directly requested, while protocol knowledge was treated as implicit or obvious, when this was only true for Miltenyi operators already familiar with the Prodigy. The lack of protocol clarity contributed to the operator errors previously described, while poor communication about planned work and a lack of trust bred from reluctance in data sharing lead to duplication in troubleshooting efforts.

4.7.1.1 Process Robustness

Process robustness is a prerequisite for a technology transfer. An unreliable process is slow and expensive to transfer due to the necessity to repeat failed process transfer steps, and ambiguous due to the difficulty in demonstrating comparability between processes with highly variable outputs. The effects of low process robustness for CCU expansion are clearly illustrated by the bacterial infection and subsequent process failure which occurred during stage 1 of the process transfer. This failure occurred during the single opportunity for trainee operators to observe an experienced operator performing the process in the established laboratory and meant that they later performed stages of the process which they have never observed working successfully. The presence of infections during the first two process runs at Loughborough University highlight the significant issues present in the process as delivered by Miltenyi.

It is unclear whether the differentiation process, as performed with H9 cells, is robust enough to reliably produce the desired mesDA progenitor cell product in its current state, as variability and unpredictable yields for the Lund mesDA differentiation process is noted by other groups (Fedele *et al.*, 2017; Drummond *et al.*, 2018). (Nolbrant *et al.*, 2017) states that extensive cell death is typical for H9 cells after day 4, and that cell death may be alleviated through the addition of B27 supplement on differentiation days 0 to 11. It is also noted that the addition of B27 requires increased CHIR concentration to achieve successful VM patterning, and that earlier FGF8b exposure may also be beneficial or detrimental depending on the exposure period. The extensive use of supplements and additional small molecules to drive the process back towards a normal operating range indicate an underlying fragile process, and one for which quality characteristics would quickly fall outside of the acceptable range without the use of biochemical blunt instruments.

Otx2 and FoxA2 are the key markers selected for quality control to confirm the product as consisting of mesDA progenitor cells. Otx2 is a marker of the midbrain and forebrain and is used to exclude the possibility of hindbrain cell contamination. It is expected to be somewhat high in pluripotent cells and above 85% for product cells (Neurostemcellrepair, 2018). As no clear change in expression is expected between pluripotent and product cells, this marker must be used in conjunction with others to give confidence in proper product identification. FoxA2 is a midbrain floor plate marker present in the in the anterior ventral midbrain, posterior ventral midbrain and ventral hindbrain (Kirkeby and Parmar, 2012). It is expected to be negative in pluripotent cells and above 85% expression in product cells (Neurostemcellrepair, 2018), however, this value was not reached by Loughborough or Miltenyi during the process transfer. This threshold has been highlighted by Miltenyi as an area likely to receive future

revisions. FoxA2 was also highlighted as having only small differences in expression between high quality product cells and cells otherwise far away from passing product quality control, limiting the ability to determine cell quality and suggesting that FoxA2 may be a poor measure of product quality.

4.7.1.2 Device Robustness

For a process to be robust it must be tolerant to a degree of input variability. For complex systems, designing for robustness includes designing to avoid positive feedback situations, where a single failure causes further failures, which themselves contribute towards further failures. A robust process can absorb a high degree of variability within a subprocess, preserving the wider process. Due to the dynamic and sensitive nature of the living product in cell therapy manufacturing, positive feedback situations are common. Where product understanding is limited, such as in process development, the availability of quality monitoring and manual intervention for rework opportunities to reduce variability are the primary way in which positive feedback situations may be avoided.

The key drawback to most automated, closed and integrated processes is the reduced flexibility and a resulting dependence on reliable operation. In the case of the Prodigy, the CCU is locked within a cultivation chamber which may only be accessed by aborting the running program. Limitations such as these remove the possibility of quality monitoring through microscopy or sampling, as well as the opportunity for re-works such as addition or removal of liquid. While these interventions should almost never be required in a reliable manufacturing process, no process is entirely without fault and current manufacturing technology for adherent cells is not mature. The lack of quality monitoring and rework capabilities on the Prodigy is a key factor in the failure of long-lasting processes.

An operator error during the expansion phase of process run 3 in which the CCU setup program was accidentally aborted during the coating wait period resulted in the presence of coating mixture in the CCU with no method of draining. There is no method of resuming a program at a desired point, and single unit operations as well as program creation and editing are not available to end users, preventing the simple draining of the CCU. With these limitations in Prodigy software, full programs must be run as workarounds, leading to unintended consequences. The recommended method to remove the coating mixture in this situation is to restart the CCU setup program, entering 0 ml when prompted to add coating mixture, the desired volume when prompted to remove coating mixture, and zero when prompted to input coating time. Due to a software bug in CCU setup program (version 131072), selecting to remove coating mixture without previously having opted to add coating mixture causes the

program to erroneously exit. A secondary method to remove coating mixture was employed, which involves restarting the CCU setup program, choosing neither to add or remove and coating mixture, and proceeding to prime the CCU and tubing by washing with EDTA buffer. This technique causes an unknown volume of EDTA buffer to be delivered to the CCU, with a slightly larger volume of liquid removed after priming. Due to the CCU having a dead volume of approximately 10 ml, a volume of EDTA buffer remained in the CCU during cell seeding, and as demonstrated in Section 4.4.2, is likely to have contributed towards the poor cell yields obtained during the expansion phase of process run 3. As summarised in Figure 81, the failure of this process occurred due to a chain of three failures, all of which had the potential for an escape or rework action which was not available due to artificial limitations in Prodigy software.

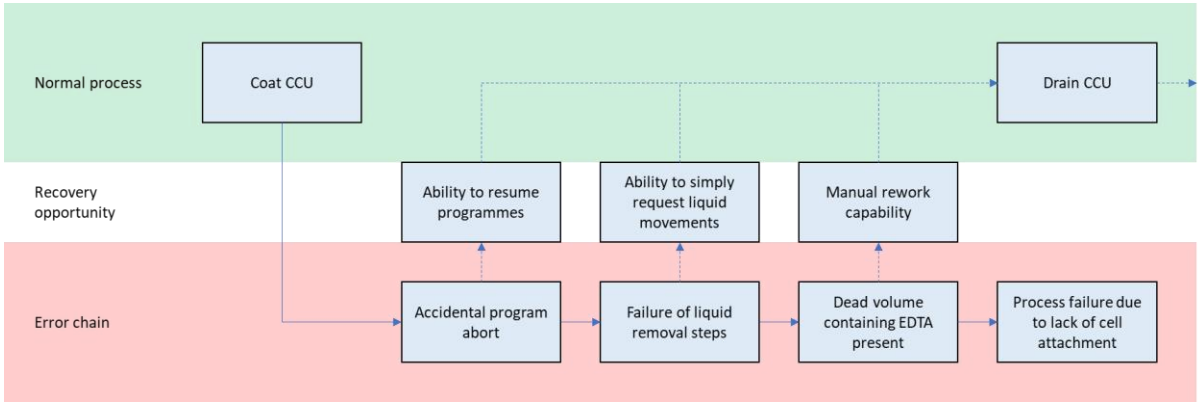

Figure 81 – Chain of events leading to process failure. Any one of the recovery opportunities would have led to normal process continuation. Only the chain of multiple errors leads to process failure.

The software issues and their potential fixes were highlighted following process run 2 in February of 2018; however, no fix was available 6 months later during process run 5 in August 2018, when the inability to drain the CCU following an operator error again lead to process failure during automated expansion. In this way, the inability of users to create, edit or install new programs (as this would effectively enable programs to be performed without purchasing software from Miltenyi) both prevents rework opportunities within a process, and prevents process robustness improvements, preventing the application of process development knowledge to reduce process risk.

4.7.2 Conclusions

The Prodigy system is notionally well matched to mesDA manufacturing process, promising automation and process closure at an appropriate scale with minimal additional equipment or facility requirements. In reality, a number of complex interactions make the Prodigy a poor match for this process, and ill-suited to external or collaborative process development in general.

The mesDA differentiation process created at Lund (Nolbrant *et al.*, 2017) is highly sensitive and requires the use of many troubleshooting steps in order to reach completion, while still failing to deliver adequate FoxA2 expression. The requirement for fresh medium on each process day prevents the use of pre-made batches, necessitating manual processing for each process intervention and negating the cost and containment benefits of closed system use. The process was found to be sensitive to unwanted medium exposure during surface coating as well as to buffer, coating solution and dissociation enzyme exposure during cell seeding and growth. In its current state the mesDA manufacturing process may not be ready for automation, requiring increased robustness to be compatible with closed and automated systems.

The Prodigy is challenging to operate as wording within the software is ambiguous, there are numerous opportunities for error, and reworks cannot be performed due to lack of program pausing and revision of inputs. The lack of ability to perform reworks such as removal of liquid from the CCU mean that the processes may be locked into chains of events resulting in process failure, where manual processes would offer multiple opportunities for recovery. The lack of online quality monitoring also makes failure mode troubleshooting challenging as data is only available at defined sampling times, as opposed to in manual culture where data can be obtained through microscopy at any time. Where knowledge is obtained during process development, it cannot be easily applied to the device as software editing and deployment is limited to Miltenyi staff. Allowing users to create and edit programmes would allow reworks during process runs and allow fixes to be rapidly implemented but would also undermine the licensing structure for Prodigy programmes. This limitation significantly hinders collaborative capability and external process development efforts.

High complexity processes may be developed on the Prodigy by enabling reworks through single unit operation programmes (to reduce process failure rates) and facilitating rapid turnaround of software changes by allowing end user editing (to allow the application of process development knowledge). Due to the understandable reluctance to open the Prodigy software environment to external developers, these essential aspects of process development are likely to remain limited to development efforts internal to Miltenyi. External process development for the Prodigy may be more suited to robust

processes of lower complexity, such as mesenchymal stem cell-based therapies, which may be more resistant to liquid contamination and coating conditions. For both internal and external process development, a high development budget may be required to absorb the additional cost of Prodigy consumables, significantly increased waste due to wash and dead volumes compared to manual culture, and increased process failure rates.

Technology transfers require a robust process and reliable equipment with comprehensive documentation and clear communication between the parties involved. The combination of a highly complex and sensitive differentiation technique with restricted process visibility and troubleshooting capability of the Prodigy as well as complex and incomplete documentation resulted in a challenging process transfer process with many costly process failures. Ultimately, the Prodigy is a successful manufacturing platform and a challenging process development platform, with many useful process development tools unavailable to external collaborators.

5 Manufacturing Considerations for Downstream Processing

Downstream processing concerns the recovery and preparation of a product for sale, and varies heavily depending on the specific needs of the product (Doran, 2013). For adherent cell therapies, downstream processing may be split into cell harvesting, purification, and cryopreservation. The downstream processing steps required for the mesencephalic dopaminergic (mesDA) progenitor cell product are summarised in Table 14, and are noteworthy for their small scale compared to mesenchymal based therapies and high container count compared to autologous therapies.

Table 14 – Downstream processing steps for a mesDA progenitor cell product.

	Harvest	Volume Reduction	Formulation	Fill and Finish	Controlled Rate Freeze	Storage and Logistics
Scale	200 ml	1 ml	1000 ml	1000 ml	1000 ml	1000 ml
Number of containers	1	1	1	500	500	500
Cell density	5×10^6	pellet	2×10^6	2×10^6	2×10^6	2×10^6
Temperature	37 °C	20 °C	20 °C	20 °C	-90 °C	-196 °C
Goal	Detach cells into single cell suspension	Remove supernatant	Resuspend in cryoprotectant	Transfer to 2 ml vials	Freeze cell suspension	Store, move and track product

Recent approvals of autologous products including Kymirah by Novartis and Yescarta from by Kite Pharma have resulted in increased attention on bioprocessing and cell therapy manufacturing capacity, however the focus has largely remained on expansion and other upstream processing steps. Downstream processing operations such as cell harvest, washing, concentration, fill and finish, and cryopreservation may become limiting factors as processes are scaled up for commercialisation.

5.1 Harvest

Adherent cell types such as stem cells and neuronal lineages are grown attached to a culture surface such as a flask, plate or carrier. These surfaces may be treated to improve hydrophilic properties and/or

be coated with proteins to facilitate specified cell attachment. Following an expansion or differentiation process step, cells must be recovered from the surface into suspension before further processing. This step is commonly achieved through the use of a dissociation enzyme such as trypsin and may be aided through physical manipulation of the culture vessel (Heng *et al.*, 2007; Nienow *et al.*, 2016).

5.1.1 Cell Detachment Manipulations

In a laboratory setting, physical manipulation is typically achieved through tapping (Thomas *et al.*, 2007), where a flask or culture plate is gently impacted to encourage rapid movement of the contained liquid and create shear forces to aid cell detachment. This technique is effective but challenging to control, as the relationships between flask acceleration, deceleration and orientation dictate liquid movement and therefore the shear forces experienced by attached cells. While microcarrier based culture systems may increase shear forces through a period of increased agitation with a magnetic stirrer or impeller (Nienow *et al.*, 2016), vessel tapping for planar culture is challenging for automated systems to perform due to the level of dexterity required. Enzyme free detachment methods have also received interest in the literature (Brun-Graeppi *et al.*, 2010; Koyama *et al.*, 2019), however these techniques have yet to see widespread usage compared to enzyme based dissociation.

Closed and automated systems may add physical manipulation to cell harvesting processes through forced liquid flow, where the dissociation enzyme and stop solution are washed over the growth surface applying shear forces to attached cells. This method is standardisable for many automated systems as the speed of liquid dispensing and vessel orientation are typically controllable but remains challenging to standardise for manual culture. Areas of the culture surface may also be challenging to access with directed liquid flow depending upon vessel shape, number of layers and the possible limited manipulations achievable on automated systems. A third possibility for automated systems is tilting or rocking of a culture vessel, allowing gravity to flow liquid from one side to the other placing shear forces on attached cells for each movement. This technique is easily standardisable and provides even coverage across a vessel surface but achieves comparatively low liquid flow speeds and therefore limited shear forces on attached cells compared to forced liquid flow.

An experiment was performed to determine the effectiveness of physical manipulations in aiding cell detachment. The performance of physical manipulation via flask tapping, forced liquid flow and flask tilting were compared, with manipulations performed according to the methods provided in Section 3.2. Flask tilting was considered the minimal physical manipulation condition, as tilting is required to

collect liquid for harvesting and therefore a zero manipulation control condition was not possible. Nine T25 flasks were seeded with RC17 cells at 2 x 10^4 cells per cm^2 and cultured for 72 hours. Flasks were harvested using the method given in Section 3.2 other than for the physical manipulation step, in which flasks were physically manipulated by either tapping the flask against an open palm, forced liquid flow via a 5ml pipette, or flask tilting with liquid then harvested into sample tubes. The harvest process was then repeated to recover any remaining cells, with all flasks physically manipulated using both extensive tapping, forced liquid flow and tilting. Liquid was then harvested into sample tubes and counted, with liquid from the second harvest representative of cells left attached to the growth surface following first harvest. Flasks and sample tubes were weighed before use, as well as before and after each harvested step to determine the liquid volume present at the time of harvest and counting, allowing determination of cells remaining in liquid dead volume.

Harvested cells are the successfully recovered portion of the primary harvest and represent the majority of cells for all detachment methods. Attached cells are those which remain attached to the culture vessel surface following the primary harvest. These cells are the target of physical manipulation techniques, which aim to improve cell detachment without increasing dissociation enzyme exposure time. Cells in the dead volume are those which were successfully detached into suspension but remain in the flask after primary harvest due to the inability of liquid manipulation techniques to recover all available liquid. Cells in dead volume may be recovered with an additional wash step after the primary harvest or discarded to save further manipulations and time. As shown in Figure 82, cell recovery for harvested cells was highest for flask tapping at 97.37%, dropping to 94.85% for cells harvested with forced liquid flow and 90.85% for cells limited to flask tilting. The proportion of cells harvested is higher with greater degrees of physical manipulation, with higher proportions of cells remaining attached when minimal physical manipulation is provided.

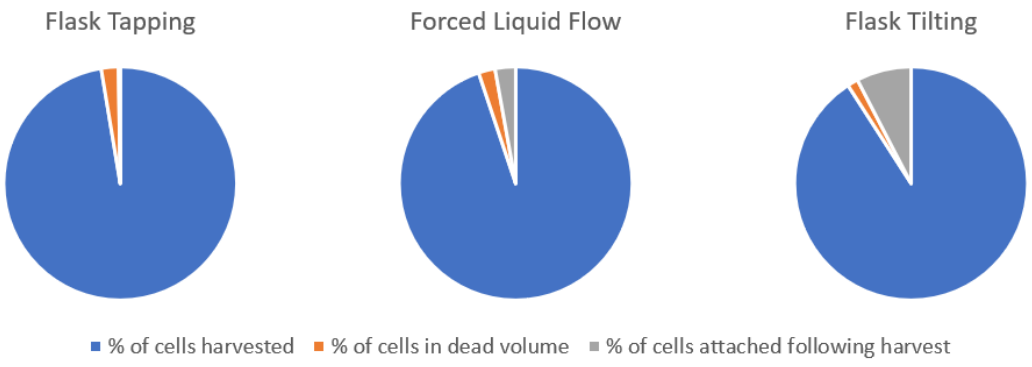

Figure 82 - Sources of cell loss during harvesting for different vessel agitation methods. Each chart represents the mean values for three biological repeats.

As shown in Figure 83, cell losses due to dead volume are stable across different physical manipulation techniques at 2.39%, 2.30% and 1.49% for tapping, forced liquid flow and flask tilting respectively. The slight trend towards higher losses for more highly manipulated methods may be due to the formation of bubbles caused by increased liquid turbulence for physical manipulation techniques with higher liquid flow. Cell losses due to incomplete detachment increase as physical manipulations are limited, rising from 0.24% for flasks harvested with tapping to 2.85% for those with forced liquid flow, and 7.62% for flasks harvested with tilting only. These losses are likely due to reduced cell detachment, as reduced shear forces allow cells to remain attached to the culture vessel surface during harvesting.

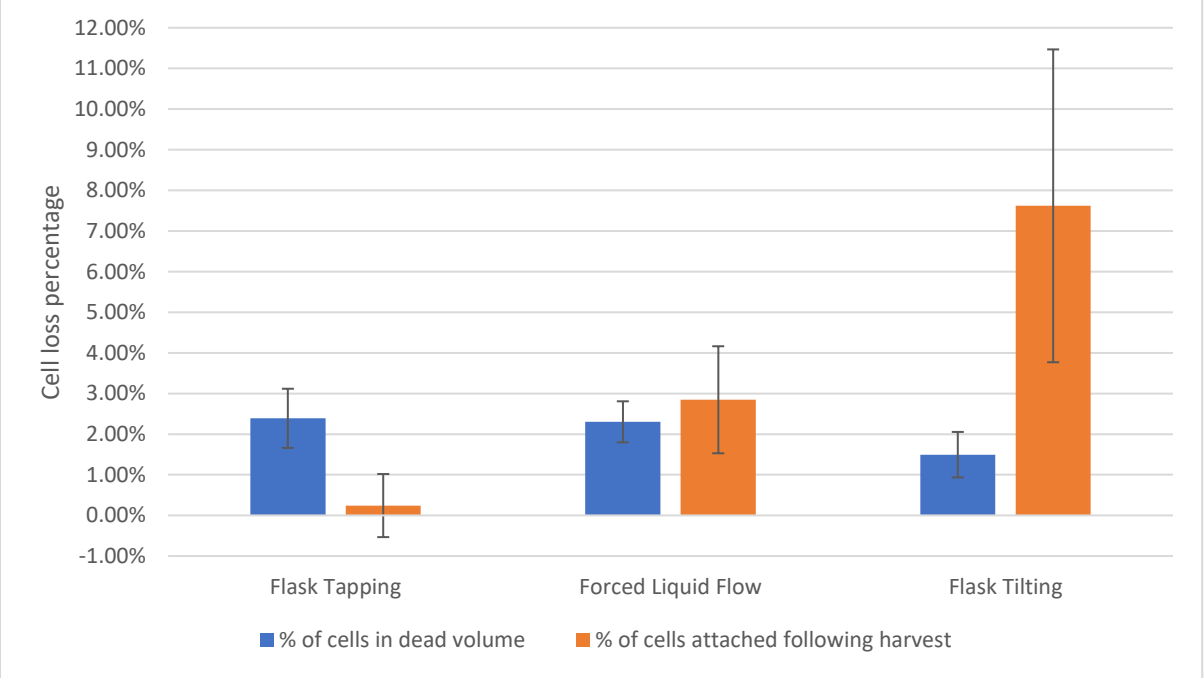

Figure 83 - Sources of RC17 cell loss during harvesting for different vessel agitation methods. Data shown as mean ± SD for biological repeats, n=3.

Flask tapping provides the highest cell recovery, however this is not always a viable approach. For large vessels such as a multilayer CellSTACK, the weight of the vessel and contained liquid is challenging to manipulate, with operators unable to deliver the sharp deceleration force required for a tap in the same way as for a small flask. Small capacity vessels such as multi-well plates also provide insufficient space for liquid to flow when tapping, limiting the techniques effectiveness. An automated device in which vessels are vibrated or impacted may provide solutions to these issues and provide the repeatability desirable for automated systems.

Forced liquid flow provides an improvement to cell losses compared to flask tilting and may be a viable option for systems which imitate the manipulations of a human operator with a robotic manipulator such as the CompacT or AUTOSTEM systems. Forced liquid flow presents an additional infection risk over the other approaches for these systems, as vessels must remain open for additional time while additional manipulations are completed (Fernandes *et al.*, 2009). This technique also relies upon vessel shape, with a requirement of access for a pipette tip to point at the culture surface, meaning that it is not suitable for large scale adherent culture on vessels such as CellSTACKs or HYPERflasks. Forced liquid flow is used to a limited degree on the Prodigy, as rotary acceleration and deceleration of the CCU provides liquid movement relative to the growth surface. For human operators, forced liquid flow may be challenging to standardise and process transfer due to the number of variables present, including range of pipette positions, degree of trigger depression on a pipette pump, placement of a pipette against the culture surface as well as time taken to perform the manipulation.

Flask tilting may be the simplest technique to achieve in both manual and automated culture of discrete vessels as it is typically the baseline of manipulation required for all harvesting processes, as vessels are tilted to allow liquid to collect in a corner to be collected. Repeating this action effectively performs flask tilting as a cell detachment aid. For built in culture vessels such as the Prodigy CCU vessel tilting is currently not a viable solution.

5.2 Purification

For stem cell derived cell therapy products (CTPs), purification refers to the removal of supernatant and debris and the transfer of cells into a defined liquid at a known concentration. Many purification techniques are split into two stages, the first being concentration; the removal of supernatant and increase in cell concentration, and the second being resuspension; the introduction of liquid and reduction in cell concentration (Cunha, Alves, *et al.*, 2015).

This section will refer to the ratio between concentration start and end volumes as the “concentration factor”, with this value indicating the degree of supernatant removal and therefore purification possible with a given method. As the degree of purification is dependent upon the ratio of supernatant removal to addition, concentration factor provides a useful comparison between purification techniques.

5.2.1 Manual Aspiration Technique

Manual open centrifugation is widely used as the go-to method for the purification of cell suspensions due to the technique's speed, ease, effectiveness, scalability, and low cost (Delahaye *et al.*, 2015). Despite its common use, the aspiration step of a manual centrifugation process is poorly standardised due to its dependence on operator judgement, a key contributing factor to process variability (Lopez *et al.*, 2010; Silverman *et al.*, 2019). The technique typically involves tilting a centrifuge tube to 45° and aspirating as close to the pellet as possible to remove all liquid, while not touching to pellet to prevent cell loss (Figure 84, A). This technique relies on operator judgement regarding how close to the pellet to stop aspirating, as well as requiring operator dexterity to not partially or completely aspirate the pellet.

A standardisable aspiration method (Figure 84, B) is proposed as the new standard practice in undergraduate laboratories to reduce the level of operator judgement and dexterity required during aspiration of supernatant from a centrifuged cell pellet. The method involves tilting the centrifuge tube until the tube shoulder (where the conical bottom transitions into the cylindrical tube walls) is at the lowest point, placing the aspirator at this point, and aspirating until the aspirator draws only air. This method removes placement of the aspiration tip from operator judgement and may reduce cell losses due to operators aspirating too close to the cell pellet. While it is recognised that this aspiration method is not new, this experiment aims to compare the performance of the two methods.

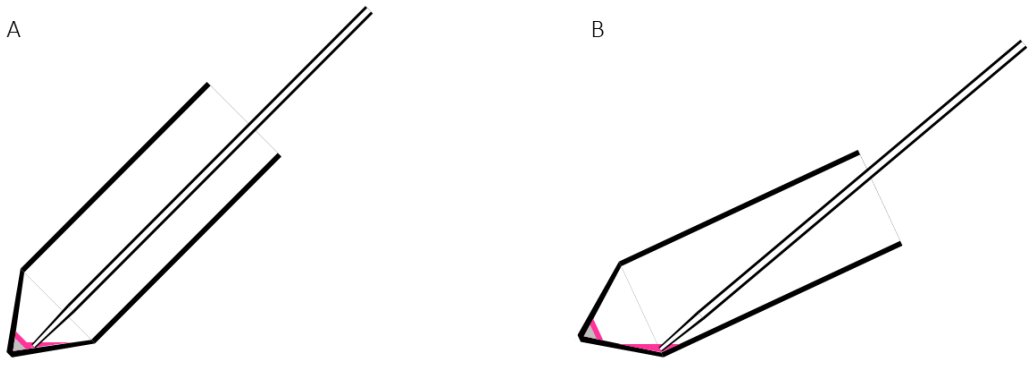

Figure 84 - Standard technique (left), aspirate down the tube until just above the pellet. Shoulder technique (right), rotate tube until the shoulder of the conical bottom is the lowest point, then aspirate liquid as it runs into this area.

RC17 cells were expanded and harvested according to the methods described in Section 3.2, then distributed between six 50 ml centrifuge tubes. Cell counts and liquid weights were measured to

determine a starting cell number for each tube. All tubes were then centrifuged according to the method given in Section 3.2.3. Three tubes were aspirated using the shoulder method described above and outlined in Section 3.2.3, while three were aspirated using the traditional aspiration technique (rotate the tube to approximately 45°, aspirate liquid, moving slowly closer to the pellet, stop aspirating when the aspirator tip is close to the pellet). For all tubes, the pellet was resuspended and counted, with liquid weight again measured to allow absolute cell number to be determined. The comparison of absolute cell number before and after centrifugation and aspiration allows for a comparison of cell recovery between the two techniques.

As shown in Figure 85, total cell recovery was higher for the shoulder aspiration technique as compared to the standard technique at 94.78% compared to 77.81%. Cell viability remained similarly unchanged for both methods, with the standard technique achieving 100.29% compared to the shoulder technique at 99.89%.

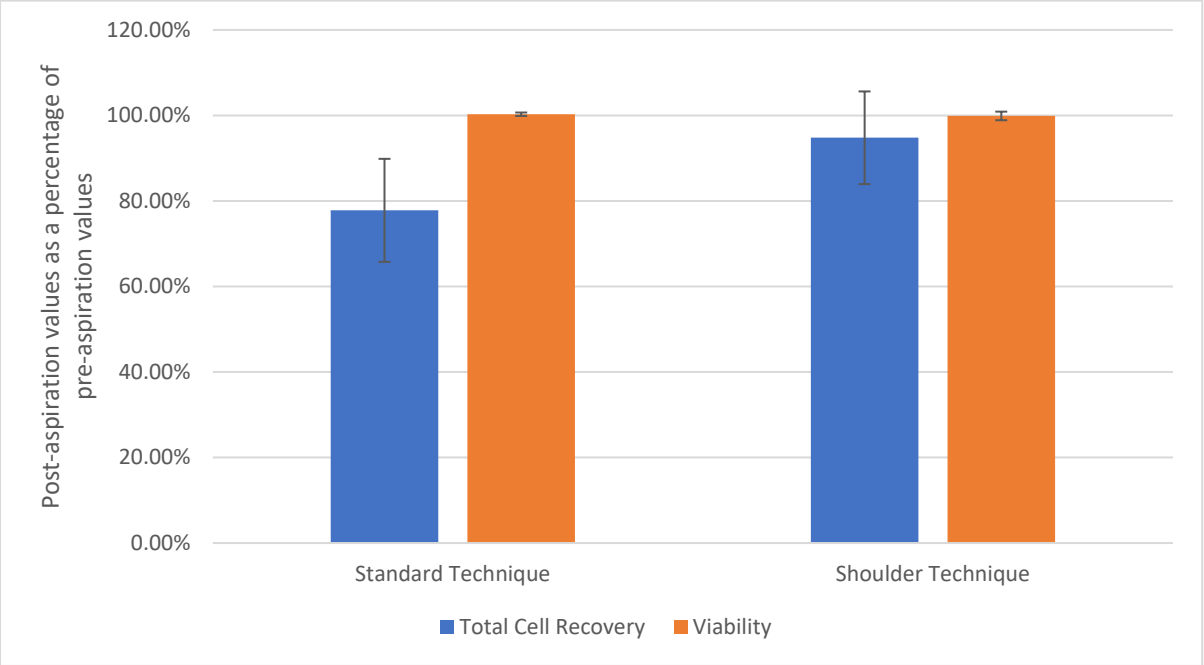

Figure 85 – Total RC17 cell count and viability before and after centrifugation at 300G for 5 minutes and aspiration using the shoulder technique and standard aspiration technique. Data shown as mean ± SD for biological repeats, n=3.

Variation for the shoulder technique is likely due to cell detachment from the pellet as liquid runs off its surface and to the lowest point during aspiration. Variation for the standard technique was expected to be higher, however variability was comparable to the shoulder technique. The experiment was performed by an operator with three years of cell culture experience and may have higher variability

and a higher chance of total pellet aspiration for novice operators. Pellet aspiration has previously been highlighted as one of the main causes for batch failure in industrial cell manufacture and is resistant to improvement actions, making it the most significant risk to processing following implementation of improvement actions (Lopez *et al.*, 2010).

5.2.2 Closed Centrifugation Tubes

Closed centrifuge tubes allow centrifugation and aspiration to be performed under fully closed conditions (Corning, 2019b), an example of closed centrifugation plasticware is show in Figure 86. Closed aspiration is achieved using a dip tube with the aspiration point, or tube opening, positioned just above the bottom of the conical portion of the centrifuge tube as shown in Figure 87, A. This effectively fixes the aspiration point above the cell pellet and allows supernatant to be removed through gentle liquid extraction. Pellet extraction can then be performed following resuspension through repeated cycles of drawing up and dispensing liquid. Closed aspiration at the scale of single closed centrifugation tubes remains a niche requirement and has not been explored in the literature. Experiments were performed to compare current closed centrifugation technology against open centrifugation techniques, and provide a reference against which other closed purification techniques could be compared.

Figure 86 - Corning 50ml and 500ml closed centrifuge tubes (Corning, 2019b).

As the aspiration point of closed systems is fixed and the aspiration point of open centrifuge tubes is operator adjustable, open systems likely offer advantages in absolute liquid removal and concentration factor, while closed systems likely offer greater consistency along with the advantages associated with closed processing, including lower infection risk and the cost benefits of processing in a lower grade of cleanroom. A comparison of aspiration for the two systems is shown in Figure 87.

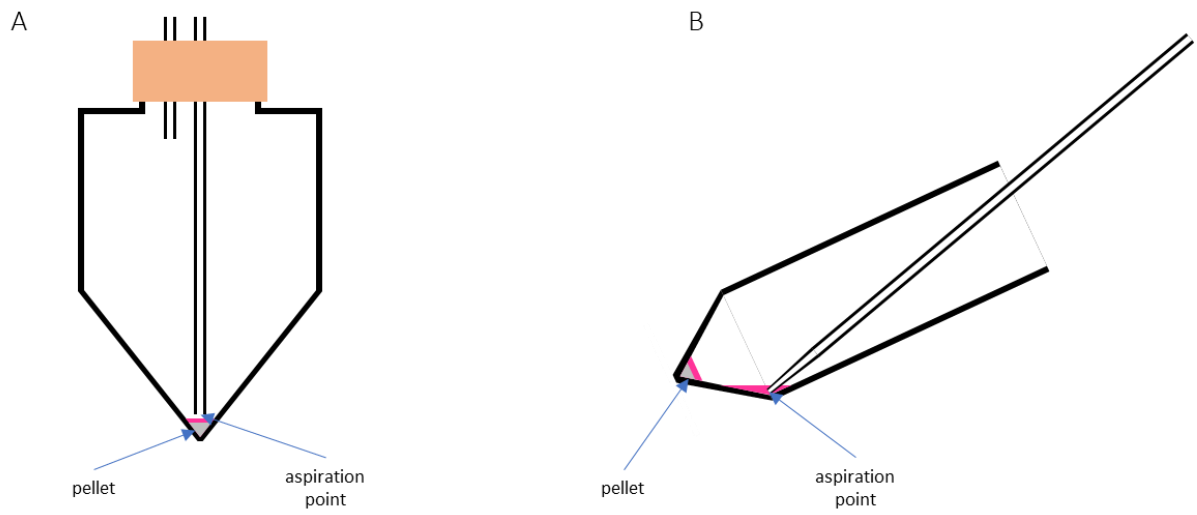

Figure 87 -Pellet and aspiration points for closed and open centrifuge tubes. Note the close proximity of the pellet and aspiration point for the closed system shown in image A.

An experiment was performed to compare purification using 50ml (Fisher, 11899640) and 500ml (Corning, 431123) open centrifuge tubes and 50ml (Corning, 11705) and 500ml (Corning, 11750) closed centrifuge tubes with dip tubes. It was expected that closed centrifuge tubes would enable effective cell purification with comparable losses to open centrifugation. All tubes were weighed prior to use to allow later weight measurements to determine contained liquid volume.

RC17 cells were harvested, resuspended in feed medium and counted according to the method outlined in Section 3.2, with 1.5 x 10^7 viable cells transferred to each type of centrifuge tube. Each centrifuge tube was filled with feed medium to 10ml total volume. Starting cell density was obtained using the method given in Section 3.5.2 while liquid volume was obtained via weighing, allowing absolute cell number to be determined for each tube. Tubes were then centrifuged at 300G for 5 minutes in a Thermo Scientific Heraeus Megafuge 40R.

Aspiration of supernatant for the open centrifuge tubes was performed using the shoulder method outlined in Section 3.2.3. Aspiration of liquid from the closed tube was achieved by connecting a 30ml

Luer threaded syringe to the dip tube portion connector of the closed centrifuge tube and drawing up liquid at a rate of approximately 0.5ml per second. This liquid draw rate was selected to minimise the effects of turbulence and shear forces disturbing the pellet which is located close to the opening of the dip tube, while remaining large enough for an operator to approximately track against the syringe volume markings. The syringe was also partially retracted prior to drawing up liquid, in order to avoid a pulse of liquid flow when overcoming the initial plunger detent.

Following aspiration, tubes were weighed to determine the pellet and remaining liquid weight. 10ml of feed medium was then added and pellets resuspended in each centrifuge tube, with counting and weighing then repeated to obtain an absolute cell count for each tube. The centrifugation and measurement cycle were repeated three times for each of the four types of centrifuge tube.

At the 50ml scale, cell recovery was comparable for open and closed centrifugation at 94.63% and 92.51% respectively. Variability of cell during recovery open centrifugation was lower with a standard deviation of 0.83% compared to the 3.82% for closed centrifugation. This increased variability is likely due to the closer proximity of the aspiration point to the cell pellet compared to open processing, and therefore higher sensitivity to variations in flow rate and induced shear forces upon the pellet. At the 500ml scale open centrifugation performed well achieving 100.35% cell yield with 3.10% standard deviation. During closed centrifugation at the 500 ml scale, the cell pellet was aspirated preventing further experimental repeats and resulting in a yield of 2.01%, as shown in Figure 88. This pellet aspiration was repeated during several reattempts at closed centrifugation at the 500 ml scale. Cell viability was unchanged in all cases other than where pellet loss occurred, with this likely attributable to the loss of healthy cells in the lost pellet and retention of non-viable cell fragments in supernatant.

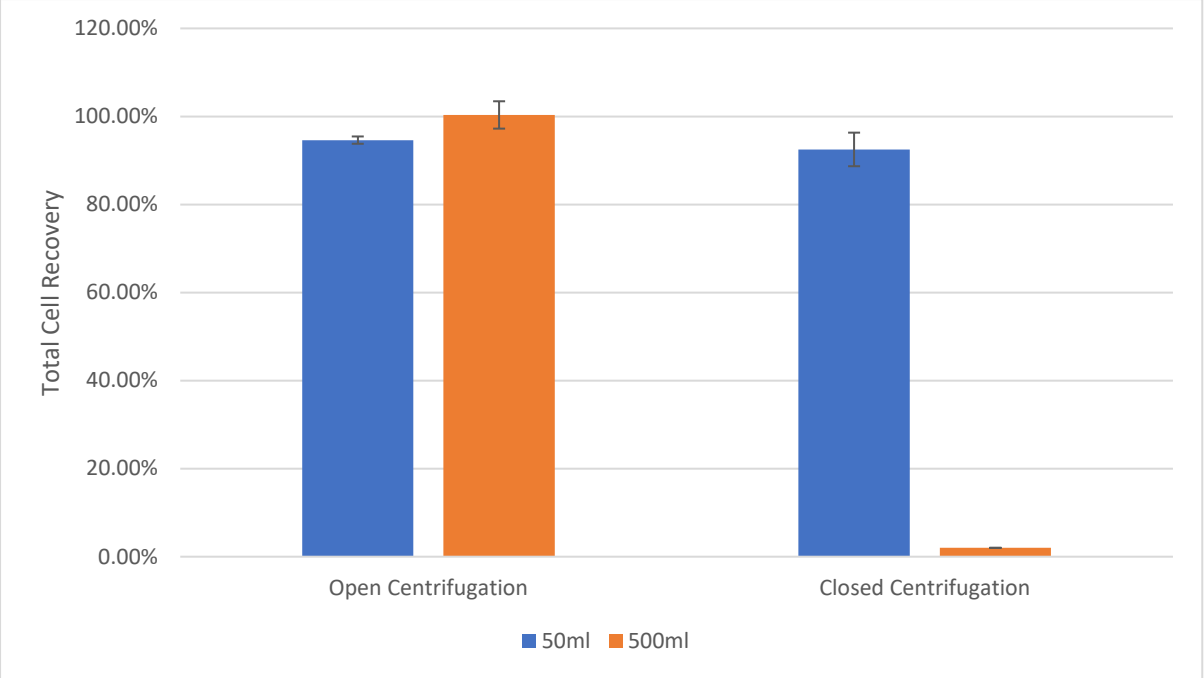

Figure 88 - Total RC17 cell recovery for open and closed centrifugation tubes following aspiration of supernatant. Recovery is consistently high for open centrifugation and high for closed centrifugation at the 50 ml scale, however, pellet aspiration during aspiration of supernatant in the 500 ml closed tube highlights the danger of placing a fixed aspiration point close to the cell pellet. Data shown as mean ± SD for biological and measurement repeats, n=3, except for the 500ml closed centrifugation bar which represents a single run.

Concentration factor is a measure of the level of purification achievable for a single use of a given method. Open centrifugation achieved high concentration factors of 157.16 at the 50 ml scale and 130.92 at the 500 ml scale, while closed centrifugation achieved lower concentration factors of 38.32 for 50 ml and 84.54 for 500 ml. These values indicate that open centrifugation provides a more thorough removal of undesirable liquids.

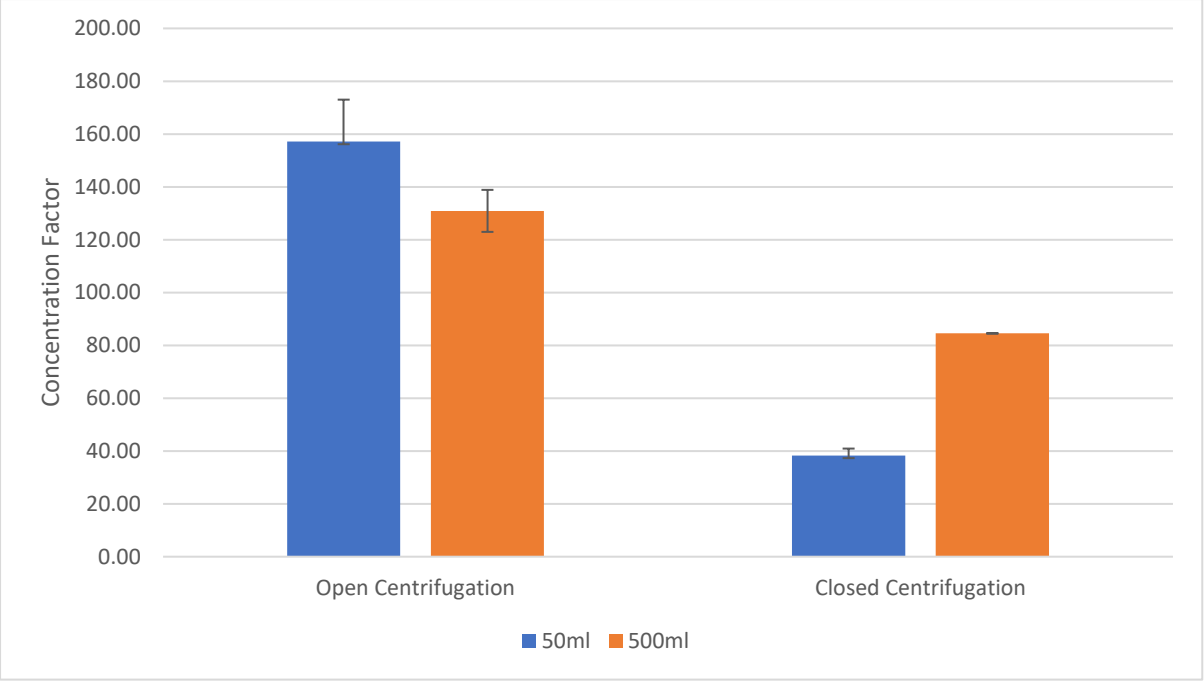

Figure 89 - Concentration factor for 50 and 500 ml open and closed centrifugation of RC17 cells. Open centrifugation offers more complete removal of supernatant regardless of processing scale. Data shown as mean ± SD for biological and measurement repeats, n=3, except for the 500ml closed centrifugation bar which represents a single run.

The failure of the closed 500 ml closed centrifugation attempt was due a pellet aspiration which occurred on further attempts to replicate similar purification conditions. Pellet aspirations are an ever-present risk during aspiration following a centrifugation, however, they are typically avoided through control of the aspiration point, either via training and protocol for open tube processing, or via tubing configuration for closed systems. The regular pellet aspirations experienced when using 500 ml closed centrifugation tubes indicate the lack of suitability of this equipment for purification of cell pellets. As previously mentioned, closed centrifugation has not been explored in the literature, with this work demonstrating the relative infancy and ineffectiveness of current technology.

5.2.3 Centrifugation on CliniMACS Prodigy

The centrifugation process on the Prodigy rotates the CentriCult chamber (CCU) to achieve the appropriate g-force. This process is shown in Figure 90 and summarised diagrammatically in Figure 91. As the CCU is entirely integrated within the Prodigy, centrifugation is only applicable to processes performed by the system, limiting its applicability. As such, CCU centrifugation has yet to be explored in the literature.

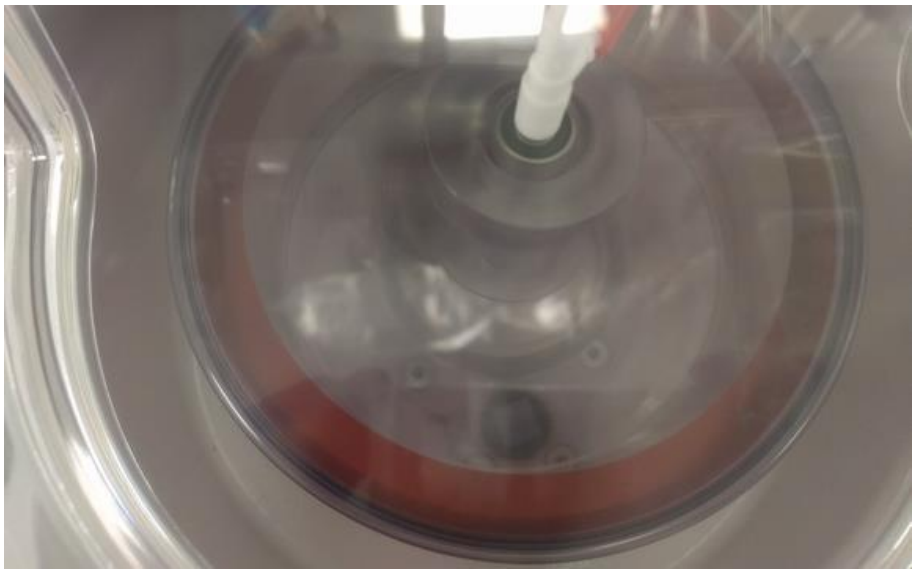

Figure 90 - Prodigy CCU during centrifugation.

For purification of harvested cells on the Prodigy, the CCU is first spun at 1500 RPM (350G) for 5 minutes. During this time cells collect against the edges of the CCU vessel as shown in Figure 91, B, in the same way that a pellet would form at the bottom of a conical tube during centrifugation. Liquid is aspirated through a hole at the perimeter of the chamber and flowed along a channel towards the centre where it is removed through the chamber spindle. The peristaltic pump used for liquid movements on the Prodigy is unable to overcome centrifugal force to move liquid from port to the spindle at the centre of the CCU when centrifuging at 1500 rpm, therefore a lower speed must be utilised. Rotation of the CCU is therefore slowed to 800 RPM (42G) in order to allow liquid to be aspirated through the lower port of the CCU as shown in Figure 91, C, with the minimum dead volume for this stage being 70ml.

To further aspirate remaining liquid, the CCU is slowed to 275 rpm (5G) and liquid is again aspirated from the lower port. Due to this reduced speed, liquid collects at the outer lower edge of the chamber due to a combination of gravity and centrifugal force as shown in Figure 91, D. Cells remain against the outer chamber edge, allowing liquid to be removed and leaving a dead volume of 30ml in the CCU. Following this aspiration step, fresh liquid is added as shown in Figure 91, F, and the chamber spun to dislodge the pellet from the CCU walls and distribute the cells within the liquid. Due to limitations in end-user accessibility to device programs and restricted access to the CCU, it was not possible to measure cell loss during centrifugation on the Prodigy, however, residual liquid volume may be modelled for a known process.

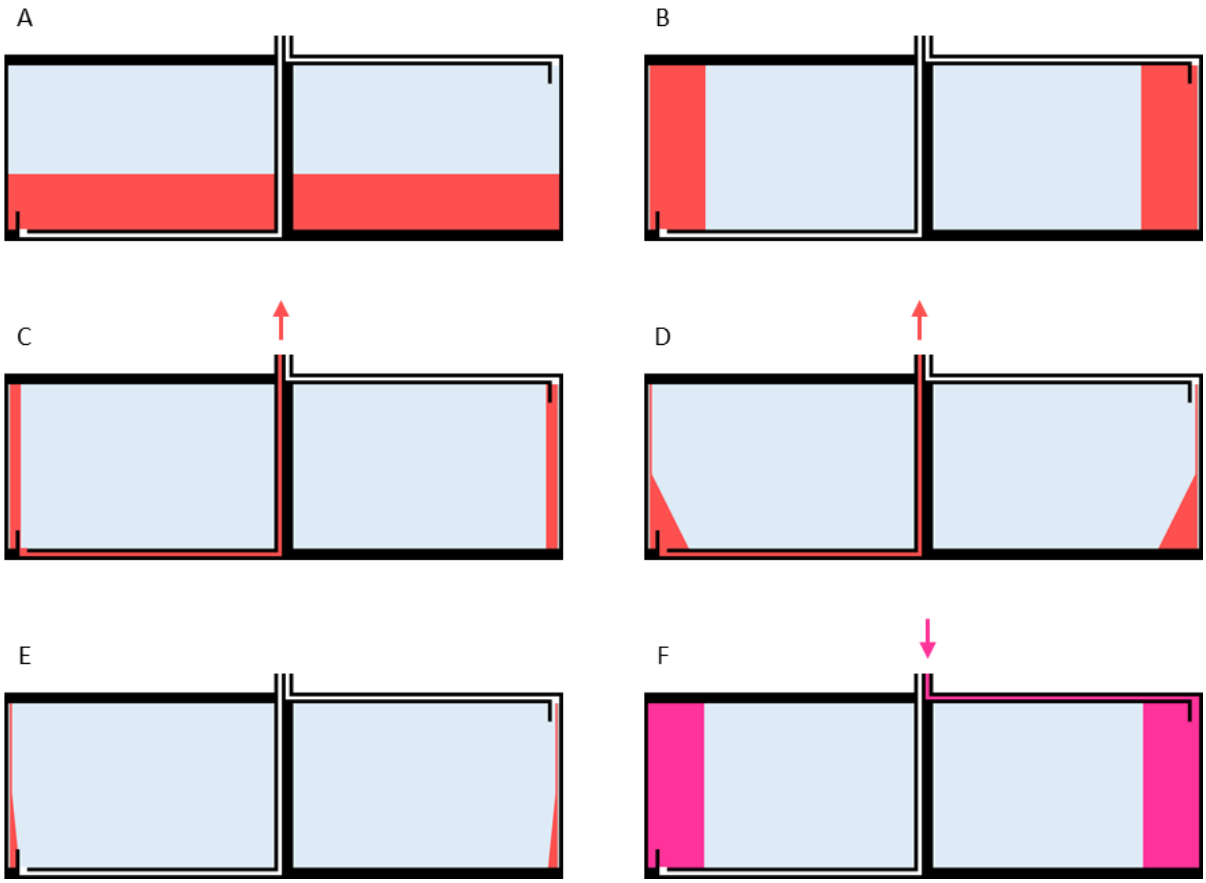

Figure 91 – Centrifugation on the Prodigy within the CCU. The CCU is first shown at rest (A). Two stages of aspiration are employed to reduce the dead volume, first to 70ml at full rotation speed (B and C), then to 30ml at reduced speed (D and E), before resuspension in fresh medium (F).

5.2.4 Tangential Flow Filtration

As previously discussed in Section 2.4.3.2.2, tangential flow filtration (TFF) is a technique in which a particle suspension is pumped in parallel to a hollow fibre filter membrane. By controlling the pressure at various points, a portion of the liquid passes through the membrane while the remaining liquid and suspended particles returns to the originating vessel (Cunha, Peixoto, *et al.*, 2015). The tangential flow of liquid across the filter membrane reduces fouling and allows for simplified positive selection processes. This technique may be used to both reduce volume and concentrate a suspension, as well as to perform a volume exchange. TFF has previously been shown to be the most cost effective technique (Hassan *et al.*, 2015) for MSC processing at medium scales, and it is therefore expected that the technique will prove equally effective in the purification of ESCs. An experiment was performed to assess the effectiveness of this method and the suitability of available TFF equipment for the

purification of small-scale embryonic stem cell (ESC) based therapies following cell harvest. It was expected that TFF would provide effective purification with increased cell loss compared to centrifugation based on experiments in the literature at similar scales to those required by the Prodigy process (Hassan *et al.*, 2015).

A filter module pore size of 0.65 µm was selected as this has previously been demonstrated to minimise losses in the purification of mesenchymal stem cells (Cunha, Peixoto, *et al.*, 2015). Membrane area was selected according to the volume of liquid to be processed, the filtrate flux rate and process time. For this work, a filter of 15 cm^2 was selected as the most cost-effective surface area, able to achieve a process time of 24 minutes for a scale of up to 150 ml based upon the filtrate flux rate of 250 $L/m^2/h$ found to be optimal in (Cunha, Silva, *et al.*, 2017). Common membrane materials include Polysulfone (PS), Polyethersulfone (PES), Modified Polyethersulfone (mPES) and Mixed Cellulose Ester (ME). ME filters are limited to pore sizes of around 0.1 µm, while mPES is the most widely available filter material across different pore sizes and was selected for this work. Volume reduction and volume exchange steps were achieved using the same filter to reduce equipment and manipulation requirements. The TFF system configuration is shown in Figure 92 and includes the SpectrumLabs KrosFlo Research II pump unit, OHAUS NavigatorXL scale, and SpectrumLabs MicroKros C02-E65U-07-S filter.

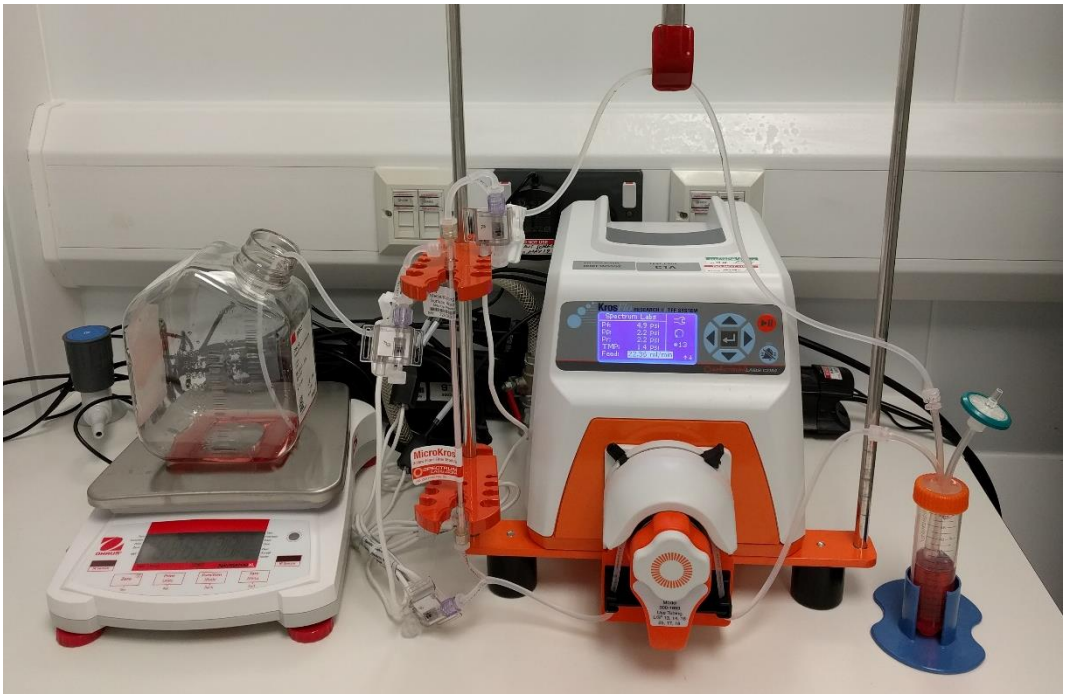

Figure 92 - TFF configuration. The sample reservoir is located on the right with liquid pumped through the pump unit and into the bottom of the TFF filter. Retentate liquid passes out the top of the TFF filter and through a manual flow restriction valve, then back to the sample vessel. Permeate liquid exits the TFF filter through a side port at the top, then passes into the waste vessel located on the scales.

The filter module was first rinsed using 50ml of PBS -/- to wet the membrane and displace air. 2.7 x 10^7 RC17 cells at passage 44 were then harvested and resuspended in 50 ml feed medium, before counting and weighing to determine the start cell concentration and volume. The sample volume was then connected to the TFF loop, which was started and monitored to maintain a shear rate of 3000 s^{-1} and filtrate flux rate of 250 L/m^2/h. After filtering the desired volume of liquid, filtration was stopped by clamping closed the permeate tube and stopping the peristaltic pump. Tubes were lifted clear of the sample vessel and the pump run in both directions to clear the loop of liquid, then the sample volume was counted and weighed to determine the post filtration cell concentration and volume. The filtration steps were repeated for volume reductions of 50 ml to 25 ml, 25 ml to 10 ml, and 10 ml to 5 ml, equating to concentration factors of 2, 5 and 10. A concentration factor of 10 was the highest achievable as the OHAUS NavigatorXL scale has a measurement resolution of 1 gram, limiting precision when processing small liquid volumes.

Diafiltration into PBS was performed by adding 25 ml of PBS -/- to the 5 ml of sample volume, then once again running the TFF system at a shear rate of 3000 s^{-1} and filtrate flux rate of 250 L/m^2/h until the sample volume returned to 5ml, equating to a 6x liquid dilution while maintaining 1x particle concentration. This diafiltration process was performed an additional three times, equating to 0.08% of the original liquid remaining following four diafiltration steps. Cells were counted and weighed between each stage of concentration and volume exchange to determine losses and changes to viability.

Following a 10-fold concentration, total cell yield had fallen to 82.58% and viability to 97.02% of the starting total. For the four stages of diafiltration performed following this, total cell yield fell to 78.02% and cell viability fell to 95.97% of the value prior to the four diafiltration process steps. The entire TFF process including x10 concentration and four stages of x6 dilution and diafiltration resulted in a total cell yields of 64.43% of the cell total prior to TFF purification, with viability having reduced from 97.3% following harvest to 90.6% following purification. These results are summarised in Figure 93.

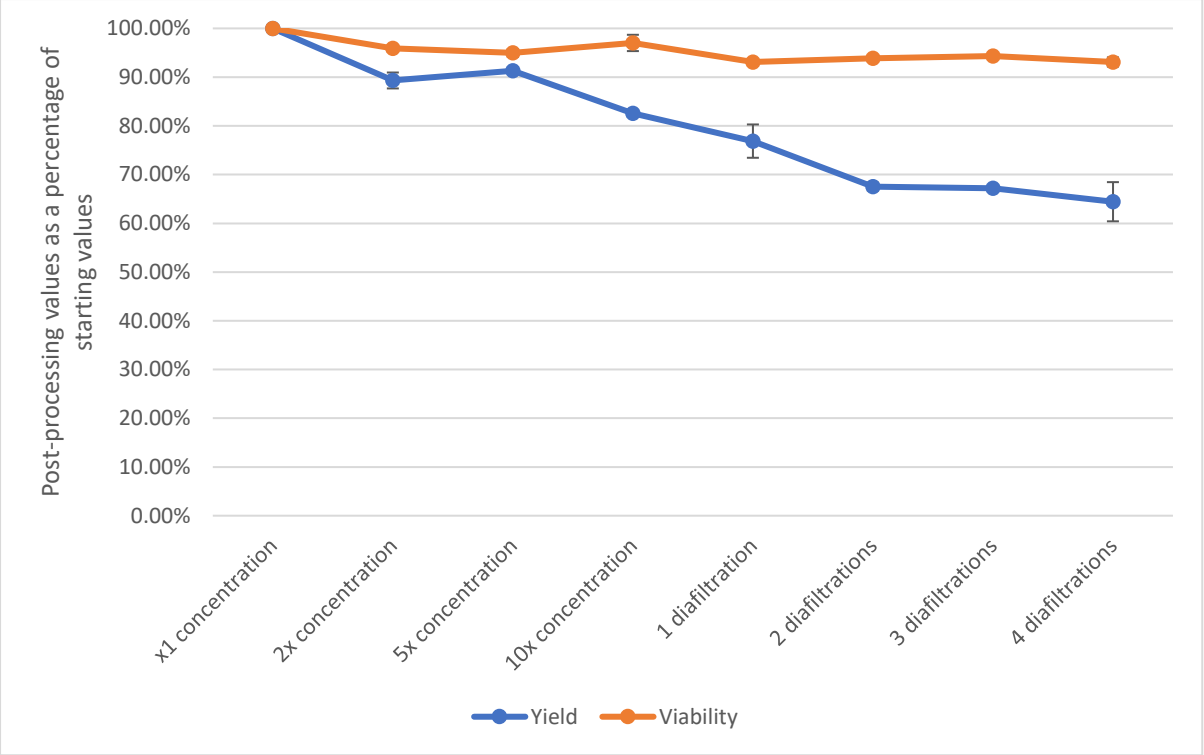

Figure 93 - Overall RC17 losses per ml of liquid passed through filter. Data shown as mean ± SD for biological repeats, n=2.

The full TFF process including concentration and diafiltration resulted in a significant loss of total cell number, however it should be noted that this technique allows for concentration factors far in excess of those achievable through batch techniques. This magnitude of cell loss has also been observed in an optimised process for the purification of mesenchymal stem cells under similar conditions (Cunha, Aguiar, *et al.*, 2017).

5.2.5 Comparison of Purification Techniques

Purification techniques must offer a high degree of unwanted liquid removal while minimising cell losses and degradation during processing. Figure 94 shows a summary of the concentration factors and cell recovery levels achievable through the purification techniques discussed in this section.

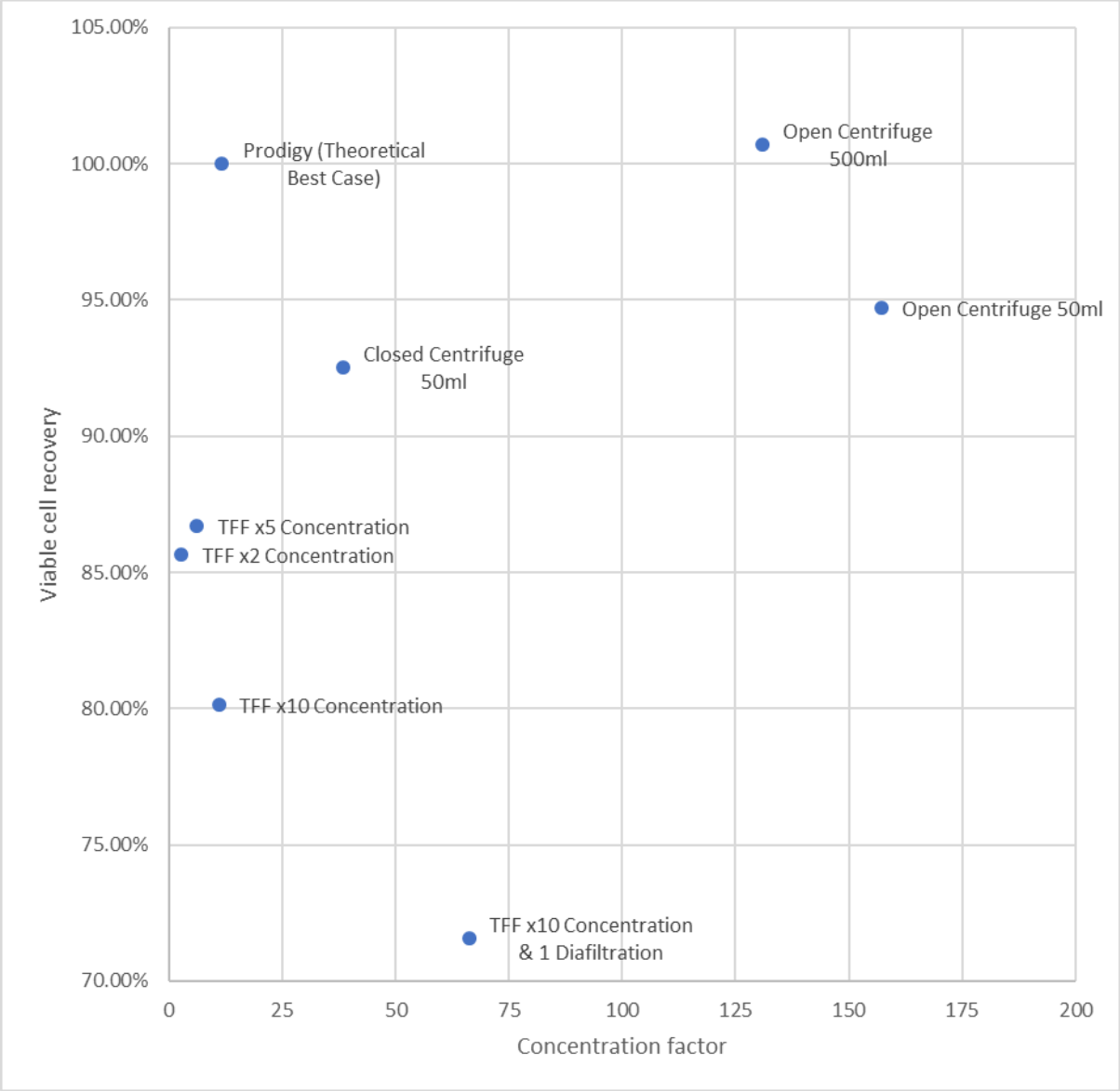

Figure 94 - Comparison of viable RC17 cell recovery % and concentration factor for various purification techniques. Closed centrifugation at the 500ml scale is excluded due to very poor cell recovery percentage archived. Only methods achieving above 80% cell recovery are shown, as this was determined to be the threshold of a successful purification operation.

Open centrifugation was arguably the most effective purification method, achieving the highest concentration factors for all discrete methods with the lowest cell losses. Open centrifugation at the 50 ml scale achieved a concentration factor of 157.16 with a high cell recovery of 94.63%. Open centrifugation at the 500 ml scale achieved a slightly reduced concentration factor of 130.92 and the highest cell recovery of 100.35%. This high level of cell recovery is also reflected in the literature, with cell hold times and management of pellet resuspension highlighted as key contributors to process quality (Delahaye *et al.*, 2015).

Closed centrifugation at the 50 ml scale achieved a concentration factor of 38.32 with a cell recovery of 92.51%. Although worse in both measures than open centrifugation, this method offers the lowest cell losses of all closed techniques measured. Closed centrifugation at the 500 ml scale is not included in Figure 94 due to the near total pellet loss experienced and resulting failure of this method. Although closed centrifugation at the 50 ml scale performed well, the loss of the pellet at the 500 ml scale speaks to the lack of reliability for this technique with available equipment, an essential factor in a manufacturing setting.

Concentration and cell recovery values for centrifugation on the Prodigy have been calculated rather than measured due to inaccessibility of the CCU. The CCU remains within a locked chamber throughout processing, processes may not be paused during an active process, and custom process configuration is not available to end-users. The achievable dead volume following centrifugation is approximately 30 ml and the highest starting capacity is 350 ml, giving a maximum achievable concentration factor of 11.67. It was not possible to determine the achievable cell recovery levels. These may be comparable to open centrifugation as the aspiration point has reasonable separation from the nearest pelleted cells, however, this value may also be significantly lower due to the cell pellet being a thin layer around the circumference of the CCU rather than a single pellet.

Unlike tube centrifugation, TFF is a continuous process and therefore has no defined end point or maximum achievable concentration for a single step, rather the losses must be balanced against desired purification and allowable process time. Some cells will always be lost to the filter surface through fouling (van Reis and Zydney, 2007). In general, cell recovery percentage decreases with the volume of liquid passed through the filter, with the hold-up volume (volume of the feed and retentate loop) forming the lower limit of liquid volume for the system. A concentration factor of 20 has previously been demonstrated for mesenchymal stem cells under similar filtration conditions (Cunha, Aguiar, *et al.*, 2017). Cell losses for high concentration factors achieved in this work are shown on a logarithmic scale in Figure 95. Although viable cell recovery decreases with increased concentration factors, the reduction plateaus for high concentration factors, demonstrating the potential effectiveness of TFF for high purity applications. TFF is less flexible than centrifugation, requiring a cell concentration of at least 1.8×10^6 cells per cm^2 to achieve high levels of cell recovery (Cunha, Peixoto, *et al.*, 2015). Processing time is also a concern for TFF as all cells must endure the entirety of the process, with extended process times contributing significantly to apoptosis and reduced future proliferation (Cunha, Peixoto, *et al.*, 2015). Processing time for centrifugation is more easily standardisable, as each process step (transfer, centrifuge, aspirate, resuspend) takes the same amount of time regardless of number of cells.

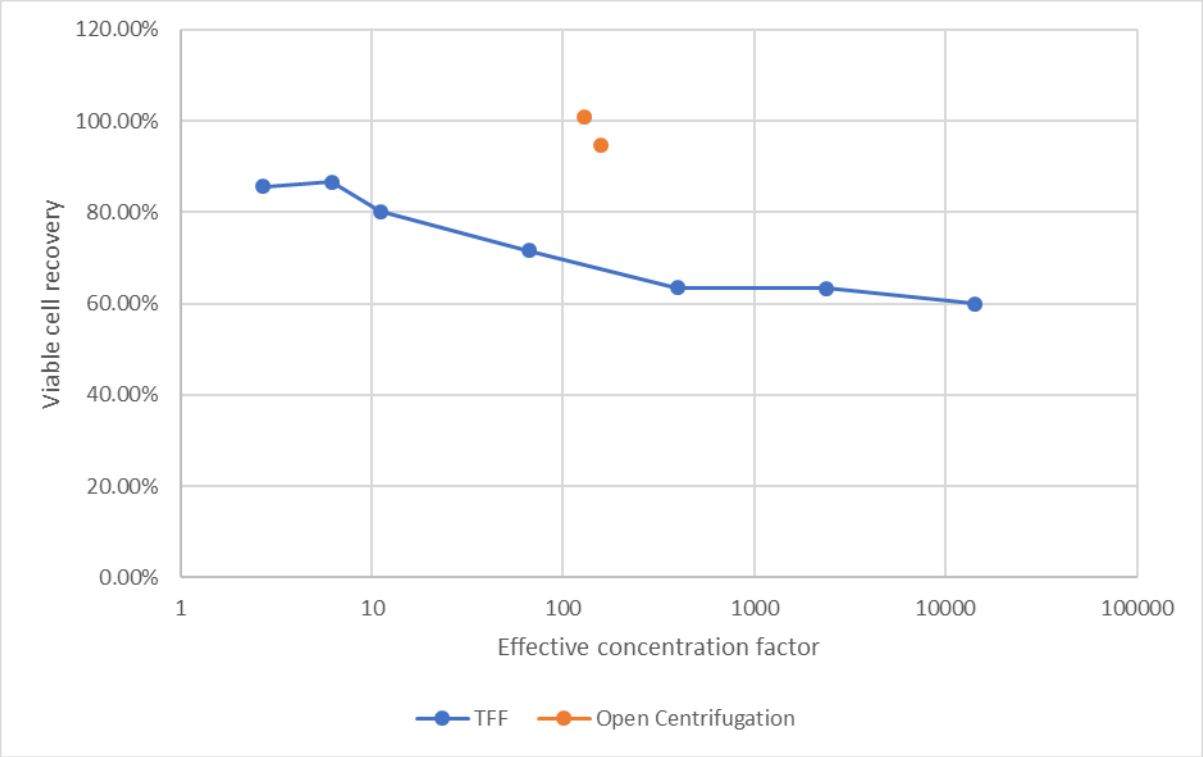

Figure 95 – Extreme concentration factors achievable via TFF, shown in comparison to those achievable in open centrifugation. Cell losses from open centrifugation might be expected to be linear, as each operation has similar losses. TFF losses after 60% were small, showing the high potential of this technique to achieve high concentration factors. Open centrifugation points are shown as mean, n=3 while TFF points are shown as mean, n=2.

5.3 Cryopreservation, Fill & Finish

Following purification and formulation, allogeneic cell therapy products are typically transferred into cryogenic storage vessels to be frozen and then stored or transported according to the specific requirements of the therapy (Nolbrant *et al.*, 2017). At the delivery side, cells will be thawed, retrieved from the cryopreservation vessel and possibly purified and reformulated, before finally being delivered to a patient, as summarised in Figure 96.

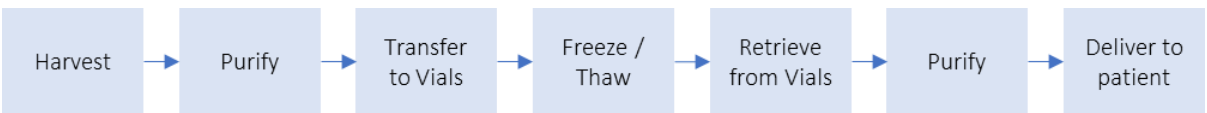

Figure 96 – Process steps for cryopreservation, from harvest to patient delivery.

5.3.1 Losses for a Typical Cryopreservation Process

Losses during downstream processing are especially costly as they represent loss of potential product cells which have received significant investments of time and materials (McCall, 2009). Small losses during manual processing for ESC cryopreservation have received little attention in currently available literature due to the abundance of techniques and equipment options at every stage, with available literature generally focussing on the performance of a newly available product against manual controls (Woods and Thirumala, 2011; Lyness, Picken and Thomas, 2019). The cumulative losses during manual cryopreservation into vials were explored due to their ubiquity in mammalian cell laboratories, and the potentially large quality and financial impacts of small but frequent cell losses during manufacture. It is expected that cell losses will be small at each processing stage but will equate to a significant portion of starting cell count over a cryopreservation process.

An experiment was performed to determine the level of cell loss and viability degradation at each stage of a standard open vial cryopreservation process as described in Section 3.2.7. RC17 cells were harvested from T25 flasks and pooled in 50 ml centrifuge tubes. Cells were then centrifuged and resuspended in cryo-protectant, transferred to vials, and transferred to a Mr Frosty freezing container for freezing in a -80 °C freezer. 24 hours later, vials were transferred to storage in LN2 and left for 1 week, after which they were thawed, resuspended in feed medium and transferred to a 50 ml centrifuge tube. Between each processing stage (other than when frozen), each of three biological repeats was weighed and counted. Total cell losses were determined by differences in total cell count and liquid volume, with viability determined during counting and results summarised in Figure 97. Total cell losses were highest for the purification step, with losses likely attributable to aspiration of cells from the pellet surface. Cell losses for vessel movements and between freeze and thaw were small and likely due to dead volumes and count variability. Changes to cell viability are highest across the freeze-thaw and centrifugation operations, possibly due to the greater strain placed on cells during these operations than during movements between containers.

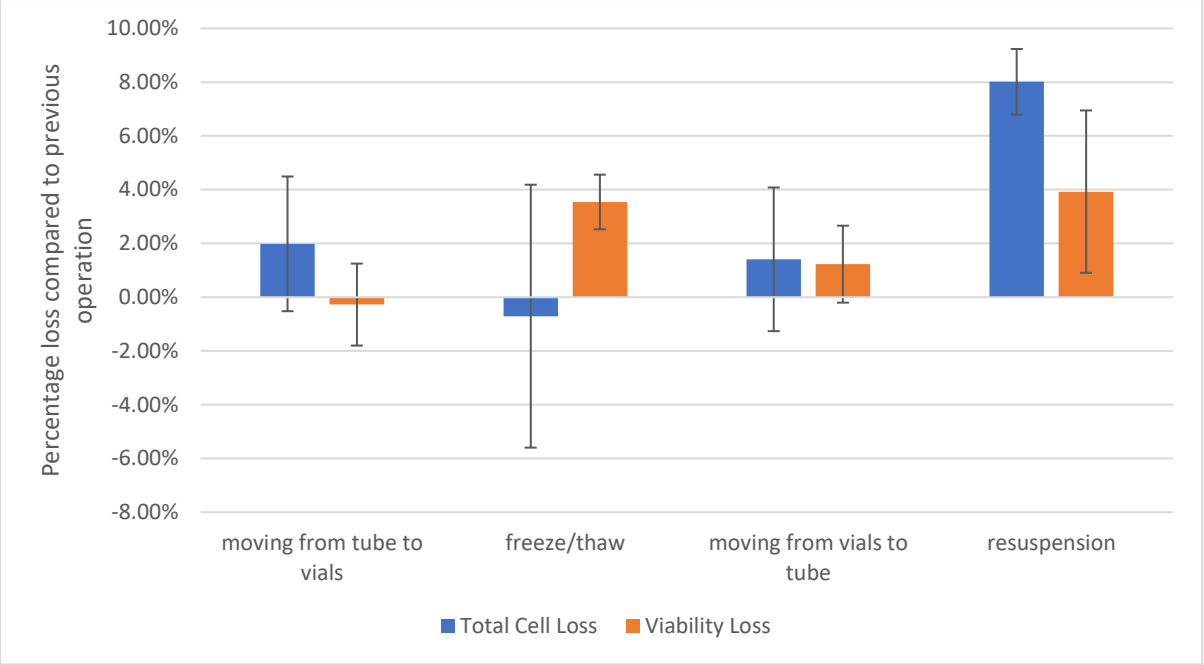

Figure 97 – Total RC17 cell count and viability changes between cryopreservation process steps. Data shown as mean ± SD for biological repeats, n=3.

Cumulative viable cell retention over the entire cryopreservation process is shown in Figure 98, with total viable cell yield for the full process at 81.85%. This level of cell loss is significant, although it is noteworthy that more cells were lost during the purification stage than for any other stage of the cryopreservation and resuscitation. The level of loss observed for purification via centrifugation is in broad agreement with those seen in Section 5.2, with significant losses in total cell number during centrifugation as part of the resuspension step, and viability losses of several percent observed due to the freeze/thaw process (Woods and Thirumala, 2011),

Figure 98 – Cumulative viable cell yield at each stage of the cryopreservation process, as compared to viable RC17 yield prior to starting cryopreservation. Data shown as mean ± SD for biological repeats, n=3.

5.3.2 Closed Cryopreservation of ESCs

Closed cryopreservation is desirable for manufacturing as it allows manipulations to be carried out in a lower grade of cleanroom than would otherwise be required, substantially decreasing overall process cost (Woods and Thirumala, 2011; Moutsatsou *et al.*, 2019). Cost benefits are most substantial for truly closed systems as they do not require any conventional grade A workspace. As a grade A environment must always transition into grade B environment where no physical barrier exists, a grade A workspace such as a biological safety cabinet (BSC) must be located inside a grade B cleanroom. In contrast, truly closed systems such as the Prodigy or a glove box isolator may operate in a grade D cleanroom, provided the closed system is not breached at any point in the process (Humpe *et al.*, 2007). Although the potential cost savings for closed processing are substantial, there is typically a higher risk of cell loss in such systems due to limited operator access and the use of tubing, which increases liquid retention and dead volumes (Woods and Thirumala, 2011).

Cryopreservation strategies and protocols are the focus of current literature due to the potentially large differences in cost and outcomes present between different approaches (Li and Ma, 2012; Coopman and Medcalf, 2014), with product focussed work largely consisting of comparisons between single products and manual controls (Woods and Thirumala, 2011; Lyness, Picken and Thomas, 2019). Due to

the small number of viable options available for the process scale and cell type of the Prodigy based mesDA manufacturing process, an experiment was performed to directly compare the level of cell loss and viability degradation present during cryopreservation in closed vials and bags compared to an open vial based control case. The expected outcome of these experiments is that closed cryopreservation will produce slightly increased cell losses following cryopreservation and resuscitation, with comparable yield performance following subsequent culture.

For each storage container, RC17s were harvested from T25 flasks then pooled and counted according to methods described in Section 3.2. Following counting, cells were centrifuged and resuspended to 1 x 10^6 cells per ml in cryoprotectant, where they were then resampled and recounted then dispensed into the cryopreservation container. For open vial freezing using 1.8 ml Cryotubes (5011-0012, ThermoFIsher), 1 ml of cell solution per vial was transferred into the vial using a 1 ml pipette tip, after which the vial lid was tightened. For closed vial freezing in 5 mL Needleless Barbed CellSeal vials (CSV-048, Cook Regentec), 5 ml of cell solution was drawn into a syringe through a blunted needle, then dispensed into each vial through the needleless Luer lock connector cap. The vials were then sealed using a heat sealer, with additional tubing trimmed from the vial. For closed bag freezing in CryoMACS 50 ml Freezing Bag 50 (200-074-400, Miltenyi Biotec), 10ml of cell solution was drawn into a syringe through a blunted needle then dispensed into each bag through a Luer connection port. Before disconnecting the syringe, the port was sealed using the pre-attached roller sealer, then excess tubing was removed from the bag using a tube heat sealer and scissors, then transferred into the overwrap. All containers were frozen using a VIA Freeze Research controlled rate freezer (Asymptote, GE Healthcare), using a program which held the cooling plate to 4 °C prior to adding the cell vessel, then cooled at 1 °C per minute to a target temperature of -90°C. All vessels were cooled within plates or racks provided by Asymptote as shown in Figure 99, with open (ASY_30061, Asymptote) and closed (ASY_30065, Asymptote) vials cooled in a plate, a single bag cooled in a plate adapter (ASY_30038, Asymptote) and multiple bags cooled in a rack adapter (ASY_30080, Asymptote). Following completion of the controlled rate freezer (CRF) run, cells were transferred to vapour phase liquid nitrogen storage.

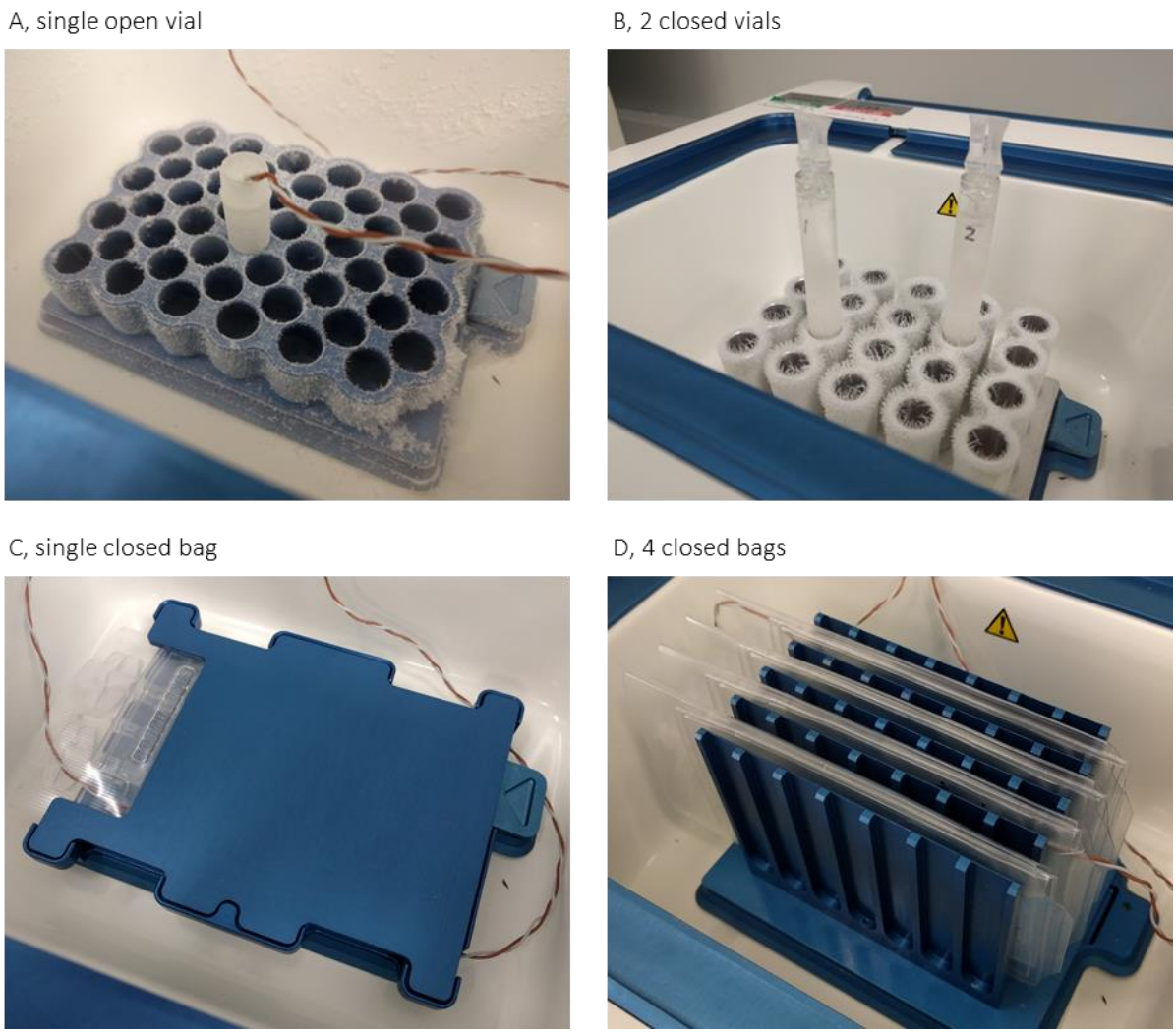

Figure 99 - Various cryopreservation container holders in the VIA Freeze Research. Images were not taken at the time of cell freezing, images from other experiments have therefore been used.

Following a storage period of 1 month, cells were retrieved from cold storage and thawed in an incubator at 37°C as described in Section 3.2.2. For open vials, the entire contents of the vial were retrieved with a 1ml pipette tip and placed into a 50 ml centrifuge tube. For closed vials, the protective film was removed from the retrieval port and the vial contents retrieved with a syringe and needle, then dispensed into a 50 ml tube. For bags, the access port cap was removed and a plastic needle with female Luer adaptor (S-F10, OrigGen Biomedical) was used to draw liquid into a syringe, then dispensed into a 50 ml tube. No additional washes were performed for any container type. In all cases, the recovered cell suspension was weighed and counted to determine cell recovery, then resuspended in seeding medium. Cryopreservation vessels were also weighed before and after use to determine liquid dead volumes, with these measurements combined with cell count data to calculate cell losses to cryopreservation vessel dead volumes. Losses due to changes in cell viability were also calculated using

cell count data. Viable cell recovery and a summary of losses is provided in Figure 100. Following post-thaw measurement, cells from each tube were seeded into laminin 521 coated 6-well plates at a density of 2 x 10^4 cells per cm^2 and transferred to an incubator. After 24 hours of growth, cells were harvested and counted to calculate growth rates for cells resuscitated following storage in each cryopreservation vessel type, with results shown in Figure 101.

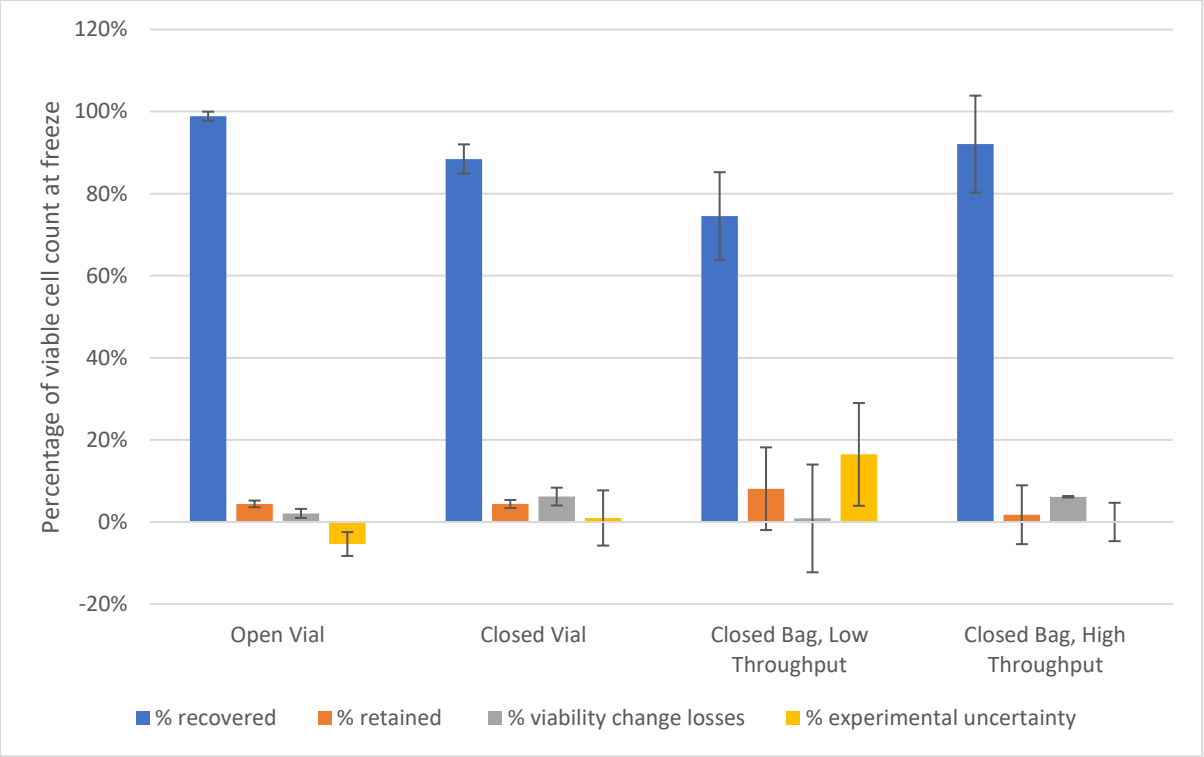

Figure 100 - Comparison of RC17 yield and cell loss for various cryopreservation vessels. Bars for open vials and high throughput closed bags shown as mean ± SD, n=3, while bars for closed vials and low throughput closed bags are shown as mean ± SD for biological repeats, n=2.

Viable cell recovery was highest for open cryopreservation vials at 98.55%, with this container type also causing the lowest variability in both recovered cell number and retained cell volume compared to closed vessel types. Closed vials delivered similar levels of variability to to open vials, likely due to the comparable cell transfer and freezing techniques employed for both vial variants than for either method of closed bag freezing. In the literature, variations on vial type cryopreservation have been shown to perform similarly to open vials (Lyness, Picken and Thomas, 2019).

Closed bags exhibited higher levels of variability in recovered cells and losses than open or closed vials. The high degree of variability in retained cells may be due to the random nature of air and liquid distribution within the bag when containing small volumes of liquid. As the distance between the sides

of the bag reduces, surface tension of the contained liquid causes it to form pockets and cease moving towards the harvest port due to gravity, preventing further liquid extraction. Operator manipulation is required to direct air pockets away from the recovery port during draining to maximise liquid retrieval, however some liquid will always be retained by surface tension and bubble formation. In the literature, closed freezing bags have generally been compared against other variations of freeze bags rather than against vials (Sputtek *et al.*, 2011; Becherucci *et al.*, 2020). These comparisons also focus on large scale suspension cell products, and may have omitted vials due to the perceived lack of crossover in scale requirements between the two vessel technologies.

The proportion of liquid recovered compared to retaining by closed bags should be equal for low and high throughput closed bag conditions as the vessel and retrieval technique used for each was identical. The disparity between recovery and retained cells in these two cases therefore highlights the high variability for closed bags compared to open and closed vials.

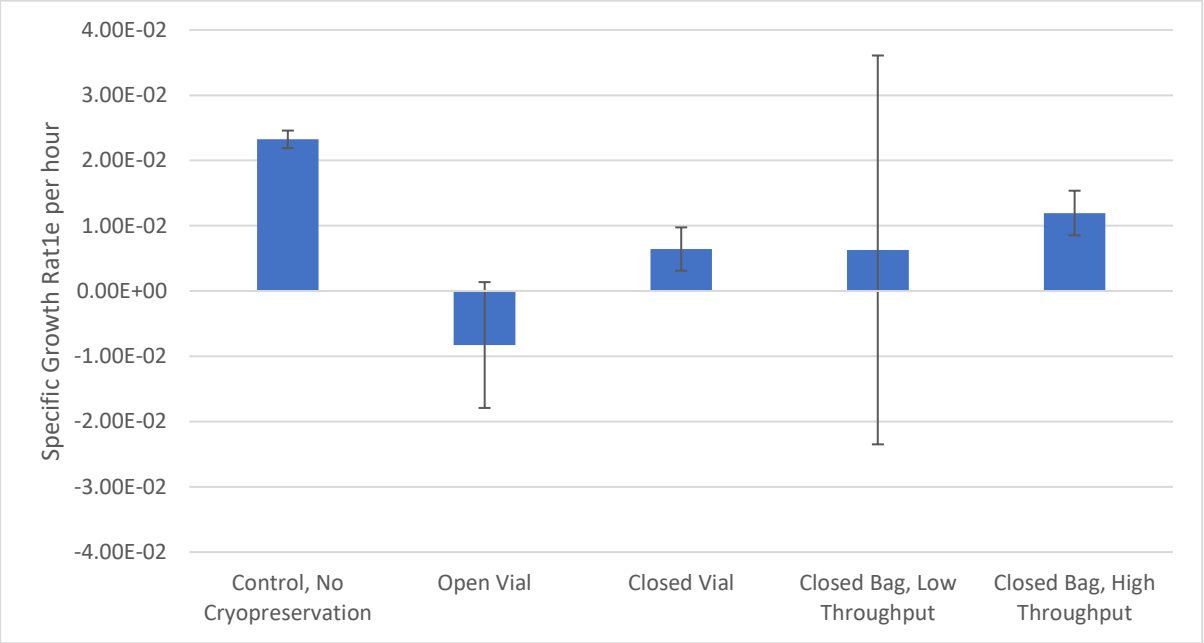

Figure 101 – Specific growth rate per hour for RC17 cells 24 hours after seeding following cryopreservation using various techniques. Bars for open vials and high throughput closed bags are shown as mean ± SD, n=3, while bars for closed vials and low throughput closed bags and control are shown as mean ± SD for biological repeats, n=2.

Cells from open vials had the lowest growth rate of -8.28 x 10^{-3} per hour and were the only vessel type to result in lost cells during the first 24 hours of growth, with cells from other cryopreservation containers achieving generally low growth rates. No or low growth is a typical behaviour for cells following cryopreservation, with an additional 24 hours of culture time typically allocated to achieve

confluency compared to a standard passage, and this experiment covering only the first 24 hours of growth. Although low, these growth values equate to a relatively small changes in cell density compared to the seeded cell density, with the overall high variability of cell growth following seeding likely being more impactful to further expansion than differences in growth rate between cryopreservation containers. These results broadly agree with the literature, that small differences in growth rate are likely following cryopreservation using different vessel types (Woods and Thirumala, 2011).

Specific growth rates 24 hours after thaw were all lower and exhibited higher variability than a standard passage for cryopreservation in all container types. This is to be expected as cells experience the stresses of a freeze-thaw cycle on top of the stresses of a typical passage during cryopreservation.

5.3.3 Controlled Rate Freezer Limitations

A key bottleneck for cryopreservation processes and therefore for downstream processing in general is controlled rate freezer throughput (Massie *et al.*, 2014). Controlled rate freezer throughput may be increased by increasing the cooling rate of a device to reduce time per batch, or by increasing the size of each batch by utilising using multiple or higher capacity-controlled rate freezers. The limiting factors for batch size are controlled rate freezer power and the capability to efficiently conduct heat away from the cell suspension to the cold plate and heat pump. Controlled rate freezer power determines the cooling rate achievable for a given thermal mass, while thermal conductivity determines the temperature differences possible between areas close to and distant from the cooling plate. High batch sizes present challenges for both factors, with high liquid volumes presenting a high thermal mass to be cooled, and large containers such as closed bags presenting significant distances and an increased number of thermal interfaces between the cold plate and cell solution. Due to the additional cost and laboratory space required for multiple or larger controlled rate freezers, the maximum batch size for a VIA Freeze controlled rate freezer was investigated.

This work is like an equipment verification effort, testing whether a CRF is able to meet its defined cooling rates for a range of vessel types and liquid volumes. Due to the nature of this work, reports on this topic are likely to be held internally to CRF manufacturers and are therefore unavailable in published literature. It was expected that the CRF would be capable of simultaneously meeting its specification for freeze rate and freeze volume regardless of the vessel type used.

For all conditions, 1.8 ml Cryotubes (5011-0012, ThermoFisher) were filled with 1 ml water and CryoMACS 50 ml Freezing Bags (200-074-400, Miltenyi Biotec) were filled with 10 ml water.

Thermocouples were used to monitor the temperature of samples at the centre and edge of each batch. In the case of vials, a hole was drilled into the vial lid to allow a thermocouple tip to rest suspended in liquid during cooling. For bags, the thermocouple tip was suspended between the bag and overwrap, as a hole could not be made in the bag without releasing the contained liquid. The same cooling profile was run for all conditions, consisting of a 4°C hold temperature followed by 1°C per minute cooling until reaching the minimum temperature of -90°C. The experiment explored the cooling capability of the controlled rate freezer with 1 ml of liquid in a single vial, 48 ml of liquid in 48 vials, 10 ml of liquid in a single closed bag, and 40 ml of liquid in 4 closed bags, as shown in Figure 102.

A, single vial

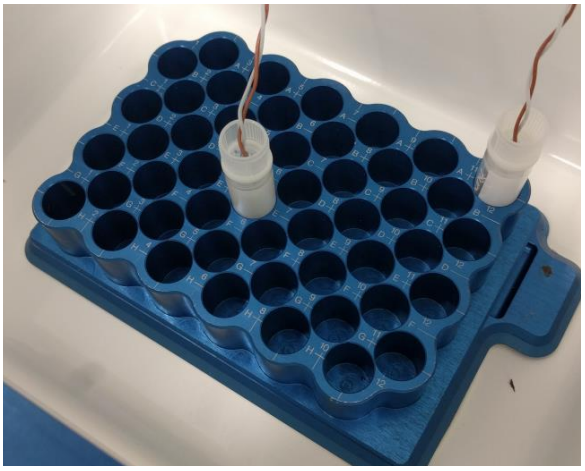

B, 48 vials

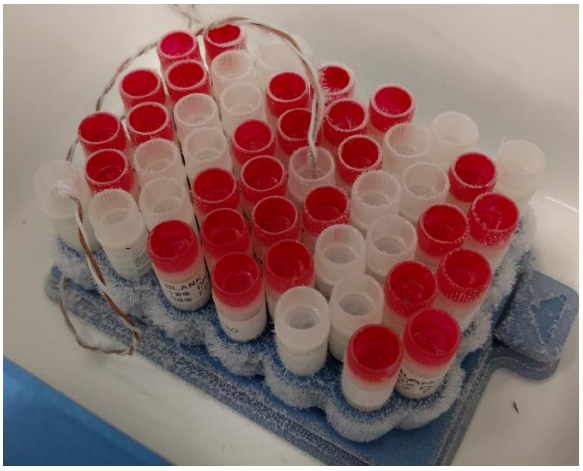

C, single bag

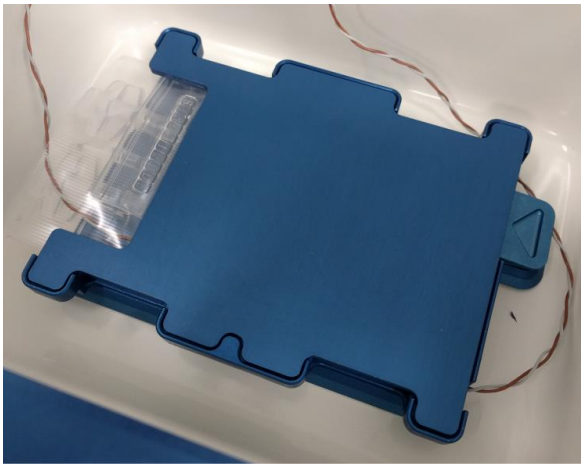

D, 4 bags

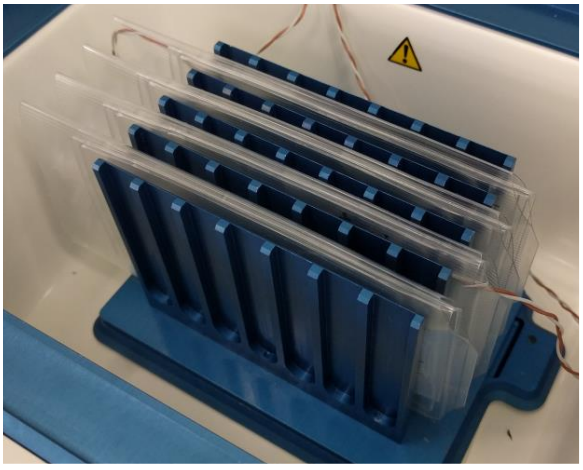

Figure 102 - Controlled rate freezer with various freezing configurations. Thermocouples were used in each case to measure liquid temperature at the centre and edge of the frozen samples. For vials, thermocouples were passed through a hole in the cap and suspended in liquid. For bags, thermocouples were positioned between the bag and bag wrap.

5.3.3.1 Output Power

The VIA Freeze series of controlled rate freezers transfer heat through a Stirling engine configured as a heat pump. The maximum input power of this heat pump is rated as 150 W at maximum power and 80 W at a hold temperature of -90°C for the VIA Freeze Eesearch (Asymptote Limited, 2017). The capability of the Stirling engine to maintain a cooling rate of 1°C per minute until reaching -90°C was tested for 2 vials (2 ml liquid volume), 48 vials (48 ml liquid volume), a single bag (10 ml liquid volume) and 4 bags (40 ml liquid volume). These volumes are all below or equal to the 48 ml sample capacity per cycle listed on the device specifications (Asymptote Limited, 2017). The performance of the system for these 4 conditions is summarised in Figure 103.

For 2 vials, 48 vials and a single bag, the cooling rate was maintained until approximately -80°C after which the cooling rate slowed. For 4 bags, the cooling rate could not be maintained upon reaching approximately -70°C. The 4-bag configuration holds less liquid than the full rack of 48 vials, however the bag holding rack arrangement has a high surface area and requires the use of a raised height lid as shown in Figure 104, reducing thermal insulation of the cryopreservation chamber and increasing the load on the Stirling engine.

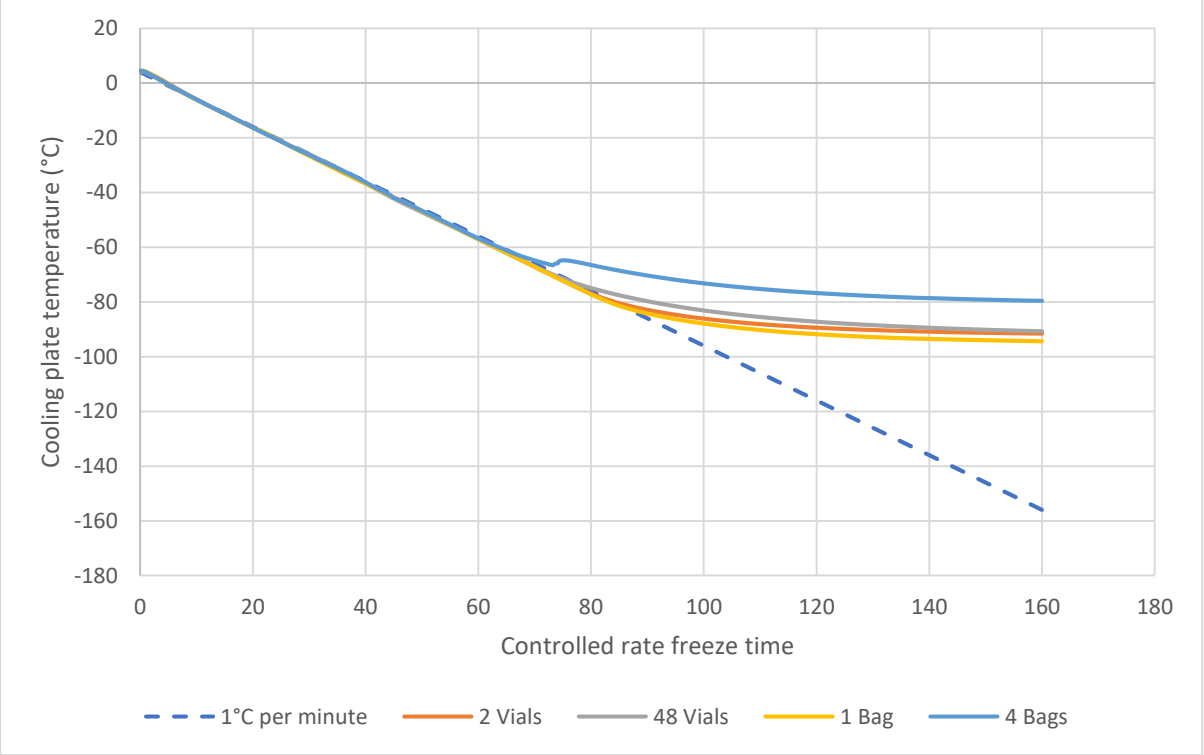

Figure 103 – Cryo-plate temperature against ideal temperature for each configuration. Cooling is on track at 1°C per minute until approximately -70°C for the 4-bag run, and approximately -80°C for other configurations.

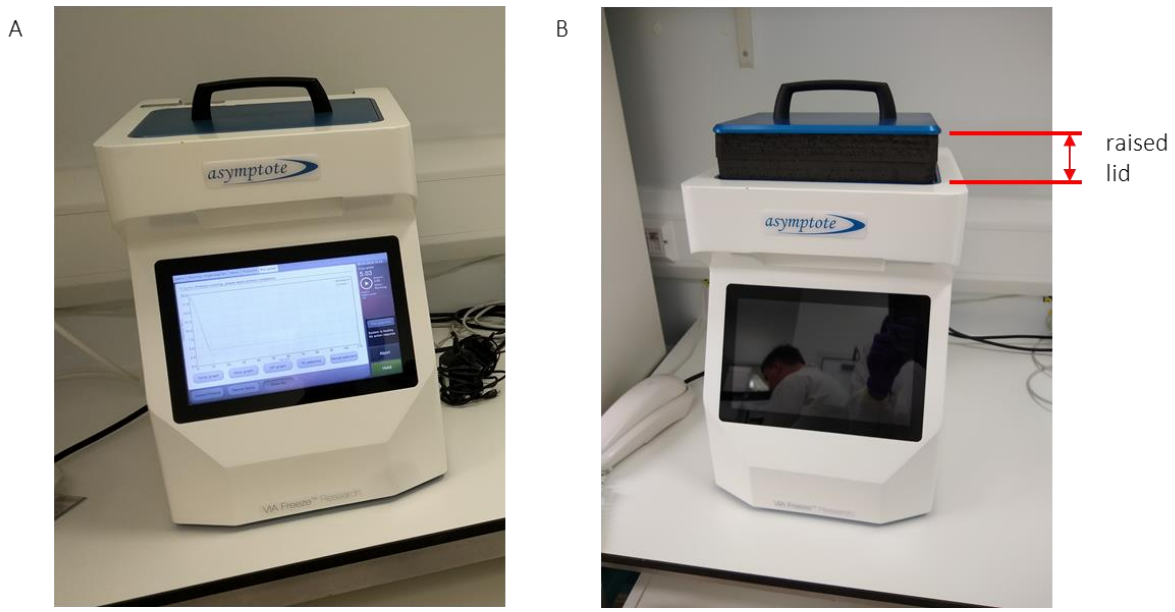

Figure 104 – Normal height lid (A) used for typical open vial cryopreservation, compared to the raised height lid (B) used for closed bag and closed vial cryopreservation.

The output power of the heat pump increases during a cryopreservation run as the thermal load is cooled to temperatures further from ambient. As the cold plate and thermal load cool, the heat pump must work harder to maintain a consistent cooling rate until it reaches 100% output power and can no longer achieve the desired rate. Under typical operation, the Stirling engine reaches its power limit near the end of the cycle when the cryo-plate and majority of samples have reached approximately -80°C. In the case of the 4-bag load, this limit is reached at approximately -70°C, as shown in Figure 105.

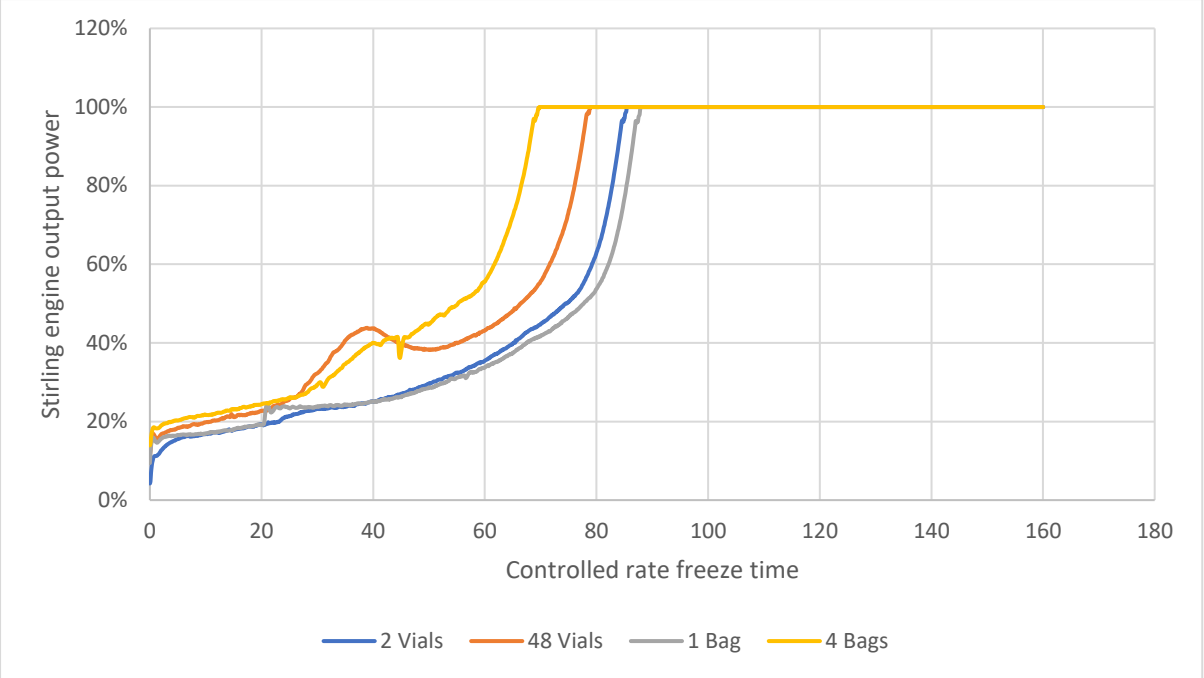

Figure 105 - Controlled rate freezer Stirling engine power output over time. When the Stirling engine reaches 100%, it can no longer increase its cooling capacity to match the 1°C per minute demand.

5.3.3.2 Thermal Conductivity

The ideal controlled rate freeze operation would homogeneously cool a cell suspension at the desired rate throughout the freezing process, regardless of volume of vessel type. In reality, thermal conductivity between the cold plate and cell suspension decreases as distance from the cold plate increases, as well as with increased numbers of material interfaces, leading to disparity in temperature between different areas of cell suspension.

For vial loads, the thermal pathway from the cell suspension to the vial, vial adaptor plate, and onto cold plate is relatively short with 3 interfaces. The same is true for the single bag holder, with the addition of the bag outer bag wrap between the bag and adaptor plate for a total of 4 interfaces. For multiple bags in a rack, portions of the cell suspension are some distance from the cold plate, with the heat transfer path passing from the liquid to the bag, through the bag wrap, onto the vertical rack support, into the horizontal rack adaptor plate and onto the cold plate for a total of 5 interfaces. The interfacing between bag, bag wrap, and vertical rack support is poor, as the lose fit of the closed bag allows for air gaps which offer poor thermal conductivity. There is an additional interface between the vertical rack support sections and the horizontal rack adaptor, with thin vertical aluminium sections making poor contact with the horizontal plate.

During testing, the VIA Freeze was run for Approximately 3 hours in order to reach a steady state in which the heat pump at full power is removing heat at the same rate at which it is heating the chamber contents, with negligible further changes to cold plate or sample temperatures. As shown in Figure 106, vial freezing for both 2 and 48 vials show an approximate 10°C difference between the cold plate and vial thermocouples, with negligible difference between the central and peripheral vials. In contrast, there is a difference of 27°C between the central and peripheral cell solution for the multiple bag freezing condition, suggesting that a batch frozen under these conditions experience a great degree of variability. The multiple bag condition also fails to reach the -80°C threshold for either central or peripheral cells, despite having a lower overall batch volume than the 48-vial condition. It is likely that a combination of larger vessel surface area, a higher number of thermal interfaces, and the use of the raised height chamber cover contributed to increased thermal conductivity between external heat sources and the cell solution, leading to worse and more variable freeze performance.

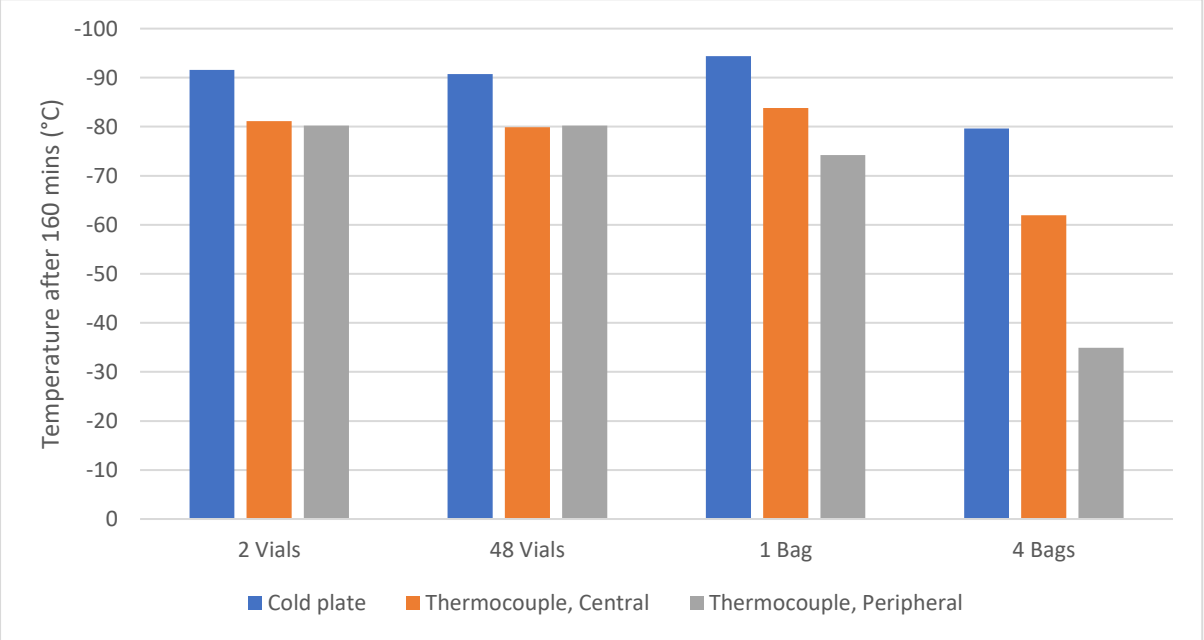

Figure 106 – Temperature of a controlled rate freezer cooling plate and cell solution after reaching a steady state following 160 minutes of cooling.

At present, the VIA Freeze controlled rate freezer meets specification for open vials but is not suitable for freezing of closed bags. Thermal conductivity may be improved for the multiple bag rack by including thermal interface material between metal on metal joints, by machining the rack from a single metal block, or by using a higher thermal conductivity material such as copper.

5.3.4 Impacts of Slow Processing

ESCs may remain cryopreserved for many years without damage, however they are highly sensitive to the freezing and thawing process (Karlsson and Toner, 1996). Cryoprotectants are commonly used to reduce damage from intracellular ice crystal formation and high solute concentrations, however cryoprotectants also have damaging effects on cells. The damaging effects of cryoprotectants are dependent upon concentration, exposure time and temperature (Benson, Kearsley and Higgins, 2012). Dimethyl sulfoxide (DMSO) is the most commonly used cryoprotectant for ESCs, however the effects of long term, low dose, room temperature DMSO exposure are not well understood. These conditions are increasingly likely as research grade slow cooling cryopreservation processes are transferred to good manufacturing practice (GMP) manufacturing conditions, which take significantly longer to perform. It is important to determine how long cells can be suspended in DMSO without significant losses to quality so that manufacturing grade processes can be best optimised for quality and time. The quantitative effects of extended pre-freeze DMSO exposure were therefore investigated, with the expectation that cell yields following thaw and subsequent culture would be reduced for cells with long hold periods.

A typical cryopreservation technique for ESCs, as described in Section 3.2.7, is to suspend cells in a cryoprotectant containing 10% DMSO and to dispense the mixture into vials, beginning freezing as soon as possible following formulation. DMSO exposure in this case is summarised in Figure 107, the exposure occurring from the point of formulation until cell freezing.

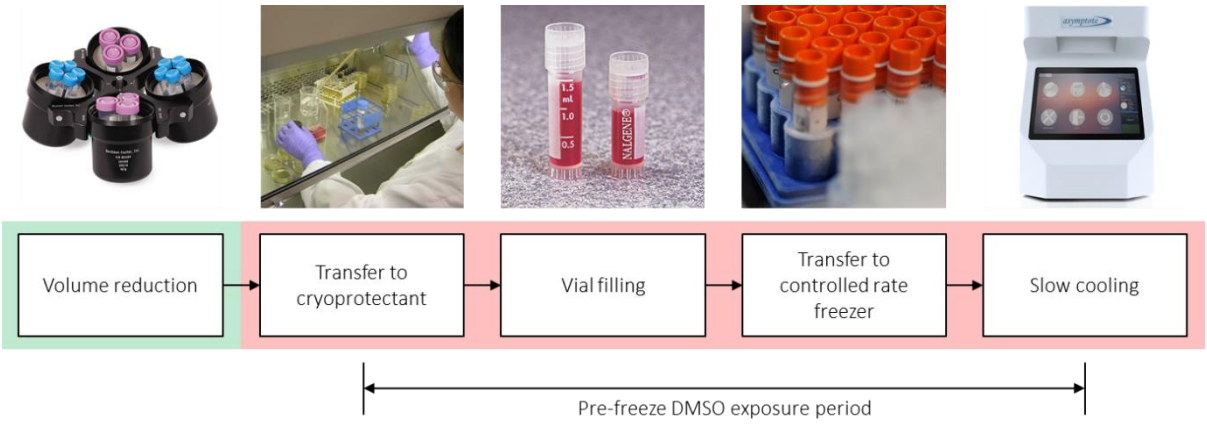

Figure 107 – A standard vialling process with process steps spend in DMSO highlighted. A volume reduction removes dissociation enzyme and inhibitor, cells are then transferred to cryoprotectant and remain exposed until frozen.

An experiment was performed in which hold steps were added between the resuspension of cells in cryoprotectant and dispensing into vials, simulating the delays present in large vialling operations and varying the exposure time of cells to DMSO. An overview of the experiment plan is provided in Figure 108. H9 cells were harvested, counted and resuspended in feed medium according to the methods outlined in Section 3.2. 4.5 x 10^6 cells were removed from the harvest and resuspended in cryoprotectant containing 10% DMSO, then dispensed into vials at 1ml each at a density of 1 x 10^6 viable cells per vial. 10 minutes later, a second batch of 4.5 x 10^6 cells was resuspended in cryoprotectant containing 10% DMSO, then dispensed into vials at 1ml each at a density of 1 x 10^6 viable cells per vial. This process was repeated two further times, giving resuspension times 10, 20 and 30 minutes after the resuspension of the first batch. Vials were transferred to a controlled rate freezer held at 4°C and began cooling at 1°C per minute 10 minutes after resuspension of the last batch, giving total pre-freeze DMSO exposure times before CRF start of 10, 20, 30 and 40 minutes. Once the CRF had reached -80°C, vials were transferred to vapour phase LN2 to be banked for 48 hours. Vials were then thawed with cells resuspended in feed medium, then counted and seeded into 6-well plates at 1 x 10^5 cells per cm^2 using the methods given in Section 3.2. Sacrificial harvests and cell counts were performed every 24 hours until a final harvest at 96 hours. This experimental design allows the use of a single pool of input cells as well as a single run of the controlled rate freezer, reducing the potential for variability which would be introduced by multiple input populations and controlled rate freezers.

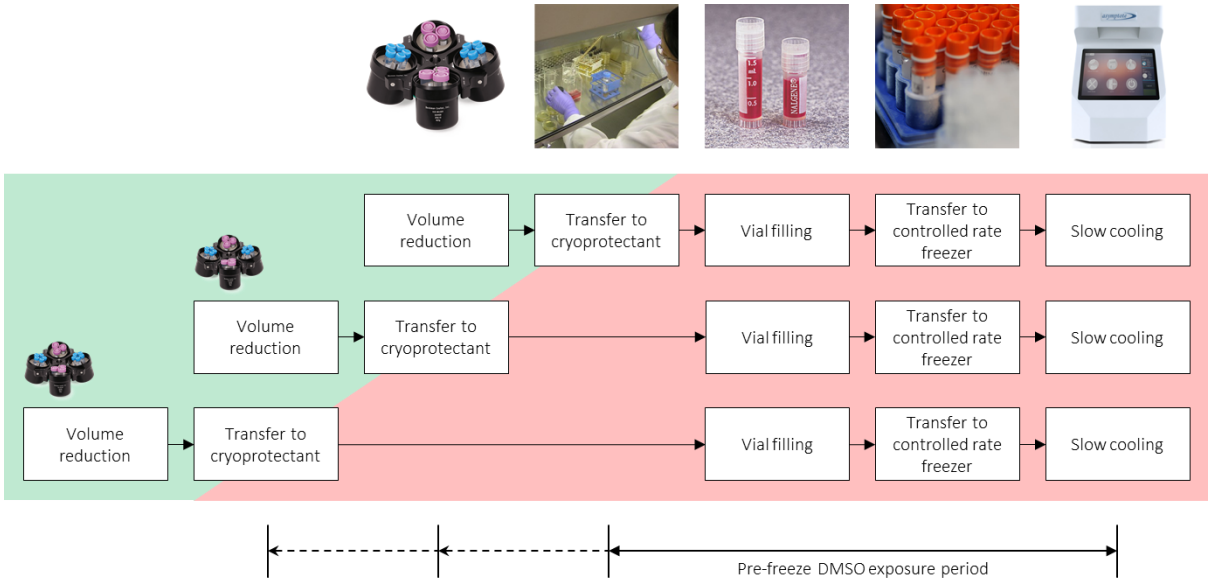

Figure 108 – Pre-freeze DMSO exposure period during a normal vialling process is shown on the top row. The centre and lower row show vialling operations with additional hold periods included, extending pre-freeze DMSO hold time.

As shown in Figure 109, an average total cell loss of 31.49% and viability loss of 2.38% was observed between cells prior to DMSO exposure and cells after DMSO exposure and a freeze thaw cycle. Total cell losses show a slight trend towards higher losses for higher DMSO exposure times, however the large variability present in these measurements suggests that the majority of losses are due to other process aspects present regardless of DMSO hold time, such as dead volumes and freeze thaw damage. Viability losses show no clear trend with regards to DMSO exposure time.

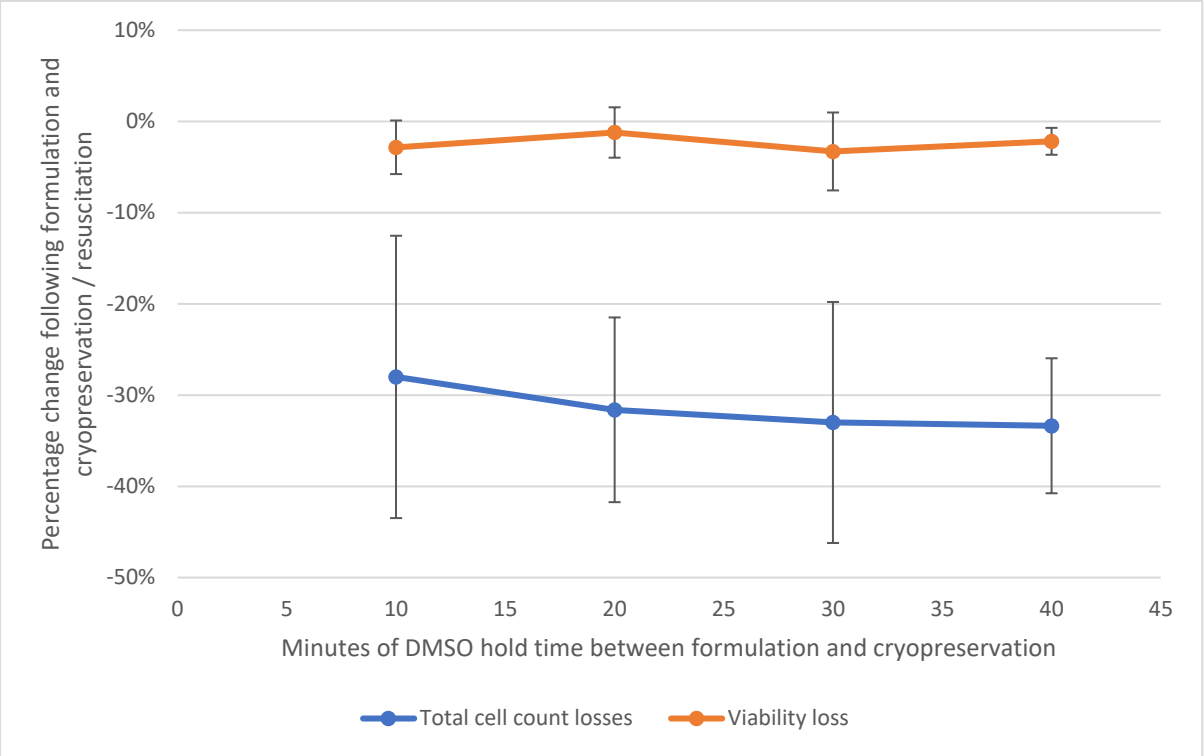

Figure 109 – Changes in total H9 cell counts and viability measurements for cells following formulation, cryopreservation and resuscitation as compared to counts performed prior to formulation, for various DMSO hold times. Data shown as mean ± SD for biological repeats, n=3.

The growth rates for 4 days following thaw were measured for 3 replicates of each DMSO hold period. As shown in Figure 110, no clear trend is present relating to DMSO exposure time, suggesting that hold periods of up to 40 minutes for H9 cells in 10% DMSO prior to freezing do not have a significant impact on cell growth directly following thaw. Although the toxicity of DMSO has been well demonstrated in the literature (Galvao *et al.*, 2014), the exposure periods in this work are significantly shorter and may account for the lack of negative impact on cell recovery and growth.

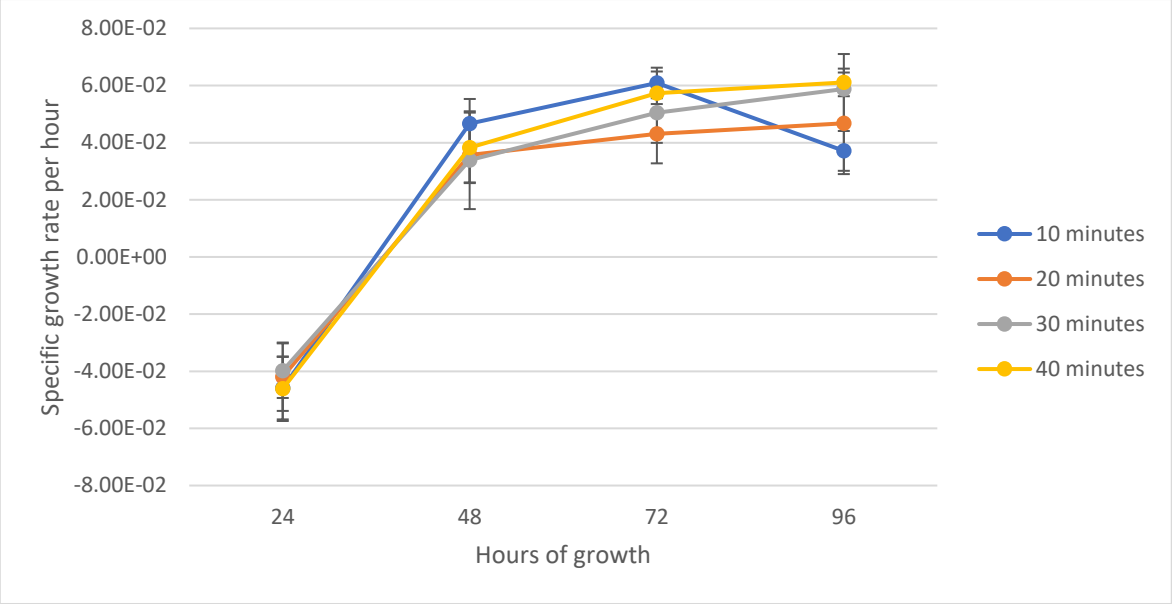

Figure 110 – Specific growth rate per hour for 4 days following thaw for extended pre-freeze DMSO exposed H9 cells. No clear pattern in cell growth is seen compared to the duration of pre-freeze DMSO hold.

The results of this experiment show little detectable effect of 10% DMSO exposure for up to 40 minutes of pre-freeze exposure time with regards to freeze-thaw recovery and growth rate for 4 days following thaw. DMSO has previously been shown to have diverse effects on ESC growth and differentiation (Pal *et al.*, 2012), with these effects being outside the scope of this experiment. These observations suggest that 40 minutes of processing time between formulation and beginning controlled rate freezing is allowable for H9 cells, however, other ESC lines or differentiated product cell types may exhibit higher sensitivity.

5.3.5 Comparison of Cryopreservation Techniques

A cryopreservation container optimised for small scale allogeneic therapies must meet basic requirements of sample sterility, stability and access (Woods and Thirumala, 2011), with combability with a process capable of truly closed filling, cryopreservation and sample retrieval being highly desirable. Open cryogenic vials are commonly used to store cells at the laboratory scale but are inherently open and require manual filling. A high degree of dexterity is required during vial filling, with the small nature of the containers and repetitive filling technique for large batches resulting in operator fatigue and increased risk of sample contamination.

Closed vials enable preservation of a fully closed system during filling and are compatible with automation but require similar levels of operator interaction as open vials for cell retrieval, limiting their suitability for closed and automated upstream processing. While automated filling systems are available, most require a biological safety cabinet or are optimised for T-cell therapies with low throughput fill and finish. Cryopreservation bags allow for large volumes to be processed more quickly due to their large size, with fill volumes ranging from 10 ml to 270 ml per bag, allowing for less manipulations and faster processing for a given liquid volume, however, bags may be too large for processes such as stem cell therapies with small dose sizes, and exhibited higher overall losses and yield variability than other vessel types. Cryo-resistant tubing on both closed vials and bags cannot be reliably sealed with the sealer provided as part of the Prodigy system, as the cryopreservation resistant tubing requires more heating than general silicone tubing. Cryo-resistant tubing is also unable to be tube welded onto silicone tubing, limiting compatibility and the possibility of closed cell retrieval.

DMSO hold experiments suggested that losses and specific growth rates are minimally impacted by prolonged DMSO exposure of up to 40 minutes prior to freezing. Although these results are promising for allowing extended processing times during batch processing, it is likely that specific functional assays will be required to determine the quality impact of cryopreservation on product cells (Marquez-Curtis *et al.*, 2016).

5.4 Discussion

Downstream processing is an essential component in cell therapy manufacturing and a key contributor to overall cost and quality loss (Hassan *et al.*, 2015). Cells are at their most valuable point during downstream processing, having received large investments of time and cost in progressing through upstream, expansion and differentiation. Downstream processing therefore concerns transferring cells from a freshly harvested solution into a defined product while minimising degradation and losses.

5.4.1 Harvest

There is a lack of research on cell losses during harvest and on the effects of physical manipulation to aid cell dissociation of planar culture. Cell damage due to cell scraping is well understood, however this technique is now obsolete in mammalian cell culture, having been replaced by enzymatic dissociation

methods (Heng *et al.*, 2007). The current lack of research may be due to the industry focus on larger scale harvesting of cells on microcarriers and in suspension, as well as the relative effectiveness of planar harvesting as a unit operation compared to other downstream processing steps. For planar cell expansion at commercial scales, growth on multi-layer vessels represents an opportunity for cell loss as manipulations are limited and detachment cannot be verified with microscopy as it can for single layer detachment at the research scale. In the absence of full diagnostics tools such as microscopy, process understanding is of utmost importance both from a manufacturing and regulatory standpoint. Consistency of cell harvests is therefore essential to stable manufacturing processes.

In this chapter, increased physical manipulation during cell harvesting was shown to correlate with reduced residual cell attachment during harvest and increase yield. The increase in cell loss of approximately 7.5% between minimally and maximally manipulated cells may be an acceptable loss depending on the specifics of the cell therapy product being produced. It is likely that higher levels of recovery may be achieved with minimal manipulation by increasing the exposure time or potency of the dissociation enzyme, at the possible cost of reduced cell quality. It may be possible to recreate the standard laboratory technique of flask tapping on robotically manipulated systems such as the CompacT SelecT, however there is a high potential for handling errors due to the reduced dexterity of robotic systems compared to human operators and rapid deceleration forces present during flask tapping. Forced liquid flow is possible to varying degrees on robotic systems featuring a serological pipet such as the CompacT SelecT, as well as on more restricted systems such as the Prodigy where the culture vessel may be rotated or otherwise moved to provide some aid to detachment. Flask tilting is the most suitable technique for closed single use tubing-based systems with otherwise stationary culture vessels but offers the lowest amount of physical manipulation. Controlled tilting of these systems may be achievable using already available technology such as bag rockers. Vessel shaking has been implemented on a CompacT SelecT system (Thomas *et al.*, 2009), and is likely to have provided harvest yield benefits between that of tilting and tapping.

It is hoped that future manufacturing processes will factor potential cell harvesting losses into decisions for closed and automated manufacturing platforms, and that the development of manufacturing platforms will allow for efficient cell harvesting through building in the capability for physical manipulation.

5.4.2 Purification

The key challenges identified for downstream processing relate to the limited options for scalable purification capable of preserving cell quality, with key concerns being processing time, sterility and mechanical stresses (Masri *et al.*, 2017). The lack of scalable tools also prevents the effective translation of manufacturing process from research to manufacturing scale, with notionally scalable techniques such as continuous flow filtration proving cost prohibitive to investigate at small scales due to current equipment (Hassan *et al.*, 2015). There is broad agreement across the literature that new developments are required to provide optimal purification for small and medium scale stem cell therapies (Pattasseril *et al.*, 2013; Hassan *et al.*, 2015), however, current closed processing equipment (summarised in Table 15) may provide solutions with acceptable levels of product loss and degradation depending on individual therapy requirements.

Table 15 - Summary of currently available purification techniques and their scalability.

Technique	Closed	Automated	Minimum Batch Size	Maximum Batch Size
Open centrifugation	No	No	any	8 litres
CCU centrifugation	Yes	Yes	30 ml	350 ml
Closed tube centrifugation	Yes	No	2 ml	2 litres
Closed bag centrifugation	Yes	No	5 ml	1 litre
Counterflow centrifugation	Yes	Possible	500 ml	12 litres
Tangential flow filtration	Yes	Possible	2 ml	5000 litres

The standard method for cell purification at the research scale is manual open centrifugation, which this chapter found to offer the highest levels of purification and lowest levels of cell loss of all methods tested. Open centrifugation is an efficient and flexible technique which is generally the default purification option at laboratory scale; however, it requires breaching of a closed process, relies heavily on manual manipulations and operator judgement, and grows challenging at scales beyond 10 litres (Pattasseril *et al.*, 2013).

Manual processing of closed centrifuge containers has the potential to provide a fully closed variant of manual centrifugation, however currently available plasticware does not feature angled dip tubes required for pellet isolation. There are limited suppliers of closed centrifuge vessels, with Corning being the only supplier represented on large laboratory product resellers for the UK and Europe. Corning's current product line for closed centrifugation consists of 50 ml (11705, Corning) and 500 ml (11750, Corning) closed centrifuge tubes, each with two tube connections configured as a full height dip tube and air balance as shown in Figure 111, A. The two-input centrifuge tubes currently available are useful for blood processing, where centrifugation is used for layer separation, however they are not well suited for cell processing as removing supernatant from a small pellet risks aspiration of the cell pellet, while for large pellets the aspiration point may lie within the pellet.

Process reservoirs produced by Corning for Repligen (formerly SpectrumLabs) for use with the KrosFlo KR2i TFF system features conical bottom vessels with three tubing connections, configured as a full height dip tube, shoulder height bent dip tube, and air balance as shown in Figure 111, B. This product is available in 15 ml (ACBT-015-C1N, Repligen), 50 ml (ACBT-050-C1N, Repligen), 250 ml (ACBT-250-C1N, Repligen) and 500 ml (ACBT-500-F1N, Repligen) capacities and is intended for use as a reservoir during TFF processing. When correctly oriented, the bent dip tube allows for centrifugation using the shoulder method within a closed system, significantly increasing the separation between aspiration point and the cell pellet. This product is not currently listed in the Corning catalogue and has limited availability from Repligen.

Equipment for open laboratory work such as pipettes and centrifuge tubes are ubiquitous and readily available with short lead times. More specialised equipment, especially made by a single or small number of suppliers, is sensitive to supply chain disruption by surges in demand and limited supply. Lead times of 77 days for 50 ml closed centrifuge tubes (11705, Corning) and 114 days for 500ml closed centrifuge tubes (11750, Corning) were experienced during this work. Supply chain issues such as these are important considerations for commercial operations, with plasticware shortages having previously impacted the manufacture of viral vectors in 2018 and mesenchymal stem cells several years prior (Stanton, 2018c).

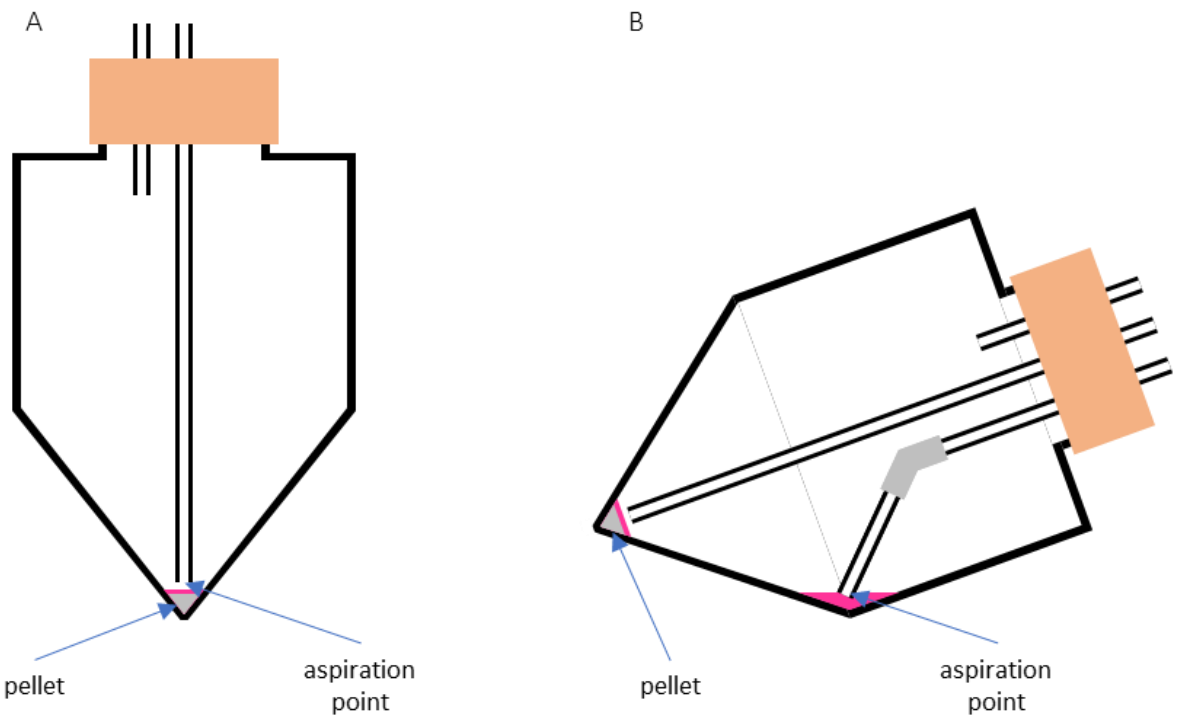

Figure 111 - Comparison of two and three tube centrifugation tubes. Tube A is a two-tube vessel of the type available from Corning and is used primarily for layer separation of blood products. If used for purification of a cell pellet, the aspiration point is too closed to the pellet, resulting in pellet loss. Tube B is a three-tube vessel featuring an angled dip tube which enables the safe removal of supernatant away from the cell pellet.

Closed processing with manual manipulations may provide a solution for small scale cell therapy manufacturing, providing cost effective purification of scales from 2ml to 2 litres per batch albeit with a reliance on operator manipulations. Due to the focus on blood processing, current products for closed centrifugation are unsuitable for removal of supernatant from a cell pellet. The three tubing connector lid shown in Figure 112, B and intended for use as a TFF processing reservoir is capable of addressing this need and is more suitable for autologous cell products than any currently available closed centrifuge tube, but currently suffers from supply issues. The fact that the most suitable plasticware is currently sold for a different purpose also highlights the lack of awareness of plasticware manufacturers of the requirement for closed cell centrifugation equipment.

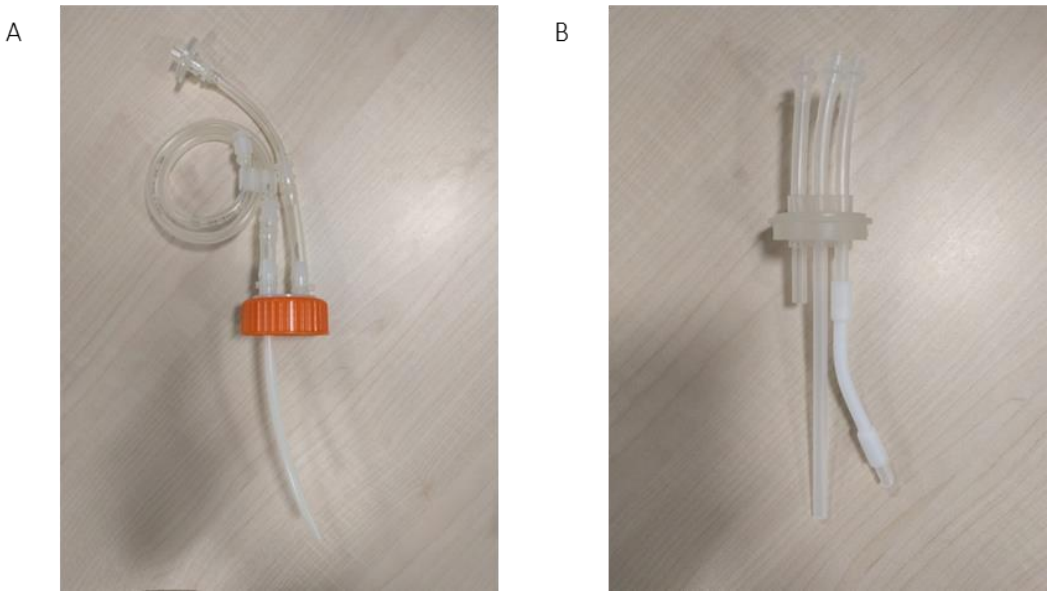

Figure 112 – Comparison of a 500 ml closed centrifugation product (11750, Corning) versus conical bottom process reservoir (ACBT-500-F1N, Repligen). Both products are produced by Corning and feature common vessel bodies and cap threading.

For processes featuring cell expansion on the Prodigy, CCU purification comes fully integrated into the closed tubing system, however, the high cost and complexity of the Prodigy and its consumables means that it is unlikely to be integrated into other closed and automated processes to perform purification as a single unit operation. As previously mentioned, counterflow centrifugation was not assessed as part of this chapter due to cost and equipment limitations. The technique has been shown to achieve 84% viable cell recovery for induced pluripotent stem cells (iPSCs) (Hasan *et al.*, 2017; Gaskell *et al.*, 2018) and may be expected to perform similarly for ESCs. Counter flow centrifugation offers a fully closed and automation compatible solution to centrifugation, however it is cost prohibitive for even exploratory work at small scales, requiring a minimum cell input of approximately 5 x 10^8 to function efficiently (Roberts, 2013; Hassan *et al.*, 2015).

In this chapter, TFF has been shown to achieve viable cell recovery levels of approximately 80% when producing a degree of purification comparable to CCU centrifugation, and levels approaching 60% for very high levels of purification. TFF has the potential to be integrated with single-use tubing-based processes such as the Prodigy but would require additional equipment including weighing scales and flow restrictors as shown in Figure 113, as well as for the Prodigy to either interact with external control software, or for Miltenyi to develop TFF control software for the Prodigy. The Prodigy pump also has limitations on tubing diameter and pump speed which translate to limitations on sheer rates and filter flux, reducing process efficiency at large scales. The extra tube routing associated with the Prodigy also results in a higher hold up volume, limiting minimum volume and concentration factor and making this

configuration unsuitable for small volume processing. Although integration of TFF with a system such as the Prodigy is achievable, it would likely make more sense to transfer the product suspension to a to a dedicated TFF system for purification. Although restrictive in many ways, TFF has the added utility of compatibility with continuous filtration processes (Cunha, Alves, *et al.*, 2015), although continuous processing options for other elements of stem cell therapy manufacturing processes are currently limited.

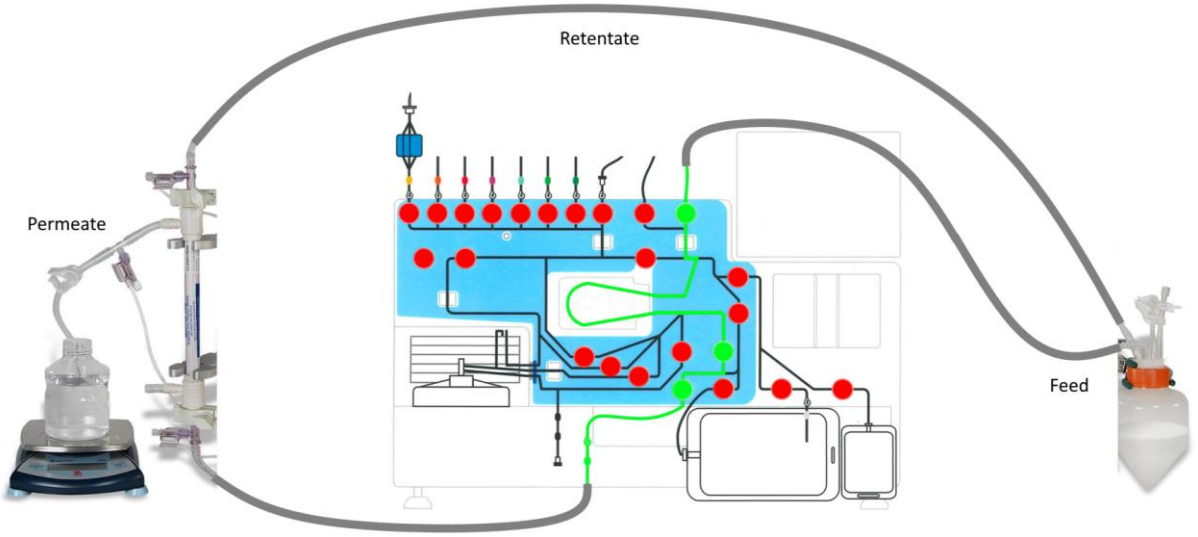

Figure 113 - Possible configuration of TFF performed through the Prodigy pump and tubing system, using external weighing scales and flow restrictors.

For allogeneic stem cell therapies, TFF is the optimal closed purification technique for low scale allogeneic stem cell therapies (Hassan *et al.*, 2015), however cell losses are significantly higher than in manual open centrifugation. Closed centrifugation in conical bottom process reservoirs may offer a solution for small scale processing, however this requires equipment with limited supply to be used outside of its intended purpose. The development of small-scale counter flow centrifugation systems, or options for smaller chambers on existing systems, would offer an attractive alternative to TFF for small scale purification, however this equipment is not currently available. Although TFF is notionally possible down to scales of around 2 ml, current limitations in software update rate and measurement precision mean there is insufficient data for the maintenance of optimal shear and filtrate flux rates required for efficient filtration at these scales.

5.4.3 Cryopreservation

Cryopreservation is the final processing step performed with an active product in liquid form, with further processing such as storage and logistics performed on notionally inactive cells in a solid and more easily handled form. Cells are extremely valuable at the point of cryopreservation, having received the full investment of banking, expansion, differentiation and purification stages, meaning that product loss at this point translates directly to lost doses. Variability in the outcome of cryopreservation and resuscitation processes is highlighted in the literature as a key challenge for stem cell therapy manufacture, and one which has received little attention compared to optimisation of isolation and expansion protocols (Coopman and Medcalf, 2014). There is a need to reduce risks and improve process robustness to enable commercial cell therapy products (Mitchell *et al.*, 2014).

The key considerations for cryopreservation vessels highlighted in the literature are vessel integrity in liquid nitrogen, maintenance of a sterile product, and accessibility of the product following thaw (Woods and Thirumala, 2011). Screw top vials are the standard vessel for small scale stem cell cryopreservation but do not form a complete seal against liquid nitrogen, potentially compromising the contained product and making them unsuitable for clinical use (Parisse, 2017). Because of this, closed vessels are gaining momentum as the vessel for commercial stem cell products, however, characterisation of performance and process suitability, especially with regards to processing time for these vessels is limited.

In this chapter, the performance of closed cryopreservation vials and bags were compared to the performance of standard screw top vials and were found to produce higher cell losses and viability degradation, as well as higher levels of variability in cell recovery and degradation. Closed bags produced the highest levels of variability and were challenging to manipulate during both filling and product retrieval, with potentially large volumes of liquid retained following product retrieval.

While processing of closed vials has more potential for dead volume losses than screw top vials, vial filling manipulations are relatively simple and are performed via a single Luer lock entry point on a short length of relatively stiff freeze resistant tubing. In contrast, filling of closed cryopreservation bags is challenging due to the number of connections and long flexible tubing paths present on each bag, as shown in Figure 114. Bag filling instructions specify that no gas should be present in the bag during freezing, however, bags ship containing a small volume of air and also take in air on the first removal of a Luer lock cap, necessitating the later removal of air with a syringe. The additional processing required to remove air after adding product liquid adds several challenging and judgement dependant manipulations of Luer lock tubes and syringes, each of which presents an opportunity for bubble

formation, product loss and contamination. After filling each bag and removing air, bags must be slipped into a protective sleeve before being transferred to a CRF. Taken together, these steps add considerable processing time and are challenging for a single operator to reliably complete.

Current closed cryopreservation vessels have been designed for patient delivery and product retrieval with a needle or Luer lock syringe. Although closed bags offer an option for sterile tube welding for product filling, the weldable section of tubing is removed prior to freezing, leaving only freeze resistant tubing which is unsuitable for tube welding. No currently available cryopreservation vessel offers closed product retrieval, limiting the suitability for fully closed cell banking applications.

Figure 114 - CryoMACS freezing bag, with three Luer lock fill ports (Miltenyi Biotec, 2020b).

Liquid nitrogen free controlled rate cooling is promoted as the new standard for cryopreservation (Asymptote Limited, 2017), providing robust and repeatable processing with record keeping suitable for commercial processing. Due to the time sensitivity of cells and batch processing nature of most CTP manufacturing processes, controlled rate freezer throughput is emerging as an issue for medium scale processing.

This chapter has highlighted issues with CRF throughput and limitations beyond those captured in device specifications, with closed vessels experiencing high levels of deviation from the desired cooling rate and variability between vessels in the same batch compared to a run of similar volume using screw top vials. Despite runs with all vessel types lying within the device specification in terms of overall product volume, the reduced chamber insulation, increased surface area and reduced thermal conductivity present when freezing closed bags allowed a large temperature differences to form

between different regions of a cryopreserved product, negating the high degree of control assumed to be present in controlled rate freezers.

Processing time is a consideration for CTP cryopreservation due to quality implications of potential cell activity and cytotoxic effects, as well as the cost implications of length processes for operator and facilities requirements (Hunt, 2019). In this chapter, periods of between 10 and 40 minutes of DMSO exposure prior to freezing were shown to have minimal impacts to H9 quality following cryopreservation and resuscitation, with this period potentially being too short to discern cytotoxic effects from background variability.

5.4.4 Conclusions

The key findings of this chapter are the significance of potential losses during cell harvest and the limited suitability of notionally well-matched purification and cryopreservation solutions to small scale stem cell therapy product processing.

Cell losses during harvest, purification and cryopreservation stack to produce high levels of overall product loss, translating directly to lost cell doses and impacting the cost of goods for each produced dose. The mesDA process introduced in Section 2.2.1 produces a high number of doses per batch and has the potential for high profit margins, making it more resilient to losses while remaining profitable, however this also means that any product loss has a higher than typical loss in potential profit.

Centrifugation based closed purification is limited by available plasticware but offers the potential for fully closed and highly efficient purification albeit with a high degree of operator involvement. Centrifugation in the Prodigy is closed and automated, but offers a low degree of purification per run, with a high consumable and device cost and challenging integration environment. TFF offers a notionally scalable solution, but one in which optimal conditions grow challenging to maintain at small scales due to the precision of current equipment. Counter flow centrifugation was not investigated in this chapter due to the cost prohibitive scale and cell density required for each run but may provide an optimal solution if small scale devices are made available.

Cryopreservation is currently based around screw-top vials and is moving towards closed systems, but efforts have largely been focussed on low vessel count autologous therapies. Closed vials offer a closed and automatable solution but present problems for controlled rate freezers due to their increased size and cooling chamber requirements. Controlled rate freezer throughput is a potential problem for even small-scale therapies, with this chapter highlighting ways in which deviations may occur when using

closed vessels, even when freezing within device specifications and using manufacturer provided equipment.

These problems represent an unmet need for small scale closed processing, an area largely left behind in the development of solutions for high batch size therapies such as those based on mesenchymal stem cells (MSC). This presents problems both for the manufacture of small-scale therapies, as well as for product and product development in general, preventing the use of comparable scale down models and making product development prohibitively expensive for high material cost therapies.

6 Process Cost and Quality

A process for the expansion and differentiation of embryonic stem cells (ESCs) to mesencephalic dopaminergic (mesDA) progenitor cells was developed by Lund University and transferred onto the Prodigy system by Miltenyi Biotec. A technology transfer was attempted to transfer the automated process from Miltenyi to Loughborough University for good manufacturing practice (GMP) development and to enable the use of the clinically relevant RC17 cell line. As discussed in Chapter 4, the technology transfer suffered difficulties due to low process robustness, equipment issues and a lack of available documentation.

This chapter proposes a method of process improvement capable of identifying cost and quality optimised process changes. This chapter first provides a process economics model with which a baseline process cost is identified the cost of process changes may be measured. The probable root cause of differentiation failure on the Prodigy identified in Section 4.6.3 is then characterised in order to define quality thresholds for H9 and RC17 cells. The quality impact of each possible mitigation strategy is then modelled for each cell line. The impact of each mitigation strategy on process cost is then weighed against the quality benefit, and finally an optimal order of process changes to meet cell line specific quality thresholds is presented. The method presented in this chapter may be applied to other processes in which the cost and quality impact upon a single critical quality attribute (CQA) must be compared for many potential process improvements.

6.1 Process Economics Model

For this work, a limited form of COGs model (referred to as a process economics model) was developed to establish a baseline cost for the mesDA product manufacturing process. A holistic style model was selected for its ability to calculate costs across many stages of processing; however, the scope was limited to costs directly affected by variations in the manufacturing process or equipment used. As such, this model enables simulation of the impact of process changes on material, operator, facility and machinery costs, as well as on the number of doses produced and cost per dose, but avoids the complexity of business decision focussed models which seek to model the full cost of goods, or costs associated with bringing a therapy to market (Lipsitz *et al.*, 2017).

6.1.1 Establishing a Baseline Process Cost for Manual and Open Processing

The baseline cost of the mesDA progenitor manufacturing process outlined in Section 3.3.3 was first modelled with the assumption that five days of ESC expansion and sixteen days of differentiation into mesDA progenitors were performed via manual manipulation in a biological safety cabinet (BSC). Downstream processing via open centrifugation was also modelled using an assumed loss figure of 5%, equal to those observed in Section 5.2.1 for open centrifugation at the 50 ml scale.

The cost of the manual process was determined to be £12,960, a breakdown of which is provided in Figure 115. Material costs constituted approximately 20% of process costs for the manual mesDA process, a figure found to be in broad agreement with those calculated for other processes of similar scales (Lipsitz *et al.*, 2017; Lopes, Sinclair and Frohlich, 2018a). Operator costs were also calculated as broadly similar to those described in literature at approximately 30% of overall process costs, and are noted as being highly dependent upon the labour intensity and length of a given process (Lipsitz *et al.*, 2017; Lopes, Sinclair and Frohlich, 2018a). Facilities costs for the mesDA process were calculated to be approximately 50% of overall process costs, with this figure being higher than is typically described in the literature (Lipsitz *et al.*, 2017; Lopes, Sinclair and Frohlich, 2018a). Facilities costs commonly represent a large portion of COG due to the high cost of maintaining manufacturing grade cleanroom facilities, with this fact being especially impactful for the mesDA process due to unusually long 21-day process run time throughout which cleanrooms are required.

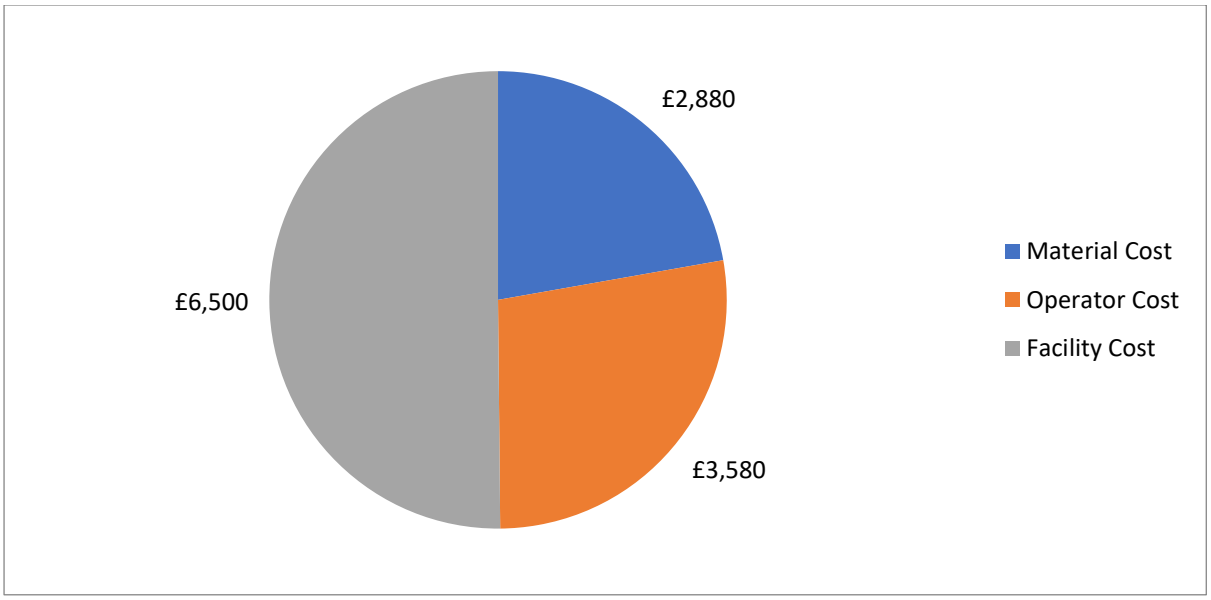

Figure 115 - Process costs for manufacture of a single mesDA batch performed in manual culture. The values in this figure have been calculated using the process economics model given in Section 6.1.

6.1.2 Cost Impact of Closed and Automated Processing

The cost of the mesDA progenitor manufacturing process using closed and automated processing as outlined in Section 3.4 was also determined. Expansion and differentiation were modelled as having been performed on the Prodigy, with media preparation performed manually in a BSC. Downstream processing losses were assumed to be 20%, equalling those seen in counterflow centrifugation at low cell concentrations (Roberts, 2013) and those observed during 10x concentration using tangential flow filtration (TFF) in Section 5.2.4.

A machinery cost was added to account for the cost of the Prodigy device, which cannot be used for other processes throughout the 21-day run time of the mesDA manufacturing process. The list price of the Prodigy is £163,909 and for clinical applications must be purchased with an IQOQ (Installation Qualification, Operational Qualification) priced at approximately £8880. The device is also likely to be purchased with a service contract priced at approximately £13,075 per year. Presuming that the Prodigy, IQOQ and service contract are bought at list price and that best case utilisation is achieved (where a new 21-day mesDA manufacturing process is begun on the day after harvest of the previous run, allowing 17 full process runs per year with 8 inactive days) for a device lifetime of 10 years, the Prodigy device cost per process run equals £1785.53.

The cost of the closed and automated process was calculated as £20,106, a breakdown of which is provided in Figure 116. Process costs have risen in all aspects as compared to the manual process, with facilities and operator cost rises due to the increased processing time required, and material costs rising due to the increase of dead and wash volumes increasing process wastage compared to the manual process. Due to the additional dead volumes present when harvesting cells using the Prodigy, the automated process produces 423 doses per batch compared to 549 doses per batch for manual processing, assuming a dose concentration of 2×10^6 cells. The reduced number of doses per batch further increases the cost per dose of automated processing compared to manual, as shown in Figure 117.

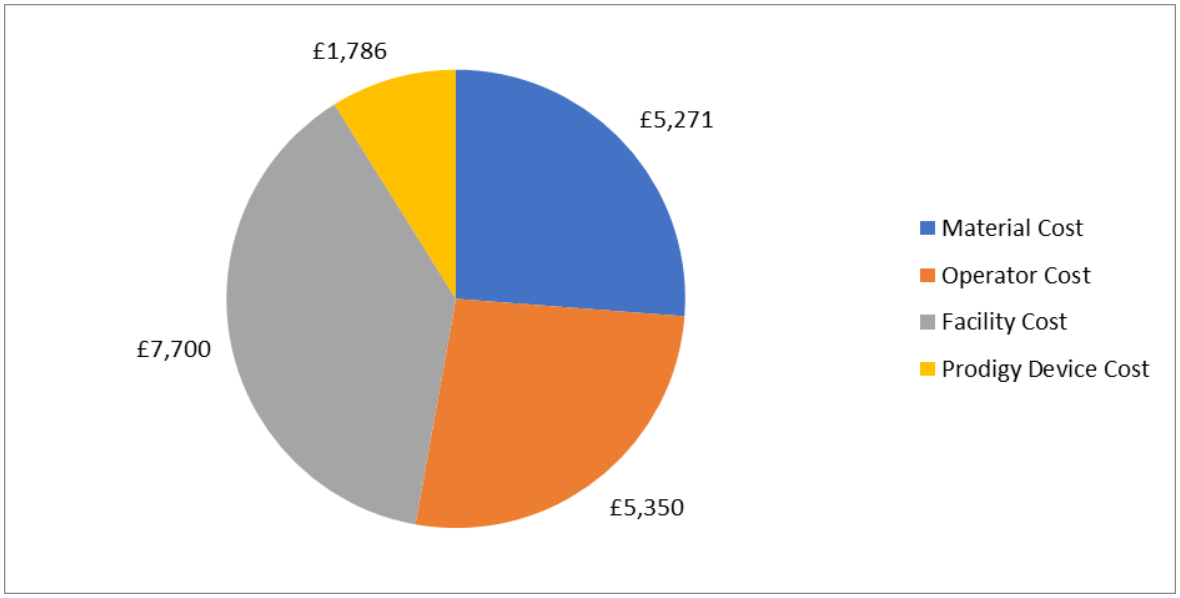

Figure 116 - Process costs for manufacture of a single mesDA batch performed on the closed and automated Prodigy system. The values in this figure have been calculated using the process economics model given in Section 6.1, with the device cost as derived in Section 6.1.2.

This cost increase is at odds with the majority of published models (Lipsitz *et al.*, 2017; Lopes, Sinclair and Frohlich, 2018b) which typically assume a significant decrease in operator resource requirements when transitioning to automated processing. The level of operator cost and level of possible saving due to automation is highly process dependant, with one highly optimised model suggesting a reduction in operator cost of 84% (Lipsitz *et al.*, 2017). A possible reason for this disparity is the lack of integration and increase in process complexity for automated processing on the Prodigy, with any savings as a result of automation cancelled out through reduced yields and inefficiencies of the system. Similar issues are highlighted in a comparison of manual, partially and fully automated manufacture of autologous dendritic cells, in which labour costs decrease for partial automation and increase for full automation (Lopes, Sinclair and Frohlich, 2018b). Labour is highlighted in publications and in surveys as a key area for cost reduction, with automation highlighted as a key industry demand (Lipsitz *et al.*, 2017; Lopes, Sinclair and Frohlich, 2018b).

Materials cost changes show disagreement within the literature, with some models showing modest cost savings (Lopes, Sinclair and Frohlich, 2018b) while others predict significant cost increases (Lipsitz *et al.*, 2017). An 83% increase in material costs were calculated for the automated mesDA process, with the change largely due to the inefficient use of differentiation medium as a tube wash and purification dilatant during processing on the Prodigy.

Facilities costs for the mesDA process showed a small increase, with this following the pattern described in the literature (Lipsitz *et al.*, 2017; Lopes, Sinclair and Frohlich, 2018b), although it is noteworthy that the increase in facilities cost was smaller for the automated mesDA process than for the more complete level of process automation described in most models.

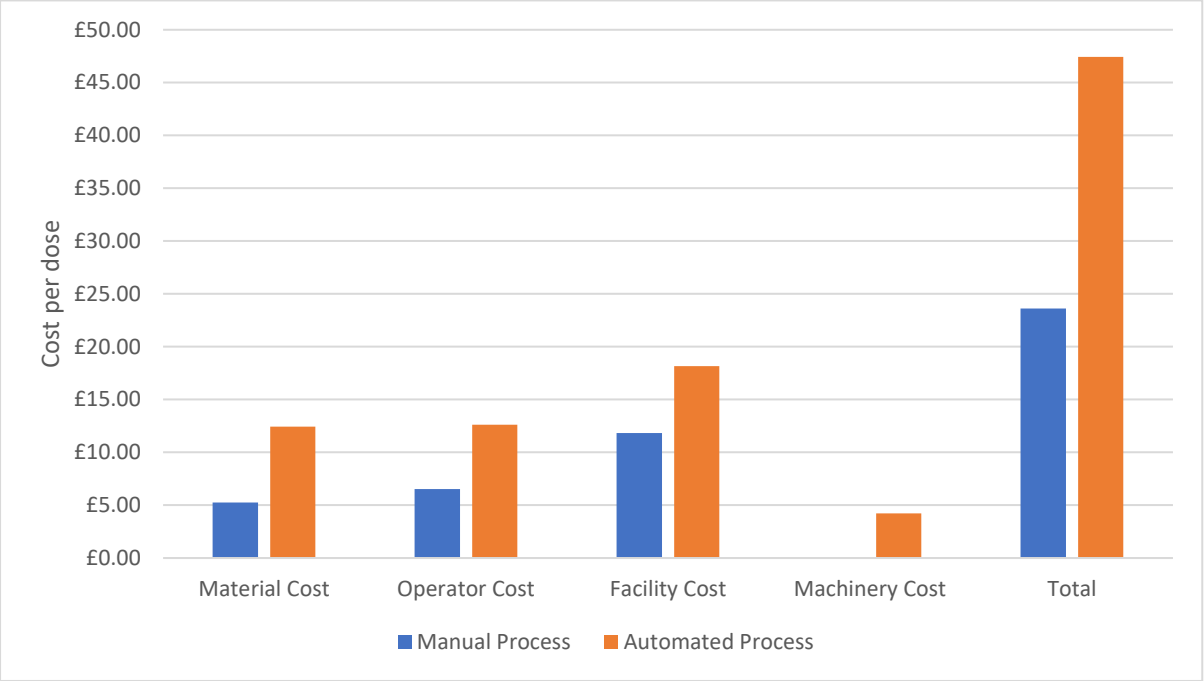

Figure 117 – Process costs per dose for the expansion, differentiation and downstream processing of a process to produce mesDA progenitor cells. Comparison of costs for the process performed manually and automated via the Prodigy, as calculated using the process economics model given in Section 6.1.

6.2 Quality Impact of Incomplete Centrifugation

Quality and cost must always be balanced in manufacturing. In the manufacture of physical components, reduced tolerance thresholds lead to increased costs as more precise and time-consuming methods are required to achieve increased quality demands (Muthu, Dhanalakshmi and Sankaranarayanasamy, 2009). In cell therapy product (CTP) manufacturing, tightening a specification for allowed contaminants increases the effort and cost required to reach the increased level of quality.

Cell quality is challenging to define and encompasses many possible cell attributes (Lipsitz, Timmins and Zandstra, 2016). Cells are required to be of adequate quality to meet a quality target product profile for release, as well as to maintain a level of quality throughout processing to prevent process failure. CQA for a cell during processing may include minimum allowable growth rates and specific morphology,

both of which are suggestive of cell health and ability to withstand further processing. Maintenance of these CQAs is dependent upon many process parameters, of which the presence of TrypLE and Defined Trypsin Inhibitor (DTI) was identified in Section 4.6.3.5 as having a critical influence on cell growth and morphology. This section focusses on quality with regards to contamination of CTPs with undesirable excipients which may be addressed through additional processing. Contamination of CTPs with adventitious agents is treated as irreversible due to challenges in removal and verifying the absence of a biological contaminant, as well as the ability of adventitious agents to multiply and so increase the level of contamination following purification. All future references to contamination within this chapter refer to non-biological contamination with TrypLE and DTI in a 1:1 ratio.

Quality management requires the balancing of process risks against the cost of mitigation strategies. The probable root cause of process failure during automated differentiation on the Prodigy identified in section 4.6 was contamination of the cell solution and seeding medium with TrypLE and Defined Trypsin Inhibitor (DTI). This contamination arose due to incomplete centrifugation on the Prodigy CCU and resulted in a lack of cell attachment during process runs performed according to the Miltenyi 2018 protocol. As the use of dissociation reagents such as TrypLE are ubiquitous in processing of adherent cells and their behaviour as a low concentration contaminant is poorly characterised, this section aims to quantify the effects of TrypLE contamination. This characterisation will provide greater understanding of the failure mode experienced during the Prodigy automation project, allow potential mitigation strategies to be modelled and optimised, and highlight the potential implications of this failure mode on other systems with reduced levels of purification compared to manual processing. The techniques detailed in this chapter are applicable to cost and quality management of other CQAs and manufacturing processes.

6.2.1 Cell Yield Response to TrypLE and DTI Contamination During Seeding

The effect of TrypLE contamination on cell growth is poorly characterised despite ubiquitous use in adherent cell culture applications. TrypLE is a trypsin replacement commonly used to aid detachment of adherent cells by cleaving peptide bonds on the carboxyl side of lysine and arginine. TrypLE also includes ethylenediaminetetraacetic acid (EDTA) at a concentration of 1 mM, which aids detachment through chelation of calcium and magnesium molecules from the cell surface, improving TrypLE efficiency. Extended exposure of the cell surface to TrypLE / EDTA may cause apoptosis through unwanted proteolysis of surface proteins. TrypLE is commonly used for a period of around 5 minutes, or until cells have detached from the culture surface. DTI is a soybean-based trypsin inhibitor and is

commonly used in a 1:1 ratio with trypsin or trypsin replacement to halt its action following cell detachment. Trypsin is created in the digestive system of many animals to break down proteins for digestion, while Trypsin inhibitor is created by plants including soybeans, pineapples and papaya as a defence mechanism.

6.2.1.1 Characterisation of Contamination During RC17 Differentiation Seeding

The growth of RC17 cells following exposure to various concentrations of TrypLE and DTI contamination during cell seeding of a differentiation was first determined. This work builds upon experiments performed in Section 4.6.3.5, providing further characterisation of the cell response to contamination of the type present during manufacture of the mesDA progenitor product on the Prodigy, and providing a baseline response to contamination against which variations of the process may be compared.

A pool of cells was obtained by harvesting, counting and purifying a culture of pluripotent RC17 cells using the methods described in Section 3.2. Cells were distributed into 50ml conical tubes containing day 0 differentiation medium and an appropriate volume of 1:1 TrypLE Select and DTI solution. The range of contamination values were 0.5% to 5.5% TrypLE & DTI in 0.5% increments. The cell suspensions were then distributed to 6-well plates coated with laminin-111 according to the method described in Section 3.3.1, with each well seeded at a density of 2.5 x 10^4 cells per cm^2 with 2ml of medium. 6-well plates were then transferred to an incubator for maintenance as detailed in Section 3.3. After 24 hours of growth, each well was harvested with 0.5ml TrypLE and diluted with 0.5ml of feed medium. A 190 µl sample was collected from each well and counted using the NC-3000 image cytometer.

Cell yields obtained following 24 hours of growth followed a dose response curve in relation to the concentration of TrypLE and DTI contamination in the cell seeding medium, as shown in Figure 118. Data was analysed and a dose response curve fitted with Origin data analysis software (OriginLab Corporation, USA). The dose response curve is defined by the formula:

$$y = A1 + \frac{(A2-A1)}{1+10^{(log(x0)-x)p}} \quad (3)$$

Where A1 is the bottom asymptote, A2 is the top asymptote, $\log(_x0)$ is the centre and p is the hill slope. Values for the curve produced by RC17 response to TrypLE and DTI contamination during seeding of a differentiation are provided in Table 16.

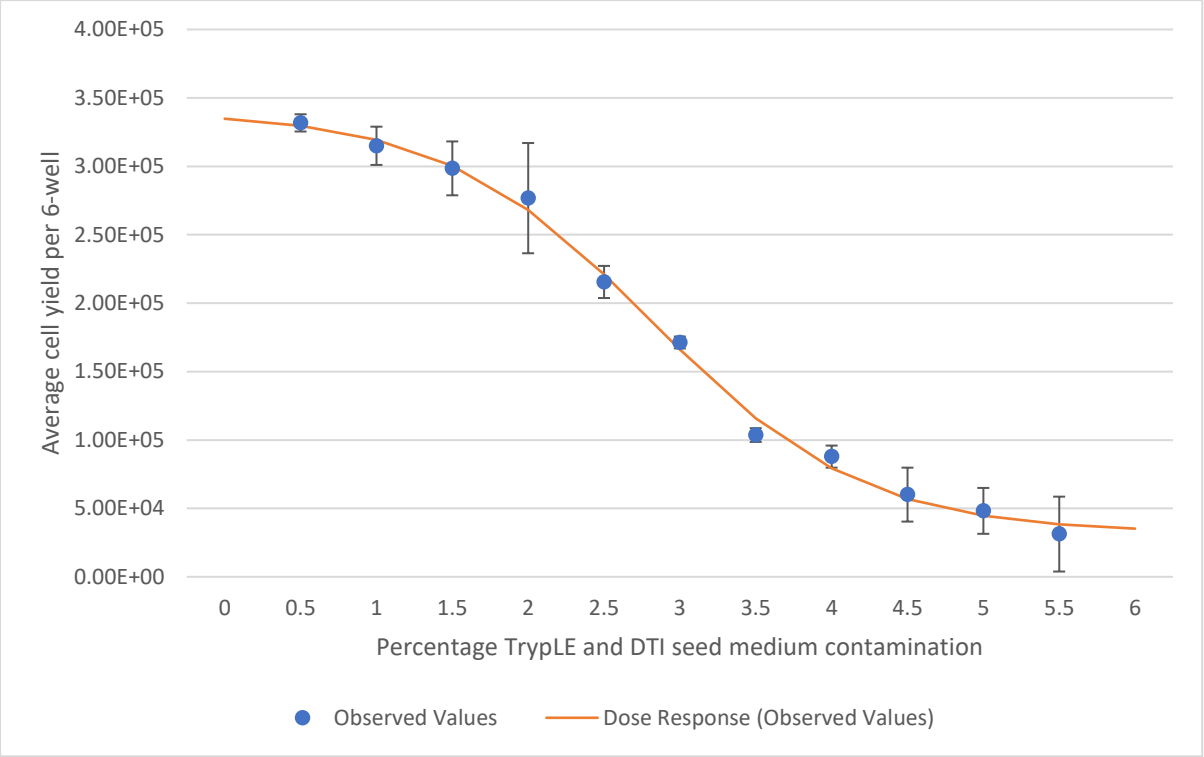

Figure 118 – Dose response curve formed by RC17 response to TrypLE and DTI contamination during seeding of differentiation onto laminin-111. Cell yields after 24 hours are reduced with increasing contamination percentage, with the highest rate of change at approximately 2.8% contamination (1.4% TrypLE and 1.4% DTI). Data shown as mean ± SD for biological repeats, n=2.

Table 16 – Dose response curve data for contamination of RC17 cells with TrypLE and DTI during seeding of differentiation.

Variable	Symbol	Value	Standard Error
bottom asymptote	A1	32208.66018	7832.1608
top asymptote	A2	339845.7358	9539.55534
centre	LOGx0	2.82029	0.06995
hill slope	p	-0.63036	0.06734
abs(A1-A2)	span	307637.0756	14894.77931

6.2.1.2 Characterisation of Contamination During RC17 and H9 Expansion and Differentiation Seeding

During the manufacture of mesDA progenitors, the keys points at which TrypLE and DTI may contaminate seeding is during seeding of the CellSTACK on differentiation days 0 and 11. Because of this, the main characterisation effort focussed on the clinically relevant RC17 cell line and the response of cells entering differentiation on a laminin-111 coated surface. Due to the prevalence of TrypLE and related dissociation enzyme use in adherent cell culture, as well as the popularity of the H9 cell line

across many applications, the characterisation of TrypLE and DTI contamination was expanded to both H9 and RC17 cell lines being seeded into both expansion on laminin-521 and differentiation on laminin-111. An experiment was performed to assess the relative sensitivity to TrypLE and DTI contamination of H9 cells compared to RC17s for both expansion and differentiation.

Pools of H9 and RC17 cells were obtained by harvesting, counting and purifying cells as described in Section 3.2. RC17 and H9 cells were seeded into expansion on laminin-521 and differentiation on laminin-111 using the method described in Sections 3.2.1 and 3.3.1, with contamination values ranging from 0% to 5% TrypLE & DTI in 1% increments.

6.2.1.2.1 RC17 and H9 Response to Contamination during Differentiation Seeding

Both RC17 and H9 cells follow a dose response curve as the concentration of TrypLE and DTI is increased at the point of cell seeding, as shown in Figure 119. Values for the dose response curves are provided in Table 17. RC17 cells are more sensitive to TrypLE and DTI contamination, with the centre of the dose response curve occurring at a contamination percentage of 2.8% compared to a 3.6% in H9 cells. This finding agrees with results previously thought to be contradictory, as Miltenyi reported successful differentiation of H9 cells when seeded in medium containing 2.5% TrypLE and DTI, whereas RC17 seeding was observed to be highly unreliable in medium containing approximately 2.5% TrypLE and DTI.

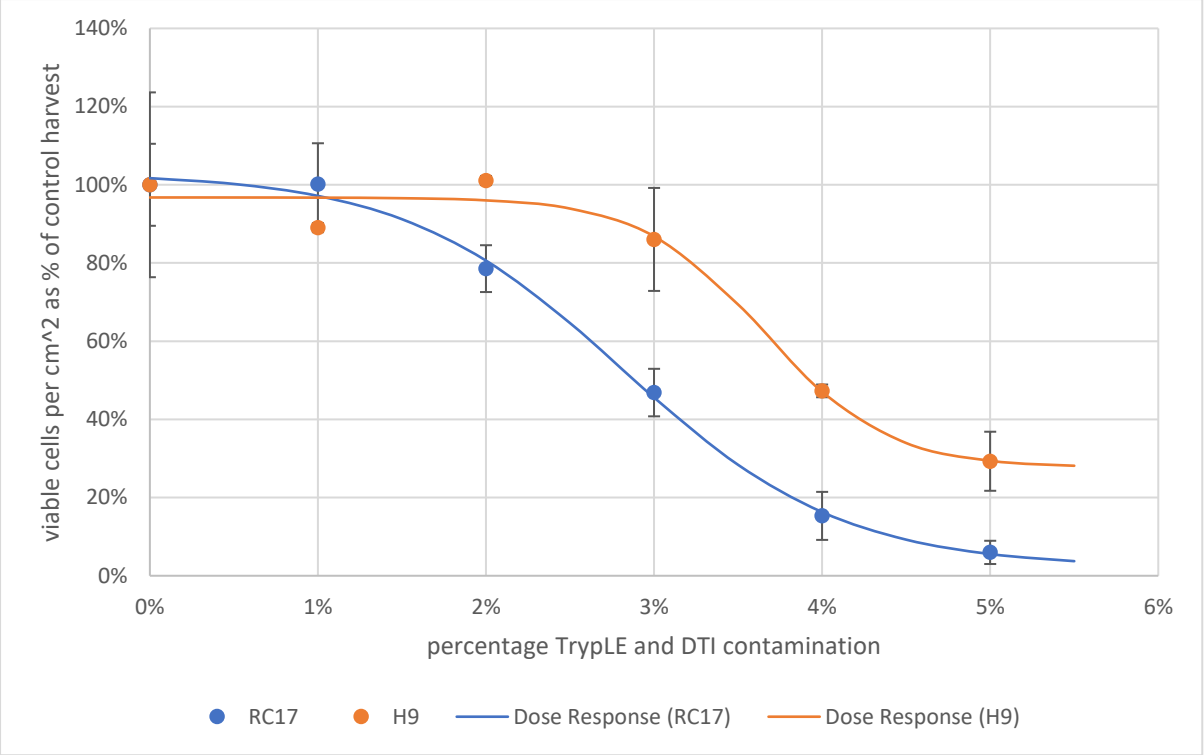

Figure 119 - Viable cell yield 24 hours after seeding RC17 and H9 cells for differentiation onto laminin-111, as a percentage of uncontaminated cell yield. Both cell lines follow a dose response pattern, with RC17s showing higher sensitivity than H9 cells. Data shown as mean ± SD for biological repeats, n=2.

Table 17 - Dose response curve data for contamination of RC17 and H9 cells with TrypLE and DTI during seeding of differentiation onto laminin-111.

Variable	Symbol	RC17		H9	
		Value	Standard Error	Value	Standard Error
bottom asymptote	A1	0.02105	0.04395	0.27689	0.08768
top asymptote	A2	1.03025	0.0327	0.96763	0.04246
centre	LOGx0	0.02818	0.00102	0.03654	0.00218
hill slope	p	-66.53067	10.35657	-118.36974	50.49327
abs(A1-A2)	span	1.0092	0.06429	0.69074	0.1018

As shown in Figure 120, cell morphology shows differences between H9 and RC17 culture in all cases. For the 0% contamination condition, H9 cells form smaller cultures with a higher rate of cell death compared to larger cultures with less cell death for RC17 cells. As discussed in Section 3.5.1, subtle differences in morphology and cell death behaviour is typical in healthy culture of H9 and RC17 cells.

At 1% and 2% contamination conditions, RC17 cells grow increasingly more rounded but maintain a small number of projections reaching into available space surrounding a culture, while H9 cells appear similar to the control condition with minimal colony rounding. For 3% contamination, RC17 cells appear

entirely rounded in large clumps while H9 cells exhibit a small amount of extension into empty space, with a large number of dead cells in single cell suspension. This same pattern is present for 4% and 5% contamination conditions, with RC17 cells forming clumps and H9 cells remaining in single cell suspension.

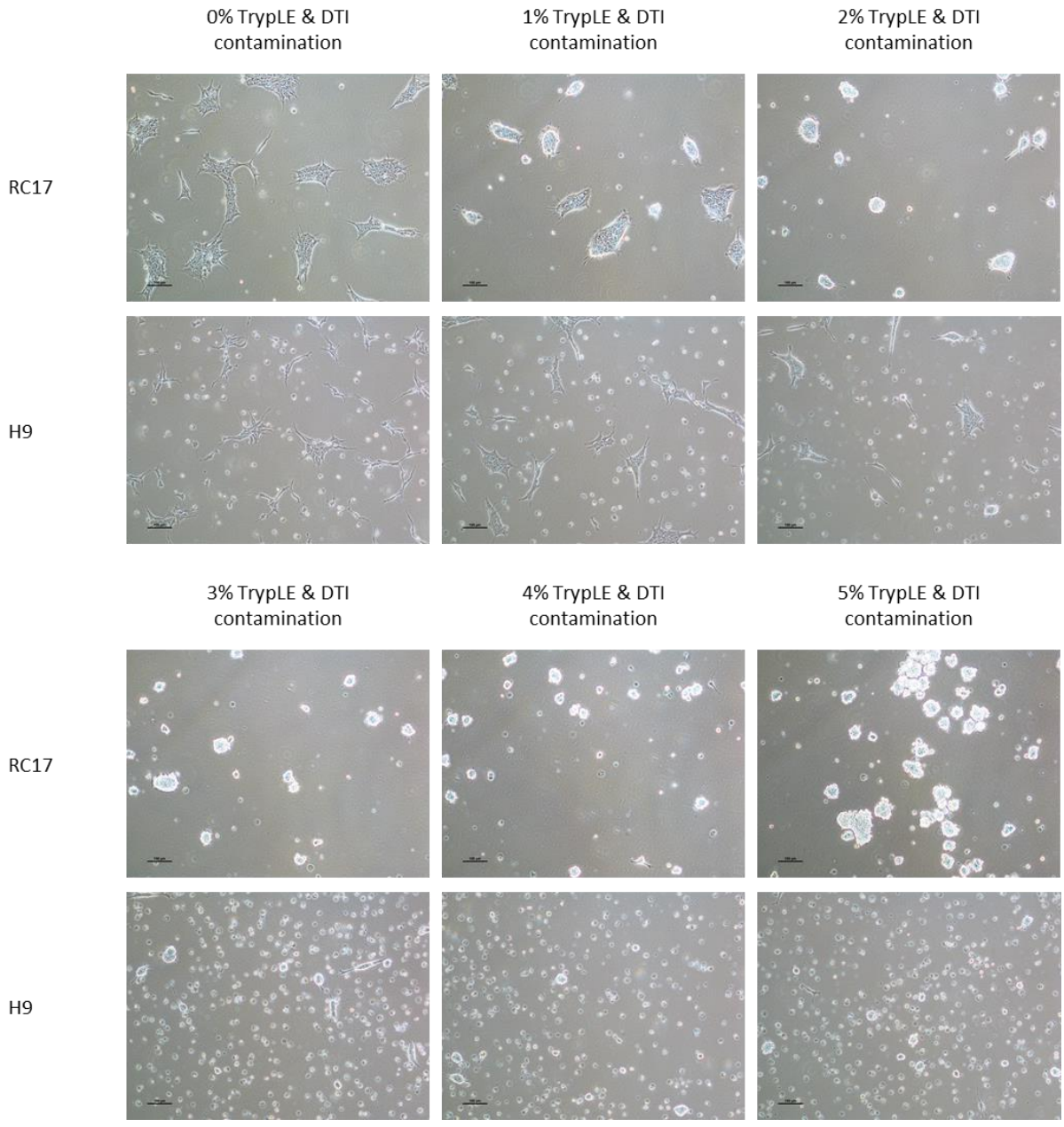

Figure 120 – RC17 and H9 morphology 24 hours after seeding a differentiation onto laminin-111 with various concentrations of TrypLE and DTI contamination. Scale bars for all images are equal to 100 µm.

6.2.1.2.2 RC17 and H9 Response to Contamination during Expansion Seeding

RC17 and H9 cells demonstrate comparable behaviour during expansion on laminin-521, with both cell lines experiencing a gradual decline in viable cells per cm^2 as the percentage of TrypLE and DTI contamination increases, as shown in Figure 121.

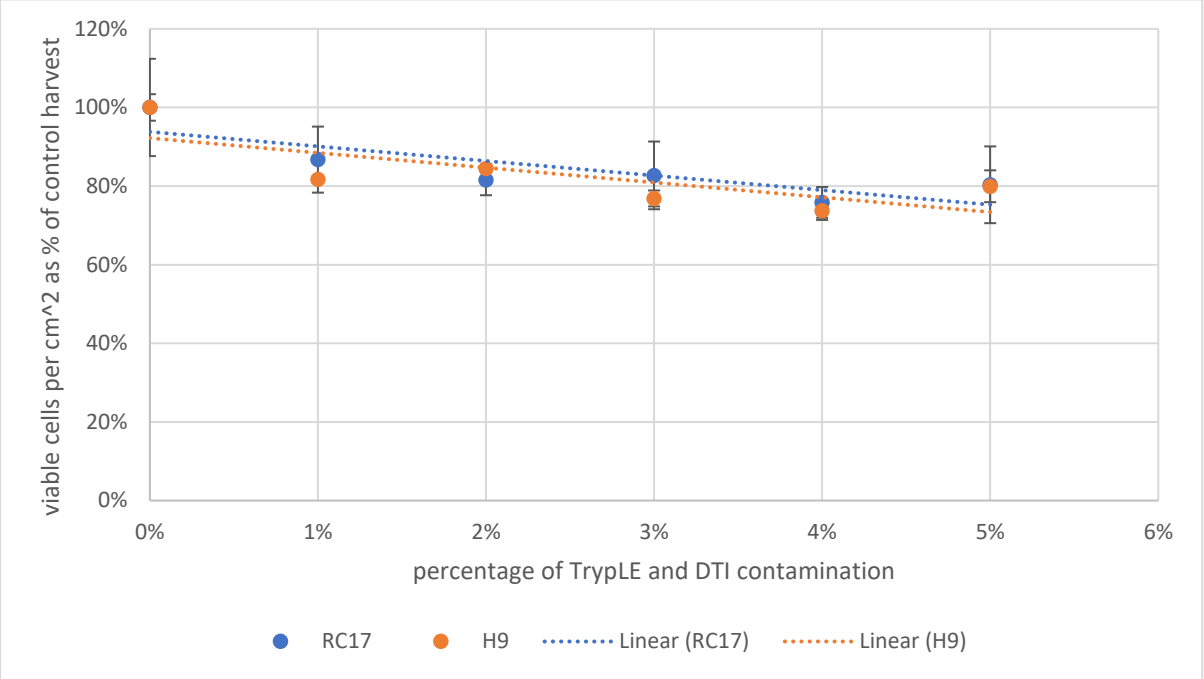

Figure 121 - Viable cell yield per cm^2 24 hours after seeding RC17 and H9 cells for expansion onto laminin-521. Data shown as mean ± SD for biological repeats, n=2.

Cell morphology is similar across various levels of TrypLE and DTI contamination, with more pronounced differences present between the RC17 and H9 cell lines than between 0% and 5% contamination, as shown in Figure 122. RC17s across all conditions form large colonies which reach into surrounding available growth space. The morphology of RC17s is fairly consistent, with a slight increase in colony roundness and decrease in outreaching branches as concentration percentage increases. H9 cells in all contamination conditions form smaller and more spread out colonies, with a higher degree of branching into open culture space. Similarly to RC17s, H9 cells form larger and less spread out colonies with less branching as TrypLE and DTI concentration increases.

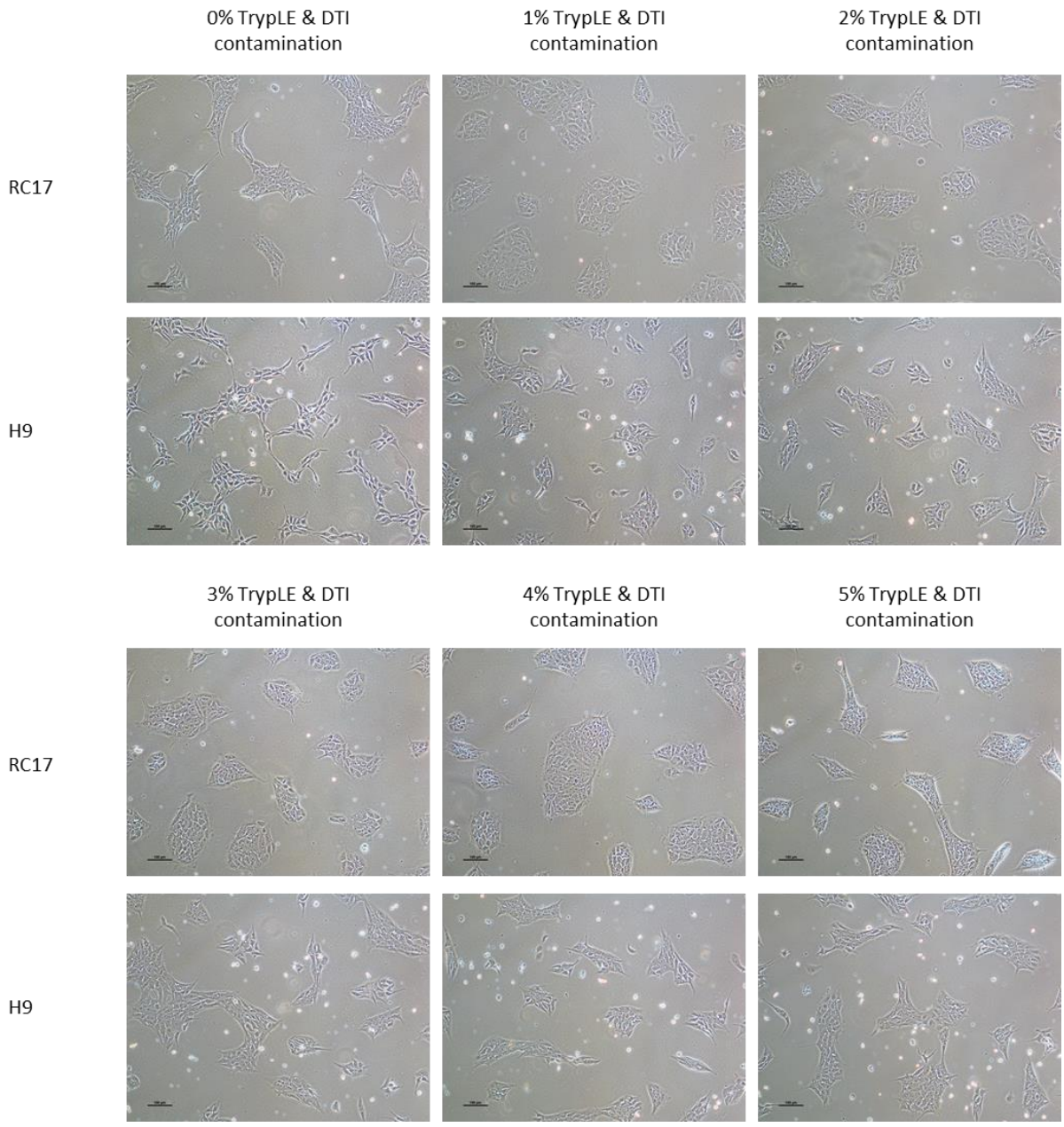

Figure 122 - RC17 and H9 morphology 24 hours after seeding an expansion onto laminin-521 with various concentrations of TrypLE and DTI contamination. Scale bars for all images are equal to 100 µm.

Although TrypLE and DTI seeding contamination levels of 5% and below shows little impact on cell morphology and yields after 24 hours, a contamination level at which cells can no longer attach for effective expansion must exist as contamination approaching 100% is comparable to a standard dissociation process. It may be that the trends shown in Figure 121 represent the upper plateau of a dose response curve which takes effect at higher levels of contamination, or that a reduction in availability of cell medium eventually restricts cell growth. For typical processing with sub-optimal purification, TrypLE and DTI contamination do not pose a significant risk to expansion process seeding.

6.2.2 Cell Yield Response to TrypLE Only, DTI Only, and Combined Contamination

TrypLE and DTI are used in a 1:1 ratio following cell harvest in the closed and automated mesDA manufacturing process, therefore previous experiments have focussed on the behaviour of both elements in concentrations likely to be present during processing on the Prodigy. As TrypLE is a dissociation enzyme, it is likely to be the main contributor to negative effects during cell seeding. It is not known whether the presence of DTI reduces the damaging effects of TrypLE, whether its effect is comparable to an equal volume of seeding medium, or whether DTI in some way contributes to the negative effects observed.

A pool of RC17 cells was prepared by harvesting, counting and purifying cells as detailed in Section 3.2. Cells were resuspended in differentiation day 0 seeding medium as detailed in Section 3.3 and transferred into 4 lots of 9.5 x 10^5 cells in 8 ml of liquid, with tube 1 containing no contamination, tube 2 containing 2.5% contamination made up of TrypLE and DTI in 1:1 ratio, tube 3 containing a 1.25% TrypLE contamination and tube 4 containing a 1.25% DTI contamination. Cells from each tube were then seeded into laminin-111 coated 6-well plates prepared using methods described in Section 3.3 and transferred to an incubator for 24 hours. Wells were then harvested and counted according to the methods described in Section 3.2.

As shown in Figure 123, cells seeded under the control condition with no contamination produced an average yield of 3.54 x 10^4 viable cells per cm^2 24 hours after seeding, while cells seeded with 1.25% DTI contamination producing a comparable average of 3.45 x 10^4 viable cells per cm^2 after the same period. Cells seeded with 2.5% combined contamination (similar to seeding conditions following harvest on the Prodigy) produced an average yield of 2.33 x 10^4 viable cells per cm^2 24 hours after seeding, equivalent to a 34.26% reduction in yield. Cells seeded with 1.25% TrypLE contamination produced an average yield of 1.16 x 10^4 viable cells per cm^2 24 hours after seeding, a reduction of 67.11% compared to the uncontaminated condition.

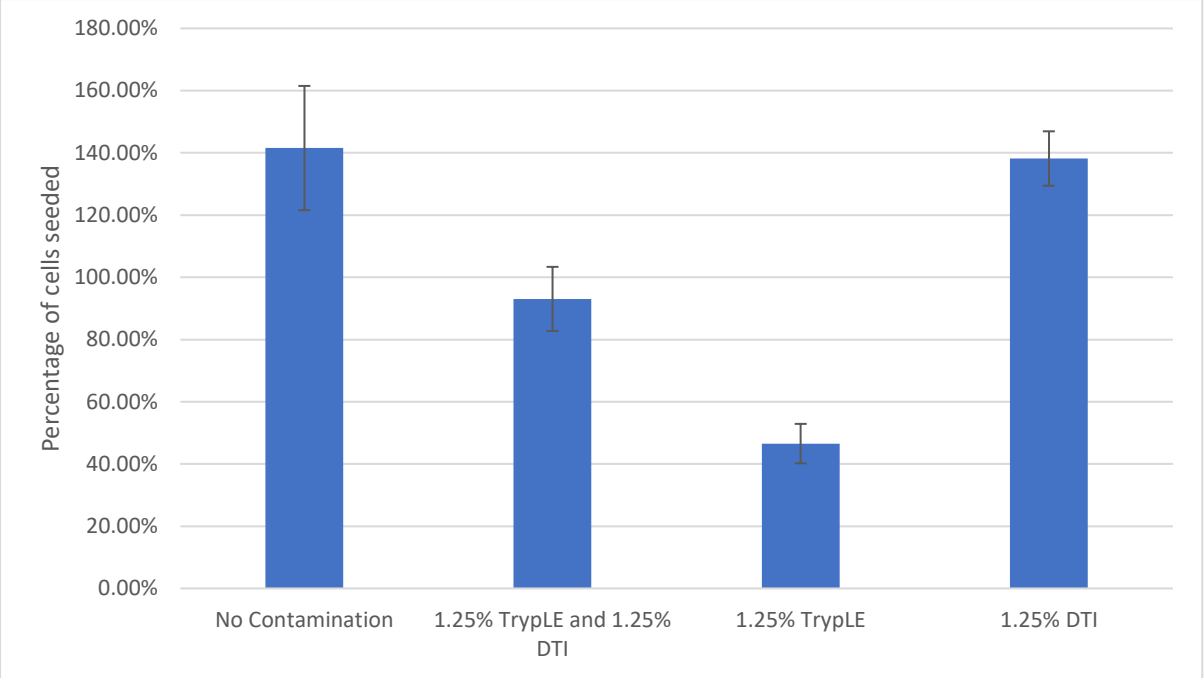

Figure 123 - Cell yield when exposed to contamination of TrypLE only, DTI only, or a combined contamination as seen in a Prodigy harvest process. Data shown as mean ± SD for biological repeats, n=3.

Cell morphology appeared healthy for cells seeded with no contamination and with 1.25% DTI contamination, with cells forming colonies and showing good attachment and projection as shown in Figure 124. Cells seeded under the 2.5% combined contamination condition, as well as under the 1.25% TrypLE only condition exhibited a rounded morphology suggesting poor attachment, with cells forming clumps and detached cells appearing similar to those attached to the laminin-111 coated surface.

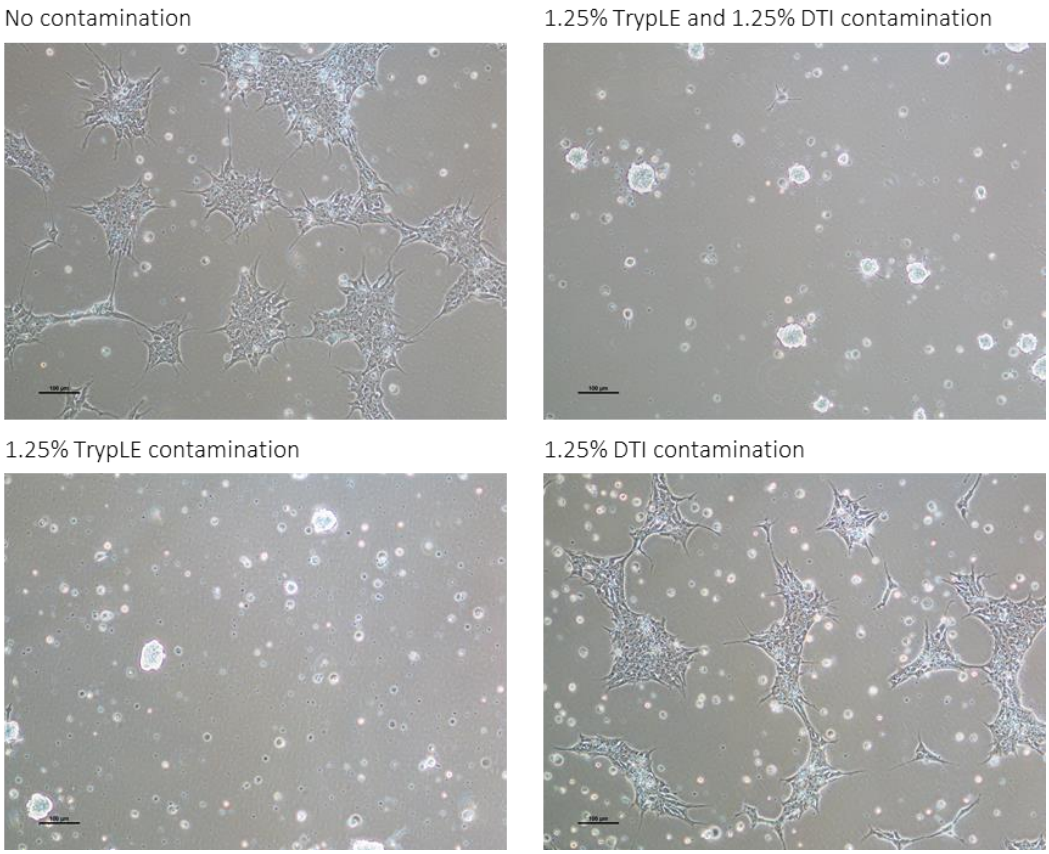

Figure 124 - Microscope images 24 hours after seeding RC17 cells under various contamination conditions. Black bar at lower left of images is representative of 100µm.

RC17 cells seeded with 1.25% DTI exhibited no significant difference in either yield or morphology after 24 hours compared to the uncontaminated condition. Cells seeded with 1.25% TrypLE produced lower cell yields and comparable morphology to than those seeded with 1.25% TrypLE and 1.25% DTI. Taken together, these observations suggest that DTI alone has neutral impact on cell growth, while TrypLE is the cause of negative cell responses to TrypLE and DTI contamination. Furthermore, DTI lessens the negative impacts of TrypLE to a greater extent than does a comparable volume of seeding medium.

6.2.3 Cause of Reduced Yields Due to TrypLE and DTI Contamination

TrypLE and DTI contamination has been shown to impact RC17 and H9 cells when present as a low-level contaminant in seeding medium. The cause of reduced yields may be due to reduced cell attachment at the time of seeding, effectively holding cells in suspension and lowering the attached cell seeding density. A second potential cause of reduced yields may be apoptosis due to continuous exposure to enzymes present in TrypLE, as proteins are continuously broken down until either apoptosis is

triggered, or cell membranes are ruptured leading to necrosis. TrypLE and DTI may also inhibit cell growth, damaging cells enough to prevent proliferation while not significantly promoting causing cell death. An experiment was performed to determine which of these factors is the primary reason for reduced cell yields when TrypLE and DTI are present. Cells were seeded into a differentiation and harvested according to the method described in Section 3.2, with one group maintained for 24 hours and a second for 72 hours prior to harvesting, as shown in Figure 125.

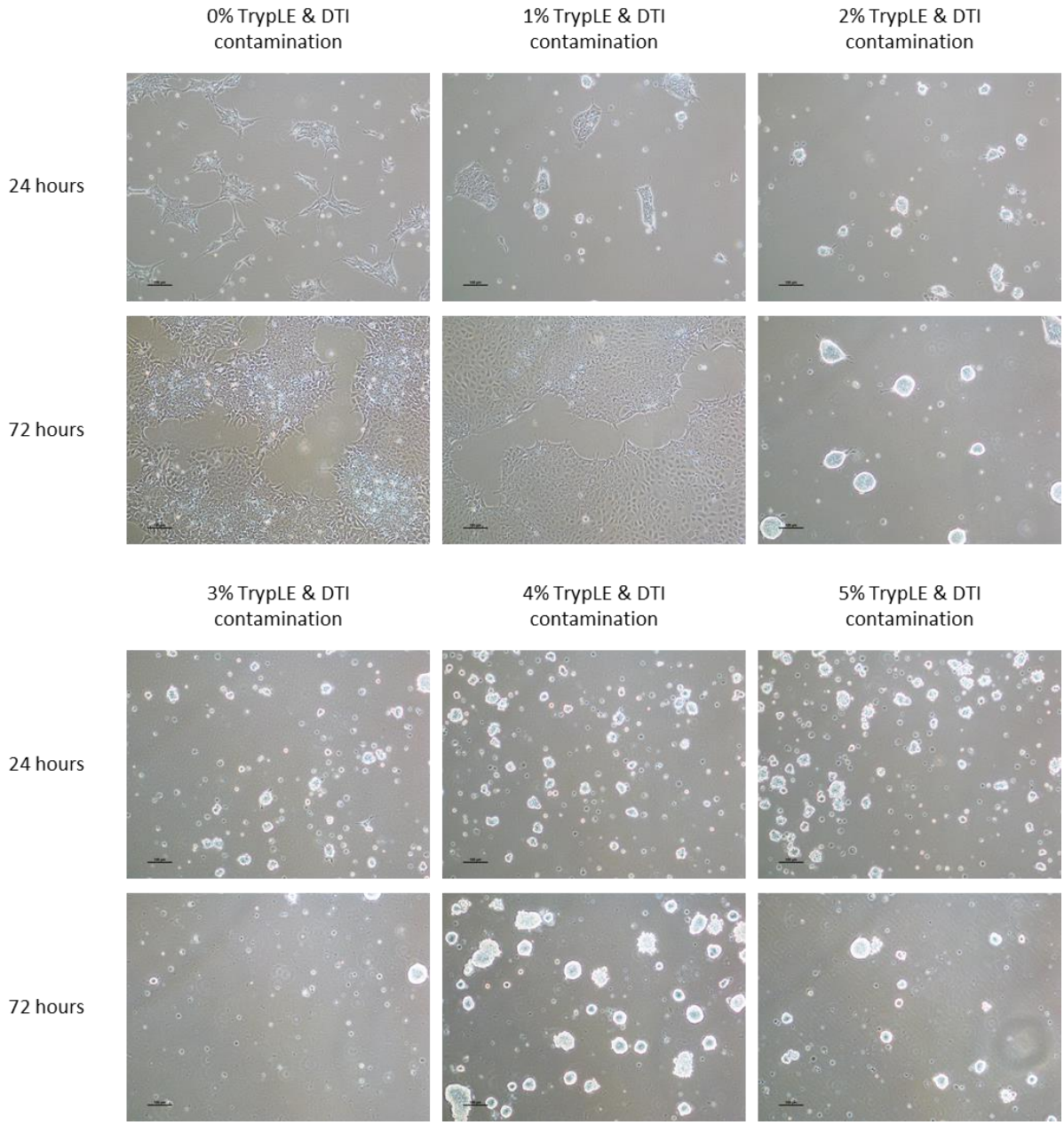

Figure 125 – For 0% contamination, RC17 cells appear flat with arms reaching into nearby space. At 1% contamination, cells appear more rounded with less extension into nearby free space.

6.2.3.1 TrypLE and DTI Impact on Cell Attachment

TrypLE and DTI may have prevented cell attachment to the culture surface, effectively holding cells in suspension and lowering the attached cell seeding density. Ongoing cell detachment was determined by measuring the number of cells present in suspension in feed medium after 24 and 72 hours as a percentage of the number of cells initially seeded, a summary of which is shown in Figure 126. There is a trend towards a higher proportion of detached cells for higher levels of contamination and this effect may be a contributing factor, but the effect is not strong enough to explain the high level of impact to cell yields previously observed.

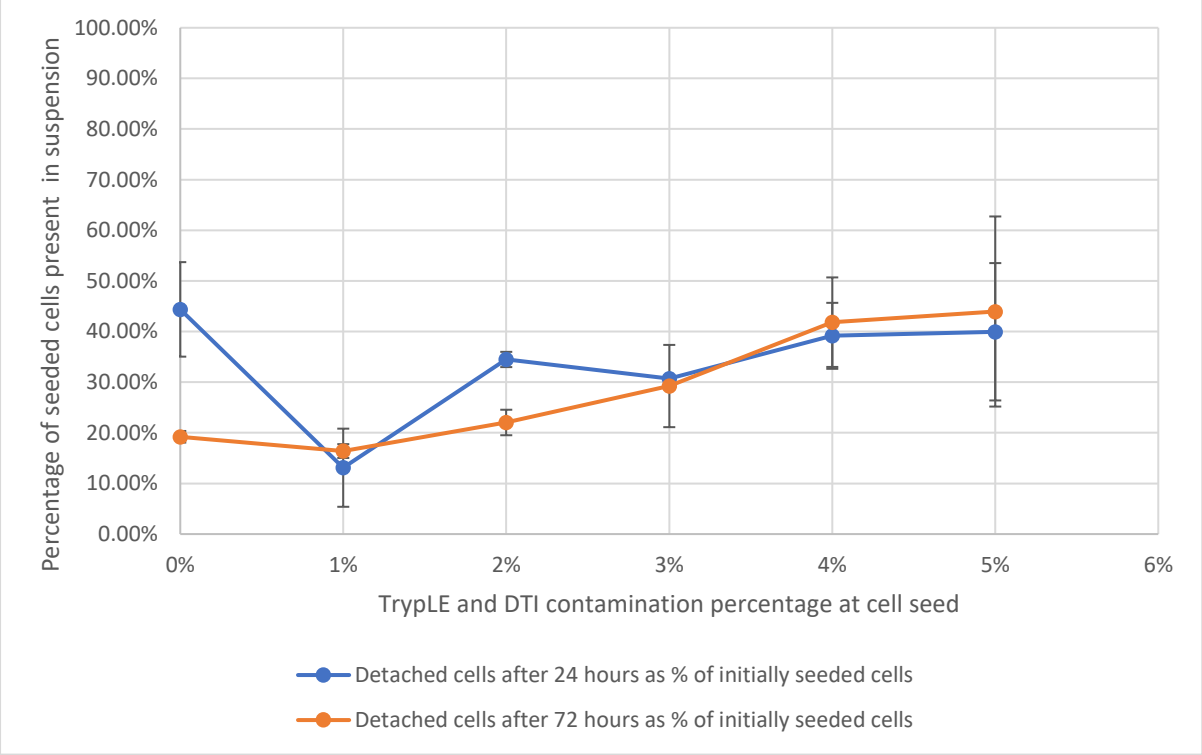

Figure 126 – Total detached RC17 cells after 24 and 72 hours as a percentage of the number of cells initially seeded. Data shown as mean ± SD for biological repeats, n=2. A high number of cells are detached after 24 hours at the 0% contamination baseline. A relatively high number of detached cells compared to attached cells is normal during early differentiation culture as cells adapt to the new conditions, with a high degree of variability in early differentiation culture being typical. The value of 44.4% at the baseline is higher than expected while the value of 13.1% at the 1% contamination for 24 hours, however it is likely that these values align closely with those for the other contamination conditions and 72-hour measurements.

6.2.3.2 TrypLE and DTI Impact on Apoptosis

Continuous exposure to TrypLE and DTI may cause apoptosis, as surface proteins are continuously broken down until cell death and deterioration is triggered. Apoptosis was measured by comparing cells present after 24 hours against cells initially seeded, including both attached cells and those which had detached and were present in suspension. These results are summarised in Figure 127 which shows the total cells present after 24 hours as a percentage of the number initially seeded. 0% and 1% contaminated cases produce approximately 10% increases in total cell number between days 0 and 1. At 2% contamination, approximately 30% of cells seeded are not present in either spent medium and PBS wash (detached) or in attached cell yield (attached) after 24 hours. For cells seeded into 3%, 4% and 5% contamination conditions, approximately 60% of initially seeded cells have been lost, being unaccounted for in either waste liquid or during cell harvest. These results suggest deterioration due to apoptosis is a significant contributor to reduced cell yields during TrypLE and DTI contamination.

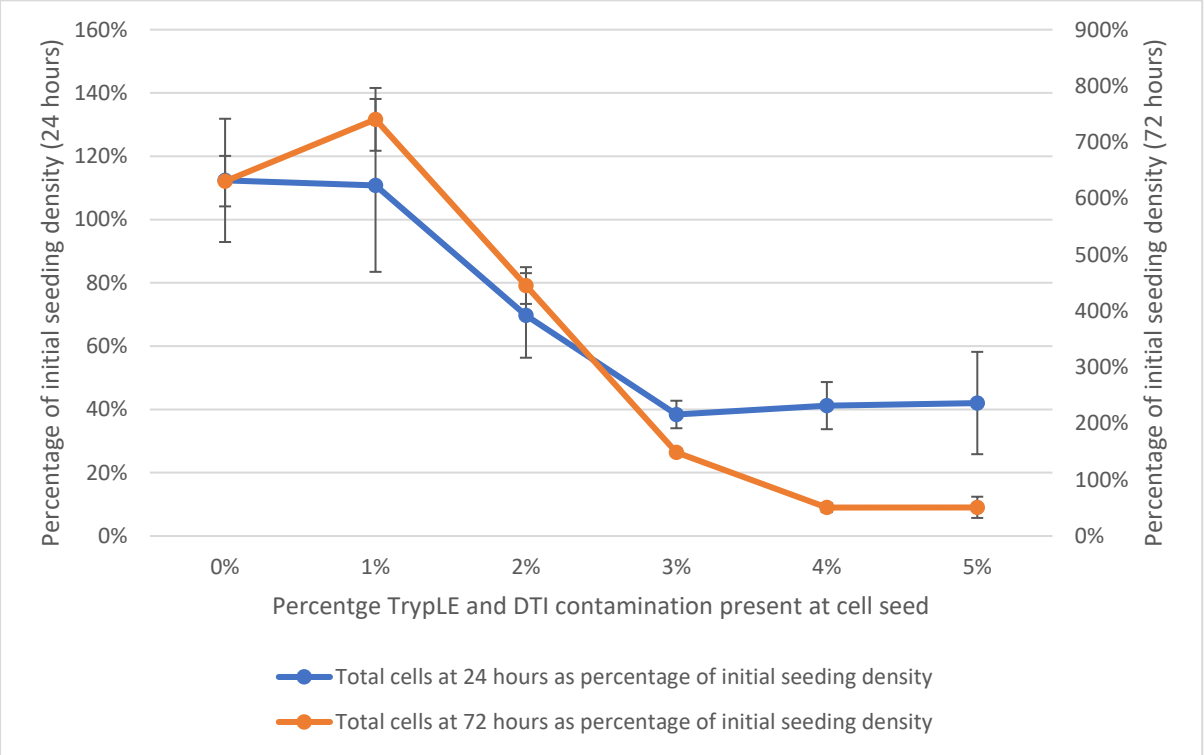

Figure 127 – Total RC17 cells present at 24 hours (left axis) and 72 hours (right axis) as a percentage of the number of cells initially seeded. Data shown as mean ± SD for biological repeats, n=2.

6.2.3.3 TrypLE and DTI Impact on Cell Proliferation

TrypLE and DTI may inhibit cell growth by damaging cells enough to prevent proliferation while not causing cell deterioration. The impact of TrypLE and DTI on prevention of cell proliferation was determined by measuring the specific growth rate of cells, using the functional seeding density determined in Section 6.2.3.1 as the initial cell count for each condition. The functional seeding density was obtained by calculating total cells minus detached cells present at 24 hours, as detached cells may be presumed to be non-proliferative. Specific growth rates were measured between the periods of initial seeding to 24 hours of growth and between 24 hours and 72 hours of growth, with results shown in Figure 128. The specific growth rate of cells between initial seeding and 24 hours of growth follows a dose response pattern, while specific growth rate between 24 and 72 hours of growth show no significant trend. These results suggest that proliferation inhibition is an important factor for reduced cell yield during the initial 24 hours following seeding, but that this effect diminishes after 24 hours. The lack of effect after 24 hours may be due to cell adaption of resistance to the denaturing effects of TrypLE, or the degradation or complete quenching of the TrypLE enzyme after a period of cell culture. The growth rates for low contamination percentages are comparable to normal healthy culture, with 24 hours of negligible change followed by an increased growth rate until approaching confluence.

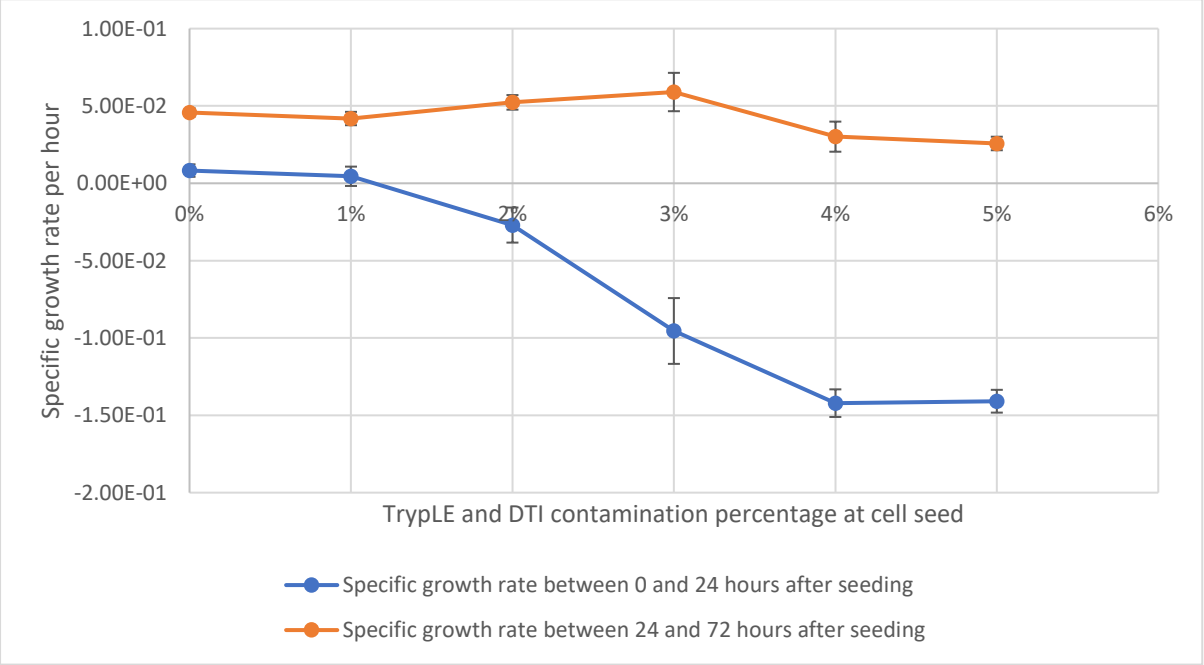

Figure 128 – Specific growth rate per hour of RC17 cells between 0 to 24 and 24 to 72 hours. The starting cell value was taken as seeded cells minus suspended cells after 24 hours (as these cells are unlikely to have contributed to growth), with the values for 24 hours and 72 hours taken as their respective harvest value, excluding suspension cells. Data shown as mean ± SD, n=2.

6.2.3.4 Identification of Root Cause of Reduced Yields

These results suggest that the primary action of TrypLE in reducing cell yields is the reduction of cells proliferative abilities, and the deterioration of cells to the point at which they are no longer detected in cell counts. This is demonstrated in Figure 127 by the loss of cell number compared to the number of cells seeded for high TrypLE and DTI contamination values, as well as in Figure 128 by the reduction in specific growth rate for the first 24 hours for high TrypLE and DTI contamination conditions. It may be that the effects of TrypLE and DTI contamination on preventing cell attachment are low enough to be lost in typical variation during the start of differentiation, or that cells which TrypLE and DTI cause to detach were lost to apoptosis before the first sampling point at 24 hours.

6.3 Definition of Quality Threshold

Following characterisation of cell yield response to contamination during cell seeding, a threshold may be determined for each cell line to indicate the maximum level of contamination for which an acceptable cell yield is achievable. The relationship between the percentage of baseline cell growth and contamination threshold is shown in Figure 129. High quality thresholds indicated by near-baseline levels of cell yields require increasingly reduced contamination percentages.

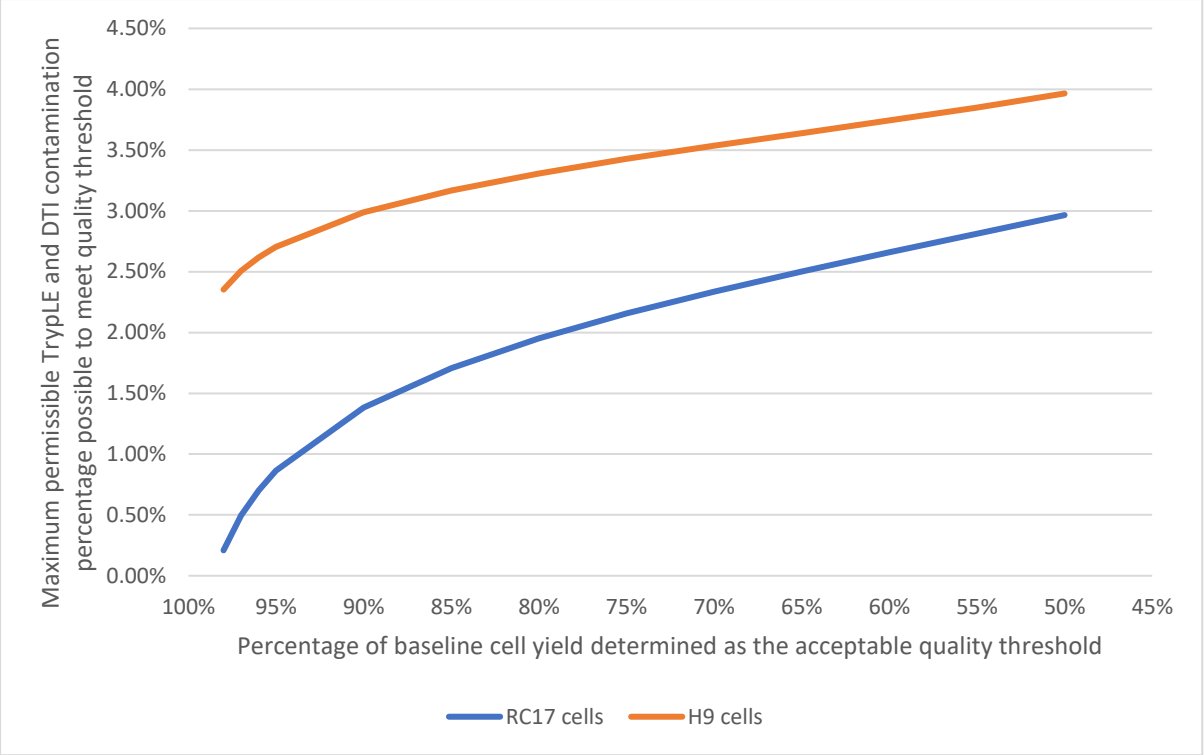

Figure 129 – A quality threshold may be set using the uncontaminated condition as a baseline. For cell yields 24 hours into differentiation to remain within 90% of the uncontaminated condition, the level of TrypLE and DTI contamination must be below 1.38%, for 80% of the uncontaminated condition, contamination must remain below 1.95%, and for 75% of the uncontaminated condition, contamination must be below 2.16% of the seeding volume.

A cell yield of at least 80% of the uncontaminated condition was selected as the minimum threshold to be met for a process to be classified as successful. This value was selected to provide a balance between the process requirements of cell quality and yield, while remaining achievable for the purification system of the Prodigy. It is likely that a higher threshold and stricter purification requirements would be sought as a process improvement measure in a manufacturing environment, as this would allow for a greater degree of process variation while avoiding the steepest region of the dose response curve, translating to a higher degree of process robustness.

Based on these decisions and the dose response curves defined by the data in Table 16 and Table 17, H9 cells require a TrypLE and DTI contamination level of below 3.31%, while RC17 cells require a TrypLE and DTI contamination level of below 1.95%. For the remainder of this chapter, these values will used as the upper thresholds of acceptable contamination percentage for their respective cell type. Process variations calculated to produce contamination percentages higher than these values will be treated as having failed to meet quality standards, while process variations resulting in lower contamination values will be treated as having met this quality criteria.

6.4 Potential Mitigation Strategies for Incomplete Centrifugation

The presence of TrypLE and DTI during RC17 and H9 differentiation seeding has been shown to reduce cell yields and contribute to process failure. Dissociation enzymes are ubiquitous for the harvesting of adherent cells, and TrypLE is used during the closed and automated manufacture of the mesDA progenitor product, as detailed in Section 3.3. Due to the sub-optimal purification provided by the CCU discussed in Section 5.2.3, TrypLE and DTI was calculated to be present at concentrations of approximately 3% to 6% during cell seeding following harvesting on the Prodigy. This section explores possible methods for reducing TrypLE and DTI concentration during cell seeding and defines the practical limits of each process change, as well as weighing the quality benefits against the complexity and increased process costs required for implementation. The Miltenyi 2018 protocol is used as the baseline protocol against which process changes are be compared. As TrypLE and DTI are used in a 1:1 ratio during cell harvest, these reagents are referred to as a single contaminant percentage consisting of equal parts TrypLE and DTI unless otherwise specified. This section concentrates on optimisation efforts for seeding of cells on differentiation day 0, however optimisation efforts also directly apply to seeding of cells on day 11, as the cell harvest, purification and seeding processes are common.

Operator controllable variables for the automated dissociation process on the Prodigy consist of: TrypLE volume for dissociation, DTI volume for quenching, wash medium for transferring cells into the output bag, cell seeding volume, and cell feed volume. A flow diagram of the dissociation, centrifugation and seeding steps performed by the Prodigy is shown in Figure 130 and highlights the points at which user selectable values contribute to the overall process.

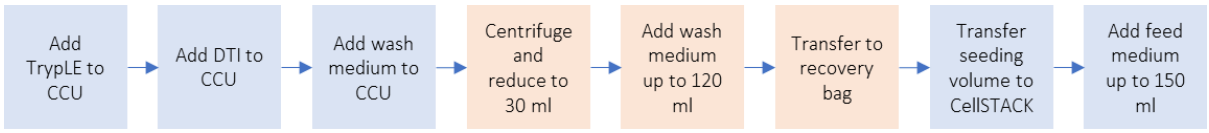

Figure 130 – Dissociation, centrifugation and seeding steps performed by the Prodigy. Steps shown in blue are those which may be varied by the operator and offer the potential for mitigation strategies for TrypLE and DTI contamination. Steps shown in red are fixed and not user configurable.

The variables outlined have complex interactions, with process changes having the potential to add significant cost to the mesDA progenitor manufacturing process. To enable exploration of these options, a tool was developed to calculate the level of TrypLE and DTI contamination during cell seeding for a range of input values, as shown in Table 18.

Table 18 - Tool to simulate the amount of TrypLE and DTI reaching the CellSTACK during cell seeding, allowing values of TrypLE, inhibitor, media wash, cell yield (which dictates cell seeding volume) and CellSTACK feed volume to be adjusted. Blue highlighted values are user controllable inputs, while the green box represents the tool output. The table shown uses default input values from the Miltenyi 2018 protocol of 100 ml for dissociation volume, inhibitor volume and wash volume, 150 ml stack feed volume, 8 x 10^7 CCU yield and 2.5 x 10^4 seeding density, producing a TrypLE and DTI contamination percentage of 2.92% during cell seeding.

	Process Step	TrypLE (ml)	DTI (ml)	Seed / Wash Medium (ml)	Total (ml)	TrypLE + DTI (ml)	TrypLE + DTI (%)
1	Drain medium	0	0	0	0	0	0.00%
2	Add TrypLE – user entered "dissociation volume"	100	0	0	100	100	100.00%
3	Wait for 8 minutes	100	0	0	100	100	100.00%
4	Add DTI – user entered "stop-solution volume"	100	100	0	200	200	100.00%
5	Add wash medium – user entered "wash volume"	100	100	100	300	200	66.67%
6	Centrifuge	100	100	100	300	200	66.67%
7	Reduce to 30 ml	10.00	10.00	10.00	30	20.00	66.67%
8	Add seed medium to make up to 120 ml CCU volume – calculated value	10.00	10.00	100.00	120	20.00	16.67%
9	Move to harvest bag – bag volume set to 110 ml (+/- 5 ml)	9.17	9.17	91.67	110	18.33	16.67%
10	Perform count - 10 ml sample extracted	8.33	8.33	83.33	100	16.67	16.67%
11	Seed stack	2.19	2.19	21.86	26.24	4.37	16.67%
12	Add medium to make up to 150 ml	2.19	2.19	145.63	150.00	4.37	2.92%

The yield of pluripotent cells obtained from the CCU dictates the volume of cells to be seeded into a CellSTACK, and therefore influences the level of TrypLE and DTI contamination present during cell seeding. When seeded in an expansion at a density of 1 x 10^4 and maintained for 5 days as detailed in Section 3.2, RC17s typically achieve a CCU yield of 8 x 10^7 while H9s typically achieve a CCU yield of approximately 4 x 10^7 cells per cm^2 under the same seeding conditions. As RC17s are intended as the source material for CTP this process intends to create, the cell density typically achieved with RC17s will be used as the reference CCU yield value from which cell seeding volume is calculated for this section, however the cost implications for both cell lines will be discussed.

6.4.1 Reduced TrypLE and DTI Volume

The first configurable process step capable of influencing TrypLE and DTI contamination during cell seeding is the volume of TrypLE added as the dissociation agent to detach cells from the CCU surface during cell harvest. The Miltenyi 2018 protocol uses 100 ml of TrypLE in a CCU with 100 cm^2 of culture area. This volume of dissociation reagent is higher than the 0.067 ml per cm^2 recommended in manufacturer guidance at 1 ml per cm^2 and may therefore provide scope for reduction. A higher TrypLE volume is required to guarantee full surface coverage within the CCU than is typically used for manual flasks, as the manual technique of tilting to ensure coverage is not possible on the Prodigy. Based on experience from previous process attempts, a volume of at least 25 ml will achieve reliable coverage of the CCU surface and will therefore be treated as the minimum allowable value.

DTI is added following the dissociation period and acts to prevent further dissociation enzyme action. The Miltenyi 2018 protocol uses 100 ml to quench the CCU harvest, a ratio of 1:1 with the volume TrypLE added. The volume of TrypLE and DTI shall be kept equal for all mitigation strategies in accordance with manufacturer guidance. DTI may therefore be reduced in parity with TrypLE volume, reducing to 25ml in cases where 25 ml of TrypLE is used. Using the tool shown in Table 18, the level of TrypLE and DTI contamination at the point of cell seeding was calculated for TrypLE and DTI input volumes from 100 ml to 25 ml, with results shown in Figure 131. For a reduction in TrypLE and DTI volume from 100 ml to 25 ml, a typical RC17 process will see a reduction in contamination from 2.92% to 1.46% and a typical H9 process will see a reduction from 5.83% to 2.92%.

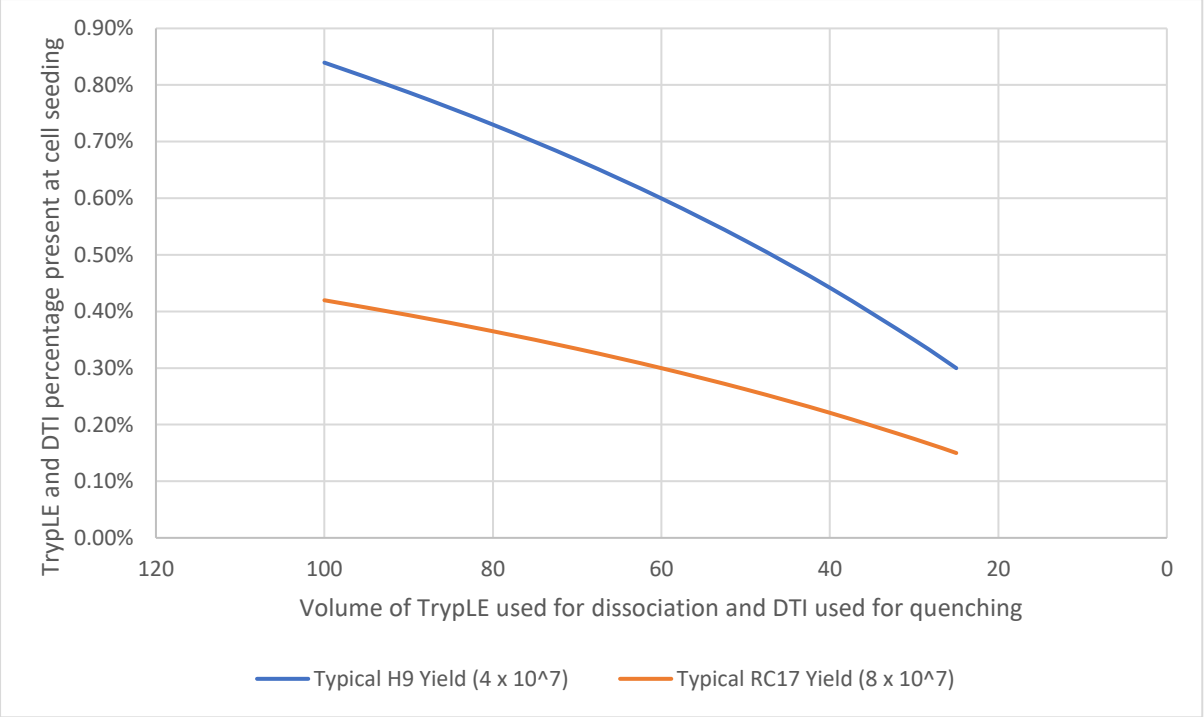

Figure 131 – Contamination response to a reduction in the volume of TrypLE and DTI added during cell dissociation and quench steps as calculated using the tool shown in Table 18. Larger reductions in contamination level occur for higher initial contamination concentrations.

6.4.2 Reduced Cell Seeding Volume *via* Reduced Seeding Density

The volume of cell suspension required to seed the CellSTACK at differentiation day 0 is dependent upon the yield obtained from the CCU during expansion, as well as the cell seeding density defined by the differentiation process. As the TrypLE and DTI contaminant are contained within the cell seeding volume, higher seeding volumes transferred to the CellSTACK translate to higher levels of contamination during cell seeding. The maximum cell suspension volume available for seeding is 100 ml. The worst-case contamination scenario is one in which all available cell suspension is required for cell seeding, with all contaminant therefore transferred to the CellSTACK during seeding and resulting in a contamination percentage of 11.11%.

Seeding volume cannot be manually selected for a given seeding density, however, protocols may be adjusted to reduce the required seeding density and to therefore reduce the seeding and contaminant volumes transferred into the CellSTACK during seeding. An experiment was performed to determine the lower threshold of acceptable seeding density for RC17 cells. Cells were seeded into pluripotent expansion and differentiation day 0 of the Miltenyi 2018 method as described in Sections 3.2 and 3.3.3. Cells were seeded at densities of between 6.25 x 10^2 and 2 x 10^4, then maintained for 48 hours and

harvested and counted using the methods detailed in section 3.2. The specific growth rate for these cells are shown in Figure 132, with higher cell seeding densities correlating with higher specific growth rates after 48 hours, indicating healthier cell culture. Based on these results, a seeding density of 1 x 10^4 as used in the Lund 2017 protocol will be assumed to be the minimum possible seeding density without compromising process quality.

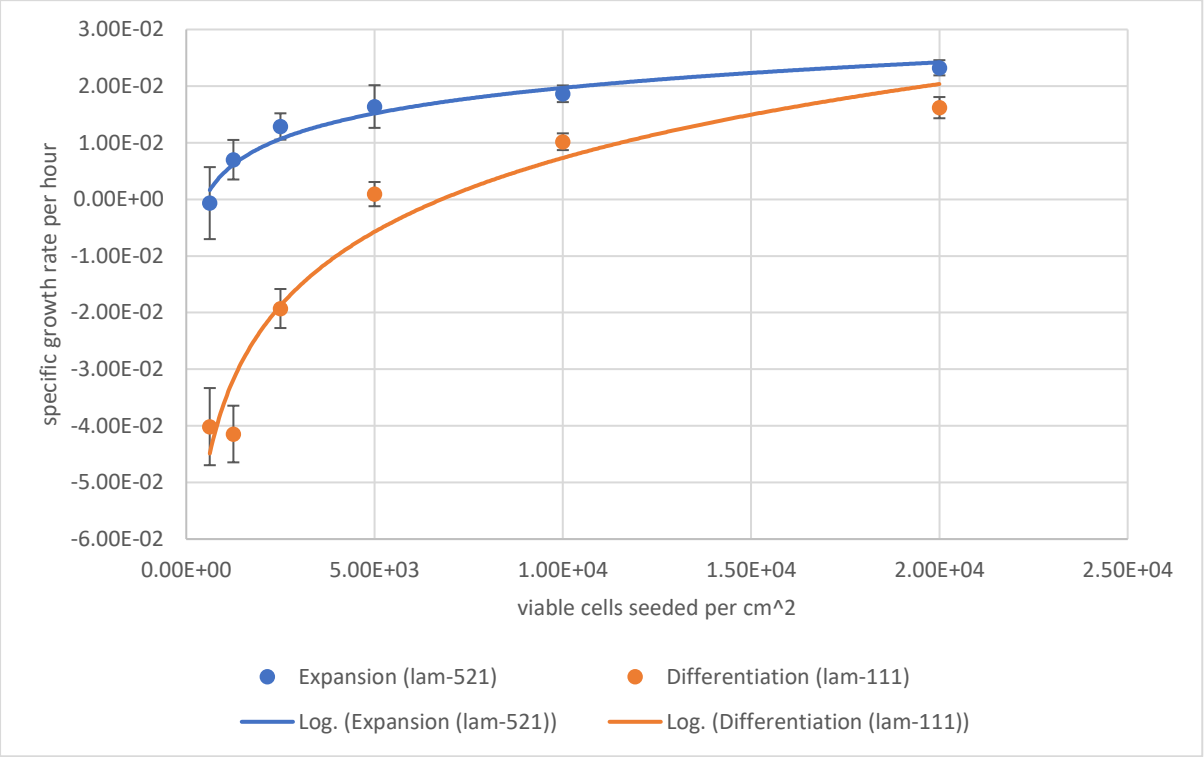

Figure 132 - Specific growth rate per hour 48 hours after seeding RC17 cells at densities ranging from 6.25 x 10^2 to 2 x 10^4 cells per cm^2 as calculated using the tool shown in Table 18. Typical seeding densities used in RC17 culture range from 1 x 10^4 to 2 x 10^4 cells per cm^2. The use of lower seeding densities would allow for less cell seeding volume, reducing TrypLE and DTI contaminant present during cell seeding.

The tool shown in Table 18 was used to calculate the level of TrypLE and DTI contamination at the point of cell seeding for cell seeding densities of between 2.5 x 10^4 cells per cm^2 as specified in the Miltenyi 2018 protocol, and 1 x 10^4 cells per cm^2 as determined to be the minimum safe seeding density and as used in the Lund 2017 protocol. Reductions in cell seeding density have a significant impact on resulting contamination level as shown in Figure 133, with a reduction from 2.5 x 10^4 cells per cm^2 to 1 x 10^4 cells per cm^2 resulting in a change in potential contamination level from 5.83% to 2.33% for a typical H9 process, and from 2.92% to 1.17% for a typical RC17 process.

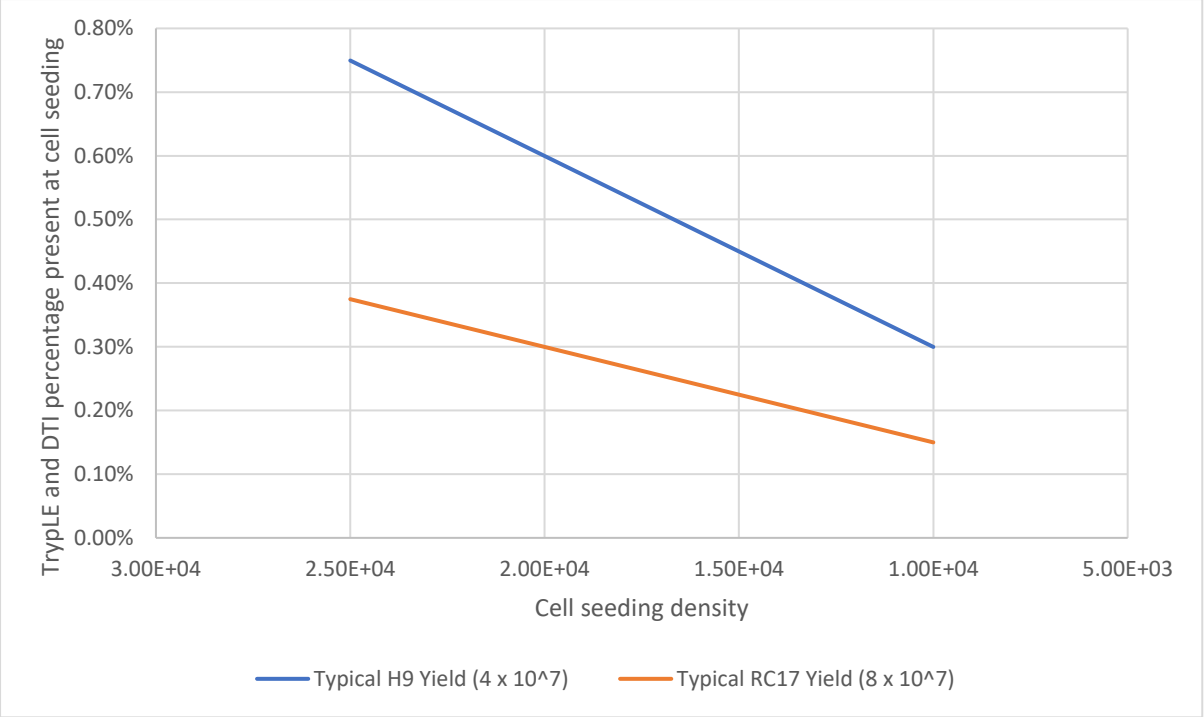

Figure 133 – Contamination response to a reduction in cell seeding density from the 2.5 x 10^4 cells per cm^2 specified in the Miltenyi 2018 protocol to the 1 x 10^4 cells per cm^2 determined to be the minimum safe seeding density and used in the Lund 2017 protocol. Values were calculated using the tool shown in Table 18.

6.4.3 Increased Feed Volume

The feed volume is the volume of medium required to top the CellSTACK up to an appropriate volume for cell maintenance, specified as 150 ml in the Miltenyi 2018 protocol. As the feed volume is configurable in software, it is possible to increase the feed volume and therefore dilute contaminant present in the CellSTACK, reducing its concentration. The feed volume recommended by Corning for a single layer CellSTACK is 130ml to 200ml (Corning, 2011). The Miltenyi 2018 process uses feed volumes of 250 ml during differentiation days 6 and onwards, this value will therefore be considered the true maximum feed volume. The impact of increased feed volume for typical RC17 and H9 yields are shown in Figure 134. Increasing feed volume from 150 ml to 250 ml results in a reduction of TrypLE and DTI concentration during cell seeding from 5.83% to 3.50% for a typical H9 process and from 2.92% to 1.75% for a typical RC17 process.

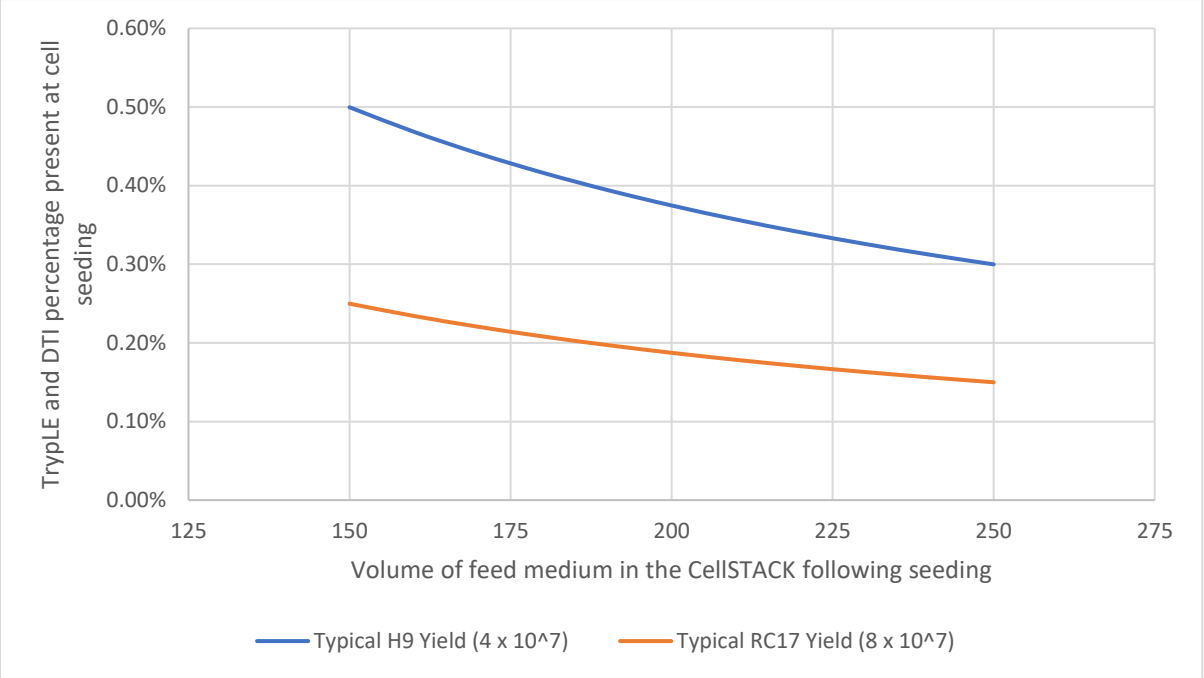

Figure 134 – Contamination response to an increase in feed volume from the 150 ml defined in the Miltenyi 2018 protocol to the maximum value of 250 ml. Feed volumes of beyond 250 ml are possible in multi-layer CellSTACK vessels. Values were calculated using the tool shown in Table 18.

6.4.4 Increased Wash Medium Volume

Wash medium is added to the CCU prior to centrifugation and dilutes cells during purification, lowering the cell density of the liquid contained within the CCU and increasing the concentration factor of the centrifugation. The ratio of wash media to TrypLE and DTI during centrifugation when performed according to the Miltenyi 2018 protocol is 1:2 (100ml wash medium to 100ml TrypLE plus 100ml DTI). Increasing the volume of wash medium added prior to centrifugation increases this ratio, with high ratios translating to higher levels of contaminant removal. The maximum capacity of the CCU during centrifugation is 350ml, therefore the maximum possible wash volume is equal to 350 ml minus the volume of TrypLE and DTI previously added. With no other changes to the Miltenyi 2018 protocol, the maximum wash volume is 150 ml (350 ml CCU capacity minus 100 ml TrypLE and 100 ml DTI) resulting in a ratio of 3:4, however if TrypLE and DTI volume are reduced to 25 ml each, the maximum wash volume rises to 300 ml (350 ml CCU capacity minus 25 ml TrypLE and 25 ml DTI) resulting in a ratio of 6:1. The effects of increased wash medium volume on contamination percentage at the point of cell seeding are shown in Figure 135. Increasing wash volume from 100 ml to a maximum of 300 ml results in a reduction of TrypLE and DTI concentration during cell seeding from 5.83% to 3.50% for a typical H9 process and from 2.92% to 1.75% for a typical RC17 process.

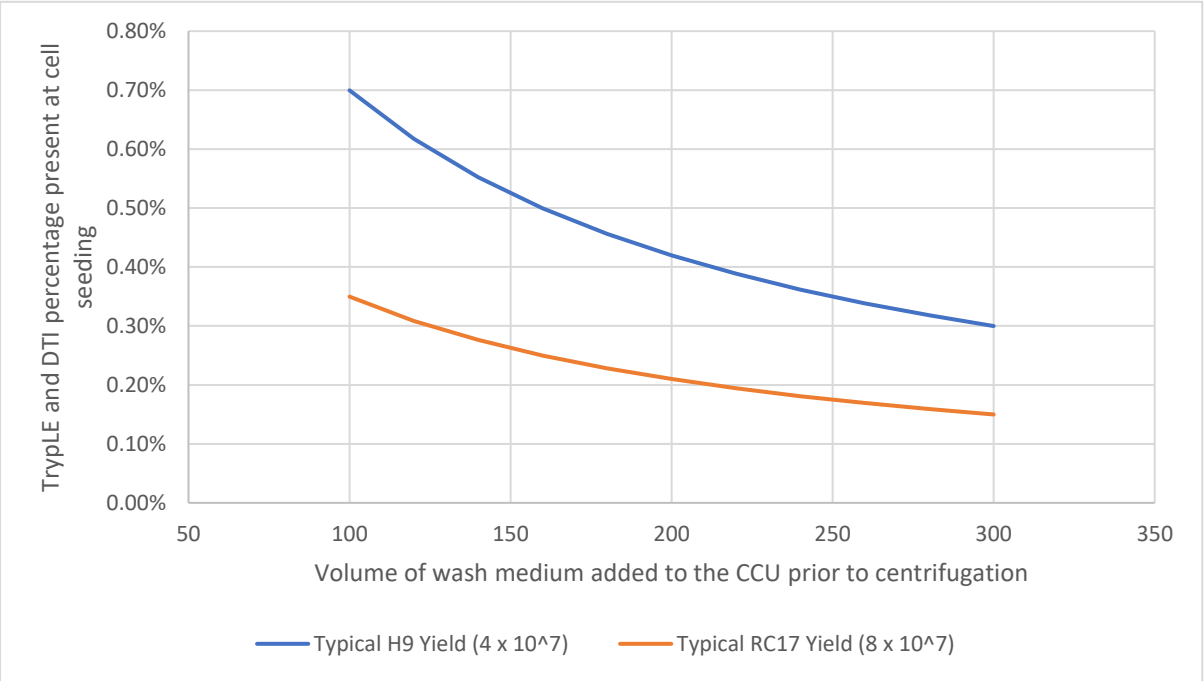

Figure 135 – Contamination response to an increase in wash volume from the value of 100 ml defined in the Miltenyi 2018 protocol to a maximum possible value of 300 ml. Values were calculated using the tool shown in Table 18.

6.4.5 Additional Stages of Centrifugation

Process changes other than changes to cell seeding density and reagent volumes are possible but introduce added complexity through additional equipment or processing steps. A variable not included in the current Prodigy software but possible with software changes is the inclusion of additional centrifugation repeats. This would require the use of additional wash medium for each additional centrifugation, as well as increased processing time and therefore use of operator and cleanroom resources. This option allows purification levels beyond those achievable through volume changes, as centrifugation can theoretically be performed as many times as required if cell losses and damage are managed.

Based on purification data in Section 5.2.5, purification in the CCU is able to achieve a best-case (maximum starting volume of 350 ml and minimum end volume of 30 ml) concentration factor of 11.67, meaning that 8.57% of any contaminant present in the supernatant at the start of centrifugation remains following a single centrifugation run. For open centrifugation using the dead volumes achieved in Section 5.2.2 for 500 ml tubes, a best-case concentration factor of 1304.79 is achievable, equating to 0.077% of any starting contaminant remaining following a single centrifugation run. For the Prodigy

to equal the level of purification achievable using manual open centrifugation, CCU centrifugation would need to be repeated 112 times. In practice, this number of repeats is impractical due to cell degradation and severely extended process times.

The level of purification delivered by open centrifugation is far higher than the minimum threshold required for TrypLE and DTI contamination for this process, with 2 centrifugation runs required to meet the 1.95% contamination threshold defined in Section 6.3. The impact of additional CCU centrifugations for the Miltenyi 2018 protocol are summarised in Figure 136, with resulting costs summarised in Table 19.

Table 19 – Process costs associated with additional centrifugation steps assuming that each additional centrifugation takes 30 minutes of additional operator and cleanroom time.

	H9 Threshold and Typical Yield 4×10^7	RC17 Threshold and Typical Yield 8×10^7
Centrifugation steps required	Two	Two
Additional wash medium required	65.4 ml	58.6 ml
Additional materials costs	£124.91	£111.93
Additional operator costs	£82.5	£82.5
Additional facilities costs	£100	£100
Total process cost increase	£307.41	£294.43

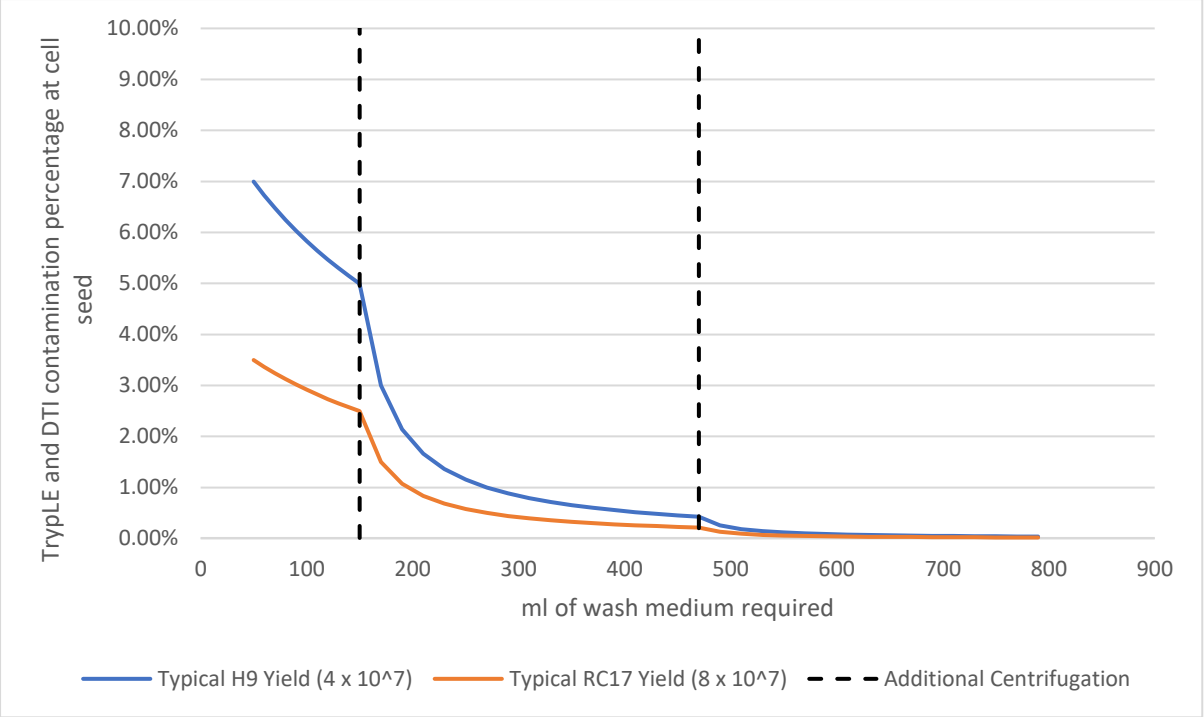

Figure 136 - Contamination response to three additional centrifugation stages. The initial centrifugation stage is represented by the region left of the left black dotted line, the second centrifugations stage is represented by the area between the two black dotted lines, and the third centrifugation is represented by the area to the right of the right-hand dotted line. Values were calculated using the tool shown in Table 18.

Aside from the added costs, cell degradation would occur due to additional time taken during processing steps as well as due to increased physical strain from repeated centrifugation, pellet formation and resuspension. Due to software limitations of the Prodigy, it was not possible to test the extent of cell degradation due to repeated CCU centrifugation.

6.5 Optimisation of Preventative Actions

The variables discussed in the previous section feature complex interactions and hold a high potential for both quality improvement and process cost impact. It is therefore important that the implementation of actions to lower TrypLE and DTI contamination are performed optimally, that is, to achieve the maximum possible level of purification quality with the minimum possible increase in process cost. Process costs were modelled by reducing or increasing reagent values within the process economics model presented in Section 6.1, while process quality improvements were modelled using the TrypLE and DTI calculation tool provided in Section 6.4. A summary of potential process changes and the cost of their implementation per unit of quality improvement is shown in Figure 137.

Reducing TrypLE and DTI volume results in both quality and cost improvements and is therefore displayed as a negative process cost. Seeding density requires no reagent changes and so is cost neutral while being beneficial to quality. Both feed volume increases, wash volume increases, and additional centrifugations have a cost of implementation to achieve quality benefits. Increases to feed volume provide the highest quality return per unit cost spent of these three changes. Additional centrifugation provides a higher quality benefit than increasing wash volume in terms of reduction of TrypLE and DTI contamination percentage during cell seeding, however, additional stages of centrifugation has the potential to introduce additional quality drawbacks. For this reason, additional centrifugation will be treated as the change of least priority, as its relatively small cost impact must be considered alongside the drawbacks of uncharacterised negative quality impacts and additional process complexity.

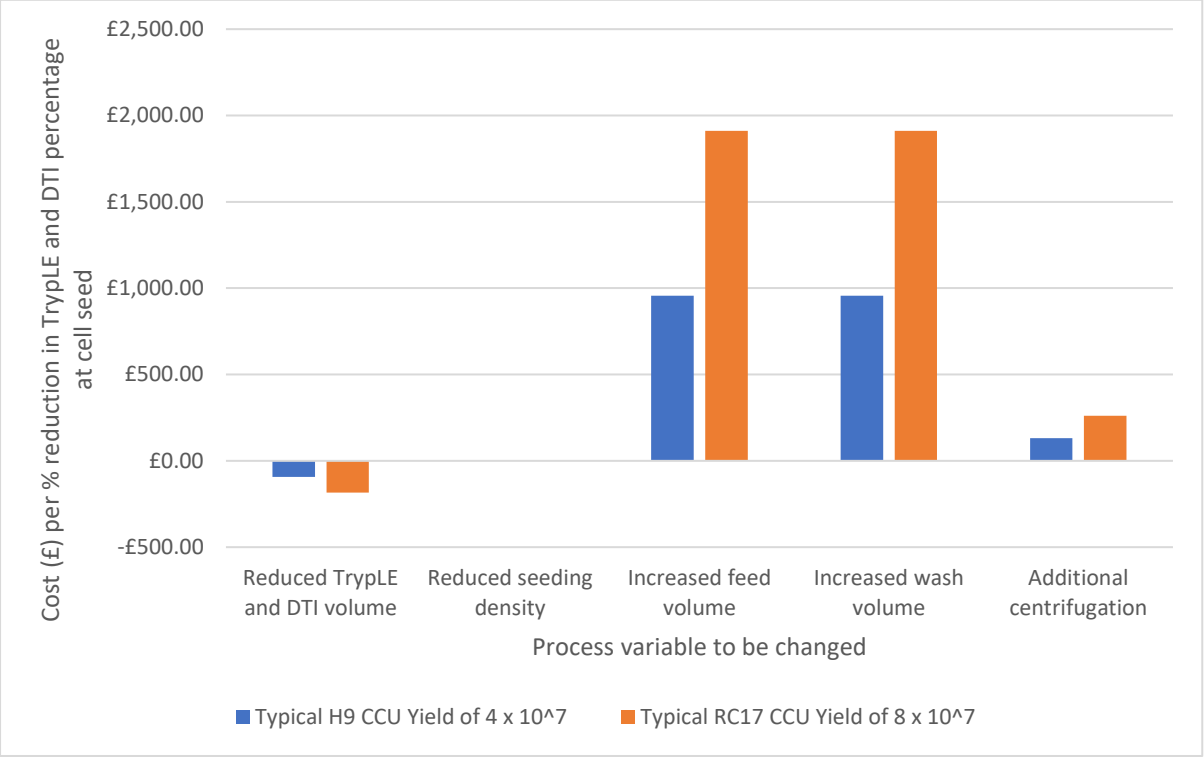

Figure 137 – Process cost increase per percentage of TrypLE and DTI reduction at cell seed. Values were calculated using the optimised volumes calculated in Section 6.4 and cost per ml for reagents given in the process economics model discussed in Section 6.1.

Based on these findings, the optimal order for mitigation strategies is to first reduce TrypLE and DTI from 100 ml to 25 ml each, then to lower seeding density from 2.5 x 10^4 to 1 x 10^4 cells per cm^2, then increase feed volume from 150 ml to 250 ml, then increase wash volume from 100 to 300ml then perform one additional centrifugation.

A new method for graphing process changes was developed and is outlined in Figure 138. The X axis represents process cost, with arrows pointing to the left indicating a cost reduction and arrows pointing right indicating a cost increase. The Y axis indicates the quality measure, in this case TrypLE and DTI contamination percentage, with a downwards arrow indicating an improvement and an upwards arrow indicating a worsening in that quality attribute. The baseline process is represented as the base of an arrow, with a proposed change indicated by the arrow tip. Arrows may be linked to represent multiple process changes chained together to produce greater overall effects.

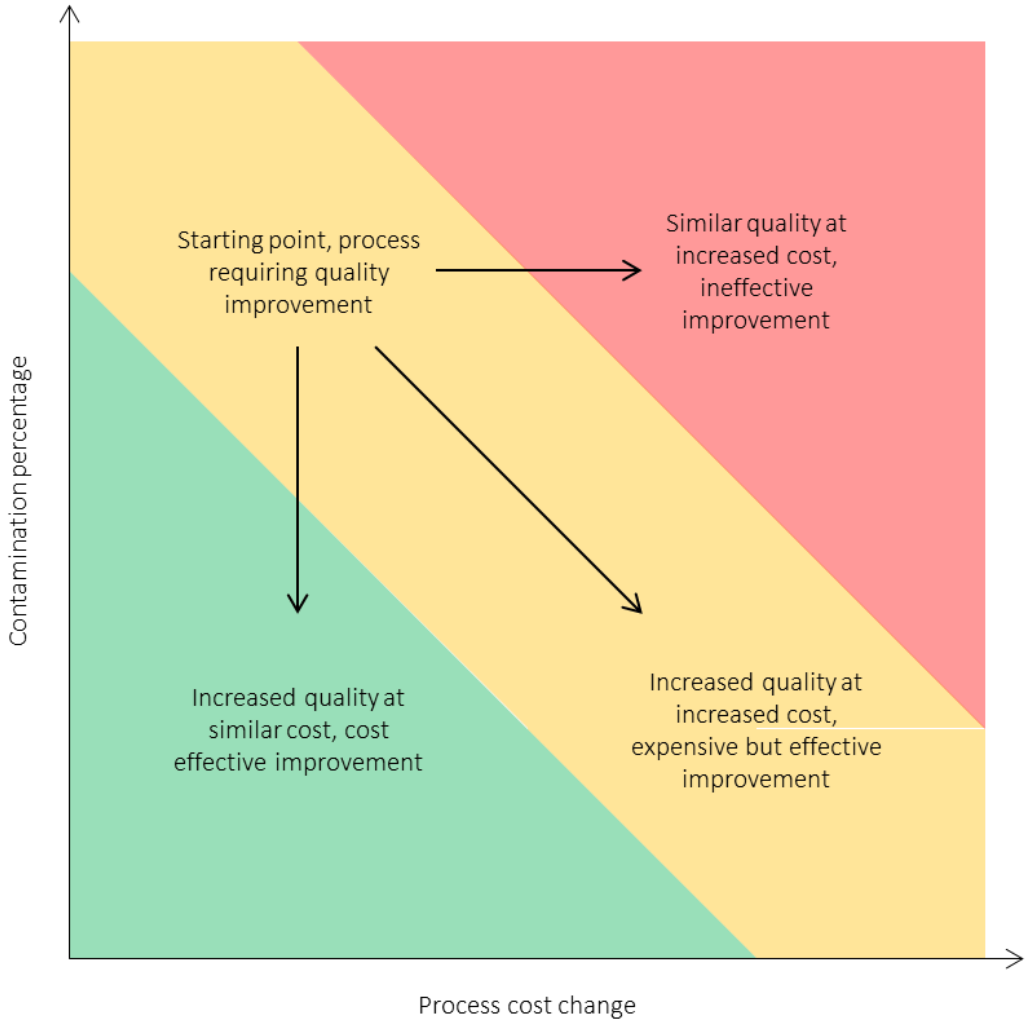

Figure 138 – Summary of process changes and their representation in arrow graphs in this section.

The quality and cost impacts of these process changes for yields seen during a typical RC17 process is modelled in Figure 139. For a Prodigy based Miltenyi 2018 protocol using RC17 cells and achieving an expansion yield of 8 x 10^7 cells from the CCU, only a reduction in TrypLE and DTI volume is required to

meet the RC17 quality threshold of less than 1.95% TrypLE and DTI contamination during cell seeding. The cost of implementing this change is shown at the point at which the quality threshold is crossed which for this process equates to a saving of £29.77 per process run.

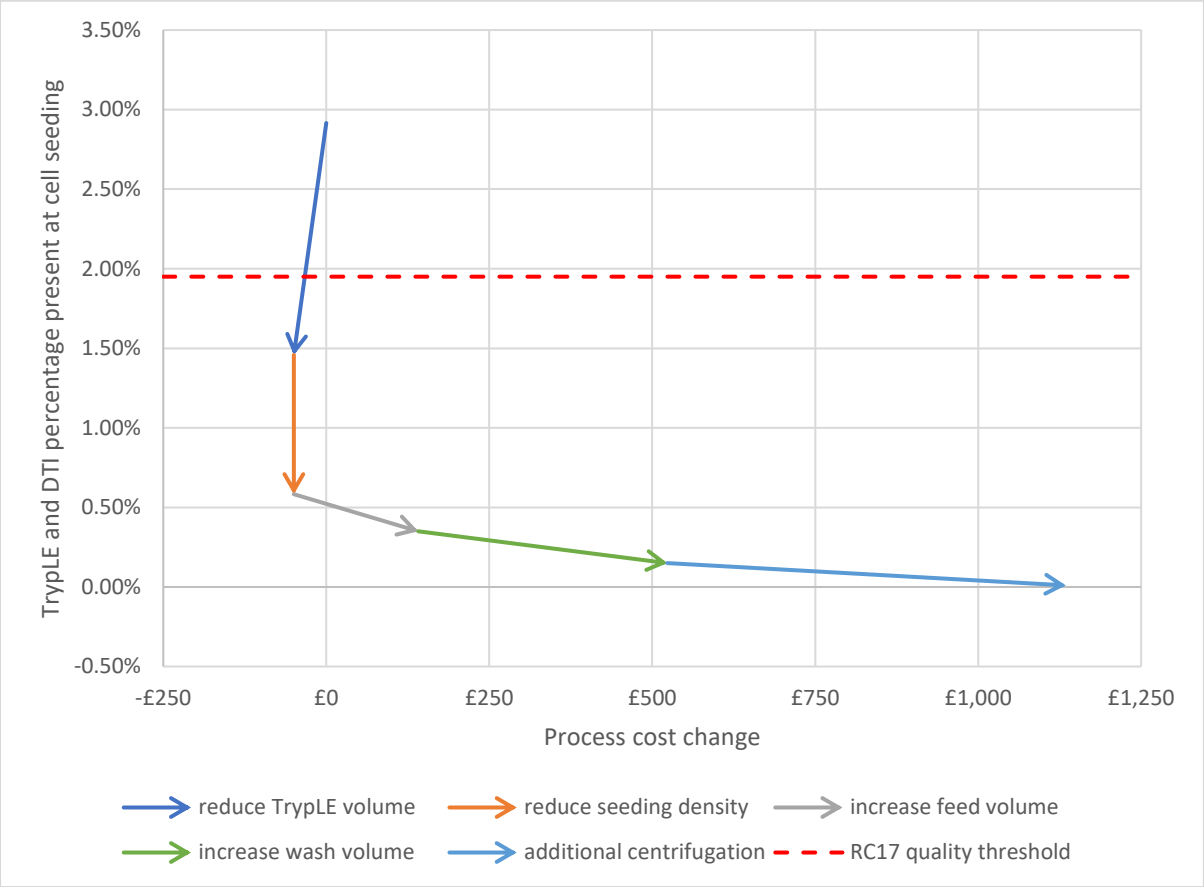

Figure 139 – Cost and quality impact of optimised process changes for a CCU yield of 8 x 10^7, the typical harvest for RC17 cells. Arrows represent shifts in process cost and TrypLE and DTI contamination level during cell seeding as process changes are implemented. The dotted red line represents the RC17 quality threshold defined in Section 6.3 of less than 1.95% TrypLE and DTI contamination percentage during cell seeding. Assuming a typical RC17 CCU yield of 8 x 10^7, only a reduction in TrypLE and DTI volume is required to meet this threshold, shown by the first arrow crossing the dotted red line. This process change results in a cost saving of £29.77. Percentage changes were calculated using the tool provided in Table 18, while costs were calculated using cost per ml values given in the process economics model discussed in Section 6.1.

For a Prodigy based Miltenyi 2018 protocol using H9 cells and assuming a typical yield of 4 x 10^7 cells from the CCU during expansion, only a reduction in TrypLE and DTI volume is required to meet the H9 quality threshold of less than 3.31% TrypLE and DTI contamination during cell seeding. The cost of this change equates to a saving of £43.00 per process run. Further quality improvements for both cell lines may be achieved by progressing down the arrows, improving quality with additional cost as further changes are implemented.

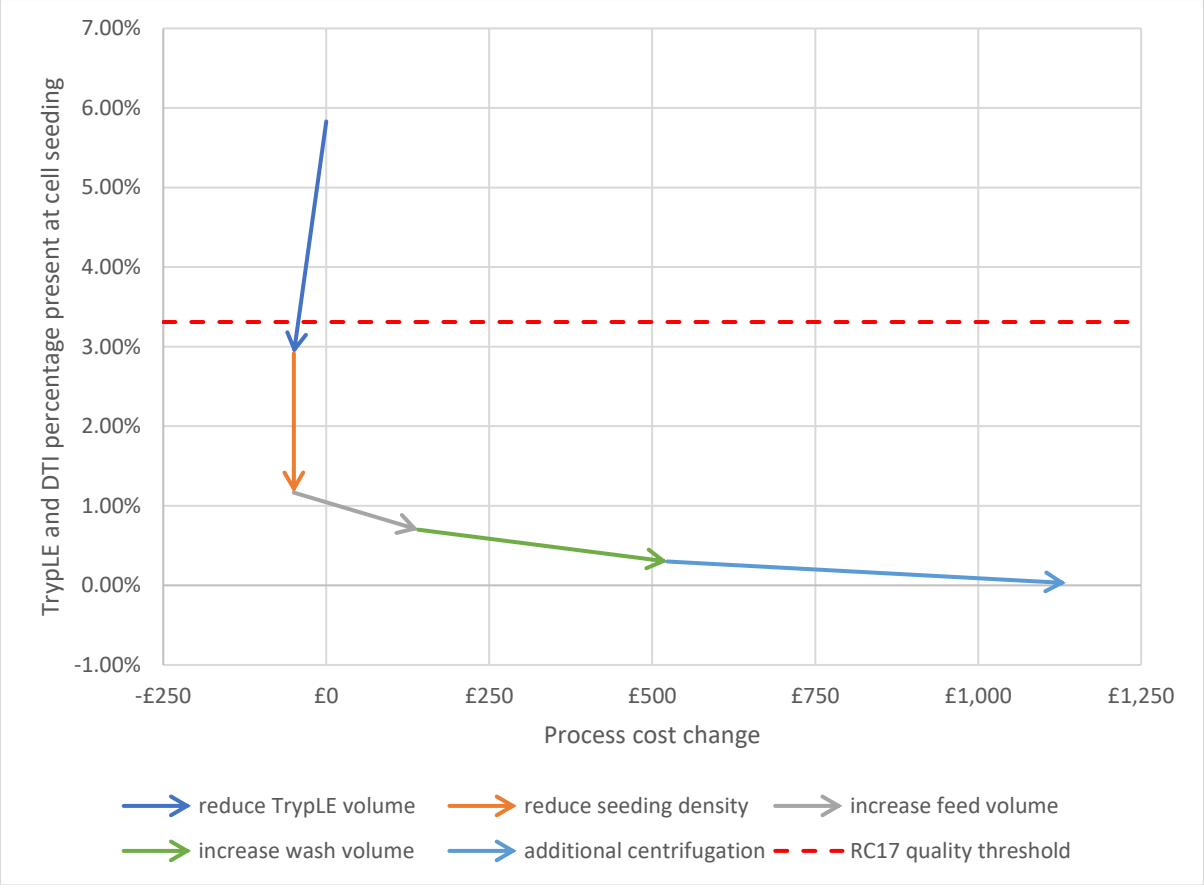

Figure 140 - Cost and quality impact of optimised process changes for a CCU yield of 4 x 10^7, the typical harvest for H9 cells. Arrows represent shifts in process cost and TrypLE and DTI contamination level during cell seeding as process changes are implemented. The dotted red line represents the H9 contamination threshold defined in Section 6.3 of less than 3.31% TrypLE and DTI contamination percentage during cell seeding. To meet this threshold and assuming a typical H9 CCU yield of 4 x 10^7 cells, a reduction in TrypLE and DTI volume is required, represented by the first crossing the dotted line. This process change results in a cost saving of £43.00. Percentage changes were calculated using the tool provided in Table 18, while costs were calculated using cost per ml values given in the process economics model discussed in Section 6.1.

Process change requirements have thus far been calculated for purification of typical H9 and RC17 CCU yields, with both cases requiring only a single process change of reducing TrypLE and DTI volume to meet the quality thresholds defined in Section 6.3. However, a robust process must provide sufficient purification for lower than typical CCU yields so as not to cause process failure under these conditions.

The differentiation process described in the Miltenyi 2018 protocol requires a minimum of 6.36 x 10^6 cells for seeding, assuming 636 cm^2 growth area and use of the lowest reliable seeding density of 1 x 10^4 cells per cm^2 as shown in Section 6.4.2. Due to losses during the purification process, a minimum CCU yield of 8.4 x 10^6 cells is required to produce 6.36 x 10^6 cells for seeding, with a lower CCU yield producing insufficient cells for correct seeding. The value of 8.4 x 10^6 therefore defines a requirement of the differentiation process on the expansion process, for which process changes to minimise TrypLE and DTI contamination have no influence.

The purification process requires additional resources to achieve the defined quality thresholds as CCU yields reduce. A CCU yield of 8.4 x 10^6 cells is the lowest yield for which the process can continue successfully, therefore this is the minimum CCU yield for which purification is required. Any resource used to improve the purification process for CCU yields lower than 8.4 x 10^6 does not add value, as the process will fail regardless of purification outcome due to insufficient cell seeding. Figure 141 shows the process changes required to meet contamination quality thresholds for the lowest allowable CCU yield of 8.4 x 10^6 cells. The thresholds required for purification of both H9 and RC17 cells are shown.

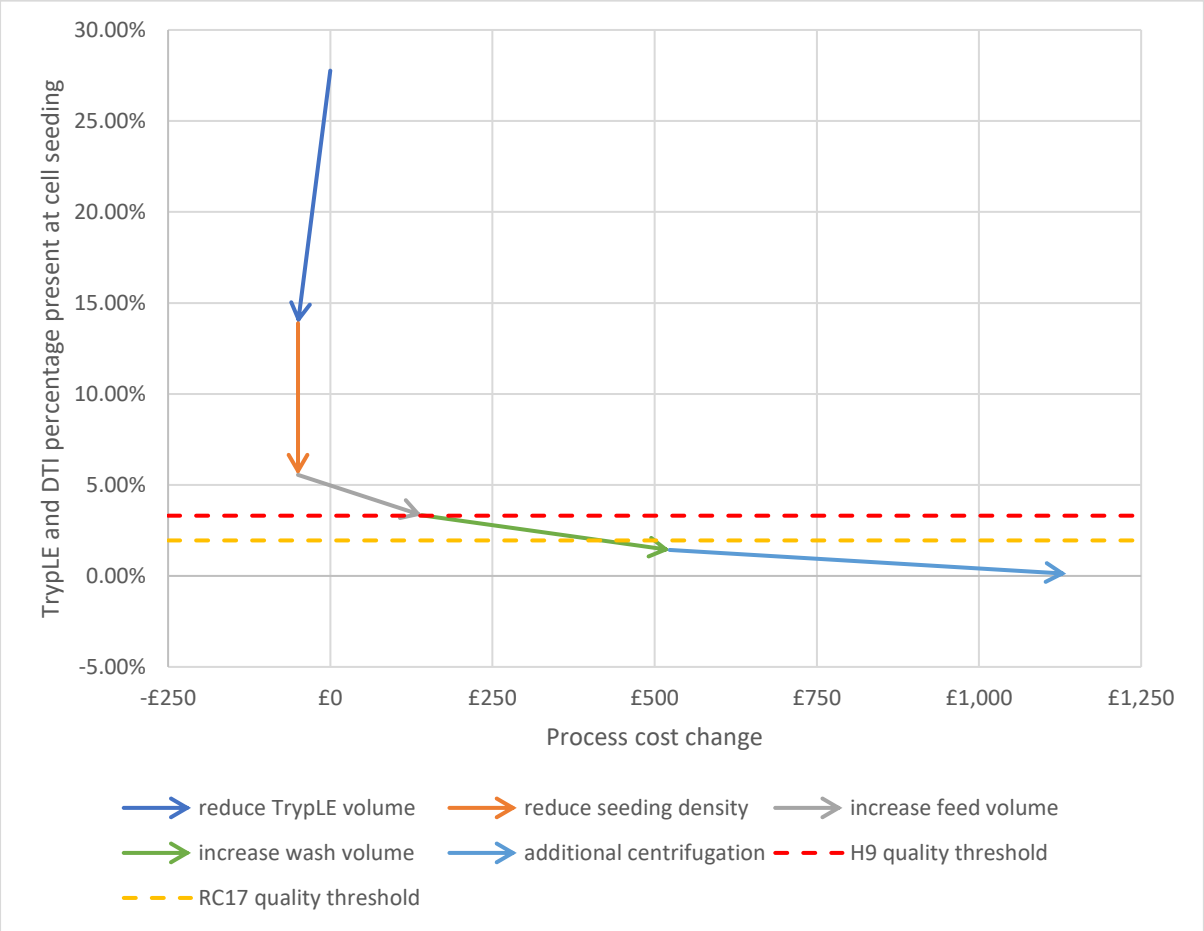

Figure 141 - Cost and quality impact of process changes for a worst case CCU yield of 8.4 x 10^6. Arrows represent shifts in process cost and contamination level during cell seeding as process changes are implemented. The dotted red line represents the H9 contamination threshold of 3.31%, while the dotted yellow line represents the RC17 contamination threshold of 1.95%. Percentage changes were calculated using the tool provided in Table 18, while costs were calculated using cost per ml values given in the process economics model discussed in Section 6.1.

6.5.1 Comparison to Non-Optimal Process Changes

Optimisation of process changes was performed to deliver the quality thresholds defined in Section 6.2 for the lowest possible level of process cost increase to the Miltenyi 2018 protocol. Figure 142 shows most and least optimal process change pathways for a lowest allowable CCU yield of 8.4×10^6. The most optimal process change pathway achieves the highest level of process improvement for the least possible process cost increase, with the least optimal process change pathway representing the least cost-efficient route to process quality improvement.

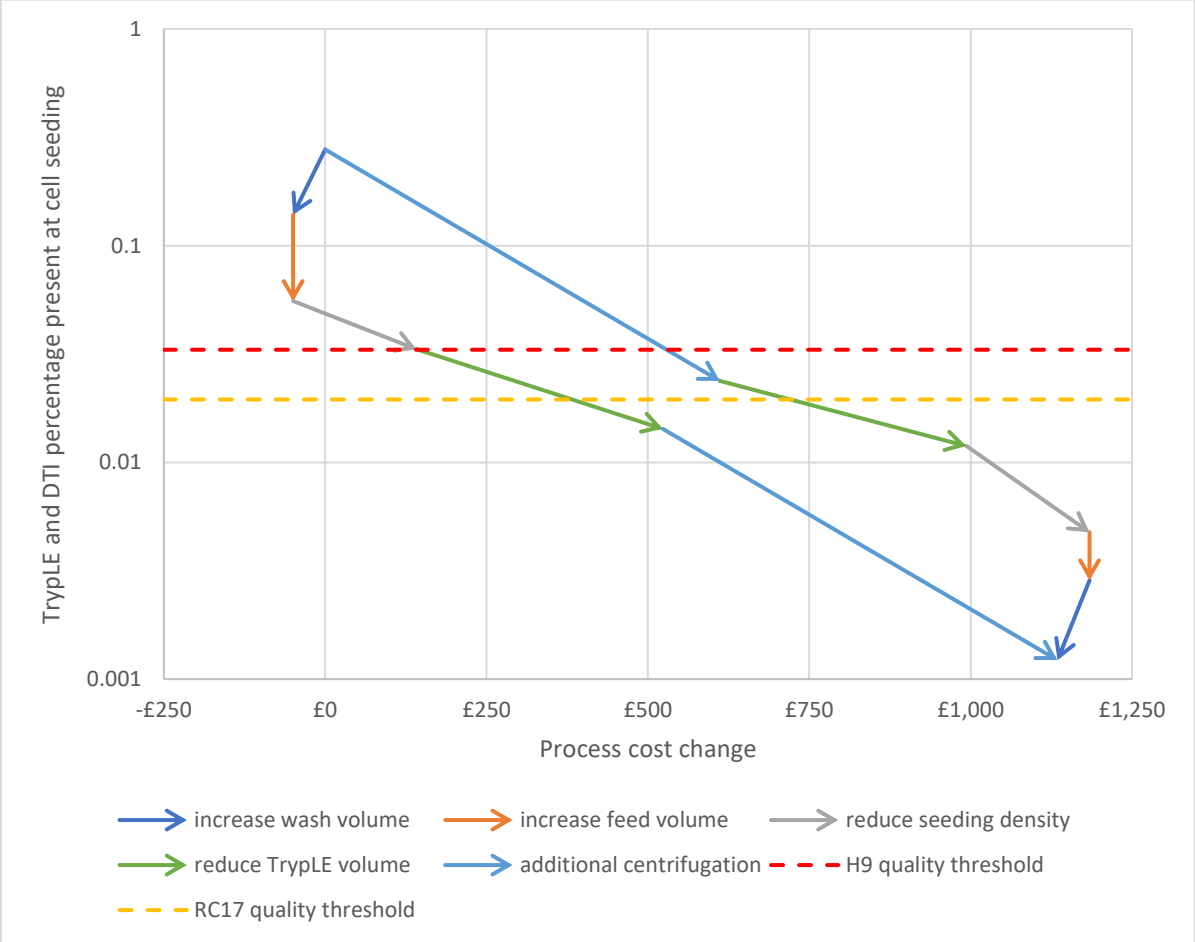

Figure 142 – Most and least optimal process change pathways for reduction of contamination for a lowest allowable CCU yield of 8.4×10^6. The lower left arrow path represents the optimal change order, achieving maximum quality improvement for the least process cost. The upper right path represents non-optimized process changes, achieving the least quality improvement for the most process cost. Both arrow paths start from the point of no process changes with no additional cost and end at the point of all explored process changes with maximum possible cost. Dotted lines represent the quality thresholds defined for each cell line. The Y-axis is represented logarithmically to provide visibility of process changes at low values of contamination. Percentage changes were calculated using the tool provided in Table 18, while costs were calculated using cost per ml values given in the process economics model discussed in Section 6.1.

The points at which the most and least optimal process change pathways (represented as arrow chains) cross the quality thresholds for each cell line (represented as dotted lines) in Figure 142 represent the points at which quality thresholds have been reached. The X-axis value of these intersections represents the process cost associated with the changes required to meet the threshold, the values of which are summarised in Figure 143.

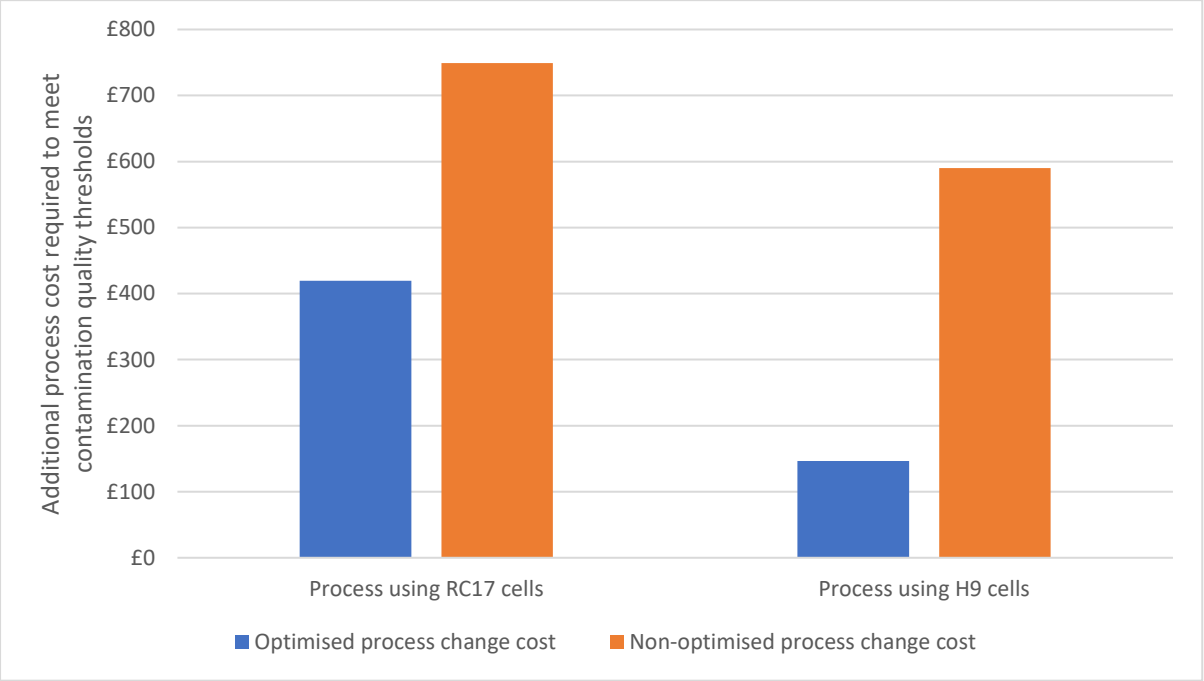

Figure 143 – Costs of process changes required to achieve contamination quality thresholds for RC17 and H9 cells using optimised and non-optimised process changes, assuming a lowest allowable CCU yield of 8.4 x 10^6.

The optimisation of process changes represents a saving of up to £330 per run for RC17s and £444 per run for H9s when compared to non-optimised process changes, despite achieving the same standard of quality improvement. Figure 143 highlights the potential for cost savings when making data driven process changes, and the potential for unnecessary process costs when making process changes which are not cost optimised. Although these savings represent a small proportion of overall process cost, they are the result of optimised process changes for only a single element of the wider process, suggesting that there is still much scope for process improvement and cost optimisation within the mesDA manufacturing process.

6.6 Discussion

Process quality is essential to CTPs as it relates directly to safety and ability to deliver a clinical benefit. The quality of intermediate products influences the quality of the overall product and dictates process robustness, with intermediate products of insufficient quality contributing to process failure. Process costs for CTPs are a limiting factor in commercialisation and process and development, therefore it is essential that product quality thresholds are achieved at the minimum possible cost.

6.6.1 TrypLE and DTI Contamination During Miltenyi Automated Process Development

The Miltenyi 2018 protocol was developed in partnership with Lund and initially used a seeding density of 1 x 10^4 cells per cm^2 for differentiation day 0 as defined in the Lund 2017 protocol. Due to restrictions on embryonic stem cell research in Germany, Miltenyi were unable to use RC17s during development, therefore the Miltenyi 2018 protocol was developed using H9 cells.

Assuming a seeding density of 1 x 10^4 cells per cm^2 and the use of H9 cells, the CCU yield required for healthy cell growth (within 20% of the uncontaminated condition) is 2.83 x 10^7 cells. H9 expansion performed according to the Miltenyi 2018 protocol typically produces a yield of 4 x 10^7 cells, 32.46% higher than required for healthy cell seeding. Because of this, reduced cell yields due to TrypLE and DTI did not occur during early development and were not identified as a problem by Miltenyi.

As process development progressed, process changes were implemented by Miltenyi including a change in seeding density from 1 x 10^4 cells per cm^2 as specified by Lund to 2.5 x 10^4 cells per cm^2. An unintended consequence of this process change was a larger volume of cell seeding solution transferred to the CellSTACK, resulting in increased TrypLE and DTI contamination at the point of cell seeding. During later stages of development, Miltenyi did not perform full process runs to validate changes, preferring to test only the process subsection for which a change was directly applied and inadvertently bypassing the problematic CCU purification step. If full validation runs had been performed, typical H9 yields of 4 x 10^7 cells would have been 56.66% of the number required to achieve successful purification under the Miltenyi 2018 protocol, resulting in significantly reduced cell yield losses and increased process failure rates due to TrypLE and DTI contamination. A summary of typically achieved yields and yields required to meet quality thresholds is provided in Figure 144.

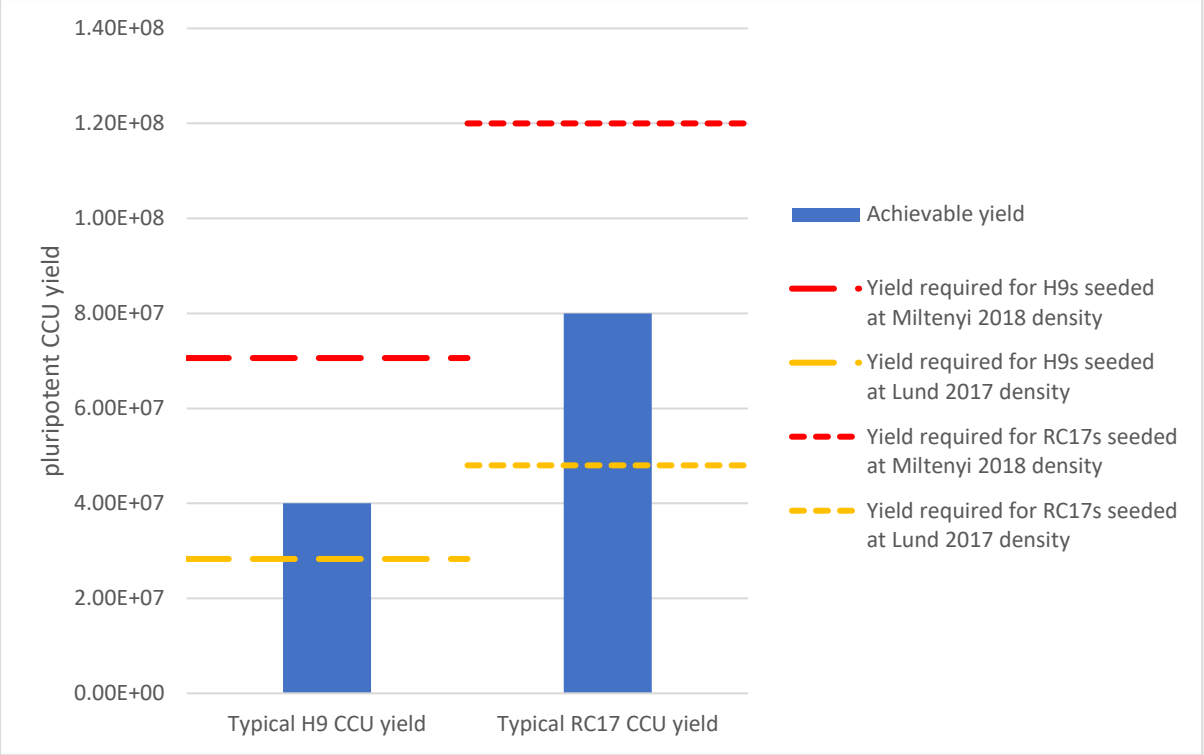

Figure 144 – Typical CCU yields for H9 and RC17 cell expansion compared to yields required to meet quality thresholds for both 1 x 10^4 cells per cm^2 and 2.5 x 10^4 cells per cm^2 seeding densities.

As full validation runs were not performed, the process detailed in the Miltenyi 2018 protocol was transferred to Loughborough having never been performed by Miltenyi. Prodigy based differentiation attempts performed at Loughborough resulted in process loss due to lack of cell attachment 24 hours after differentiation seeding, as discussed in Section 4.6.1. Based on characterisation data identified in Section 6.2.1.1, the Miltenyi 2018 protocol received by Loughborough would be expected to result in 71.2% reduced cell yield for H9 cells and 48.53% reduced cell yield for RC17 cells after 24 hours, with significantly altered cell morphology compared to an uncontaminated control.

Based on the findings of this chapter, the Miltenyi 2018 protocol is unlikely to be capable of producing mesDA progenitor cells without external purification in its current form. This is due to the high level of cell damage caused by TrypLE and DTI contamination during differentiation seeding which is a result of insufficient purification of cells harvested from the CCU. This problem was not identified during development by Miltenyi as full process verification was not performed. The use of external purification to prepare cells for the verification of the differentiation step inadvertently masked problems with substandard CCU centrifugation, effectively removing this step from verification efforts. This meant that the effort to transfer the mesDA manufacturing process from Miltenyi to Loughborough was

performed for a process which had never been run in its entirety and was unlikely to achieve successful differentiation without significant process changes.

This work highlights the potential for unintended consequences of process changes, and the importance of fit-for-purpose process verification following protocol alterations. Miltenyi increased seeding density from 1 x 10^4 to 2.5 x 10^4 cells per cm^2 in an attempt to increase process reliability, as increased seeding density typically results in healthier cell culture. In reality, increasing cell density resulted in increased TrypLE and DTI concentration in the CellSTACK during cell seeding, reducing process reliability to the point of failure under typical yield conditions. Had this change been verified as part of a full process run it is likely that it would have been identified prior to process transfer efforts.

6.6.2 Cell Line Differences

This work highlights the significant impact on cell quality of TrypLE and DTI contamination at the point of cell seeding and during cell culture for H9 and RC17 cell lines. Of particular interest is the difference in response of the two notionally identical cell lines, H9s and RC17s, and the impact on the level of process change and resource investment required to meet defined quality thresholds for each cell line.

H9 cells are commonly used in research due to their early derivation date, breadth of characterisation data and relative ease of obtaining ethics approval (Löser *et al.*, 2010). Much development is performed using H9 cells with the assumption that established processes will translate to other ESC lines. In the case of the mesDA progenitor CTP, differences in yield and sensitivity to TrypLE and DTI during seeding have the potential to impact process cost and robustness to the point of process failure.

RC17 cells were shown to be more sensitive to TrypLE and DTI contamination, exhibiting a 20% loss in cell yields after 24 hours compared to an uncontaminated control at a contaminating level of 1.95%, compared to 3.31% for H9 cells, as summarised in Figure 145. RC17 cells also produce nearly double the typical H9 yield in pluripotent culture as defined in Miltenyi 2018 protocol. While these differences may be due to variation within the cell lines as a result of extended culture, cell yields obtained at Loughborough are comparable to those reported by Lund and Miltenyi, and the H9 response to TrypLE and DTI characterised in Section 6.2.1.2.1 agrees with that observed at Miltenyi. The impact of cell line differences is high for all allogeneic therapies and suggests a need for extensive verification following migration to a new cell line. The differences between similarly sourced cell lines mirrors the high level of input material variability understood to be part of autologous processing.

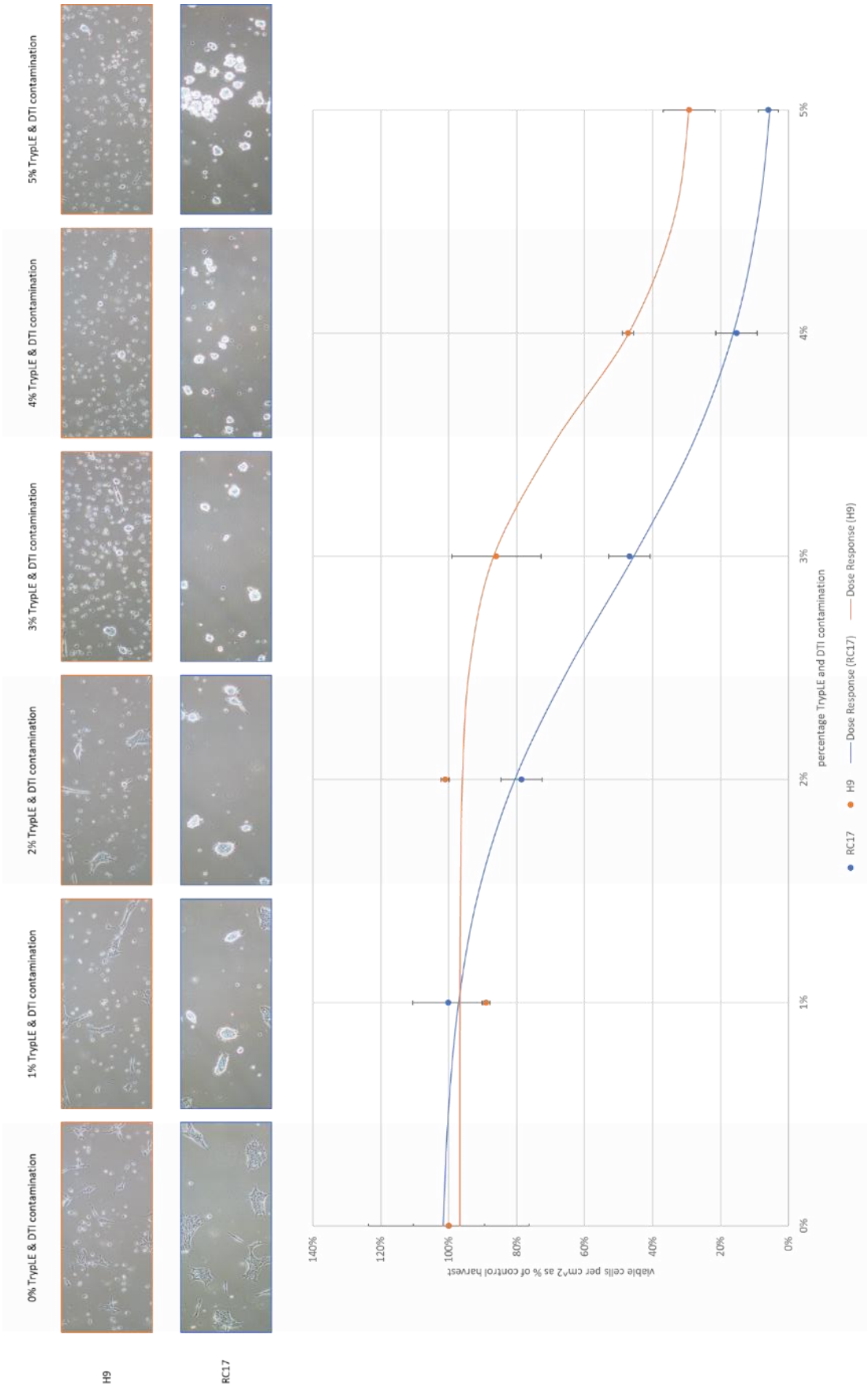

Figure 145 – RC17 and H9 cell lines follow a dose response pattern to TrypLE and DTI contamination during seeding, with RC17s showing higher sensitivity to reduced yields than H9 cells. Data shown as mean ± SD for biological repeats, n=2.

6.6.3 Process Change Complexity

The process changes discussed in this chapter have complex interactions with other elements of the manufacturing process. Each potential process change has an effect magnitude which varies depending upon process changes already implemented, the cell line used and the CCU yield obtained during expansion. Some variable changes are also limited or enabled by other changes, while others depend upon software modifications to the Prodigy and therefore not currently possible.

A number of these limitations have been simplified to facilitate creation of the process change sequencing models presented in Section 6.4. A key assumption for these models is that each process changes produce a linear response, when in fact mitigation strategies may produce combinations of linear and logarithmic responses. This simplification was made as it has no bearing on change sequence priority, and therefore would have no impact on the process change priority recommendations.

Additional complexities specific to each process variable and not included in the process change model are summarised in Table 20. These additional complexities were excluded from the process change sequencing models presented in Section 6.5 as they describe changes with the potential for significant secondary effects which would require substantial characterisation before being implemented in the process change sequence model.

The assumption of linear changes and exclusion of additional complexity summarised in Table 20 was performed in order to minimise assumptions regarding cell response outside of the verified process parameter ranges. This pragmatic approach has produced a model capable of both determining optimal process change sequencing and calculating the resulting cost impact for process changes with minimal risk of secondary effects, while avoiding unnecessary expense required to validate process changes with a high risk of negative secondary effects.

Table 20 – Summary of limitations and considerations not included in the cost and quality model for each process variable.

Process Variable	Limitations Modelled	Considerations Not Modelled
TrypLE and DTI volume	No less than 25 ml due to requirement for reliable CCU coverage without agitation. TrypLE and DTI volume limit allowable wash volume.	Agitation of CCU may enable volumes lower than 25 ml to produce reliable coverage. Agitation is dependent upon software and may include device specific factors, e.g. age of CCU rotation mechanism influences deceleration.
Cell seeding volume	Dependent upon seeding density, for which a minimum of 1×10^4 cells per cm^2 was determined in Section 6.4.2, and CCU yield, typically 4×10^7 for H9 cells and 8×10^7 for RC17 cells but may vary.	Lower seeding densities may be able to produce sufficient cells to perform the differentiation process given the extended culture period. Behaviour of low seeding densities later in differentiation is not characterised.
Feed volume	Maximum CellSTACK feed volume is specified by the Miltenyi 2018 protocol as 250 ml (Miltenyi Biotec, 2018a).	Higher feed volumes may be possible but also reduce gas volume of chamber, potentially limiting correct gassing and impacting cell growth. Slight angle of shelving in incubator will also influence liquid level and air gap.
Wash medium volume	Maximum possible wash medium volume is determined by the maximum CCU capacity of 350 ml minus the volume of TrypLE and DTI used for dissociation.	It may be possible to add wash volume during centrifugation to bypass the CCU capacity limitation. This is not possible in current software. There are many variables relating to input and output transfer speed and timing, rotation speed and forces etc.
Additional stages of centrifugation	No physical limitation for additional centrifugations, however they are not currently possible with Prodigy software.	Each additional centrifugation places further stress on cells and extends processing time, potentially impacting cell health and robustness. Additional centrifugations may be performed with any wash volume, further increasing variables.

6.6.4 Conclusions

This chapter first presents a process economics model for mesDA progenitor manufacture based upon the Miltenyi 2018 protocol, comparing the process costs of manual manufacture to that of a comparable closed and automated process. The impact of TrypLE and DTI contamination during cell seeding on yields was then characterised, with H9 and RC17 cells found to produce a dose response behaviour to contamination during differentiation seeding. Dose responses of cells to reagents are common (Palmer *et al.*, 2013), however, this work describes the first characterisation of H9 and RC17 yield losses due to TrypLE and DTI contamination. This work may prove useful to other processes due to the ubiquity of dissociation enzymes in adherent cell culture, as well as the adoption of less effective purification techniques when transferring to closed and automated processing.

Acceptable levels of TrypLE and DTI contamination for H9 and RC17 cells were then defined, and potential mitigation strategies and their cost and quality impacts explored. Mitigation strategies were then optimised, and an optimal process change sequence presented to produce the highest level of process improvement for the least possible process cost increase. Finally, this work highlights the cost benefits of data driven process change and identifies several key differences between the H9 and RC17 cell lines which may have significant implications for manufacturing of ESC derived CTPs.

The method presented in this chapter may be used to investigate the cost and quality benefits of competing process change options affecting a single CQA. The advantage the method presented in this chapter as opposed to conventional process development as practiced at Miltenyi is the logical progression towards an optimal endpoint, and the balanced use of exploratory experiments alongside model-based analysis of competing options. The process cost and quality graphs presented in Section 6.5 are a novel method of displaying the cost and quality impacts of potential process changes and provide a useful tool to display competing process change opportunities, and the order in which they should be optimally applied.

7 Conclusions

This work has explored issues which are prevalent in cell therapy product (CTP) development and manufacturing processes. While many of these issues are recognised at a surface level, this work has explored complexities which are only revealed during real world process development and presents findings at the technical implementation level of detail. These conclusions therefore identify pieces of knowledge which are seemingly obvious, but which are in fact highly nuanced and vital to understand for real world process implementation.

The cell therapy industry has recently seen success with chimeric antigen receptor T cells (CAR-T) therapies such as Kymriah (Novartis, Switzerland) and Yescarta (Kite Pharma, US) receiving market authorisation and delivering clinical benefits in Europe, the US and Japan. Outside of CAR-T, a number of previously approved therapies have been withdrawn due to commercial difficulties in the case of Provenge (Dendreon, US), ChondroCelect (TiGenix, Belgium) and Glybera (uniQure, Netherlands), as well as challenges in establishing a manufacturing site in the case of MACI (Vericel, Denmark).

CTPs offer the opportunity to address unmet clinical needs for many conditions, however, the high costs associated with their development and manufacture is a key barrier to widespread adoption. High development and manufacturing costs result from the use of expensive labour due to product and process complexity, high facility costs associated with GMP cleanrooms to enable sterile processing, as well as expensive reagents and consumables (Stanton, 2019). These costs are exacerbated by inefficiencies and high levels of product loss and degradation during processing (Hassan *et al.*, 2015), high batch failure rates observed during CTP manufacture (Julien and Whitford, 2008; Langer, 2008, 2016), and in the case of small scale allogeneic CTPs, a lack of processing equipment at suitable scales for development or manufacture.

Cost has been highlighted as the key limiting factor for the advancement of CTPs; cost reduction measures are therefore essential to the advancement of the field. Economies of scale are well understood as key drivers of cost reduction across many industries, and have been identified as a key cost driver for allogeneic products (Lipsitz *et al.*, 2017). While autologous therapies are limited in scale up of batch size to the output required by a single patient, allogeneic therapies face no similar limitation and may be scaled up as far as patient demand or manufacturing capacity allows. Cost of goods (COGs) has been highlighted as the key reason for the high costs associated with CAR-T therapies, which at present are too expensive to be widely used by world healthcare systems (Stanton, 2019). Allogeneic therapies offer the potential to reduce cost of goods by orders of magnitude, potentially bringing CTPs

into price parity with traditional pharmaceuticals and enabling their use by budget limited healthcare providers.

Although it is not possible to produce autologous mesencephalic dopaminergic (mesDA) progenitors using the manufacturing process given in 3.3.3 due to the use of embryonic stem cells (ESCs) as a source material, the approximate process costs for a comparable one to one process may be calculated. The closed and automated mesDA manufacturing process given in Section 3.4 produces approximately 425 doses per batch, with facilities and labour accounting for approximately 70% of process costs as given in Section 6.1.2. Facilities and labour requirements would remain largely constant for batch sizes of either one or 425 doses per batch. Presuming negligible material costs for a single dose, the cost per process run of a one to one process is likely to be approximately 70% that of an allogeneic process, consisting of only facilities and labour costs. Producing the mesDA product using allogeneic processing therefore yields 0.235% the doses of autologous processing while retaining 70% of the required costs, translating to an approximate 300-fold decrease in process cost per dose for autologous processing compared to a comparable one to one process. Due to the limitation of one dose per batch, this translates to a decrease in process costs from £14,835.53 per dose for a one to one process to £47.44 per dose for a comparable allogeneic process, as calculated in Section 6.1.1.

This vast cost decrease is an agreement with the literature, which notes that allogeneic products benefit from economies of scale to a similar degree as pharmaceuticals, while autologous therapies see little cost benefit from scale out (Lipsitz *et al.*, 2017). A cost decrease of this magnitude significantly improves profitability and potential market size for a CTP. The true cost benefit for allogeneic as compared to an autologous therapy is likely to be even greater than calculated for an allogeneic one to one therapy, as these figures do not account for further costs associated with the additional processing steps required and increased variability of autologous material.

7.1 Need for Process-Appropriate Equipment

CTPs cannot be terminally sterilised and therefore require sterile conditions throughout every stage of manufacture. CTP manufacture is made possible by the availability of suitable plasticware and processing systems, with this dependency increasing as CTP manufacture moves towards the use of closed systems and automation. As CTP manufacture has shifted towards the use of closed and automated processing in pursuit of improved sterility, scale and control, equipment has become a limiting factor in process and product development.

Current CTP manufacturing equipment has mainly been developed for large scale processing of mesenchymal stem cell (MSC) based therapies, requiring scales of up to 10^{13} per batch (Jossen *et al.*, 2018), or autologous therapies such as CAR-T, at similar scales to allogeneic ESC derived therapies but with drastically different dose and verification requirements. While stirred tank bioreactors are a proven option for large scale processing, such systems are unsuitable for small scale processes. Much currently available equipment is notionally suitable for processing of small-scale adherent CTPs but presents unforeseen challenges during real world use. Examples of this behaviour include inadequate purification during CCU centrifugation on the Prodigy, the limited level of process control awarded by tangential flow filtration (TFF) at small scales, the high risk of pellet aspiration with current closed centrifugation tubes, as well as the inability of controlled rate freezers (CRF) to deliver adequate cooling to closed cryopreservation vessels. In many cases, only small changes to existing equipment would be required to create effective solutions for small scale allogeneic therapies. In the case of Prodigy purification, insufficient purification may be overcome through balancing reagent volumes and seeding density; TFF may be improved at small scales by increasing the update rate and precision of measurement equipment and monitoring software; and closed centrifugation tubes may be adapted for use with pelleted cells through the addition of an angled aspiration tube, as already implemented in liquid reservoirs for TFF. Where equipment is available, it is currently challenging to integrate due to a lack of standardization between manufacturers (Stanton, 2019).

The development of enabling technology for small scale autologous CTPs may depend on a pioneering allogeneic therapy leading the way to build industry motivation and awareness. Such a therapy would need to make use of currently available equipment, likely translating to higher losses and greater variability and therefore higher costs than would be possible on purpose designed equipment. Understanding the real-world limitations and quality impacts of sub-optimal equipment will allow small scale allogeneic therapies to be manufactured.

7.2 Cell Therapy Manufacturing Processes as Complex Systems

It is understood that biological cells are complex entities, with the characterisation of interactions and emergent behaviours being key to developing basic science understanding and in the application of knowledge for the development of new therapies (Kitano, 2002). Manufacturing processes for biological cells may therefore be considered as complex systems, with outputs varying significantly and unpredictably in response to small changes in material or process inputs.

The high sensitivity of CTP manufacturing processes to a wide array of process inputs is well understood and is evidenced in the high rates of failure seen in CTP as compared to other manufacturing industries. Deviations from process parameters resulting from process faults or operator errors are generally understood to result in loss of critical quality attributes in complex and unpredictable ways. Process changes are distinct from deviations, being purposeful alterations to a defined process made with the intention of producing an improvement in either quality or cost. As purposeful changes are based on current process understanding it is assumed that they will produce a desired effect with minimal impact on other process elements, however, changes to complex systems are likely to include complex and unpredictable effects, regardless of intent.

7.2.1 Sensitivity to Process Changes

Complex systems exhibit complex relationships between process parameters and quality attributes, with a high sensitivity to change. While the aim of technology transfer is the direct transfer of a process and related knowledge between sites or institutions, transfers inevitably introduce numerous process changes due to differences in equipment, materials and processes. Process transfers are understood to be challenging with the potential to delay projects by months or years (Perry, 2010).

Throughout Chapter 4, several process changes made by Miltenyi during the technology transfer process were identified as having unintended interactions and consequences. As discussed in Section 4.7, Miltenyi experienced frequent process failures during differentiation and were unsure of the cause. A process change was made from a day 0 differentiation seeding density of 1 x 10^4 cells per cm^2 as specified by Lund (Nolbrant *et al.*, 2017) to an increased seeding density of 2.5 x 10^4 cells per cm^2. This change was made with the knowledge that increased seeding density generally improves robustness of ESC culture. As a result of this change, an increased volume of TrypLE contaminated cell solution was transferred to the CellSTACK during cell seeding resulting in process failure during a full process run. This minor process change was presumed to have negligible impact on the overall process but resulted in complete process failure and product loss due to interactions between the process and equipment of the manufacturing process. Despite basic verification efforts by Miltenyi, the full consequences of this process change only manifested during a full-scale process run using CCU based purification on the Prodigy. Had verification efforts been fit for purpose and included testing of the new seed density parameter using CCU based purification, this issue would have been picked up several months earlier saving significant process development time and money. This example illustrates the need to

understand non-obvious process and machine interactions, and to consider the system wide impact of process changes when developing change proposals and verification strategies.

7.2.2 Sensitivity to Cell Line Changes

Although starting material is recognised as a key cause of variability in the manufacture of autologous CTPs (Williams *et al.*, 2016), the behaviour of cell lines as input material for allogeneic therapies is assumed to be largely consistent. H9 cells are commonly used in research due to the breath of characterisation data and relative ease of obtaining ethical approval for the cell line (Löser *et al.*, 2010). The widespread use of H9s in the development of CTPs exposes the industry to the risk of a regulatory ban on therapies derived from the cell line, a possible response if harm were to result from a H9 derived therapy. If this were to occur, therapies developed using H9 cells would be required to transition to other cell lines, potentially losing the ability to manufacture a given therapy to a comparable standard or at an acceptable cost.

As demonstrated in Section 6.6.1, subtle differences in cell growth and TrypLE sensitivity between H9 and RC17 cells resulted in a 70% increase in required yield for the primary expansion during the mesDA manufacturing process. In the case of the mesDA progenitor therapy this increase would be addressable through changes to cell seeding density; however, the effects are complex and highly process specific, meaning that changes to starting material may result in other therapies being uneconomical to manufacture due to cell line specific failure modes. The differences in TrypLE sensitivity observed in Section 6.2 and summarised in Figure 145 are likely to have implications for many therapies due to the ubiquity of dissociation enzymes in adherent cell processing. The sensitivity of processes to notionally comparable input material also suggests that variability between cell banks originating from the same cell line, and even between vials within a bank has the potential to result in significant impacts to quality attributes, and therefore to process cost and robustness.

7.2.3 Sensitivity to Variability

Variability is present in all manufacturing processes and is introduced via input materials and in the execution of processing steps. As explored in Chapter 5, cell losses and degradation for each manipulation during processing are relatively small but may combine to produce unpredictable behaviours over an entire process. Because of this, a CTP manufacturing process must be viewed

holistically, with potential quality impacts affecting and being affected by all subsequent processing steps. These effects may be more pronounced in ESC processing, which are generally performed at lower scales and are considered more sensitive than cell types such as MSCs.

Sensitivity to process variability has previously been observed in MSC manufacturing on the CompacT SelecT (Sartorius Stedim TAP, UK), where variability in cell yields resulted in variations in Trypsin/EDTA contamination during cell seeding. Pour-away purification resulted in contamination of cell seeding medium with 1% to 4% Trypsin/EDTA, with the concentration dependent upon cell yields of the prior expansion. High initial yields resulted in low contamination levels for subsequent passages, allowing for good yields and continued low contamination levels. Small reductions in cell growth early in the process were shown to produce process failure, as lower initial yields resulted in higher contamination values which then contributed to even lower cell yields for subsequent passages. In this way, a positive feedback loop was established resulting in process failure (Thomas *et al.*, 2007). Cryopreservation has also been identified as a key source of variability in ESC manufacturing, impacting processes both prior to the main expansion and following product formulation (Mitchell *et al.*, 2014). Losses and degradation, however slight, must also be considered from an economic standpoint, as even small losses may represent many potential lost doses due to the low cell density requirement of many ESC derived therapies. Due to the high profit margins achievable with allogeneic therapies, losses may also represent a substantial loss of potential profit.

7.3 Contributions to Knowledge

While areas such as cell expansion receive much attention by equipment manufacturers and in published research, all steps in a manufacturing process contribute to product quality and impact cost of goods. A key aim of the work described in this thesis was to characterise elements of CTP manufacturing system which typically receive little attention, and to explore the wider quality and cost impacts of these elements and their interactions on a systems scale. A summary of knowledge gained and remaining challenges for each key process step is shown in Table 21.

Table 21 – Summary of prior knowledge, knowledge gained and remaining challenges for each major process step.

Process Step	Prior Knowledge	Knowledge Gained	Remaining Challenges
Sourcing	Assumption of comparability between ESC cell lines.	Difference in cell line behaviour for both expansion & differentiation yields as well as TrypLE contamination behaviour.	Characterisation of cell line specific failure modes other than TrypLE contamination.
Laminin Coating	Knowledge that laminin performance degrades with drying.	Characterisation of laminin drying.	Comparison of drying behaviour with other coatings. Modelling of process cost impact to determine allowable delay.
	No prior knowledge regarding albumin and laminin competitive binding.	Sensitivity to growth surface contamination with albumin.	Measurement of minimum allowable albumin contamination.
Seeding	TrypLE assumed to be quenched with DTI.	Sensitivity to contamination with TrypLE and inability of medium or DTI to prevent cell damage.	Measurement of alternative dissociation enzymes.
Feed	Assumption that losses on closed systems are minimal.	Dead volumes add significant volume and cost to automated process.	Modelling of cost impact of dead volumes due to closed processing.
Harvest	Physical manipulation used in manual culture, benefit not quantified.	Characterisation of physical manipulation as aid to detachment	Testing the impact of physical manipulations using defined forces producible by automated systems. Explore possibility of bag agitation requirement to avoid cell settling during seeding.
Purification	Lack of standardisation of aspiration technique	Definition and measurement of shoulder aspiration method.	Defined method to be included in future protocol publications.
	Much closed equipment considered suitable due to notional compatibility.	Equipment is poorly optimised for small scale in practice (e.g. closed centrifugation and TFF).	Development and testing of equipment improvements (e.g. additional dip tubes and more sensitive and responsive TFF equipment).

Table 21 continued - Summary of prior knowledge, knowledge gained and remaining challenges for each major process step.

Process Step	Prior Knowledge	Knowledge Gained	Remaining Challenges
Purification (continued)	Poor robustness of mesDA manufacturing process, reasons unknown.	Poor CCU purification leads to TrypLE degrading cell growth in mesDA process. Characterisation of failure.	Exploration of TrypLE failure mode on other processes and automated systems.
	Increasing wash volume to improve purification considered but not quantified.	Mitigation strategies are complex and increase process cost. High levels of purification are challenging to achieve.	Validation of TrypLE contamination mitigation strategies.
Fill and Finish	Compatibility of closed tubes and bags with ESC processing.	High losses for closed cryopreservation solutions, variability of bag-based freezing.	Characterisation of variability and losses during closed cryopreservation, assessment of cost impacts.
	Assumed impact on growth of ESCs exposed to DMSO prior to cryopreservation.	Stability of ESCs in 5% DMSO prior to freezing for up to 40 minutes.	Measurement of DMSO impact at higher concentrations, longer hold times and for mesDA progenitor product cells.
Freeze	CRF throughput as a process bottleneck due to high device cost.	CRFs unable to maintain controlled freeze for multiple bags, falling out of spec. Throughput is dependent upon vessel type, and is reduced for closed bags.	Development and testing of mitigation strategies (e.g. improved racks and chamber insulation).
Resuscitation	Closed cryopreservation systems assumed to provide a closed process.	Weldable vials and bags incompatible with welding following cryopreservation. Necessity of open processing for cell retrieval.	Development of new storage vessel capable of closed cell retrieval.
	Cryopreservation recognised as significant contributor to process variability. Closed and automated systems assumed to reduce variability.	High variability of bag-based freezing. Substantial contribution to variability from purification.	Development of new storage vessels with a focus on reduction of dead volumes and repeatable cell retrieval.

Based upon the knowledge gained in this work, an updated process design specification for a closed and semi-automated mesDA manufacturing process is shown in Figure 146. This process is generalisable to other ESC based allogeneic CTPs with similar dose size requirements and features parallels with traditional pharmaceutical supply chains and organisational structures.

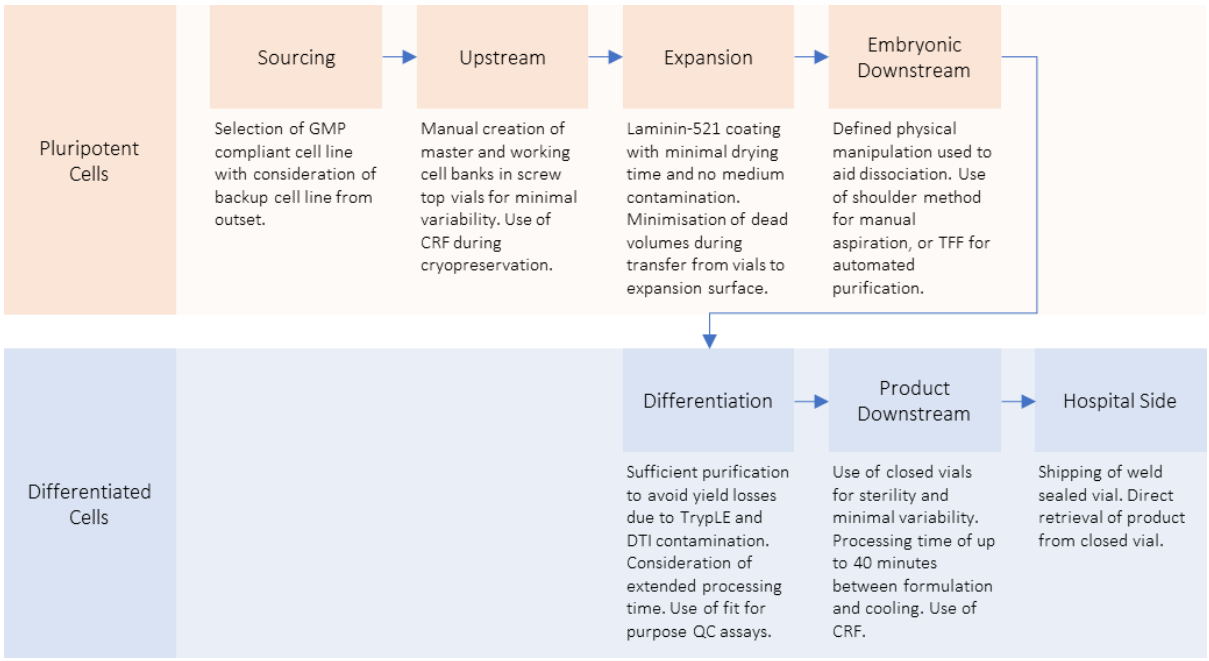

Figure 146 – Process design specification for a closed and semi-automated mesDA manufacturing process.

The additional detail present in the process design specification in Figure 146 compared to the high level process overview provided in the literature review in Figure 5 represents process knowledge for steps typically overlooked in published research. Robustness focussed process changes may be common knowledge within commercial entities familiar with CTP manufacture, however this level of process knowledge was not evident in the process provided by Miltenyi during the mesDA project or during the technology transfer. During this work, it was not possible to set statistical confidence limits or to assess the cost impact of process risk as the process is not yet fixed, and runs are prohibitively costly to perform enough process repeats to produce adequate data for robustness analysis.

Seemingly small contributions of cell loss, degradation and variability are present throughout the entire process chain and may interact to produce significant effects. It is only by understanding these neglected process steps and considering their impact on a holistic, system wide level that system level robustness can be achieved.

7.4 Outlook

The success of CAR-T therapies has directed industry focus towards autologous therapies; however, the potential benefits of these therapies are limited by high cost of goods resulting in affordability incompatible with world healthcare budgets (Stanton, 2019). Despite current equipment limitations for small scale processing of allogeneic CTPs, the potential profitability of these therapies makes them an attractive prospect. Allogeneic therapies using standardised biological input material offer the potential to produce a high number of doses per product batch, drastically reducing cost per batch and maintaining compatibility with established manufacturing, quality and regulatory paradigms. The profitability of allogeneic CTPs is likely to provide motivation for equipment manufacturers to develop optimised systems at an appropriate scale, in the same way as has occurred for CAR-T and similar autologous therapies.

As allogeneic CTPs move towards mainstream adoption, manufacturing processes must be continuously improved to maximise economic benefit while maintaining pace with the developing GMP and regulatory landscapes. While elements of the manufacturing process will benefit from characterisation of isolated elements, such experiments typically design out complexity present in real world systems. As in most manufacturing settings, truly representative data best capable of driving optimisation efforts will be obtained from real production runs. As such process runs are cost prohibitive during development, process optimisation efforts must capture system complexity, taking a systems wide view in order to gain applicability to real world process implementations.

7.5 Future Work

Key areas of future work required to achieve a reliable mesDA manufacturing process include the validation of TrypLE contamination mitigation strategies discussed in Chapter 6. Once a suitable level of process robustness has been demonstrated, the mesDA manufacturing process may transition from a state of active development to one of continuous improvement. An abundance of data from production runs will enable powerful statistical sensitivity analyses of critical process parameters such as laminin drying time and sensitivity to low level contaminants, allowing fine optimisation of standard operating procedures.

The development of equipment improvements discussed in Section 5.4 would provide benefit to the mesDA manufacturing process and have the potential to satisfy unmet needs in the wider field. Closed

purification for small to medium batches of adherent cells is frequently discussed as a limiting factor for both manufacturing and product development, and may be achieved through the modification of closed centrifugation bottles to include angled aspiration ports, or through the increased precision and responsiveness of TFF measuring hardware and real-time control systems. CRF throughput may also be increased through improved rack and chamber insulation designs, especially for closed vessels such as tall tubes or stacked bags. Storage vessels also require improvements to enable closed liquid retrieval and to reduce dead volumes and variability. The move from functionally closed to truly closed processing also requires the development of new storage vessels with a focus on reduction of dead volumes and repeatable closed cell retrieval.

The sensitivity of two ESC cell lines to low level TrypLE contamination may prove to be of significant impact to any therapy which includes an adherent stem cell expansion phase. Due to the ubiquity of trypsin and similar dissociation enzymes and the current push towards closed processing, many processes may see lower yields due to increased dissociation enzyme contamination during expansion as a result of less effective closed purification processes. Improvements to purification techniques therefore offer the opportunity to increase yields both through reduced purification losses, as well as through increased expansion rates due to effective dissociation enzyme removal.

Differences in cell response to TrypLE contamination also highlight issues around the assumption of comparability between and within cell lines, suggesting that characterisation of cell bank and even vial specific failure modes may be of great importance in large scale commercial cell therapy manufacture.

8 References

Abou-El-Enein, M. *et al.* (2013) 'Good Manufacturing Practices (GMP) manufacturing of advanced therapy medicinal products: a novel tailored model for optimizing performance and estimating costs', *Cytotherapy*, 15(3), pp. 362–383. doi: https://doi.org/10.1016/j.jcyt.2012.09.006.

Adewumi, O. *et al.* (2007) 'Characterization of human embryonic stem cell lines by the International Stem Cell Initiative', *Nature biotechnology*. Nature Publishing Group, 25(7), p. 803.

Adler, A. F. *et al.* (2019) 'hESC-Derived Dopaminergic Transplants Integrate into Basal Ganglia Circuitry in a Preclinical Model of Parkinson's Disease', *Cell Reports*, 28(13), pp. 3462-3473.e5. doi: https://doi.org/10.1016/j.celrep.2019.08.058.

Adler, S. *et al.* (2006) 'The effects of solvents on embryonic stem cell differentiation.', *Toxicology in vitro : an international journal published in association with BIBRA*. Elsevier, 20(3), pp. 265–71. doi: 10.1016/j.tiv.2005.06.043.

Allegrucci, C. and Young, L. E. (2006) 'Differences between human embryonic stem cell lines', *Human Reproduction Update*, 13(2), pp. 103–120. doi: 10.1093/humupd/dml041.

Alliance for Regenerative Medicine (2019) *Alliance for Regenerative Medicine, 2019 Q3 Report*.

Alper, J. (2009) 'Geron gets green light for human trial of ES cell–derived product', *Nature Biotechnology*. Nature Publishing Group, 27, p. 213. Available at: https://doi.org/10.1038/nbt0309-213a.

Amps, K. *et al.* (2011) 'Screening a large, ethnically diverse population of human embryonic stem cells identifies a chromosome 20 minimal amplicon that confers a growth advantage', *Nature Biotechnology*, 29(12), pp. 1132–1144. doi: 10.1038/nbt.2051.

Amps, K. J. *et al.* (2010) 'In situ cryopreservation of human embryonic stem cells in gas-permeable membrane culture cassettes for high post-thaw yield and good manufacturing practice', *Cryobiology*. Elsevier, 60(3), pp. 344–350. doi: 10.1016/j.cryobiol.2010.03.007.

Apel, M. *et al.* (2013) 'Integrated clinical scale manufacturing system for cellular products derived by magnetic cell separation, centrifugation and cell culture', *Chemie-Ingenieur-Technik*. Wiley Online Library, 85(1–2), pp. 103–110. doi: 10.1002/cite.201200175.

Asymptote Limited (2017) *Asymptote Website*. Available at: http://asymptote.co.uk/VIAFreeze2.php.

Bagga, V., Dunnett, S. B. and Fricker-Gates, R. A. (2008) 'Ascorbic acid increases the number of dopamine neurons in vitro and in transplants to the 6-OHDA-lesioned rat brain', *Cell Transplantation*, 17(7), pp. 763–773. doi: 10.3727/096368908786516774.

Baharvand, H. *et al.* (2010) 'An efficient and easy-to-use cryopreservation protocol for human ES and iPS cells', *Nature protocols*. Nature Publishing Group, 5(3), p. 588.

Bakken, A. M., Bruserud, O. and Abrahamsen, J. F. (2003) 'No differences in colony formation of peripheral blood stem cells frozen with 5% or 10% dimethyl sulfoxide', *Journal of hematotherapy & stem cell research*. Mary Ann Liebert, Inc., 12(3), pp. 351–358.

Balint, B. *et al.* (1999) 'The cryopreservation protocol optimal for progenitor recovery is not optimal for preservation of marrow repopulating ability', *Bone Marrow Transplantation*, 23(6), p. 613. doi: 10.1038/sj.bmt.1701623.

Ball, O. *et al.* (2018) 'Bioprocessing automation in cell therapy manufacturing: Outcomes of special interest group automation workshop', *Cytotherapy*, 20(4), pp. 592–599. doi: https://doi.org/10.1016/j.jcyt.2018.01.005.

Bally-Cuif, L., Cholley, B. and Wassef, M. (1995) 'Involvement of Wnt-1 in the formation of the mes/metencephalic boundary', *Mechanisms of development*. Elsevier, 53(1), pp. 23–34.

Banfalvi, G. (2008) 'Cell cycle synchronization of animal cells and nuclei by centrifugal elutriation', *Nature Protocols*. Nature Publishing Group, 3, p. 663. Available at: https://doi.org/10.1038/nprot.2008.34.

Barker, R. A. *et al.* (2015) 'G-Force PD: a global initiative in coordinating stem cell-based dopamine treatments for Parkinson's disease', *NPJ Parkinson's disease*. Nature Publishing Group, 1, p. 15017. doi: 10.1038/npjparkd.2015.17.

Barker, R. A. *et al.* (2016) 'Are Stem Cell-Based Therapies for Parkinson's Disease Ready for the Clinic in 2016?', *Journal of Parkinson's disease*. IOS Press, (Preprint), pp. 1–7.

Barker, R. A. *et al.* (2019) 'Designing stem-cell-based dopamine cell replacement trials for Parkinson's disease', *Nature Medicine*, 25(7), pp. 1045–1053. doi: 10.1038/s41591-019-0507-2.

Barker, R. A., Drouin-Ouellet, J. and Parmar, M. (2015) 'Cell-based therapies for Parkinson disease - past insights and future potential', *Nature Reviews Neurology*. Nature Publishing Group, 11(9), pp. 492–503.

Becherucci, V. *et al.* (2020) 'Comparison of CryoMACS Freezing Bags with Maco Biotech Freezing-Ethinyl Vinyl Acetate Bags for Hematopoietic Progenitor Cells Cryopreservation Using a CD34+-Enriched

Product', *Biopreservation and Biobanking*. Mary Ann Liebert, Inc., publishers. doi: 10.1089/bio.2019.0135.

Benson, J. D., Kearsley, A. J. and Higgins, A. Z. (2012) 'Mathematical optimization of procedures for cryoprotectant equilibration using a toxicity cost function', *Cryobiology*. Elsevier, 64(3), pp. 144–151. doi: 10.1016/j.cryobiol.2012.01.001.

Bersenev, A. and Kili, S. (2018) 'Management of "out of specification" commercial autologous CAR-T cell products', *Cell Gene Therapy Insights*, 4(11), pp. 1051–1058. Available at: https://insights.bio/cell-and-gene-therapy-insights/?bio_journals=management-of-out-of-specification-commercial-autologous-car-t-cell-products.

Berz, D. *et al.* (2007) 'Cryopreservation of hematopoietic stem cells', *American journal of hematology*. Wiley Online Library, 82(6), pp. 463–472.

BioLamina (2018) 'BioLamina and Novo Nordisk Partner to Advance Stem Cell Based Therapies for Three Common Medical Conditions', *PR Newswire*.

Björklund, A. *et al.* (1980) 'Reinnervation of the denervated striatum by substantia nigra transplants: functional consequences as revealed by pharmacological and sensorimotor testing', *Brain research*. Elsevier, 199(2), pp. 307–333.

Björklund, A. and Stenevi, U. (1979) 'Reconstruction of the nigrostriatal dopamine pathway by intracerebral nigral transplants', *Brain Research*. Elsevier, 177(3), pp. 555–560. doi: 10.1016/0006-8993(79)90472-4.

Bjorklund, L. M. *et al.* (2002) 'Embryonic stem cells develop into functional dopaminergic neurons after transplantation in a Parkinson rat model', *Proceedings of the National Academy of Sciences*. National Acad Sciences, 99(4), pp. 2344–2349. doi: 10.1073/pnas.022438099.

Bretzner, F. *et al.* (2011) 'Target Populations for First-In-Human Embryonic Stem Cell Research in Spinal Cord Injury', *Cell Stem Cell*, 8(5), pp. 468–475. doi: https://doi.org/10.1016/j.stem.2011.04.012.

Brun-Graeppi, A. K. A. S. *et al.* (2010) 'Thermoresponsive surfaces for cell culture and enzyme-free cell detachment', *Progress in Polymer Science (Oxford)*. Elsevier, 35(11), pp. 1311–1324. doi: 10.1016/j.progpolymsci.2010.07.007.

Brundin, P. and Björklund, A. (1998) *Survival of expanded dopaminergic precursors is critical for clinical trials*, *Nature neuroscience*. doi: 10.1038/2773.

Bubela, T. *et al.* (2015) 'Bringing regenerative medicines to the clinic: the future for regulation and

reimbursement.', *Regenerative medicine*. Future Medicine, 10(7), pp. 897–911. doi: 10.2217/rme.15.51.

Buckler, R. L. *et al.* (2016) 'Technological developments for small-scale downstream processing of cell therapies', *Cytotherapy*, 18(3), pp. 301–306. doi: https://doi.org/10.1016/j.jcyt.2015.12.003.

Bueno, C., Montes, R. and Menendez, P. (2010) 'The ROCK Inhibitor Y-27632 Negatively Affects the Expansion/Survival of Both Fresh and Cryopreserved Cord Blood-Derived CD34+ Hematopoietic Progenitor Cells', *Stem Cell Reviews and Reports*, 6(2), pp. 215–223. doi: 10.1007/s12015-010-9118-5.

Cambridge University Institute for Manufacturing (2016) *Emerging Industries, Aims and Outputs*. Available at: http://www.ifm.eng.cam.ac.uk/research/eip/aims/ (Accessed: 15 August 2017).

Canham, M. a. *et al.* (2015) 'The Molecular Karyotype of 25 Clinical-Grade Human Embryonic Stem Cell Lines', *Scientific Reports*. Nature Publishing Group, 5, p. 17258. doi: 10.1038/srep17258.

Chambers, I. *et al.* (2003) 'Functional Expression Cloning of Nanog, a Pluripotency Sustaining Factor in Embryonic Stem Cells', *Cell*, 113(5), pp. 643–655. doi: https://doi.org/10.1016/S0092-8674(03)00392-1.

Chambers, S. M. *et al.* (2009) 'Highly efficient neural conversion of human ES and iPS cells by dual inhibition of SMAD signaling', *Nat.Biotechnol.* Nature Publishing Group, 27(1546-1696 (Electronic)), pp. 275–280.

Chaudhuri, K. R., Healy, D. G. and Schapira, A. H. V (2006) 'Non-motor symptoms of Parkinson's disease: Diagnosis and management', *Lancet Neurology*, 5(3), pp. 235–245. doi: 10.1016/S1474-4422(06)70373-8.

Chen, G. (2012) 'Splitting hESC/hiPSC lines with EDTA in feeder free conditions', *StemBook [Internet]. Cambridge, MA: Harvard Stem Cell Institute. doi*, 10.

Chen, Y. *et al.* (2008) 'NS21: Re-defined and modified supplement B27 for neuronal cultures', *Journal of Neuroscience Methods*. Elsevier, 171(2), pp. 239–247. doi: 10.1016/j.jneumeth.2008.03.013.

Choi, J.-S. *et al.* (2015) 'Effects of Donor Age, Long-Term Passage Culture, and Cryopreservation on Tonsil-Derived Mesenchymal Stem Cells', *Cellular Physiology and Biochemistry*, 36(1), pp. 85–99. Available at: http://www.karger.com/DOI/10.1159/000374055.

Claassen, D. A., Desler, M. M. and Rizzino, A. (2009) 'ROCK inhibition enhances the recovery and growth of cryopreserved human embryonic stem cells and human induced pluripotent stem cells', *Molecular reproduction and development*. Wiley Online Library, 76(8), pp. 722–732.

Coopman, K. and Medcalf, N. (2014) 'From production to patient: challenges and approaches for delivering cell therapies', in *StemBook [Internet]*. Harvard Stem Cell Institute.

Corning (2011) *Corning CellSTACK Culture Chambers*. Available at: https://cdn.stemcell.com/media/files/manual/MADX21631-Corning_CellSTACK_Culture_Chambers.pdf.

Corning (2019a) *Corning 500 mL Easy Grip Polystyrene Storage Bottles with Dip Tube, with 0.2 µm MLL/FLL Filter, MLL*. Available at: https://ecatalog.corning.com/life-sciences/b2c/US/en/Bioprocess-and-Scale-up/Closed-System-Bottles-and-Tubes-and-Flasks/Corning®-Easy-Grip-Polystyrene-Storage-Bottles/p/11665.

Corning (2019b) *Corning Preassembled Closed Systems Solution Centrifuge Tubes*. Available at: https://ecatalog.corning.com/life-sciences/b2c/US/en/Liquid-Handling/Tubes,-Liquid-Handling/Centrifuge-Tubes/Corning®-Preassembled-Closed-Systems-Solution-Centrifuge-Tubes/p/preassembledClosedSystemSolutionsForCentrifugeTubes.

Crosby, P. B. (1979) *Quality is free: The art of making quality certain*. McGraw-hill New York.

Cunha, B., Alves, P. M., *et al.* (2015) 'Exploring continuous and integrated strategies for the up- and downstream processing of human mesenchymal stem cells', *Journal of Biotechnology*. Elsevier, 213, pp. 97–108. doi: 10.1016/j.jbiotec.2015.02.023.

Cunha, B., Peixoto, C., *et al.* (2015) 'Filtration methodologies for the clarification and concentration of human mesenchymal stem cells', *Journal of Membrane Science*, 478, pp. 117–129. doi: https://doi.org/10.1016/j.memsci.2014.12.041.

Cunha, B., Aguiar, T., *et al.* (2017) 'Bioprocess integration for human mesenchymal stem cells: From up to downstream processing scale-up to cell proteome characterization', *Journal of Biotechnology*, 248, pp. 87–98. doi: 10.1016/j.jbiotec.2017.01.014.

Cunha, B., Silva, R. J. S., *et al.* (2017) 'Finding the design space of a filtration-based operation for the concentration of human pluripotent stem cells', *Journal of Membrane Science*, 542, pp. 399–407. doi: https://doi.org/10.1016/j.memsci.2017.08.036.

Czysz, K., Minger, S. and Thomas, N. (2015) 'Dmso efficiently down regulates pluripotency genes in human embryonic stem cells during definitive endoderm derivation and increases the proficiency of hepatic differentiation', *PLoS ONE*. Public Library of Science, 10(2), p. e0117689. doi: 10.1371/journal.pone.0117689.

DeFrancesco, L. (2009) 'Fits and starts for Geron', *Nature Biotechnology*, 27(10), p. 877. doi:

10.1038/nbt1009-877b.

Delahaye, M. *et al.* (2015) 'An ultra scale-down analysis of the recovery by dead-end centrifugation of human cells for therapy', *Biotechnology and Bioengineering*. Wiley Online Library, 112(5), pp. 997–1011. doi: 10.1002/bit.25519.

Doran, P. M. (2013) *Bioprocess Engineering Principles*, *Academic Press*. Academic press. Available at: https://books.google.at/books?id=wZSylDhgEXMC.

Draper, J. S. *et al.* (2004) 'Recurrent gain of chromosomes 17q and 12 in cultured human embryonic stem cells', *Nature biotechnology*. Nature Publishing Group, 22(1), p. 53.

Drummond, N. *et al.* (2018) 'Tools to monitor the production of a midbrain dopaminergic precursor cell product', in *Parkinson's UK*.

Dunnett, S. B. *et al.* (1983) 'Intracerebral grafting of neuronal cell suspensions. IV. Behavioural recovery in rats with unilateral 6-OHDA lesions following implantation of nigral cell suspensions in different forebrain sites', *Acta physiologica Scandinavica. Supplementum*, 522, pp. 29–37. Available at: http://europepmc.org/abstract/MED/6426250.

Eaker, S. *et al.* (2013) 'Concise review: Guidance in developing commercializable autologous/patient-specific cell therapy manufacturing', *Stem cells translational medicine*. Wiley Online Library, 2(11), pp. 871–883.

EudraLex (2014) *The rules governing medicinal products in the European Union*. Volume.

EudraLex (2017) *Guidelines on Good Manufacturing Practice specific to Advanced Therapy Medicinal Products*.

European Medicines Agency (2014) *Guideline on the use of porcine trypsin used in the manufacture of human biological medicinal products*. Available at: https://www.ema.europa.eu/en/documents/scientific-guideline/guideline-use-porcine-trypsin-used-manufacture-human-biological-medicinal-products_en.pdf.

European Medicines Agency (2019) 'Legal framework: Advanced therapies'. Available at: https://www.ema.europa.eu/en/human-regulatory/overview/advanced-therapies/legal-framework-advanced-therapies.

Evans, M. J. and Kaufman, M. H. (1981) 'Establishment in culture of pluripotential cells from mouse embryos', *Nature*, 292(5819), pp. 154–156. doi: 10.1038/292154a0.

FDA (2004) 'Sterile Drug Products Produced by Aseptic Processing: Current Good Manufacturing

Practice', *Guidance for Industry*, (September), pp. 1–63. Available at: http://www.fda.gov/downloads/Drugs/GuidanceComplianceRegulatoryInformation/Guidances/ucm070342.pdf.

FDA (2008) 'CGMP for phase 1 investigational drugs', *Guidance for Industry*, (July), pp. 301–827. Available at: http://www.fda.gov/cder/guidance/index.htm%5Cnhttp://www.fda.gov/cber/guidelines.htm.

FDA (2018a) 'CFR - Code of Federal Regulations Title 21'. Available at: https://www.accessdata.fda.gov/scripts/cdrh/cfdocs/cfCFR/CFRSearch.cfm?fr=1271.10.

FDA (2018b) *Hospira Inc. A Pfizer Company, McPherson, KS, 483 issued 08/08/2018*.

Fedele, S. *et al.* (2017) 'Expansion of human midbrain floor plate progenitors from induced pluripotent stem cells increases dopaminergic neuron differentiation potential', *Scientific reports*. Nature Publishing Group, 7(1), p. 6036.

Fernandes, A. M. *et al.* (2009) 'Successful scale-up of human embryonic stem cell production in a stirred microcarrier culture system', *Brazilian Journal of Medical and Biological Research*. SciELO Brasil, 42(6), pp. 515–522. doi: 10.1590/s0100-879x2009000600007.

Frame, S., Cohen, P. and Biondi, R. M. (2001) 'A common phosphate binding site explains the unique substrate specificity of GSK3 and its inactivation by phosphorylation', *Molecular cell*. Elsevier, 7(6), pp. 1321–1327.

Frantz, S. (2012) 'Embryonic stem cell pioneer Geron exits field, cuts losses.', *Nature biotechnology*. Nature Publishing Group, pp. 12–13. doi: 10.1038/nbt0112-12.

Freed, C. R. *et al.* (2001) 'Transplantation of Embyonic Dopamine Neurons for Severe Parkinson's Disease', *New England Journal of Medicine*. Mass Medical Soc, 344(10), pp. 710–719.

Freund, T. F. *et al.* (1985) 'Efferent synaptic connections of grafted dopaminergic neurons reinnervating the host neostriatum: a tyrosine hydroxylase immunocytochemical study', *Journal of Neuroscience*. Soc Neuroscience, 5(3), pp. 603–616.

Fricker-Gates, R. A. and Gates, M. A. (2010) 'Stem cell-derived dopamine neurons for brain repair in Parkinson's disease.', *Regenerative Medicine*. Future Medicine, 5(2), pp. 267–278. doi: 10.2217/rme.10.3.

Galmés, A. *et al.* (1999) 'Long-term storage at− 80° C of hematopoietic progenitor cells with 5-percent dimethyl sulfoxide as the sole cryoprotectant', *Transfusion*. Wiley Online Library, 39(1), pp. 70–73.

Galvao, J. *et al.* (2014) 'Unexpected low-dose toxicity of the universal solvent DMSO', *The FASEB Journal*. Federation of American Societies for Experimental Biology Bethesda, MD, USA, 28(3), pp. 1317–1330.

Gaskell, T. *et al.* (2018) 'Addressing the challenges of controlled, scalable and affordable expansion of hPSCs for therapeutic use', in *ISSCR Proceedings*.

Girling, A. *et al.* (2010) 'Early-stage valuation of medical devices: the role of developmental uncertainty', *Value in Health*. Elsevier, 13(5), pp. 585–591.

Godoy-Hernández, G. and Vázquez-Flota, F. A. (2012) 'Growth measurements: Estimation of cell division and cell expansion', *Methods in Molecular Biology*. Unidad de Bioquímica y Biología Molecular de Plantas, Centro de Investigación Científica de Yucatán, Mérida, Yucatán, México. ggodoy@cicy.mx, 877, pp. 41–48. doi: 10.1007/978-1-61779-818-4_4.

Godthardt, K. *et al.* (2019) 'Efficient GMP compliant expansion of mesenchymal stromal cells (MSCs) from umbilical cord, bone marrow and adipose tissue using a closed cultivation system.', *Cytotherapy*, 21(5), pp. S90–S91. doi: 10.1016/j.jcyt.2019.03.522.

Grealish, S. *et al.* (2014) 'Human ESC-derived dopamine neurons show similar preclinical efficacy and potency to fetal neurons when grafted in a rat model of Parkinson's disease', *Cell Stem Cell*. Elsevier, 15(5), pp. 653–665. doi: 10.1016/j.stem.2014.09.017.

Griffiths, J. B. *et al.* (1979) 'Changes in cell size during the cooling, warming and post-thawing periods of the freeze-thaw cycle', *Cryobiology*. Elsevier, 16(2), pp. 141–151.

Hadpe, S. R. *et al.* (2017) 'ATF for cell culture harvest clarification: mechanistic modelling and comparison with TFF', *Journal of Chemical Technology and Biotechnology*. John Wiley & Sons, Ltd, 92(4), pp. 732–740. doi: 10.1002/jctb.5165.

Hallett, P. J. *et al.* (2015) 'Successful Function of Autologous iPSC-Derived Dopamine Neurons following Transplantation in a Non-Human Primate Model of Parkinson's Disease', *Cell Stem Cell*, 16(3), pp. 269–274. doi: http://dx.doi.org/10.1016/j.stem.2015.01.018.

Hanslick, J. L. *et al.* (2009) 'Dimethyl sulfoxide (DMSO) produces widespread apoptosis in the developing central nervous system', *Neurobiology of disease*. Elsevier, 34(1), pp. 1–10. doi: 10.1016/j.nbd.2008.11.006.

Harris, I. R., Meacle, F. and Powers, D. (2016) 'Automation in Cell Therapy Manufacturing', *BioProcess International*, April. Available at: http://www.bioprocessintl.com/manufacturing/cell-therapies/automation-in-cell-therapy-manufacturing/.

Harrison, R. P. *et al.* (2017) 'Decentralized manufacturing of cell and gene therapies: Overcoming challenges and identifying opportunities', *Cytotherapy*, 19(10), pp. 1140–1151. doi: https://doi.org/10.1016/j.jcyt.2017.07.005.

Hasan, J. *et al.* (2017) 'A semi-automated cost-efficient process for the closed expansion and harvest of pluripotent stem cells using a hollow fibre bioreactor and continuous centrifugation', *Cytotherapy*. Elsevier, 19(5), p. S158. doi: 10.1016/j.jcyt.2017.02.245.

Hassan, S. *et al.* (2015) 'Allogeneic cell therapy bioprocess economics and optimization: Downstream processing decisions', *Regenerative Medicine*. Future Medicine, 10(5), pp. 591–609. doi: 10.2217/rme.15.29.

Heathman, T. R. J. *et al.* (2015) 'The translation of cell-based therapies: clinical landscape and manufacturing challenges', *Regenerative medicine*. Future Medicine, 10(1), pp. 49–64.

Heng, B. C. *et al.* (2006) 'Low temperature tolerance of human embryonic stem cells', *International Journal of Medical Sciences*. Ivyspring International Publisher, 3(4), p. 124.

Heng, B. C. *et al.* (2007) 'Mechanical dissociation of human embryonic stem cell colonies by manual scraping after collagenase treatment is much more detrimental to cellular viability than is trypsinization with gentle pipetting', *Biotechnology and applied biochemistry*. Wiley Online Library, 47(1), pp. 33–37.

Heng, B. C. (2009) 'Effect of Rho-associated kinase (ROCK) inhibitor Y-27632 on the post-thaw viability of cryopreserved human bone marrow-derived mesenchymal stem cells', *Tissue and Cell*, 41(5), pp. 376–380. doi: 10.1016/j.tice.2009.01.004.

Hirsch, L. *et al.* (2016) 'The Incidence of Parkinson's Disease: A Systematic Review and Meta-Analysis', *Neuroepidemiology*, 46(4), pp. 292–300. doi: 10.1159/000445751.

Hourd, P. *et al.* (2008) 'Regulatory challenges for the manufacture and scale-out of autologous cell therapies', *StemBook*. Harvard Stem Cell Institute, pp. 1–13. doi: 10.3824/stembook.1.96.1.1.

Humpe, A. *et al.* (2007) 'Cryopreservation of cellular products in a closed-bag system with an incorporated dimethyl sulfoxide-resistant sterile filter outside of cleanroom facilities', *Transfusion*. Wiley Online Library, 47(6), pp. 1033–1041. doi: 10.1111/j.1537-2995.2007.01232.x.

Hunt, C. J. (2017) 'Cryopreservation: Vitrification and Controlled Rate Cooling', in *Stem Cell Banking: Concepts and Protocols*. Springer New York, pp. 41–77.

Hunt, C. J. (2019) 'Technical considerations in the freezing, low-temperature storage and thawing of stem cells for cellular therapies', *Transfusion Medicine and Hemotherapy*. Karger Publishers, 46(3), pp.

134–150.

Hyman, C. *et al.* (1991) 'BDNF is a neurotrophic factor for dopaminergic neurons of the substantia nigra', *Nature*. Nature Publishing Group, 350(6315), pp. 230–232. doi: 10.1038/350230a0.

ICH (1995) 'Stability Testing of Biotechnological/Biological Products Q5C', *ICH Harmonised Tripartite Guideline*, (November), pp. 1–8.

ICH (1999) *Q6A Specifications: Test Procedures and Acceptance Criteria for New Drug Substances and New Drug Products: Chemical Substances*.

ICH (2000) 'Good Manufacturing Practice Guide for Active Pharmaceutical Ingredients Q7', *ICH Harmonised Tripartite Guideline*, (November).

ICH (2001) 'Derivation and Characterisation of Cell Substrates Used for Production of Biotechnological/Biological Products Q5D', *ICH Harmonised Tripartite Guideline*.

ICH (2008) 'Pharmaceutical Quality System Q10', *ICH Harmonised Tripartite Guideline*, 4.

ICH (2009) 'Pharmaceutical Development Q8(R2)', *ICH Harmonised Tripartite Guideline*, 4.

ISO (2015) 'ISO 9000:2015'.

ISPE (2003) *Good Practice Guide: Technology Transfer*.

Jankovic, J. (2008) 'Parkinson's disease: clinical features and diagnosis', *Journal of Neurology, Neurosurgery & Psychiatry*, 79(4), pp. 368 LP – 376. Available at: http://jnnp.bmj.com/content/79/4/368.abstract.

John Morris, G. and Acton, E. (2013) 'Controlled ice nucleation in cryopreservation – A review', *Cryobiology*, 66(2), pp. 85–92. doi: http://dx.doi.org/10.1016/j.cryobiol.2012.11.007.

Josephson, R. *et al.* (2007) 'Qualification of embryonal carcinoma 2102Ep as a reference for human embryonic stem cell research', *Stem cells*. Wiley Online Library, 25(2), pp. 437–446.

Jossen, V. *et al.* (2018) 'Manufacturing human mesenchymal stem cells at clinical scale: process and regulatory challenges', *Applied microbiology and biotechnology*. Springer, 102(9), pp. 3981–3994.

Julien, C. and Whitford, W. (2008) 'The Biopharmaceutical Industry's New Operating Paradigm', *BioProcess International*. INFORMA LIFE SCIENCES GROUP, 6, p. 6.

Kaiser, A. D. *et al.* (2015) 'Towards a commercial process for the manufacture of genetically modified T cells for therapy.', *Cancer gene therapy*. Nature Publishing Group, 22(2), pp. 72–8. doi: 10.1038/cgt.2014.78.

Kallur, T. *et al.* (2017) 'Quality Assurance in Stem Cell Banking: Emphasis on Embryonic and Induced Pluripotent Stem Cell Banking', in *Stem Cell Banking: Concepts and Protocols*. Springer, pp. 11–16.

Kandel, E. R. *et al.* (2000) *Principles of Neural Science*. McGraw-hill New York.

Karlsson, J. O. M. and Toner, M. (1996) 'Long-term storage of tissues by cryopreservation: critical issues', *Biomaterials*, 17(3), pp. 243–256. doi: https://doi.org/10.1016/0142-9612(96)85562-1.

Katkov, I. I. *et al.* (2006) 'Cryopreservation by slow cooling with DMSO diminished production of Oct-4 pluripotency marker in human embryonic stem cells', *Cryobiology*. Elsevier, 53(2), pp. 194–205.

Kawasaki H, Mizuseki K, Nishikawa S, Kaneko S, Kuwana Y, Nakanishi S, Nishikawa SI, S. Y. (2000) 'Induction of midbrain dopaminergic neurons from ES cells by stromal cell derived inducing activity', *Neuron*. Elsevier, 28(1), pp. 31–40.

Kerby, J. *et al.* (2017) 'Transfer and optimisation of ATMP manufacturing', *Cytotherapy*. Elsevier, 19(5), p. S115.

Kim, J. H. H. *et al.* (2002) 'Dopamine neurons derived from embryonic stem cells function in an animal model of Parkinson's disease', *Nature*. Nature Publishing Group, 418(6893), pp. 50–56. doi: 10.1038/nature00900.

Kirkeby, A. *et al.* (2012) 'Generation of Regionally Specified Neural Progenitors and Functional Neurons from Human Embryonic Stem Cells under Defined Conditions', *Cell Reports*. Elsevier, 1(6), pp. 703–714. doi: 10.1016/j.celrep.2012.04.009.

Kirkeby, A. *et al.* (2017) 'Predictive Markers Guide Differentiation to Improve Graft Outcome in Clinical Translation of hESC-Based Therapy for Parkinson's Disease', *Cell Stem Cell*. Elsevier, 20(1), pp. 135–148. doi: 10.1016/j.stem.2016.09.004.

Kirkeby, A., Nelander, J. and Parmar, M. (2012) 'Generating regionalized neuronal cells from pluripotency, a step-by-step protocol.', *Frontiers in cellular neuroscience*. Frontiers Media SA, 6(January), p. 64. doi: 10.3389/fncel.2012.00064.

Kirkeby, A. and Parmar, M. (2012) 'Building authentic midbrain dopaminergic neurons from stem cells – Lessons from development', *Translational Neuroscience*, 3(4), pp. 314–319. doi: 10.2478/s13380-012-0041-x.

Kirkeby, A., Parmar, M. and Barker, R. A. (2017) 'Strategies for bringing stem cell-derived dopamine neurons to the clinic: A European approach (STEM-PD)', *Progress in Brain Research*. Elsevier. doi: 10.1016/bs.pbr.2016.11.011.

Kitano, H. (2002) 'Systems biology: a brief overview', *science*. American Association for the Advancement of Science, 295(5560), pp. 1662–1664.

Koehler, K. R. *et al.* (2011) 'Extended passaging increases the efficiency of neural differentiation from induced pluripotent stem cells', *BMC Neuroscience*. BioMed Central, 12(1), p. 82. doi: 10.1186/1471-2202-12-82.

Koyama, S. *et al.* (2019) 'Alternating electric field application induced non-contact and enzyme-free cell detachment', *Cytotechnology*. Springer, 71(2), pp. 583–597.

Langer, E. S. (2008) 'Biotech Facilities Average a Batch Failure Every 40.6 Weeks', *BioProcess International*. Available at: https://bioprocessintl.com/analytical/downstream-validation/biotech-facilities-average-a-batch-failure-every-40-6-weeks-183158/.

Langer, E. S. (2016) 'Average Batch Failure Rate Worsens', *Genetic Engineering & Biology News*. Available at: https://www.genengnews.com/magazine/average-batch-failure-rate-worsens/.

Li, Y. and Ma, T. (2012) 'Bioprocessing of cryopreservation for large-scale banking of human pluripotent stem cells.', *BioResearch open access*. 140 Huguenot Street, 3rd FloorNew Rochelle, NY 10801USA: Mary Ann Liebert, Inc. 140 Huguenot Street, 3rd Floor New Rochelle, NY 10801 USA, 1(5), pp. 205–14. doi: 10.1089/biores.2012.0224.

Lindvall, O. *et al.* (1990) 'Grafts of fetal dopamine neurons survive and improve motor function in Parkinson's disease.', *Science (New York, N.Y.)*, 247(4942), pp. 574–577. doi: 10.1126/science.2105529.

Lindvall, O. and Björklund, A. (2004) 'Cell therapy in Parkinson's disease.', *NeuroRx : the journal of the American Society for Experimental NeuroTherapeutics*. Elsevier, 1(4), pp. 382–93. doi: 10.1602/neurorx.1.4.382.

Lineage Cell Therapeutics (2010) *Safety Study of GRNOPC1 in Spinal Cord Injury*, *ClinicalTrials.gov*. Available at: https://clinicaltrials.gov/ct2/show/NCT01217008.

Lipsitz, Y. Y. *et al.* (2017) 'A roadmap for cost-of-goods planning to guide economic production of cell therapy products', *Cytotherapy*. Elsevier, 19(12), pp. 1383–1391.

Lipsitz, Y. Y., Timmins, N. E. and Zandstra, P. W. (2016) 'Quality cell therapy manufacturing by design', *Nat Biotechnol*. Nature Publishing Group, 34(4), pp. 393–400. doi: 10.1038/nbt.3525.

Lopes, A. G., Sinclair, A. and Frohlich, B. (2018a) 'Cost analysis of cell therapy manufacture: autologous cell therapies, part 1', *BioProcess Int*, 16(3).

Lopes, A. G., Sinclair, A. and Frohlich, B. (2018b) 'Cost analysis of cell therapy manufacture: autologous

cell therapies, part 2', *BioProcess Int*.

Lopez, F. *et al.* (2010) 'A Quality Risk Management Model Approach for Cell Therapy Manufacturing', *Risk Analysis*. Wiley Online Library, 30(12), pp. 1857–1871. doi: 10.1111/j.1539-6924.2010.01465.x.

Löser, P. *et al.* (2010) 'Human embryonic stem cell lines and their use in international research', *Stem cells (Dayton, Ohio)*. Wiley Subscription Services, Inc., A Wiley Company, 28(2), pp. 240–246. doi: 10.1002/stem.286.

Lovelock, J. E. (1953) 'The haemolysis of human red blood cells by freezing and thawing', *Biochimica et Biophysica Acta*, 10, pp. 414–426. doi: http://dx.doi.org/10.1016/0006-3002(53)90273-X.

Lovelock, J. E. and Bishop, M. W. H. (1959) 'Prevention of freezing damage to living cells by dimethyl sulphoxide.', *Nature*, 183(4672), pp. 1394–5. doi: 10.1038/1831394a0.

Lyness, A. M., Picken, A. and Thomas, R. (2019) 'Evaluation of a vial adaptor to ensure safe and efficient needle-free transfer of cells post-cryopreservation in preparation for drug delivery', *Cytotherapy*. Elsevier, 21(5), p. S38.

MacLeod, R. A. F. *et al.* (1999) 'Widespread intraspecies cross-contamination of human tumor cell lines arising at source', *International Journal of Cancer*. Wiley Online Library, 83(4), pp. 555–563.

Magnasco, A. *et al.* (2008) 'Mesenchymal Stem Cells Protective Effect in Adriamycin Model of Nephropathy', *Cell Transplantation*. SAGE Publications Inc, 17(10–11), pp. 1157–1167. doi: 10.3727/096368908787236567.

Marquez-Curtis, L. A. *et al.* (2016) 'Beyond membrane integrity: Assessing the functionality of human umbilical vein endothelial cells after cryopreservation', *Cryobiology*, 72(3), pp. 183–190. doi: 10.1016/j.cryobiol.2016.05.005.

Mason, C. and Dunnill, P. (2008) 'A brief definition of regenerative medicine'. Future Medicine.

Mason, C. and Dunnill, P. (2009) 'Assessing the value of autologous and allogeneic cells for regenerative medicine', *Regenerative Medicine*. Future Medicine, 4(6), pp. 835–853. doi: 10.2217/rme.09.64.

Mason, C. and Hoare, M. (2006) 'Regenerative medicine bioprocessing: the need to learn from the experience of other fields.', *Regenerative medicine*. Future Medicine, 1(5), pp. 615–623. doi: 10.2217/17460751.1.5.615.

Masri, F. *et al.* (2017) 'Challenges and advances in scale-up of label-free downstream processing for allogeneic cell therapies', *Cell Gene Therapy Insights*, 3(6), pp. 447–467. doi: 10.18609/cgti.2017.041.

Massie, I. *et al.* (2014) 'GMP Cryopreservation of Large Volumes of Cells for Regenerative Medicine: Active Control of the Freezing Process.', *Tissue engineering. Part C, Methods*. 140 Huguenot Street, 3rd FloorNew Rochelle, NY 10801USA: Mary Ann Liebert, Inc., 20(9), pp. 1–46. doi: 10.1089/ten.TEC.2013.0571.

Masui, S. *et al.* (2007) 'Pluripotency governed by Sox2 via regulation of Oct3/4 expression in mouse embryonic stem cells', *Nature cell biology*. Nature Publishing Group, 9(6), p. 625.

Mazur, P. (1963) 'Kinetics of Water Loss from Cells at Subzero Temperatures and the Likelihood of Intracellular Freezing', *The Journal of General Physiology*, 47(2), pp. 347 LP – 369. Available at: http://jgp.rupress.org/content/47/2/347.abstract.

Mazur, P., Leibo, S. P. and Chu, E. H. Y. (1972) 'A two-factor hypothesis of freezing injury. Evidence from Chinese hamster tissue-culture cells', *Experimental Cell Research*, 71(2), pp. 345–355. doi: 10.1016/0014-4827(72)90303-5.

McCall, M. J. (2009) *HYPERStack Expansion of hBM-MSC to Differentiation and DSP*.

Mei, S. H. J. *et al.* (2010) 'Mesenchymal stem cells reduce inflammation while enhancing bacterial clearance and improving survival in sepsis', *American journal of respiratory and critical care medicine*. American Thoracic Society, 182(8), pp. 1047–1057.

Miltenyi Biotec (2018a) *Differentiation of human pluripotent stem cells into mesencephalic dopaminergic progenitor cells*. Available at: https://www.miltenyibiotec.com/upload/assets/IM0022462.PDF.

Miltenyi Biotec (2018b) *GMP-compliant human pluripotent stem cell expansion process*. Available at: https://www.miltenyibiotec.com/upload/assets/IM0022463.PDF.

Miltenyi Biotec (2020a) *CliniMACS Prodigy*. Available at: https://www.miltenyibiotec.com/GB-en/products/cell-manufacturing-platform/clinimacs-prodigy/clinimacs-prodigy-instrument/clinimacs-prodigy-r.html (Accessed: 10 April 2019).

Miltenyi Biotec (2020b) *CryoMACS Freezing Bag 50*. Available at: https://www.miltenyibiotec.com/GB-en/products/cell-manufacturing-platform/cell-culture-and-freezing-bags/cryomacs-freezing-products/cryomacs-r-freezing-bags.html#.

Mitchell, P. D. *et al.* (2014) 'A quality-by-design approach to risk reduction and optimization for human embryonic stem cell cryopreservation processes', *Tissue Engineering Part C: Methods*. Mary Ann Liebert, Inc. 140 Huguenot Street, 3rd Floor New Rochelle, NY 10801 USA, 20(12), pp. 941–950.

Moutsatsou, P. *et al.* (2019) 'Automation in cell and gene therapy manufacturing: from past to future', *Biotechnology Letters*, 41(11), pp. 1245–1253. doi: 10.1007/s10529-019-02732-z.

Munk, M. (2017) 'The Industry's Hesitation to Adopt Continuous Bioprocessing: Recommendations for Deciding What, Where, and When to Implement', *BioProcess International*, April. Available at: http://www.bioprocessintl.com/manufacturing/continuous-bioprocessing/industrys-hesitation-adopt-continuous-bioprocessing-recommendations-deciding-implement/.

Muthu, P., Dhanalakshmi, V. and Sankaranarayanasamy, K. (2009) 'Optimal tolerance design of assembly for minimum quality loss and manufacturing cost using metaheuristic algorithms', *International Journal of Advanced Manufacturing Technology*. Springer, 44(11–12), pp. 1154–1164. doi: 10.1007/s00170-009-1930-1.

Neurostemcellrepair (2018) *Final Report Summary - NEUROSTEMCELLREPAIR (European stem cell consortium for neural cell replacement, reprogramming and functional brain repair)*. Available at: https://cordis.europa.eu/result/rcn/219184_en.html.

Nichols, J. *et al.* (1998) 'Formation of Pluripotent Stem Cells in the Mammalian Embryo Depends on the POU Transcription Factor Oct4', *Cell*, 95(3), pp. 379–391. doi: https://doi.org/10.1016/S0092-8674(00)81769-9.

Nienow, A. W. *et al.* (2016) 'Agitation conditions for the culture and detachment of hMSCs from microcarriers in multiple bioreactor platforms', *Biochemical Engineering Journal*, 108, pp. 24–29. doi: 10.1016/j.bej.2015.08.003.

Nolbrant, S. *et al.* (2017) 'Generation of high-purity human ventral midbrain dopaminergic progenitors for in vitro maturation and intracerebral transplantation', *Nature Protocols*. Nature Publishing Group, a division of Macmillan Publishers Limited. All Rights Reserved., 12(9), pp. 1962–1979. doi: 10.1038/nprot.2017.078.

Ock, S.-A. and Rho, G.-J. (2011) 'Effect of dimethyl sulfoxide (DMSO) on cryopreservation of porcine mesenchymal stem cells (pMSCs)', *Cell Transplantation*. College of Veterinary Medicine, Gyeongsang National University, Jinju, Republic of Korea., 20(8), pp. 1231–1239. doi: 10.3727/096368910X552835.

Olanow, C. W. *et al.* (2003) 'A double-blind controlled trial of bilateral fetal nigral transplantation in Parkinson's disease', *Annals of Neurology*. Wiley Online Library, 54(3), pp. 403–414. doi: 10.1002/ana.10720.

ONS (2019) *United Kingdom population mid-year estimate*.

Osafune, K. *et al.* (2008) 'Marked differences in differentiation propensity among human embryonic

stem cell lines.', *Nature biotechnology*. Nature Publishing Group, 26(3), pp. 313–315. doi: 10.1038/nbt1383.

OzoneLab Instruments (2020) 'OzoneLab Laboratory Research Peripherals'. Available at: http://www.ozonelab.com/pricing/pricelists/OLP-lab.htm.

Pal, R. *et al.* (2012) 'Diverse effects of dimethyl sulfoxide (DMSO) on the differentiation potential of human embryonic stem cells', *Archives of toxicology*. Springer, 86(4), pp. 651–661.

Pall Life Sciences (2003) *Introduction to Tangential Flow Filtration for Laboratory and Process Development Applications*.

Palmer, J. A. *et al.* (2013) 'Establishment and assessment of a new human embryonic stem cell-based biomarker assay for developmental toxicity screening', *Birth Defects Research Part B - Developmental and Reproductive Toxicology*. Wiley Online Library, 98(4), pp. 343–363. doi: 10.1002/bdrb.21078.

Parent, M. and Parent, A. (2010) 'Substantia Nigra and Parkinson's Disease: A Brief History of Their Long and Intimate Relationship', *Canadian Journal of Neurological Sciences / Journal Canadien des Sciences Neurologiques*. 2014/12/02. Cambridge University Press, 37(3), pp. 313–319. doi: DOI: 10.1017/S0317167100010209.

Parisse, J.-S. (2017) 'The importance of fill & finish in the commercialization of your cell & gene therapy', *Cell Gene Therapy Insights*, 3(6), pp. 405–408. doi: 10.18609/cgti.2017.043.

Park, Y. Bin *et al.* (2008) 'Alterations of proliferative and differentiation potentials of human embryonic stem cells during long-term culture.', *Experimental & molecular medicine*. Korean Society for Biochemistry and Molecular Biology, 40(1), pp. 98–108. doi: 10.3858/emm.2008.40.1.98.

Parkinsons UK (2017) *The cost of Parkinson's: the financial impact of living with the condition*. Available at: https://www.parkinsons.org.uk/sites/default/files/2017-07/CS2547 Cost of Parkinson%27s report 2017 - UK_1.pdf.

Pattasseril, J. *et al.* (2013) 'Downstream Technology Landscape for Large-Scale Therapeutic Cell Processing | BioProcess International', *Bioprocess Int*, 11(3), pp. 38–47. Available at: http://www.bioprocessintl.com/upstream-processing/bioreactors/downstream-technology-landscape-for-large-scale-therapeutic-cell-processing-340981/.

Pereira Chilima, T. D., Moncaubeig, F. and Farid, S. S. (2018) 'Impact of allogeneic stem cell manufacturing decisions on cost of goods, process robustness and reimbursement', *Biochemical Engineering Journal*, 137, pp. 132–151. doi: https://doi.org/10.1016/j.bej.2018.04.017.

Perlow, M. J. *et al.* (1979) 'Brain grafts reduce motor abnormalities produced by destruction of nigrostriatal dopamine system.', *Science (New York, N.Y.)*. American Association for the Advancement of Science, 204(May), pp. 643–647. doi: 10.1126/science.571147.

Perry, S. (2010) 'Tech Transfer: Do It Right the First Time', *Pharma Manufacturing*. Available at: https://www.pharmamanufacturing.com/articles/2010/007/?show=all.

Piccini, P. *et al.* (1999) 'Dopamine release from nigral transplants visualized in vivo in a Parkinson's patient.', *Nature neuroscience*. Nature Publishing Group, 2(12), pp. 1137–1140. doi: 10.1038/16060.

Piccini, P. *et al.* (2000) 'Delayed recovery of movement-related cortical function in Parkinson's disease after striatal dopaminergic grafts', *Annals of Neurology*, 48(5), pp. 689–695. doi: 10.1002/1531-8249(200011)48:5<689::AID-ANA1>3.0.CO;2-N.

Piccini, P. *et al.* (2005) 'Factors affecting the clinical outcome after neural transplantation in Parkinson's disease', *Brain*. Oxford Univ Press, 128(12), pp. 2977–2986. doi: 10.1093/brain/awh649.

Pigeau, G. M., Csaszar, E. and Dulgar-Tulloch, A. (2018) 'Commercial Scale Manufacturing of Allogeneic Cell Therapy', *Frontiers in Medicine*, p. 233. Available at: https://www.frontiersin.org/article/10.3389/fmed.2018.00233.

Pijuan-Galitó, S. *et al.* (2016) 'Human serum-derived protein removes the need for coating in defined human pluripotent stem cell culture', *Nature Communications*. Nature Publishing Group, 7(1), pp. 1–12. doi: 10.1038/ncomms12170.

Plagnol, A. C. *et al.* (2009) 'Industry perceptions of barriers to commercialization of regenerative medicine products in the UK', *Regenerative Medicine*. Future Medicine, 4(4), pp. 549–559.

Polge, C., Smith, A. U. and Parkes, A. S. (1949) 'Revival of spermatozoa after vitrification and dehydration at low temperatures', *Nature*, 164(4172), p. 666.

Pringsheim, T. *et al.* (2014) 'The prevalence of Parkinson's disease: A systematic review and meta-analysis', *Movement disorders*. Wiley Online Library, 29(13), pp. 1583–1590.

Puri, M. C. and Nagy, A. (2012) 'Concise review: Embryonic stem cells versus induced pluripotent stem cells: The game is on', *Stem Cells*. Wiley Online Library, 30(1), pp. 10–14. doi: 10.1002/stem.788.

Rafiq, Q. A. *et al.* (2016) 'Developing an automated robotic factory for novel stem cell therapy production', *Regenerative Medicine*. Future Medicine, pp. 351–354. doi: 10.2217/rme-2016-0040.

Rafiq, Q. A., Coopman, K. and Hewitt, C. J. (2013) 'Scale-up of human mesenchymal stem cell culture: current technologies and future challenges', *Current Opinion in Chemical Engineering*, 2(1), pp. 8–16.

doi: https://doi.org/10.1016/j.coche.2013.01.005.

Rajamani, K. *et al.* (2014) 'Genetic and Epigenetic Instability of Stem Cells', *Cell Transplantation*. SAGE Publications Inc, 23(4–5), pp. 417–433. doi: 10.3727/096368914X678472.

van Reis, R. and Zydney, A. (2007) 'Bioprocess membrane technology', *Journal of Membrane Science*, 297(1–2), pp. 16–50. doi: 10.1016/j.memsci.2007.02.045.

Reubinoff, B. E. *et al.* (2001) 'Effective cryopreservation of human embryonic stem cells by the open pulled straw vitrification method.', *Human reproduction (Oxford, England)*. Oxford University Press, 16(10), pp. 2187–94. doi: 10.1093/humrep/16.10.2187.

Richards, M. *et al.* (2004) 'An efficient and safe xeno-free cryopreservation method for the storage of human embryonic stem cells', *Stem Cells*. Wiley Online Library, 22(5), pp. 779–789. doi: 10.1634/stemcells.22-5-779.

Roberts, S. (2013) 'Lonza, Multiple Options for Large-Scale Production of Cell Therapeutics: Evaluation and Implementation', in *ISCT North America 2013 Regional Meeting*.

Rosler, E. S. *et al.* (2004) 'Long-term culture of human embryonic stem cells in feeder-free conditions', *Developmental Dynamics*. Wiley Online Library, 229(2), pp. 259–274.

Rotondi, M. C., Costariol, E. and Rafiq, Q. (2019) 'A cost/quality analysis of primary human T-Cells in different expansion systems'.

Rowley, J. *et al.* (2012) 'Meeting lot-size challenges of manufacturing adherent cells for therapy', *BioProcess International*, 10(SUPPL. 3), pp. 16–22.

Sartorius (2020) *Flexboy® 2D Bags*. Available at: https://www.sartorius.com/shop/ww/en/usd/flexboy®-2d-bags/c/M_Flexboy_Bags.

Sauer, H. *et al.* (1992) 'Cryopreservation, survival and function of intrastriatal fetal mesencephalic grafts in a rat model of Parkinson's disease', *Experimental brain research*. Springer, 90(1), pp. 54–62.

Schlenke, P. *et al.* (2008) 'The impact of the German tissue act on the manufacturing of autologous and allogeneic stem cell preparations', *Transfusion Medicine and Hemotherapy*. Karger Publishers, 35(6), pp. 446–452.

Schwartz, L. (2003) 'Diafiltration: A fast, efficient method for desalting, or buffer exchange of biological samples', *Pall Scientific & Technical Report*.

Scott, C. T. and Magnus, D. (2014) 'Wrongful termination: lessons from the Geron clinical trial', *Stem*

cells translational medicine. 2014/10/08. AlphaMed Press, 3(12), pp. 1398–1401. doi: 10.5966/sctm.2014-0147.

Shariatzadeh, M. *et al.* (2020) 'Distributed automated manufacturing of pluripotent stem cell products', *The International Journal of Advanced Manufacturing Technology*, 106(3), pp. 1085–1103. doi: 10.1007/s00170-019-04516-1.

Silani, V. *et al.* (1988) 'Human neuronal cell viability demonstrated in culture after cryopreservation', *Brain Research*, 473(1), pp. 169–174. doi: https://doi.org/10.1016/0006-8993(88)90331-9.

Silverman, L. I. *et al.* (2019) 'Identifying and Managing Sources of Variability in Cell Therapy Manufacturing and Clinical Trials', *Regenerative Engineering and Translational Medicine*, 5(4), pp. 354–361. doi: 10.1007/s40883-019-00129-y.

Simaria, A. S. *et al.* (2014) 'Allogeneic cell therapy bioprocess economics and optimization: Single-use cell expansion technologies', *Biotechnology and Bioengineering*. Wiley Online Library, 111(1), pp. 69–83. doi: 10.1002/bit.25008.

Smith, D. (2014) *Process monitoring and control using live cell imaging for the manufacturing of cell therapies*.

Soares, F. A. C. *et al.* (2014) 'Investigating the feasibility of scale up and automation of human induced pluripotent stem cells cultured in aggregates in feeder free conditions', *Journal of Biotechnology*. Elsevier, 173(1), pp. 53–58. doi: 10.1016/j.jbiotec.2013.12.009.

Soldner, F. *et al.* (2009) 'Parkinson's disease patient-derived induced pluripotent stem cells free of viral reprogramming factors', *Cell*. Elsevier, 136(5), pp. 964–977.

Sonntag, K. *et al.* (2004) 'Temporally induced Nurr1 can induce a non-neuronal dopaminergic cell type in embryonic stem cell differentiation', *European Journal of Neuroscience*. Wiley Online Library, 19(5), pp. 1141–1152.

De Sousa, P. A., Tye, B. J., *et al.* (2016) 'Derivation of the clinical grade human embryonic stem cell line RCe013-A (RC-9)', *Stem Cell Research*. Elsevier, 17(1), pp. 36–41. doi: 10.1016/j.scr.2016.04.020.

De Sousa, P. A., Downie, J. M., *et al.* (2016) 'Development and production of good manufacturing practice grade human embryonic stem cell lines as source material for clinical application', *Stem Cell Research*, 17(2), pp. 379–390. doi: 10.1016/j.scr.2016.08.011.

Specht, L. and Ph, D. (2020) 'An analysis of culture medium costs and production volumes for cultivated meat', *The Good Food Institute: Washington, DC, USA*.

Sputtek, A. *et al.* (2011) 'Bioequivalence comparison of a new freezing bag (CryoMACS®) with the Cryocyte® freezing bag for cryogenic storage of human hematopoietic progenitor cells', *Cytotherapy*. Taylor & Francis, 13(4), pp. 481–489.

Stacey, G. (2017) 'Stem Cell Banking: A Global View', in *Stem Cell Banking: Concepts and Protocols*. Springer, pp. 3–10.

Stanton, D. (2018a) 'Future market needs driving vendor innovation, says MilliporeSigma', *BioProcess International*. Available at: https://bioprocessintl.com/bioprocess-insider/upstream-downstream-processing/future-market-needs-driving-vendor-innovation-says-milliporesigma/.

Stanton, D. (2018b) 'High Octane: Lonza buys 80% of "game-changing" cell therapy tech partner', *BioProcess International*. Available at: https://bioprocessintl.com/bioprocess-insider/deal-making/high-octane-lonza-buys-80-of-game-changing-cell-therapy-tech-partner/.

Stanton, D. (2018c) 'Hyperstack Shortage Caused by Gene Therapy Surge', *BioProcess International*.

Stanton, D. (2019) 'Cost of Goods Is Crucial for the Future of Regenerative Medicine: CAR-T Cell Therapy Provides a Case Study in Perspective', *BioProcess International*. Available at: https://bioprocessintl.com/manufacturing/emerging-therapeutics-manufacturing/cost-of-goods-is-crucial-for-the-future-of-regenerative-medicine-car-t-cell-therapy-provides-a-case-study-in-perspective/.

Strauss, S. (2010) 'Geron trial resumes, but standards for stem cell trials remain elusive', *Nature Biotechnology*. Nature Publishing Group, pp. 989–990. doi: 10.1038/nbt1010-989.

Strecker, R. E. *et al.* (1987) 'Autoregulation of dopamine release and metabolism by intrastriatal nigral grafts as revealed by intracerebral dialysis', *Neuroscience*. Elsevier, 22(1), pp. 169–178.

Takahashi, J. (2019) 'Preparing for first human trial of induced pluripotent stem cell-derived cells for Parkinson's disease: an interview with Jun Takahashi', *Regenerative Medicine*. Future Medicine, 14(2), pp. 93–95. doi: 10.2217/rme-2018-0158.

Takahashi, K. and Yamanaka, S. (2006) 'Induction of pluripotent stem cells from mouse embryonic and adult fibroblast cultures by defined factors.', *Cell*. Elsevier, 126(4), pp. 663–76. doi: 10.1016/j.cell.2006.07.024.

The International Stem Cell Banking Initiative (2009) 'Consensus Guidance for Banking and Supply of Human Embryonic Stem Cell Lines for Research Purposes', *Stem Cell Reviews and Reports*, 5(4), pp. 301–314. doi: 10.1007/s12015-009-9085-x.

Thomas, R. J. *et al.* (2007) 'Manufacture of a human mesenchymal stem cell population using an automated cell culture platform', *Cytotechnology*. Springer, 55(1), pp. 31–39.

Thomas, R. J. *et al.* (2008) 'Cell Culture Automation and Quality Engineering: A Necessary Partnership to Develop Optimized Manufacturing Processes for Cell-Based Therapies', *JALA - Journal of the Association for Laboratory Automation*. SAGE Publications, 13(3), pp. 152–158. doi: 10.1016/j.jala.2007.12.003.

Thomas, R. J. *et al.* (2009) 'Automated, scalable culture of human embryonic stem cells in feeder-free conditions', *Biotechnology and Bioengineering*. Wiley Online Library, 102(6), pp. 1636–1644. doi: 10.1002/bit.22187.

Thomson, J. A. *et al.* (1998) 'Embryonic stem cell lines derived from human blastocysts', *science*. American Association for the Advancement of Science, 282(5391), pp. 1145–1147. doi: 10.1126/science.282.5391.1145.

Tomar, R. (1999) 'Total Laboratory Automation and Diagnostic Immunology', *Clinical and Diagnostic Laboratory Immunology*, 6(3), pp. 293 LP – 294. Available at: http://cvi.asm.org/content/6/3/293.abstract.

Vallejo-Torres, L. *et al.* (2008) 'Integrating health economics modeling in the product development cycle of medical devices: a Bayesian approach', *International journal of technology assessment in health care*, 24(4), p. 459.

Want, A. J. *et al.* (2012) 'Large-scale expansion and exploitation of pluripotent stem cells for regenerative medicine purposes: Beyond the T flask', *Regenerative Medicine*. Future Medicine, 7(1), pp. 71–84. doi: 10.2217/rme.11.101.

Watanabe, K. *et al.* (2007) 'A ROCK inhibitor permits survival of dissociated human embryonic stem cells.', *Nature biotechnology*. Nature Publishing Group, 25(6), pp. 681–6. doi: 10.1038/nbt1310.

Weir, S. *et al.* (2018) 'Short-and long-term cost and utilization of health care resources in Parkinson's disease in the UK', *Movement Disorders*. Wiley Online Library, 33(6), pp. 974–981.

WHO (2016) *Guidelines on Validation*. Available at: https://www.who.int/medicines/areas/quality_safety/quality_assurance/validation-without_appendices_2016_05_17.pdf?ua=1.

Williams, D. J. *et al.* (2012) 'Precision manufacturing for clinical-quality regenerative medicines.', in *Philosophical transactions. Series A, Mathematical, physical, and engineering sciences*. Boston, MA, pp. 3924–49. doi: 10.1098/rsta.2011.0049.

Williams, D. J. *et al.* (2016) 'Comparability: manufacturing, characterization and controls, report of a UK Regenerative Medicine Platform Pluripotent Stem Cell Platform Workshop, Trinity Hall, Cambridge, 14-15 September 2015.', *Regenerative medicine*. Future Medicine Ltd London, UK, 11(5), pp. 483–92. doi: 10.2217/rme-2016-0053.

Wirth, E., Lebkowski, J. S. and Lebacqz, K. (2011) 'Response to Frederic Bretzner et al. "Target Populations for First-In-Human Embryonic Stem Cell Research in Spinal Cord Injury"', *Cell Stem Cell*, 8(5), pp. 476–478. doi: https://doi.org/10.1016/j.stem.2011.04.008.

Woods, E. J. *et al.* (2003) 'A theoretically optimized method for cord blood stem cell cryopreservation', *J Hematother Stem Cell Res*. Mary Ann Liebert, Inc., 12(3), pp. 341–350. doi: 10.1089/152581603322023070.

Woods, E. J. and Thirumala, S. (2011) 'Packaging considerations for biopreservation', *Transfusion Medicine and Hemotherapy*. 2011/03/16. S. Karger GmbH, 38(2), pp. 149–156. doi: 10.1159/000326083.

World Health Organization (2011) *Annex 7 - WHO guidelines on transfer of technology in pharmaceutical manufacturing*.

World Health Organization (2019) *Medicines regulatory support*. Available at: https://www.who.int/medicines/areas/quality_safety/regulation_legislation/en/.

Yang, X. *et al.* (2015) 'Intraarticular injection of allogenic mesenchymal stem cells has a protective role for the osteoarthritis', *Chinese medical journal*. Wolters Kluwer Health, 128(18), p. 2516.

Ye, W. *et al.* (1998) 'FGF and Shh Signals Control Dopaminergic and Serotonergic Cell Fate in the Anterior Neural Plate', *Cell*, 93(5), pp. 755–766. doi: https://doi.org/10.1016/S0092-8674(00)81437-3.

Zeng, A.-P. and Bi, J.-X. (2006) 'Cell Culture Kinetics and Modeling', *Cell Culture Technology for Pharmaceutical and Cell-Based Therapies*. MARCEL DECKER, 30, p. 299.

Zhang, S.-C. *et al.* (2001) 'In vitro differentiation of transplantable neural precursors from human embryonic stem cells', *Nature biotechnology*. Nature Publishing Group, 19(12), pp. 1129–1133.

Zoro, B. J. H. *et al.* (2009) 'Regenerative medicine bioprocessing: Concentration and behavior of adherent cell suspensions and pastes', *Biotechnology and Bioengineering*. Wiley Online Library, 103(6), pp. 1236–1247. doi: 10.1002/bit.22356.

9 Appendices

Appendix A – Process Economics Model

This material is unavailable due to copyright restrictions.

Appendix B – Timeline of Prodigy Technology Transfer Troubleshooting

	Prodigy	Expansion Troubleshooting	Differentiation Troubleshooting
15/03/2017	Visited Miltenyi for stages 1 and 2 of technology transfer. Unable to complete due to an bacterial infection within the CCU.		
12/10/2017	Miltenyi development scientist visited Loughborough for technology transfer stage 3. No tube welder was available, partial process performed with water.		
29/11/2017	First Prodigy run (H9 cells), failed expansion due to insufficient cell harvest, infection and possible gassing errors.		
31/01/2018	Second Prodigy run (H9 cells), failed expansion due to fungal infection and CO2 gassing error.		
14/03/2018	Third Prodigy run (H9 cells), failed expansion due to insufficient cell harvest following coating errors.		
23/04/2018		Manual seeding of CCU, exploratory EDTA buffer exposure work.	
27/04/2018		Tested whether exposure to EDTA buffer after coating impacts cell growth, results show a negligible impact.	
14/05/2018		Laminin drying of laminin 521 at 0.1 ug per cm^2, process impact found but unlikely to be cause of process failure.	
30/05/2018	Fourth Prodigy run (H9 cells), successful automated expansion followed by near total cell death during differentiation using Lund process.		
26/06/2018		Tested whether exposure to iPS-brew before laminin coating impacts cell growth, results show significant impact, probable cause of failure.	
29/06/2018		Laminin drying of laminin 521 at 0.5 ug per cm^2, process impact found but unlikely to be cause of process failure.	
20/06/2018			New Miltenyi method discussed, changes to feed days and small molecules.
25/07/2018			Manual H9 differentiation in T25 flasks, first successful differentiation of H9 cells to mesDA using updated process at Loughborough.
07/08/2018	Fifth Prodigy run (H9 cells), failed expansion due to buffer contamination. Differentation seeded from controls but failed on day 10 due to infection.		
10/09/2018		Tested whether EDTA buffer exposure before coating impacts cell growth, impact found to be negligible.	
21/09/2018		Tested whether EDTA buffer during seeding impacted cell growth, identified as probable cause of failure.	
03/09/2018			Manual RC17 differentiation in T25 flasks, first successful differentiation of RC17 cells into mesDA progenitors at Loughborough.
24/10/2018			Tested differentiaiton seeding conditions including buffer and coating exposure, seeding from a flexible bag, and use of non-warmed culture plastic.
25/10/2018			Tested differentation seeding sensitivity to reagent temperature.
10/10/2018	Sixth Prodigy run (RC17 cells), successful expansion followed by lack of cell attachment during differentiation seeding due to TrypLE/inhibitor		
09/11/2018			Tested differentiation using CCU and flask expanded cells, flask expanded cells showed significantly higher yields.
05/12/2018			Tested the impact of TrypLE and inhibitor contamination during differentiation seeding, identified as probable cause of process failure.

Appendix C – Draft Loughborough University Protocol for the Manufacture of mesDA Progenitor Cells on the Prodigy